EXPLORING JADOMYCIN BIOSYNTHESIS IN STREPTOMYCES VENEZUELAE

by

Andrew W. Robertson

Submitted in partial fulfilment of the requirements
for the degree of Doctor of Philosophy

at

Dalhousie University
Halifax, Nova Scotia
April 2015

TABLE OF CONTENTS

LIST OF FIGURES vi
LIST OF SCHEMES ix
LIST OF TABLES x
ABSTRACT xi
LIST OF ABBREVIATIONS USED xii
ACKNOWLEDGEMENTS xv
CHAPTER 1: INTRODUCTION 1
1.1. Natural Products Discovery 1
1.2. Jadomycin History: Initial Isolation and Structural Elucidation 3
1.3. Type-II Polyketide Synthases (PKS) and the Angucyclines 4
1.4. Polyketide Elongation and Cyclization 7
1.5. JadFGH: Divergent Biosynthetic Pathways and Dead Ends 8
1.6. Dideoxy Sugar Tailoring Gene Cluster 14
1.7. Amino Acid Incorporation: Exploiting a Spontaneous Process 16
1.8. Project Objectives 18
CHAPTER 2: RESULTS AND DISCUSSION PART 1 20
2.1. Exploiting Jadomycin Biosynthesis 20
2.1.1. Derivatization of Jadomycin Oct 21
2.1.2. Structural Characterization of **58a**-**58f** 26
2.1.3. Characterization of **58** 30
2.1.4. Deprotection of **58e** 31
2.2. Probing Structural Diversity 32
2.2.1. Attempted Isolation of Jadomycin DOct (**66**) and the Derivative (**66a**) 32
2.2.2. Isolation and Characterization of Jadomycin AVA (**67**) 33
2.3. Biological Activity of Jadomycin Amides 35
2.4. L-Lysine (**56**) Fermentations 35
2.4.1. ^{15}N Labeled L-Lysine 37
2.4.2. Isolation of L-digitoxosyl-phenanthroviridin 38
2.4.3. Structural Elucidation of **70** 39

2.4.4. Cytotoxic Activity of **70** 42
CHAPTER 3: RESULTS AND DISCUSSION PART 2 48
3.1. Regulation in Jadomycin Biosynthesis 48
3.1.1 JadX Homology Studies 50
3.1.2. JadX Disruption Shifts *S. venezuelae* Natural Product Profile 51
3.2. Ligand Observed NMR Binding: JadX Binds Jadomycins and Chloramphenicol 55
3.2.1 Quantification of JadX-Ligand Binding 58
3.2.2. Competitive Binding Experiments 61
3.3. Protein Observed Binding 62
3.4. Further Discussion 65
CHAPTER 4: EXPERIMENTAL 66
4.1. General Methods 66
4.1.1. HPLC Method #1 68
4.1.2. HPLC Method #2: Compound 58d 68
4.2. *S. venezuelae* ISP5230 VS1099 Media and Growth Conditions 68
4.2.1. Labeled ^{15}N-L-lysine growths 71
4.2.2. Crude Growth Purification 71
4.3. Succinimidyl Ester Preparation (Compounds **59**-**64**) 72
4.3.1. Phenoxyacetic acid *N*-hydroxysuccinimide ester (**59**) 72
4.3.2. (2-Naphthoxy)acetic acid *N*-hydroxysuccinimide ester (**60**) 72
4.3.3. Benzoic acid *N*-hydroxysuccinimide ester (**61**) 73
4.3.4. Nonoic acid *N*-hydroxysuccinimide ester (**62**) 73
4.3.5. SuO-Fmoc (**63**) 74
4.3.6. Synthesis of SuO-F-BODIPY (**64**) 75
4.3.7. 4,4-Difluoro-1,3,5,7-tetramethyl-2-ethyl-6-(3-propanoic acid) -8-H-4-bora-3a,4a-diaza-s-indacene *N*-hydroxysuccinimide ester (**64**) 77
4.4. Jadomycin Amide Syntheses, Purification, and Characterization (**58a**-**58f**, and **66a**) 78
4.4.1. Jadomycin Oct Phenoxyacetylamide (**58a**) 78
4.4.2. Jadomycin Oct Naphthoxyacetylamide (**58b**) 82
4.4.3. Jadomycin Oct Benzoylamide (**58c**) 86

4.4.4. Jadomycin Oct Nonoylamide (**58d**) 90
4.4.5. Jadomycin Oct Fmoc amide (**58e**) 94
4.4.6. Jadomycin Oct BODIPY amide (**58f**) 97
4.4.7. Jadomycin Oct (**58**) Purification and Characterization 101
4.4.8. Deprotection of **58e** 104
4.4.9. Jadomycin AVA (**67**) Purification and Characterization 105
4.4.10. Jadomycin DOct (**66**) Crude Isolation 108
4.4.11. Jadomycin DOct Phenoxyacetylamide (**66a**) 108
4.4.12. L-digitoxosyl-phenanthroviridin (**70**) 110
4.5. Biological Activity Evaluation 112
4.5.1. Photo-mediated DNA cleavage assays 112
4.5.2. Copper-mediated DNA cleavage assays 114
4.5.3. Bacterial culture 115
4.5.4. Agar well diffusion assays 116
4.6 General Methods for JadX NMR Binding Studies 118
4.6.1. Buffers and Growth Media 118
4.6.2. HPLC Analysis 118
4.6.3. LC-MS/MS Analysis 118
4.6.4. NMR Methodologies. 119
4.7. pET28a(+)::*jadX* Plasmid Construction 119
4.7.1. Genomic DNA Isolation (Kirby Mix Procedure) 119
4.7.2. *jadX* Cloning and Amplification 120
4.7.3. pET28a(+) Plasmid Preparation 122
4.7.4. pET28a(+) and *jadX* Digestion 122
4.7.5. Overexpression and Purification of JadX 124
4.7.6. Overexpression and Purification of ^{15}N-JadX 126
4.8. Jadomycin Growths and Purification 126
4.8.1. Bacterial Strains and Growth Conditions 126
4.8.2. Jadomycin DS Production, Isolation and Characterization 126
CHAPTER 5: CONCLUSIONS 129
5.1. Precursor Directed Biosynthesis and Semi-synthesis of Novel Jadomycins 129

5.2. Functional Characterization of JadX 130
REFERENCES 131
APPENDIX A: TLC IMAGES FROM COUPLING REACTIONS WITH **58** 140
APPENDIX B: HRMS DATA 143
APPENDIX C: SPECTRAL DATA FOR PURIFIED JADOMYCINS 154
APPENDIX D: NATIONAL CANCER INSTITUTE (NCI) 60 DTP HUMAN TUMOR CELL LINE SCREENS CYTOTOXIC ACTIVITY AND COMPARE ANALYSIS 210
APPENDIX E: JADX BINDING STUDIES INCLUDING BUFFERS, LC-MS/MS ANALYSIS, SPECTRAL DATA AND DOSE REPONSE BINDING CURVES 226

LIST OF FIGURES

Figure 1. Structures of the natural products streptomycin (**1**), chlortetracycline (**2**), chloramphenicol (**3**), and vancomycin (**4**). 2

Figure 2. Structures of jadomycin A (**5**) including ring labeling and jadomycin B (**6**). 4

Figure 3. (*A*) Structures of typical type I, II and III PKS derived natural products, erythromycin (**7**), pikromycin (**8**), doxorubicin (**9**), daunorubicin (**10**), tetrahydroxynaphthalene (**11**) and flaviolin (**12**); (*B*) simplified biosynthetic mechanism for the formation of the type II PKS derived doxorubicin (**9**). 6

Figure 4. Structures of benz[*a*]anthracene (left), and the benz[*a*]anthracene derived tetrangomycin (**7**) and tetrangulol (**8**). 7

Figure 5. Structures of the 2,6-dideoxysugar L-digitoxose (**24**), and the natural products tetrocarcin A (**25**) and kijanimicin (**26**) glycosylated with L-digitoxose. 14

Figure 6. Structures of four amino acids used in *S. venezuelae* ISP5230 VS1099 growths for jadomycin production: L-ornithine (**54**), D-ornithine (**55**), L-lysine (**56**) and 5-aminopenanoic acid (**57**). 20

Figure 7. HPLC traces and LC-MS/MS fragmentations of **58a**-**58f** and **58**. 25

Figure 8. Key NMR correlations for characterization of **58a**-**58f**. 28

Figure 9. Observed ^{1}H-^{1}H COSY (bold) and HMBC (solid arrows) correlations of **58.** 30

Figure 10. Structures of D-ornithine (**55**), 5-aminovaleric acid (**65**), and the structures of the analogues incorporating these amino acids, jadomycin DOct (**66**) and jadomycin AVA (**67**). 32

Figure 11. Attempted derivatization of jadomycin DOct (**66**) 33

Figure 12. Structural characterization of jadomycin AVA (**67**) 34

Figure 13. Comparative LC-MS/MS fragmentation patterns of jadomycin L-lysine, jadomycin ε-^{15}N-L-lysine, and jadomycin α-^{15}N-L-lysine 38

Figure 14. Structures of L-digitoxosyl-phenanthroviridin (**70**) and phenanthroviridin aglycone (**71**). 39

Figure 15. HPLC and LC-MS/MS analysis of **70** 40

Figure 16. Structural elucidation and comparison of **70** 41

Figure 17. Top identified compounds by COMPARE analysis for each GI_{50}, TGI and LC_{50} correlations with **70** comparing against the NCI Standard Agents Database. 45

Figure 18. Structures of compounds from the NCI synthetic compounds database (synthetic compounds and natural products of known structure) showing highest correlations to **70** for each GI_{50}, TGI and LC_{50}. 47

Figure 19. Structures of the *Streptomyces coelicolor* produced natural products undecylprodigiosin (**89**) and actinorhodin (**90**). 48

Figure 20. Genetic organization of *S. venezuelae* ISP5230 jadomycin gene cluster 50

Figure 21. Structures of the natural products azicemicin (**91**), kinamycin A (**92**), herbimycin (**93**), geldanamycin (**94**), and methylenomycin (**95**) whose biosynthetic gene clusters code for a JadX homolog. 51

Figure 22. Structure of jadomycin DS (**96**). 52

Figure 23. *S. venezuelae* ISP5230 comparative growths of wild-type and gene-disruption mutants Δ*jadX* and Δ*jadW2*. 54

Figure 24. Selective JadX-jadomycin binding by WaterLOGSY NMR 56

Figure 25. Selective JadX-chloramphenicol (**3**) binding by WaterLOGSY NMR 57

Figure 26. JadX-**96** WaterLOGSY spectra and dose response curves 60

Figure 27. JadX-**3** WaterLOGSY spectra and dose response curves 61

Figure 28. Comparing JadX-**3** binding at different pH 63

Figure 29. JadX-ligand binding by protein observed chemical shift perturbation 64

Figure 30. Absorbance plots of *S. venezuelae* ISP5230 VS1099 growths using **54**, **55** and **65** at 60 mM. 70

Figure 31. Absorbance plots of *S. venezuelae* ISP5230 VS1099 growths using **56** at 60 mM 70

Figure 32. Atom-labeled structure of compound **58a**. 79

Figure 33. Atom-labeled structure of compound **58b**. 83

Figure 34. Atom-labeled structure of compound **58c**. 87

Figure 35. Atom-labeled structure of compound **58d**. 91

Figure 36. Atom-labeled structure of compound **58e**. 94

Figure 37. Atom-labeled structure of compound **58f**. 98

Figure 38. Atom-labeled structure of compound **58**. 101

Figure 39. Deprotection of **58e**. 104

Figure 40. Atom-labeled structure of compound **67**. 105

Figure 41. TLC and HPLC analysis of **67** 108

Figure 42. LC-MS/MS fragmentation of **66** 108

Figure 43. LC-MS/MS fragmentation of **66a** 109
Figure 44. TLC and HPLC analysis of **66a**..... 110
Figure 45. Atom-labeled structure of compound **70**. 111
Figure 46. Photo-mediated DNA cleavage assay with jadomycins **58a**-**58d**..... 114
Figure 47. Copper-mediated DNA cleavage by jadomycins **58a**-**58d**. 115
Figure 48. *Streptococcus mutans* growth plates and agar well diffusion inhibition zones from jadomycins **58a**-**58d**..... 117
Figure 49. 1% agarose gel comparing cloned amplified *jadX* from *S. venezuelae* ISP5230 WT and *S. venezuelae* ISP5230 VS1085..... 121
Figure 50. SDS-PAGE gel (15%) of JadX purification 125
Figure 51. Atom-labeled structure of jadomycin DS (**96**). 127

LIST OF SCHEMES

Scheme 1. Biosynthetic formation of the decapolyketide intermediate by JadABCJMN, followed by cyclization to UWM6 (**15**) by JadDEI. 8

Scheme 2. Secondary metabolite production by *Streptomyces venezuelae* ISP5230 upon disruption of oxygenase coding genes *jadF*, *jadG* and *jadH*. 9

Scheme 3. Natural products produced upon incubation of **17** with fermentations of *Streptomyces venezuelae* ISP5230 *jadA* deletion mutant (top), S. lividans expressing *jadFGH* (middle), and incubation with JadH (bottom). 10

Scheme 4. Enzymatic conversion of **17** to the hydroquinone CR1 (**20**) catalyzed by JadH, followed by spontaneous oxidation to form **18**. 11

Scheme 5. Jadomycin PKS and post-PKS biosynthetic pathway illustrating the function of all identified structural enzymes responsible for production of **5** and divergence of the precursor related kinamycin and gilvocarcin biosynthetic pathways... 13

Scheme 6. Proposes dideoxysugar biosynthetic pathways of *S. venezuelae* ISP5230 wild type (WT) and *S. venezuelae* ISP5230 VS1080 (*jadO* disruption-mutant) producing jadomycin B (**6**) and ILEVS1080 (**34**) respectively. 15

Scheme 7. Proposed mechanism for spontaneous amino acid incorporation forming the oxazolone ring. Incorporation of L-isoleucine is used as an example. 17

Scheme 8. Examples of jadomycin structural diversity permissible through precursor directed biosynthesis and semi-synthetic derivatization. 18

Scheme 9. Possible L-ornithine incorporation into the jadomycin backbone. 21

Scheme 10. Synthesis of activated succinimidyl esters (**59**-**64**). 22

Scheme 11. Proposed interconversion of jadomycin diastereomers. 23

Scheme 12. Semi-synthetic derivatization of jadomycin Oct (**58**). 24

Scheme 13. Deprotection of **58e** as an alternative purification route to **58**..... 31

Scheme 14. Possible L-lysine incorporation into the jadomycin backbone. 36

Scheme 15. Proposed jadomycin degredation pathway forming **70**. 42

Scheme 16. Synthesis of **64**. 76

LIST OF TABLES

Table 1. Diastereomeric ratios, isolated yields and HRMS *m/z* of jadomycin amides **58a**-**58f** and **58**. 26

Table 2. Summary of NCI 60 cancer cell line screen GI_{50}, TGI, and LC_{50} values of **70**, compared to a small library of jadomycin analogues. 43

Table 3. Quantitative comparison of JadX binding. 62

Table 4. Jadomycin Oct phenoxyacetylamide (**58a**) $3a_{Mj}$ diastereomer NMR data. 80

Table 5. Jadomycin Oct phenoxyacetylamide (**58a**) $3a_{Mn}$ diastereomer NMR data. 81

Table 6. Jadomycin Oct naphthoxyacetylamide (**58b**) $3a_{Mj}$ diastereomer NMR data. 84

Table 7. Jadomycin Oct naphthoxyacetylamide (**58b**) $3a_{Mn}$ diastereomer NMR data. 85

Table 8. Jadomycin Oct benzoylamide (**58c**) $3a_{Mj}$ diastereomer NMR data. 88

Table 9. Jadomycin Oct benzoylamide (**58c**) $3a_{Mn}$ diastereomer NMR data. 89

Table 10. Jadomycin Oct nonoylamide (**58d**) $3a_{Mj}$ diastereomer NMR data. 92

Table 11. Jadomycin Oct nonoylamide (**58d**) $3a_{Mn}$ diastereomer NMR data. 93

Table 12. Jadomycin Oct Fmoc amide (**58e**) $3a_{Mj}$ diastereomer NMR data. 95

Table 13. Jadomycin Oct Fmoc amide (**58e**) $3a_{Mn}$ diastereomer NMR data. 96

Table 14. Jadomycin Oct BODIPY amide (**58f**) $3a_{Mj}$ diastereomer NMR data. 99

Table 15. Jadomycin Oct BODIPY amide (**58f**) $3a_{Mn}$ diastereomer NMR data. 100

Table 16. Jadomycin Oct (**58**) $3a_{Mj}$ diastereomer NMR data. 102

Table 17. Jadomycin Oct (**58**) $3a_{Mn}$ diastereomer NMR data. 103

Table 18. Jadomycin AVA (**67**) $3a_{Mj}$ diastereomer NMR data. 106

Table 19. Jadomycin AVA (**67**) $3a_{Mn}$ diastereomer NMR data. 107

Table 20. L-digitoxosyl-phenanthroviridin (**70**) NMR data. 112

Table 21. Agar well diffusion tabulated results for bacterial growth inhibition by jadomycins **58a-58d**. 118

Table 22. Jadomycin DS (**96**) NMR data recorded in dPBS. 128

ABSTRACT

The soil bacterium *Streptomyces venezuelae* ISP5230 has been studied extensively for its ability to produce the jadomycin family of natural products. This family of angucyclines is distinguished by a characteristic benz[*a*]anthracene scaffold, the 2,6-dideoxysugar L-digitoxose, and an amino acid that is usually fused directly into the polyaromatic backbone as an oxazolone ring. The incorporation of the amino acid proceeds through a spontaneous process, which can be exploited through precursor-directed biosynthesis by altering the nitrogen source in *Streptomyces venezuelae* ISP5230 fermentations.

Precursor-directed biosynthesis using diamino acids L-ornithine and L-lysine are described. This resulted in the successful isolation and characterization of a structurally unique eight-membered L-ornithine ring-containing jadomycin, expanding on the structural diversity permissible from this spontaneous process. This compound was further derivatized, *via* semi-synthetic methods, to furnish a small library of jadomycin amides containing a unique eight-membered heterocycle. The isolation and characterization of the jadomycin-like analogue L-digitoxosyl-phenanthroviridin is also discussed. Bioactivities of these structurally novel jadomycins were established and the structure activity relationship was explored between these compounds and the typical oxazolone-ring containing jadomycins.

In addition, the characterization of JadX, a protein of undetermined function coded for in the jadomycin biosynthetic gene cluster is reported. The ability of JadX to bind both chloramphenicol and jadomycins and affect production of these natural products is demonstrated, suggesting a role in regulation. This work suggests JadX is a new class of "atypical" response regulator involved in the cross-regulation of disparate natural products *via* an end-product-mediated control mechanism. This is the first example of characterization of these "JadX-like" proteins and could shed light onto a previously unknown group of important regulatory proteins.

LIST OF ABBREVIATIONS USED

Abs_{526}	absorbance measured at 526 nm
ACP	acyl carrier protein
ax.	axial
BODIPY	boron-dipyrromethene
bp	base pairs
br	broad
CH_3CN	acetonitrile
COSY	correlation spectroscopy
CV	column volume(s)
d	doublet
DBU	1,8-diazabicycloundec-7-ene
DCC	*N,N′*-dicyclohexylcarbodiimide
DCM	dichloromethane
DCU	1,3-dicyclohexylurea
dd	doublet of doublets
DMSO	dimethyl sulfoxide
dPBS	deuterated phosphate buffered saline
ε	extinction coefficient (when referring to absorbance)
E. coli	*Escherichia coli*
eq.	equatorial
EtBr	ethidium bromide
EtOAc	ethyl acetate
EtOH	ethanol
FAD	flavin adenine dinucleotide
FAS	fatty acid synthase
FMN	flavin-mononucleotide
Fmoc	fluorenylmethoxycarbonyl
FPLC	fast protein liquid chromatography
GI_{50}	growth inhibition of 50%

^{1}H	hydrogen
HIC	hydrophobic interaction column
HPLC	high performance liquid chromatography
HRMS	high-resolution mass spectrometry
HSQC	heteronuclear single quantum coherence
IC_{50}	lethal dose in 50% of test subjects
in vitro	performed within a controlled environment
in vivo	performed using a living systems
J	coupling constant
KS	ketosynthase
LB	Luria-Bertani Media
LC	liquid chromatography
LC_{50}	concentration resulting in 50% lethality
LRMS	low-resolution mass spectrmetry
m	multiplet
MeOH	methanol
Mj	major diastereomer
Mn	minor diastereomer
MOPS	3-(*N*-morpholino)propanesulfonic acid
MS	mass spectrometry
MS/MS	tandem mass spectrometry
MSM	mineral salts media
MYM	maltose yeast extract media
NADPH	nicotinamide adenine dinucleotide phosphate
NCI	National Cancer Institute (USA)
NDP	nucleoside diphosphate
NMR	nuclear magnetic resonance
NTA	nitrilo triacetic acid
nOe	nuclear Overhauser effect
NTF2	nuclear transport factor 2
NTP	nucleotide triphosphate

OD_{600}	optical density measured at 600 nm
ORF	open reading frame
PAGE	polyacrylamide gel electrophoresis
PBS	phosphate buffered saline
PCR	polymerase chain reaction
PDI	photo dynamic inactivation
PKS	polyketide synthase
ppm	parts per million
q	quartet
rf	radio frequency
ROESY	rotating frame nuclear Overhauser effect spectroscopy
RPM	revolutions per minute
rt	room temperature
s	singlet (when used in a table of NMR data)
SAM	*S*-adenosylmethionine
SDS	sodium dodecyl sulfate
STD	saturation transfer difference
t	triplet
TEA	triethanolamine
TGI	concentration resulting in total growth inhibition
TLC	thin layer chromatography
UV	ultraviolet
v/v	volume percent
WaterLOGSY	water-ligand observed via gradient spectroscopy
WT	wild type
w/v	weight/volume percent (grams of solute in 100 mL of solvent)
δ	chemical shift in parts per million
λ	wavelength

ACKNOWLEDGEMENTS

I would like to first and foremost acknowledge my supervisor Dr. David Jakeman for his expertise, encouragement, patience and input on these difficult projects. My thanks are extended to all group members past and present whose work in the lab has allowed my research to succeed.

I would like to express my gratitude towards my committee members Dr. Stephen Bearne, Dr. Jan Rainey, and Dr. Norm Schepp for all their discussion and help towards the project. Special thanks are extended to Dr. Ray Syvitski, Dr. Nadine Merkley and Ian Burton of the NRC in Halifax for all their help and training on the NMR. I would also like to thank Xiao Feng for his work in acquiring the high resolution mass spectrometry data.

Very special thanks also goes out to Matt (Chris) Loranger, Stephen Beaton, Jon Moulins, Steph Forget, Ben Tardiff, Francois Lefort, Gaia Aish, Camilo Martinez-Farina and the countless others whose help and friendships have been extremely important towards the success of my research. Thank you for all the good discussions and good times I have had during the course of my graduate school career.

Finally, I would like to extend my thanks to my parents Wendy and Ralph Robertson for their help and encouragement during the difficult times. As well, thanks to my sisters Christine and Stacie Robertson for putting up with me. Special thanks to my uncle James Robertson for all of his help and support throughout my schooling. As well, thanks to all my friends and family members for their loving support throughout the years.

CHAPTER 1: INTRODUCTION

1.1. Natural Products Discovery

Many of today's clinically relevant drugs used for treatment of diseases have been isolated from or have been inspired by natural sources.[1] The use of "natural products" for treatment of disease and ailments dates back thousands of years, primarily with the use of plant extracts as medicines.[2] As science and chemical techniques advanced, interest turned to isolation and characterization of the active compounds from these traditional medicines, with some of the earliest examples including salicylic acid and morphine, both of which are still used today.[2, 3] The identification of new bioactive natural products gained interest from the pharmaceutical industry after the discovery of penicillin.[4] Isolated from *Penicillium* fungi, penicillin was found to have potent antibiotic activity and low toxicity.[5, 6] As such, pharmaceutical companies and academic laboratories began compiling large libraries of microorganisms in an effort to identify new bioactive metabolites.[5] This sudden interest in microorganisms ultimately led to the discovery of several important antibiotics including: streptomycin (**1**),[7] chlortetracycline (**2**),[8] chloramphenicol (**3**)[9, 10] and vancomycin (**4**)[11] (Figure 1). These compounds were of such clinical and societal importance, Nobel Prizes in Physiology and Medicine were awarded for these discoveries, first to Fleming, Chain and Florey for penicillin in 1945, and later to Waksman for streptomycin in 1952.

Unfortunately, as time passed, problems arose associated with the re-discovery of compounds, slowing isolation and characterization of new natural products, increasing the cost for their discovery. With increasing costs and lower rate of discovery of novel molecules, interest in natural products from the pharmaceutical industry waned.[12] Despite this reduced enthusiasm for natural products as a source of new bioactive compounds, their continued importance in the medical field cannot be overstated. A 2012 review by Newman and Cragg identified that approximately 50% of all approved drugs between 1981 and 2010 were natural products, natural product derived, or synthetic compounds with a natural product pharmacophore. Furthermore, when examining anticancer therapeutic agents approved for clinical use between 1940 and 2010, this number

increases to 64%.[13] Even today, many natural products and their derivatives continue to be evaluated for their potential as therapeutic medicines.[14] With an estimated >99% of natural bacteria yet to be cultured, nature still represents a relatively untouched reservoir of potential compounds.[15]

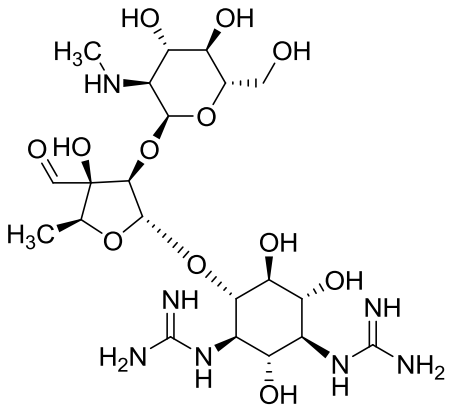

1

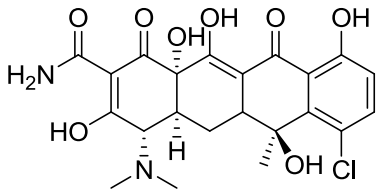

2

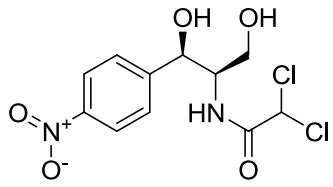

3

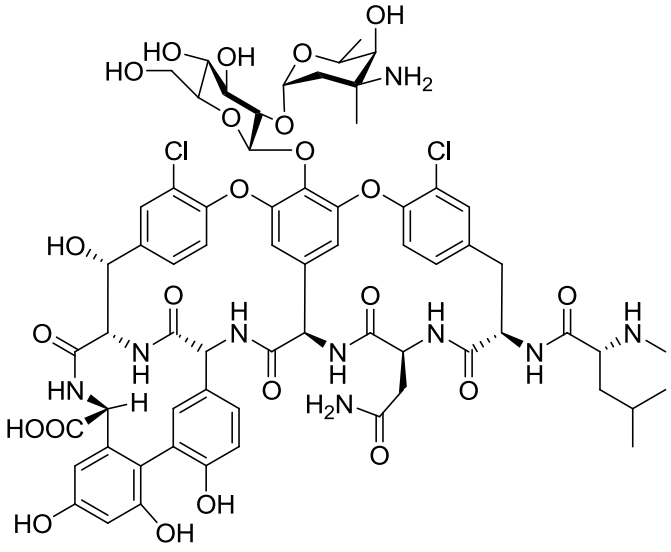

4

Figure 1. Structures of the natural products streptomycin (**1**), chlortetracycline (**2**), chloramphenicol (**3**), and vancomycin (**4**).

Of the major natural products producing organisms, the Gram-positive actinomycetes group of bacteria are among the best. Specifically, the Actinobacteria genus *Streptomyces* is one of the largest sources of bioactive natural products.[16] *Streptomyces* species are estimated to account for the production of upwards of 32% of

all identified bioactive metabolites.[17, 18] Many of these microbial natural products are classified as secondary metabolites. These compounds are not essential for cell proliferation, but, rather, are produced by the host organism often in response to physiological or environmental stress, in contrast to primary metabolites which are essential for survival and proliferation of an organism.[19] Biosynthesis of these molecules is accomplished *via* a cascade of enzymes and proteins cooperatively working together to furnish complex structures. Genes coding for these biosynthetic enzymes and proteins are often physically situated in close proximity to one another in biosynthetic gene clusters.[20, 21] Many of these biosynthetic clusters remain silent under standard culturing conditions. Only under very specific conditions will the organism activate production of these pathways, making discovery of the natural products they produce often difficult.[18] One such "cryptic" family of natural products are the jadomycins.

1.2. Jadomycin History: Initial Isolation and Structural Elucidation

The jadomycins were serendipitously discovered by Vining and coworkers while studying biosynthesis of **3** from the soil bacterium *Streptomyces venezuelae* ISP5230.[22, 23] While incubating *S. venezuelae*, an incubator malfunction resulted in overheating. Fermentations were exposed to a temperature of 37 °C overnight, effectively heat shocking the bacteria. After 24 h, cultures which were typically colourless were instead dark red. From these cultures, the first example of the jadomycin family of natural products, jadomycin A (**5**), was isolated and characterized (Figure 2).[23] Conditions for production of **5** were refined by substituting galactose (used for production of **3**) with glucose, and increasing the incubation temperature from 28 °C to 37 °C. Under these conditions, major natural product production was switched to **5**. The polyaromatic backbone of **5** suggested biosynthesis via a polyketide synthase (PKS) pathway. In addition, an L-isoleucine moiety was identified fused directly into the B-ring of the jadomycin backbone, forming a 5-membered oxazolone ring system.[23] Soon after, the glycosylated analogue jadomycin B (**6**) was isolated (Figure 2).[24] This molecule was found to contain the rare dideoxysugar L-digitoxose bound to the aglycone via an *O*-glycosidic linkage on the D-ring (Figure 2). Continued work towards the optimization of growth conditions for production of **6**, led to the discovery that in addition to heat shock,

S. venezuelae switched production from **3** to **6** upon phage infection or ethanol shock during fermentations.[25] Of these stressing conditions, ethanol treatment resulted in the highest production of **6**.[25]

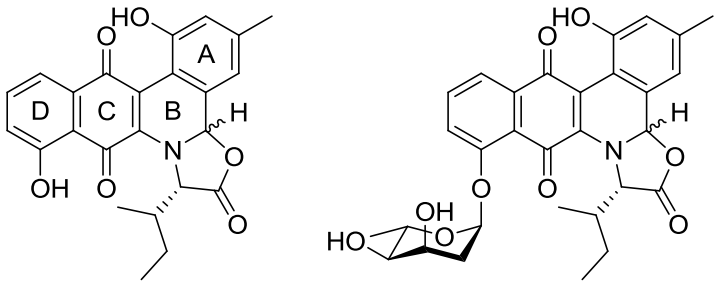

jadomycin A (**5**) jadomycin B (**6**)

Figure 2. Structures of jadomycin A (**5**) including ring labeling and jadomycin B (**6**).

1.3. Type-II Polyketide Synthases (PKS) and the Angucyclines

As previously mentioned, the actinomycetes are a large source of structurally diverse secondary metabolite natural products. Many of the compounds produced fall under the classification of polyketide natural products. Polyketides are a large family of structurally diverse compounds found throughout nature with production occurring in bacteria, fungi and plants.[26] Interest in the polyketides is mainly associated with their exceptional biological activity and potential for drug discovery, with many exhibiting antibiotic, anticancer, antifungal, anti-parasitic and even immunosuppressive activity.[26] The biosynthesis of these molecules is accomplished by a family of enzymes known as the polyketide synthases (PKSs). These enzymes act in a similar fashion to fatty acid synthases (FASs) in that they proceed via the covalent binding of a starter unit (acetyl-CoA, propionyl-CoA etc.) to an acyl carrier protein (ACP) followed by a series of elongation steps fusing units together, ultimately forming an extended chain.[27] Differential reduction, dehydration and cyclization leads to a structurally diverse group of compounds that are further derivatized, often by glycosylation or oxidation, *via* post-PKS tailoring enzymes.[28]

The PKSs are categorized into three groups: type I, type II and type III.[26] The type I PKSs are large multifunctional enzymes that act in a non-iterative fashion and are responsible for the biosynthesis of macrolides, a group of compounds containing large

lactone rings, examples include the clinically important erythromycin (**7**)[29], and the first isolated macrolide pikromycin (**8**)[30] (Figure 3*A*).

Type-II PKSs are usually complexes of multiple mono-functional proteins. The type II PKSs are only found in actinomycetes and are responsible for the production of highly cyclized, often polyaromatic natural products.[31] This is accomplished through a series of iterative condensations guided by the heterodimer ketosynthase-chain length factor (KS_α-KS_β) and an acyl carrier protein (ACP), producing a non-reduced, enzyme tethered polyketide chain (Figure 3*B*).[31] Chain extension/length of these polyketide intermediates is regulated by the KS_α-KS_β system.[31, 32] This is followed by the appropriate folding of the polyketide intermediate, again dictated by the KS_α-KS_β system, to ensure specific cyclization.[31] Finally, a series of ketoreductases, and aromatase/cyclases catalyze the ring closing, producing a fully cyclized intermediate which can then be decorated by a host of post-PKS modifying enzymes (Figure 3*B*). Some examples of type II PKS derived natural products include the clinically important doxorubicin (**9**) and daunorubicin (**10**), both currently in use as clinical chemotherapeutic agents (Figure 3*A*).[33]

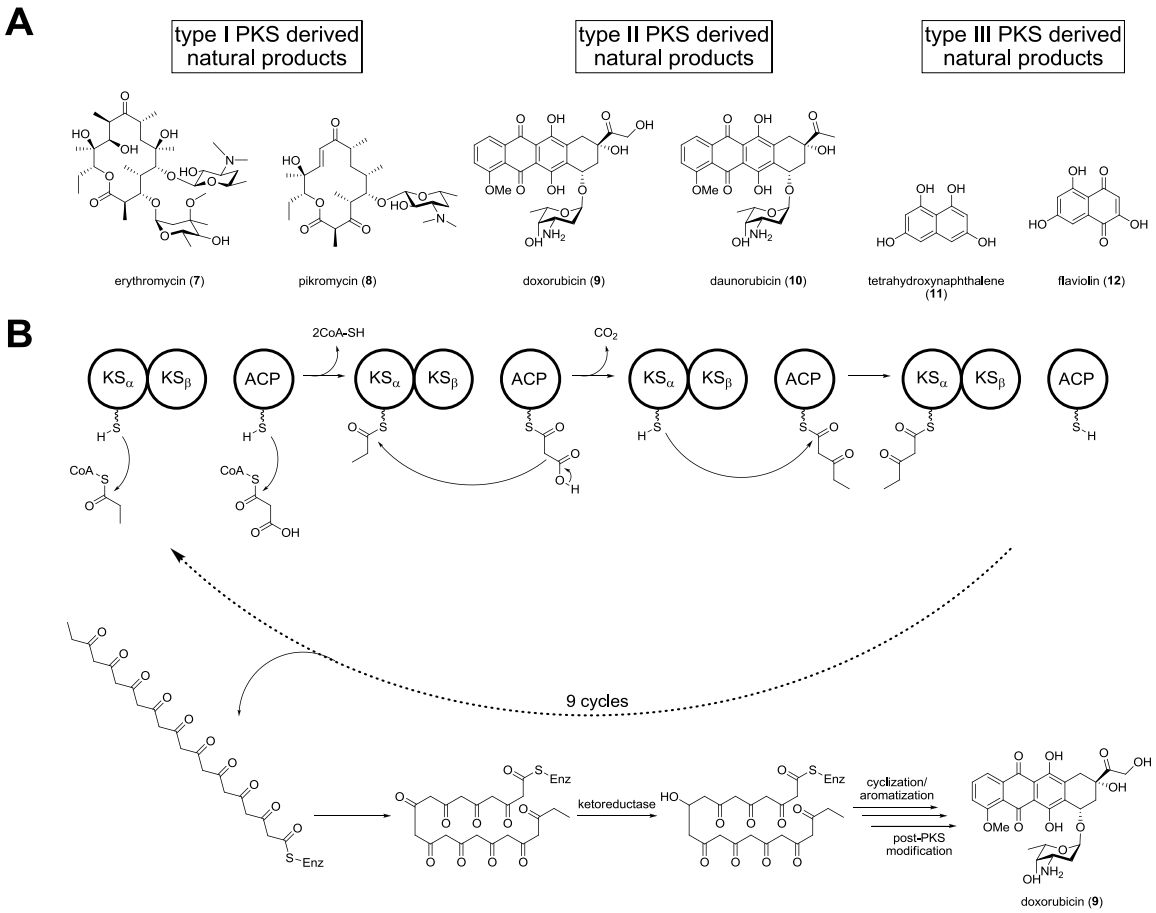

Figure 3. (*A*) Structures of typical type I, II and III PKS derived natural products, erythromycin (**7**), pikromycin (**8**), doxorubicin (**9**), daunorubicin (**10**), tetrahydroxynaphthalene (**11**) and flaviolin (**12**); (*B*) simplified biosynthetic mechanism for the formation of the type II PKS derived doxorubicin (**9**). Figure adapted from Shen.[26]

The third example of the PKSs are the type III PKSs. These are single enzymes that exist as homodimers. These dimeric systems are responsible for catalyzing initiation, elongation, and cyclization, yielding polyketide products.[34] Because of the simplicity of the homodimeric system, the type III PKS derived natural products are often not as structurally complex as those produced by the type I or type II PKSs. Examples include tetrahydroxynaphthalene (**11**) and flaviolin (**12**) (Figure 3*A*).[35]

In the case of type II PKSs, the folding of the intermediate polyketide-chain plays a large role in dictating the structure of the backbone of the final natural product. Compounds **5** and **6** structurally resemble the angucyclines, a unique group of glycosylated type II PKS derived natural products, named for the "angled" tetracyclic benz[*a*]anthracene scaffold from which they are derived (Figure 4).[36, 37] This large group

of secondary metabolites was identified in the mid-1960s with the discoveries of non-glycosylated tetrangomycin (**13**)[38] and tetrangulol (**14**)[39], and today constitutes the largest group of type II PKS derived natural products (Figure 4).[37] The structural diversity of this group arises from the configurations of polyaromatic backbone and the decoration of these scaffolds by a wide array of post-PKS tailoring enzymes, giving these compounds a wide range of bioactivities.[37] The structural similarities of **5** and **6** to the angucyclines, and ^{13}C-labeling experiments (Vining unpublished data) putatively identified the jadomycins as a group of type II PKS derived natural products.

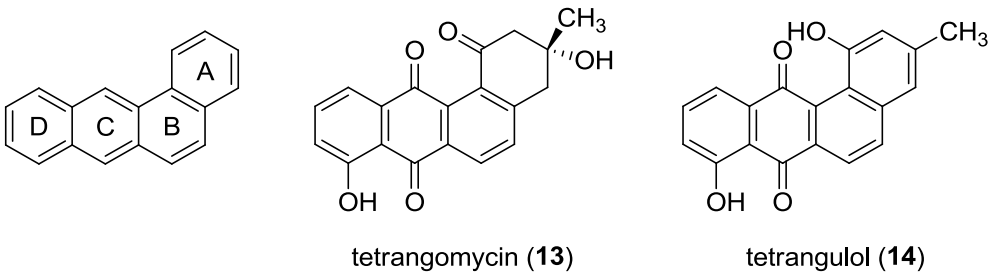

tetrangomycin (**13**) tetrangulol (**14**)

Figure 4. Structures of benz[*a*]anthracene (left), and the benz[*a*]anthracene derived tetrangomycin (**7**) and tetrangulol (**8**).

1.4. Polyketide Elongation and Cyclization

With structural similarities identified between the jadomycins and the type-II PKS derived angucyclines, Vining and coworkers began work to locate and identify the *S. venezuelae* PKS genes responsible for biosynthesis. In 1994 a gene cluster consisting of five open reading frames (ORFs) was identified.[40] Predicted amino acid sequence comparisons of the ORFs identified strong similarities to subunits of a type-II PKS system.[40] ORF1 and ORF2 (*jadA* and *jadB* respectively) were shown to likely code for the keto-synthase (KS) units, KS_α and KS_β, responsible for polyketide chain elongation and chain length determination. ORF3 (*jadC*) was identified as coding for an ACP. ORF4 (*jadD*) was putatively characterized to code for a bifunctional cyclase/dehydratase, and ORF5 (*jadE*) likely coded for a ketoreductase.[40] The discovery of *jadI* was reported soon after, and was found to be essential for cyclization of the proposed decaketide intermediate (Scheme 1). In 2000 and 2001, three more genes were identified (*jadJ*, *jadM*, and *jadN*) for their roles in initial polyketide synthesis.[41, 42] *jadJ* was identified by

sequence comparison to code for as an acyl-coenzyme A carboxylase, responsible for the carboxylation of acetyl-CoA to readily form malonyl-CoA for polyketide elongation.[41] *jadM* showed homology with a phosphopantetheinyl transferase, while *jadN* was identified as a potential acyl-CoA decarboxylase enzyme; all of which play vital roles in polyketide synthesis and chain elongation.[41] The six genes *jadABCJMN* code for the core PKS enzymes responsible for the formation of a decapolyketide intermediate, likely from one acetyl-CoA and 9 malonyl-CoA units (Scheme 1). Heterologous expression of *jadABCDEI* in *S. lividans* 1326 by Hutchinson and co-workers resulted in the isolation of the angucyclinone UWM6 (**15**) leading to belief at the time that **15** was a key intermediate in jadomycin biosynthesis.[43, 44] It was discovered later that **15** was likely not the true biosynthetic intermediate, and formed spontaneously from another jadomycin precursor in the absence of the enzymes JadFGH.[45]

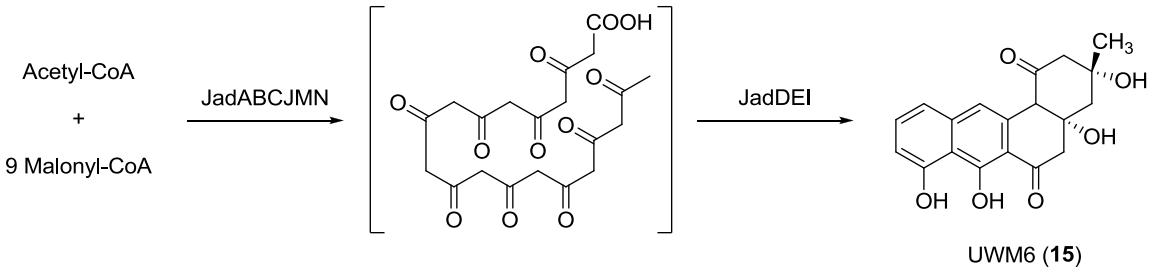

Scheme 1. Biosynthetic formation of the decapolyketide intermediate by JadABCJMN, followed by cyclization to UWM6 (**15**) by JadDEI.

1.5. JadFGH: Divergent Biosynthetic Pathways and Dead Ends

ORF6 (*jadF*), ORF7 (*jadG*) and ORF8 (*jadH*) were first reported by Vining in the late-1990s and were hypothesized to code for oxygenases, important in catalyzing post-PKS reactions to produce **5**.[46, 47] Understanding the biosynthetic mechanisms of these enzymes, and how they pertain to amino acid incorporation has been a large focus of the angucycline academic community. Initial studies identified that upon disruption of *jadF* with an apramycin-resistance gene, biosynthesis of **6** was abolished, and was accompanied by the accumulation of the previously characterized antibiotic rabelomycin (**16**) (Scheme 2).[46, 48] Compound **16** was later identified as a shunt product likely formed from a spontaneous oxidation of **15** (Scheme 2). Despite discovery of this biosynthetic

dead end, loss of jadomycin production in the absence of JadF was the first example illustrating the importance of the oxygenase enzymes for production of **5** and **6**. Following this study, Yang and Rohr published two comprehensive studies looking at the natural products profiles of *jadG*, and *jadH* disruption mutants. Disruption of *jadH* led to the production of 2,3-dehydro-UWM6 (**17**),[45] while the *jadG* disruption mutant led to the production of **16**, dehydrorabelomycin (**18**), and the glycosylated shunt product L-digitoxosyl-dehydrorabelomycin (**19**), glycosylated by the glycosyltransferase JadS (Scheme 2).[49]

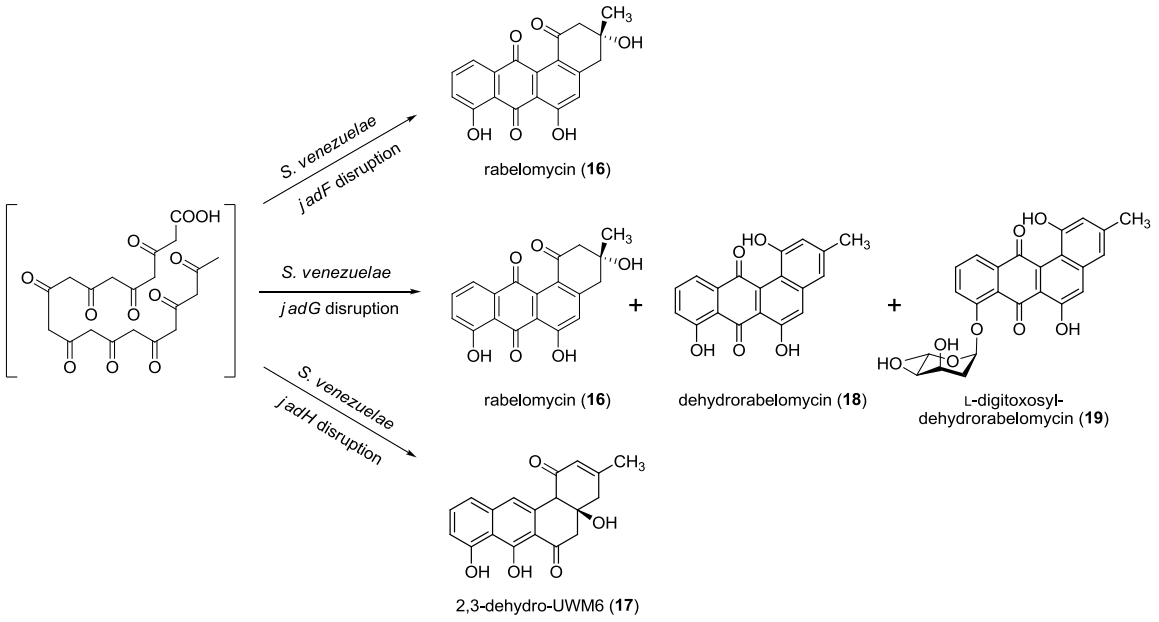

Scheme 2. Secondary metabolite production by *Streptomyces venezuelae* ISP5230 upon disruption of oxygenase coding genes *jadF*, *jadG* and *jadH*. Scheme adapted from Rix *et al*.[49]

To initiate amino acid incorporation and subsequent oxazolone ring formation, C-C bond cleavage of the B-ring of the benz[*a*]anthracene frame must first be accomplished. All products isolated from the single *jadFGH* disruption mutants contained intact B-rings, lacking amino acid incorporation, illustrating the importance of the enzymes coded for by these genes for facilitating B-ring C-C bond cleavage. The roles of these enzymes were further probed by *in vivo* and *in vitro* evaluation of compounds **15**, **16** and **17** as substrates for a series of *Streptomyces* strains and the purified enzyme JadH.[45] When **17** was incubated with a *jadA* deletion mutant of *S. venezuelae* ISP5230 lacking the ability to produce the decaketide intermediate,

production of **5** and **6** was observed (Scheme 3). This illustrated **17** was a post-PKS substrate in the jadomycin biosynthetic pathway. More interestingly, when **17** was incubated with an engineered strain of *S. lividans* expressing *jadFGH*, in the presence of L-isoleucine, conversion to **5** was observed, unequivocally demonstrating the oxygenase enzymes were responsible for the B-ring cleavage (Scheme 3). Overexpressed and purified JadH also successfully utilized **17** as a substrate, producing **18** (Scheme 3).[45]

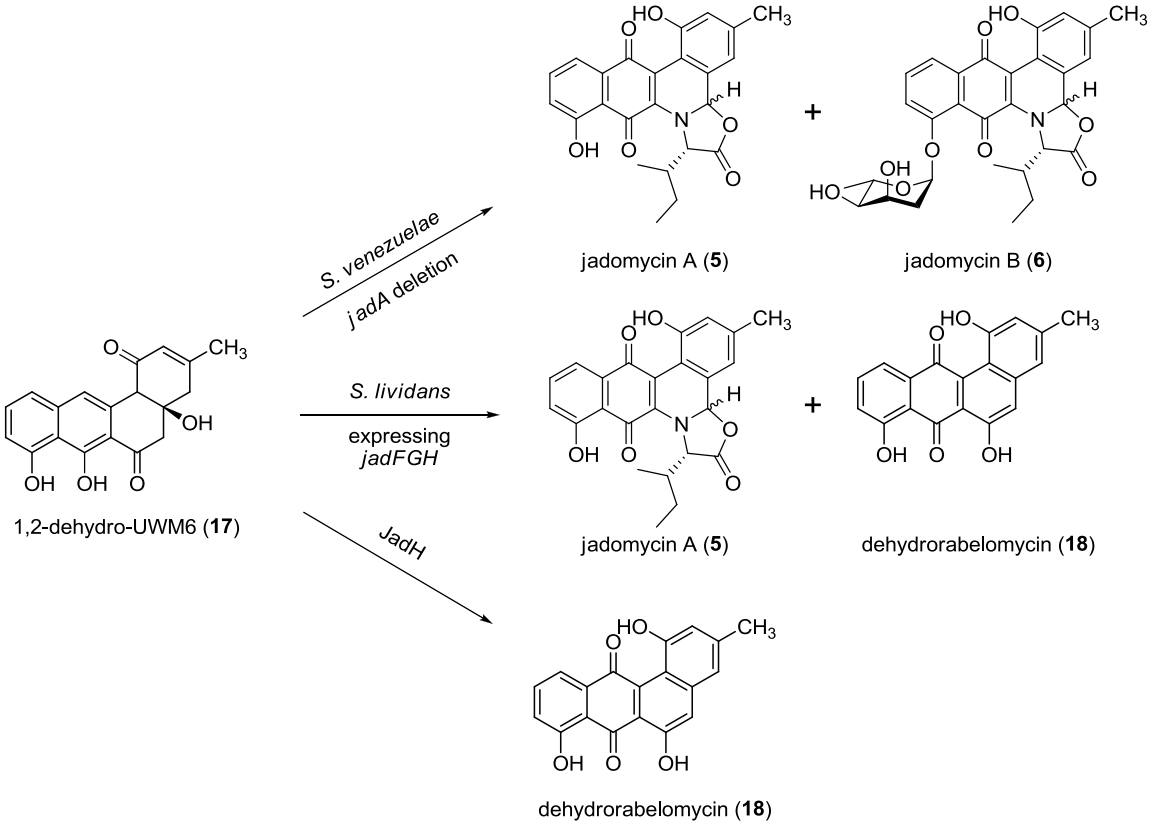

Scheme 3. Natural products produced upon incubation of **17** with fermentations of *Streptomyces venezuelae* ISP5230 *jadA* deletion mutant (top), *S. lividans* expressing *jadFGH* (middle), and incubation with JadH (bottom).[45]

A more recent re-examination of the function of JadH by Yang and coworkers identified that the enzyme was not responsible for the direct conversion of **17** to **18**, but rather, conversion of **17** to the hydroquinone intermediate CR1 (**20**) (Scheme 4). Compound **20** then undergoes spontaneous oxidation to form **18** (Scheme 4). This proved JadH was a bifunctional oxygenase-dehydrase enzyme.[45, 50]

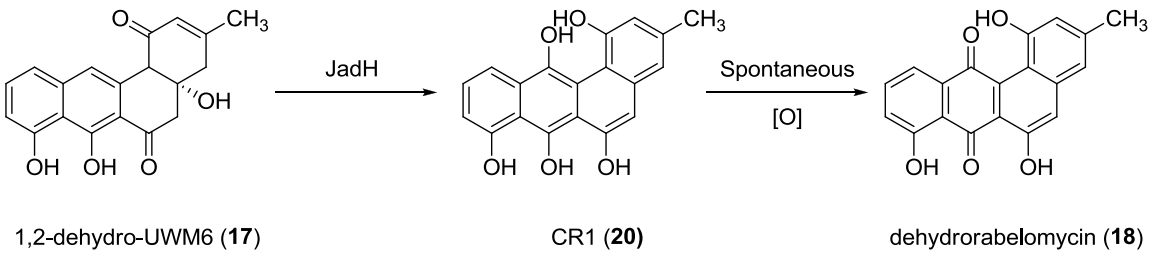

Scheme 4. Enzymatic conversion of **17** to the hydroquinone CR1 (**20**) catalyzed by JadH, followed by spontaneous oxidation to form **18**.

With JadH not directly involved in the oxidative B-ring cleavage, the potential enzymes responsible were limited to JadF or JadG. While studying the divergence of the jadomycin and the closely related gilvocarcin M (**21**) biosynthetic pathways (Scheme 5) using combinatorial biosynthetic methodologies, Rohr and coworkers showed that JadF was likely the link between the PKS and post-PKS tailoring pathways in jadomycin biosynthesis, acting as a 2,3-dehydratase responsible for hydrolysis and decarboxylation of the ACP-tethered analogue of **15** to form **17** (Scheme 5).[51, 52] This implicated the only remaining oxygenase JadG as the enzyme responsible for the C-C cleavage of the B-ring.[52, 53] Soon after the JadF finding by Rohr, two separate articles were published by Yang[53] and Rohr[54] successfully identifying JadG as the oxygenase responsible for the C-C bond cleavage. Inspired by the work of Rohr[52] illustrating the requirement of the cofactors nicotinamide adenine dinucleotide phosphate (NADPH), flavin adenine dinucleotide (FAD) and *S*-adenosylmethionine (SAM) to catalyze the full formation of **21**, Yang and coworkers identified *jadY*, an ORF in the jadomycin cluster, as responsible for coding of a flavin-mononucleotide/FAD (FMN/FAD) reductase they postulated was responsible for cofactor production for the jadomycin oxygenases. Yang went on to show upon incubation of JadY and JadG in the presence of **18**, FMN, NADH and L-isoleucine, conversion to **5** was observed (Scheme 5).[53] Although demonstrating that JadG was responsible for the B-ring cleavage, the exact mechanism of this conversion had yet to be identified. Past work by Vining and Rohr had proposed a mechanism implicating a Baeyer-Villiger-like reaction to produce a 7-membered oxepinone ring containing intermediate.[49, 55] This mechanism was confirmed upon the incubation of GilOII, the JadG homolog in the biosynthetic pathway of **21**, in the presence of **18**, together with a series of cofactors, and observing the production of the oxepinone intermediate (**22**) by high

performance liquid chromatography (HPLC) analysis (Scheme 5). The structure was confirmed by purification and subsequent nuclear magnetic resonance (NMR) spectroscopy and high-resolution mass spectrometry (HRMS) analysis.[54] It is proposed that this intermediate is cleaved by the hydrolase JadK,[47, 49] accompanied by decarboxylation, to form a reactive aldehyde intermediate (**23**). It is at this point that divergence between biosynthetic pathways producing **6**, **21** and the kinamycins is proposed (Scheme 5).[51, 54, 56] In the case of **21** and the kinamycins, a series of enzymes act on this aldehyde intermediate facilitating a structural rearrangement to furnish these atypical angucyclinones (Scheme 5). In the case of jadomycin biosynthesis, it is believed that incorporation of the amino acid proceeds spontaneously via direct interaction between the amino group and this reactive aldehyde (Scheme 5).[57] Glycosylation is then accomplished by the glycosyltransferase JadS giving the fully decorated **6** (Scheme 5).

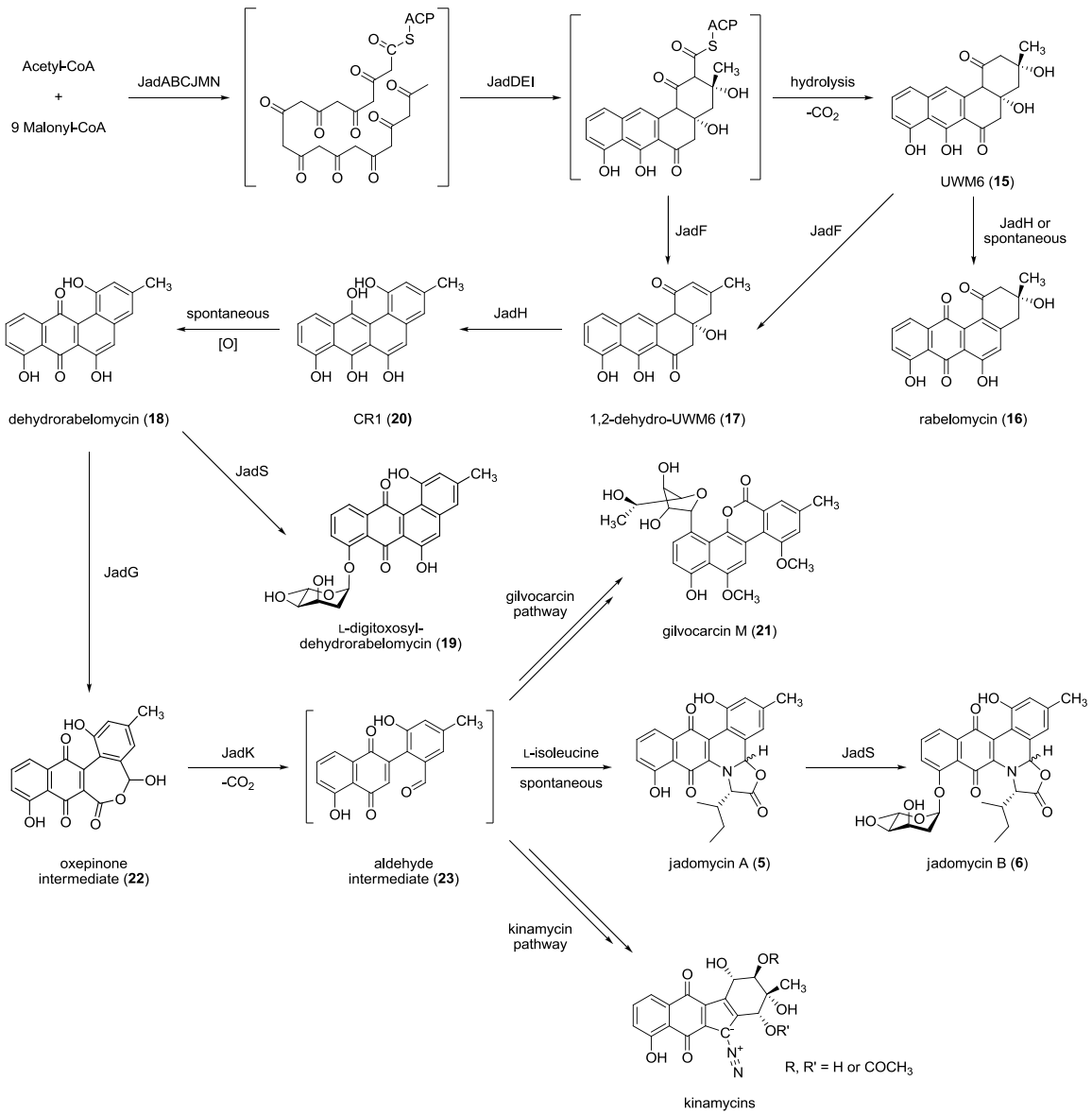

Scheme 5. Jadomycin PKS and post-PKS biosynthetic pathway illustrating the function of all identified structural enzymes responsible for production of **5** and divergence of the precursor related kinamycin and gilvocarcin biosynthetic pathways. Adapted and updated from Fan *et al*.[53]

1.6. Dideoxy Sugar Tailoring Gene Cluster

Glycosylation of natural products is widespread, and is often extremely important for the biological activity of these molecules.[58-60] As previously described, compound **6** is glycosylated with the rare 2,6-dideoxysugar L-digitoxose (**24**) at the D-ring via an *O*-glycosidic linkage (Figure 5). The 2,6-dideoxy sugars are often found within natural product steroidal glycosides, antibiotics, and antitumor compounds.[61] L-digitoxose (Figure 5) has only been reported in natural products isolated from actinomycetes[62] including the type-I PKS derived tetrocarcin A (**25**) produced by *Micromonospora chalcea* NRRL 11289[63-65] and the structurally related kijanimicin (**26**) from *Actinomadura kijaniata*, both decorated with multiple L-digitoxosyl moieties (Figure 5).[66] In the case of **6**, the JadS glycosyltransferase facilitates addition of **24**, but several enzymatic steps are required for the biosynthesis of an activated NDP-L-digitoxose substrate before this can occur.

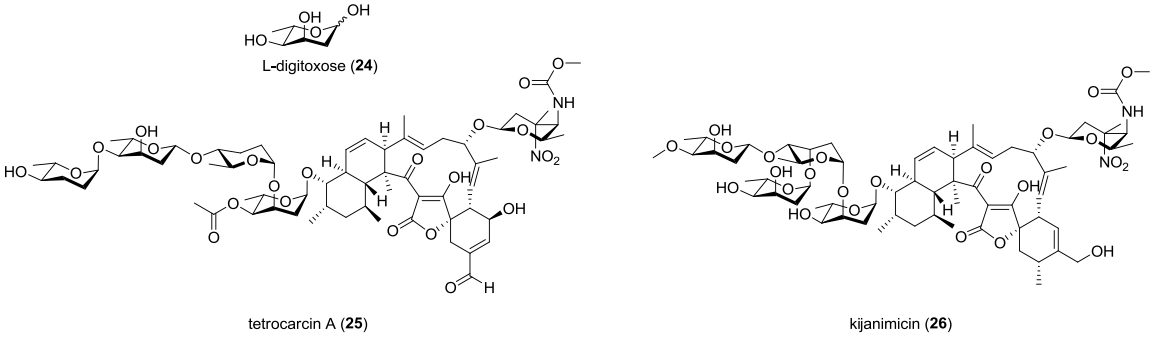

Figure 5. Structures of the 2,6-dideoxysugar L-digitoxose (**24**), and the natural products tetrocarcin A (**25**) and kijanimicin (**26**) glycosylated with L-digitoxose.

Work by Wang, White and Vining in 2004 successfully identified 8 genes (*jadXOPQSTUV*), which by sequence comparisons were found to code for a series of dideoxysugar tailoring enzymes.[67] Putative functions were assigned by sequence homology studies. A series of *S. venezuelae* ISP5230 single gene disruption mutants lacking the ability to express each of the eight enzymes were created to probe their importance for jadomycin glycosylation. The mutants were grown in the presence of L-isoleucine and the culture media was monitored for the production of both **5** and **6**. All disruption-mutants, with the exception of the *jadX* disruption-mutant, produced only **5** as the major natural product. The *jadX* disruption-mutant appeared to produce both

compounds, but at a reduced capacity compared to the wild type *S. venezuelae* ISP5230. This suggested JadX may be important for glycosylation but was not essential (*vide infra*).[67] The proposed L-digitoxose biosynthetic pathway begins with the coupling of α-D-glucose 1-phosphate (**27**) with a nucleotide triphosphate (NTP), catalyzed by nucleotidylyltransferase JadQ, to produce α-D-NDP-glucose (**28**) (Scheme 6). JadT then likely acts as a 4,6-dehydratase, removing the 6-OH and oxidizing the 4-OH position, forming the corresponding NDP-4-keto-6-deoxy-D-glucose (**29**) (Scheme 6). The dehydratase, JadO, then removes the 2-OH to form the corresponding NDP-3,4-diketo-2,6-dideoxyglucose intermediate (**30**). Compound **30** then undergoes a reduction by the ketoreductase, JadP, to form the NDP-4-keto-2,6-dideoxy-D-glucose (**31**). JadU, an epimerase, inverts the stereochemistry at C-5 to form **32**. The ketoreductase, JadV, finishes the pathway by reducing the carbonyl at C-4, forming NDP-L-digitoxose (**33**). Compound **33** is transfered to the jadomycin aglycone via the glycosyltransferase, JadS, forming the fully glycosylated compound **6** (Scheme 6).[67]

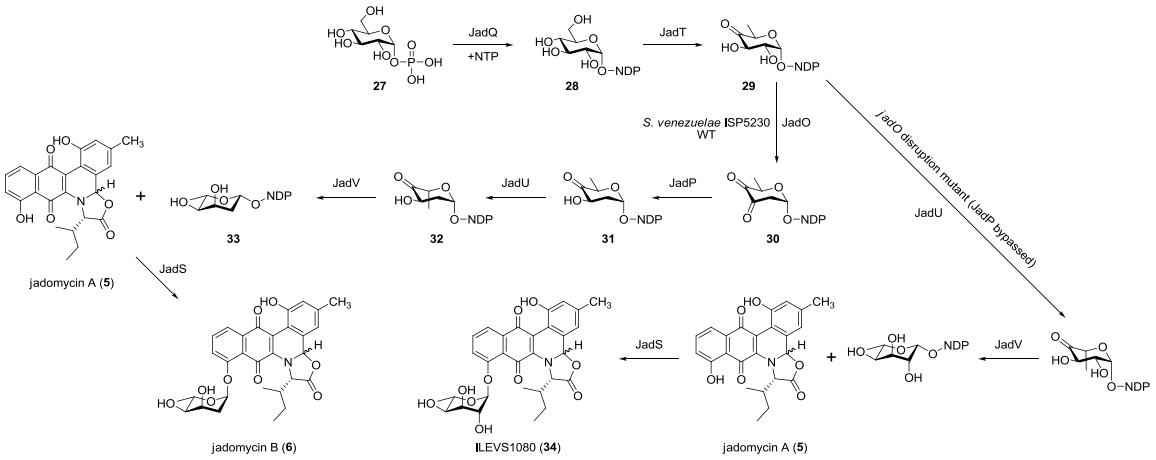

Scheme 6. Proposed dideoxysugar biosynthetic pathways of *S. venezuelae* ISP5230 wild type (WT) and *S. venezuelae* ISP5230 VS1080 (*jadO* disruption-mutant) producing jadomycin B (**6**) and ILEVS1080 (**34**) respectively.

In 2006, a study by Jakeman and coworkers[68] re-examined natural product profile of the *jadO* disruption mutant *S. venezuelae* ISP5230 VS1080[67] previously described by Vining. Using optimized conditions for improved jadomycin production,[69] *S. venezuelae* ISP5230 VS1080 was grown in the presence of L-isoleucine as the sole nitrogen source. Analysis and fractionation of the fermentation yielded the unique natural product ILEVS1080 (**34**)

glycosylated with a 6-deoxy-α-L-altropyranose moiety (Scheme 6).[69] The presence of the 2-OH group on the sugar illustrated that JadO was involved removing this hydroxyl group. Furthermore, because glycosylation of the natural product was still observed *in vivo* with the non-physiological substrate NDP-6-deoxyaltropyranose, this suggested that JadS is a promiscuous glycosyltransferase capable of accepting non-physiological substrates and incorporating them into the structure of jadomycins. Exploiting the substrate specificity of natural product glycosyltransferases is an alluring approach to structural diversification.[70]

1.7. Amino Acid Incorporation: Exploiting a Spontaneous Process

Spontaneous processes in natural product biosynthetic pathways are rare, but have been reported.[71] As previously mentioned, in the jadomycin cluster, *jadG* had been identified to code for the enzyme responsible for the B-ring opening.[51, 53] This C-C bond cleavage proceeds via a Baeyer-Villiger oxidation producing the oxepinone intermediate **22**, which is then cleaved to yield the reactive aldehyde **23** (Scheme 5).[54] Traditionally, *S. venezuelae* chloramphenicol-producing fermentations had been performed in minimal media containing a single amino acid as the sole nitrogen source.[22, 72] At the time of discovery of **5** and **6**, media was supplemented with L-isoleucine (60 mM). Isolation of **6** as the major natural product with the presence of the intact amino acid suggested the possibility of a non-enzymatic incorporation of the amino acid leading to the hypothesis that fermentations in the presence of different amino acids could lead to derivatization of the oxazolone ring.[46] The first reported use of amino acids other than L-isoleucine in jadomycin productions was by Doull, who observed differences in colour in fermentations supplemented with different amino acids, suggesting that modified derivatives of **6** may have been produced.[25] Several years later, the first isolated examples of these derivatives were characterized.[57, 73-75]

The proposed mechanism for amino acid insertion involves the spontaneous reaction of an amino acid with **23** to form an imine intermediate (Scheme 7). It is proposed that this intermediate then quickly undergoes a series of intramolecular cyclizations initiated by a Michael addition from the imine nitrogen to the quinone ring, ultimately yielding the oxazolone ring containing **5** (Scheme 7).[57]

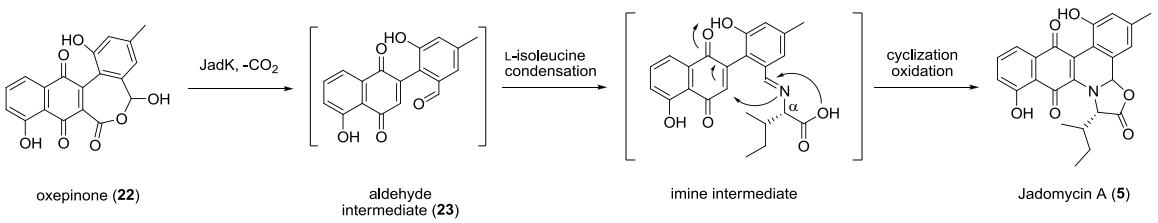

Scheme 7. Proposed mechanism for spontaneous amino acid incorporation forming the oxazolone ring. Incorporation of L-isoleucine is used as an example.

Exploitation of this unique biosynthetic step has led to the isolation and characterization of over 25 distinct jadomycin variants, containing the 5-membered oxazolone ring (**35-40**), and some analogues containing atypical cyclized rings of various sizes (**41-44**) (Scheme 8). Several of these compounds and their structures are outlined in Scheme 8.[57, 73-78] Compelling evidence for the cyclization process has also been demonstrated through the chemical synthesis of **5** by O'Doherty and later by Yu in the total syntheses of **6** and a key series of fully glycosylated jadomycins.[79, 80] Work has also been conducted on structural diversification by semi-synthetic methodologies. Jakeman and coworkers successfully produced jadomycin OPS (**45**) containing a terminal alkyne through precursor directed biosynthesis using the non-proteogenic amino acid *O*-propargyl-L-serine (Scheme 8). The alkyne functionality was then used as a chemical handle, and reacted with a series of azides to furnish a small library of jadomycin triazoles (**46-53**) (Scheme 8).[81]

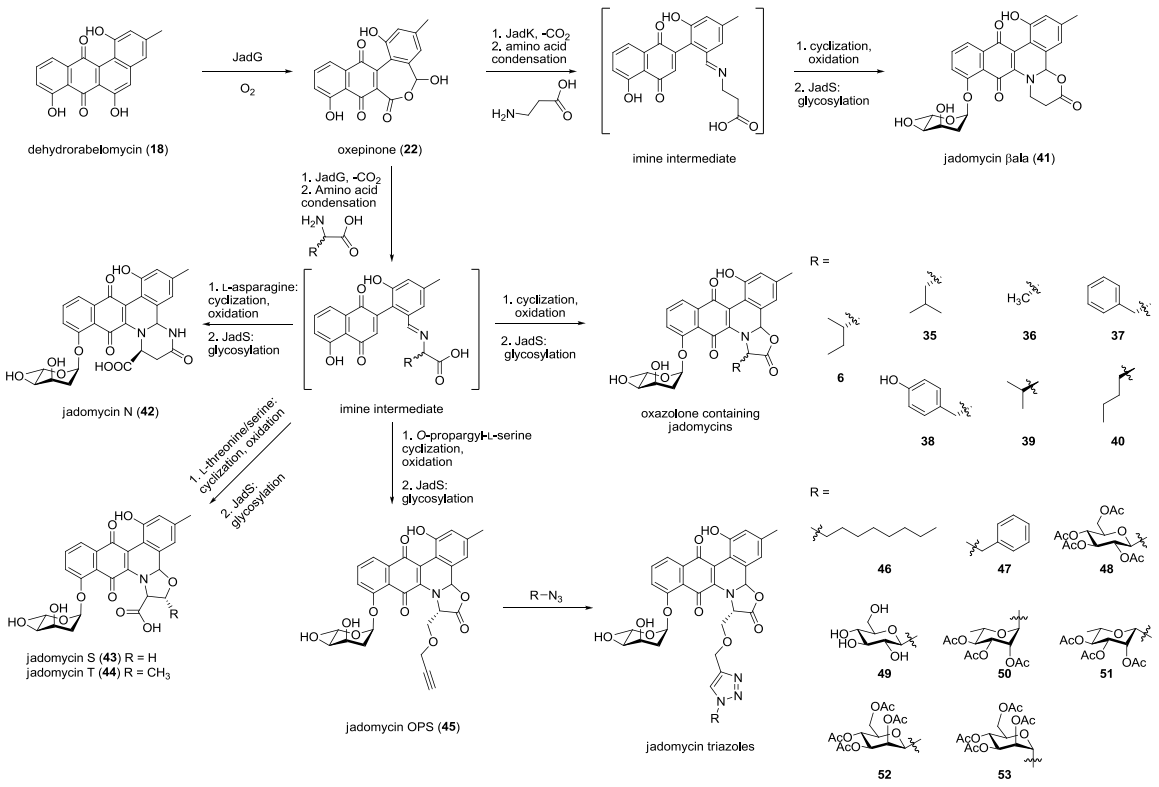

Scheme 8. Examples of jadomycin structural diversity permissible through precursor directed biosynthesis and semi-synthetic derivatization.

Like other angucyclines, the jadomycins have been shown to possess cytotoxic and antibiotic bioactivity.[77, 81-85] This bioactivity, coupled with facile methods of derivatization, has driven a continued interest in isolation and characterization of new jadomycins analogues, and the expansion and accurate mapping of the biosynthetic pathway.

1.8. Project Objectives

The aims of this thesis are two-fold: 1) expanding the jadomycin library via precursor-directed biosynthesis and developing semisynthetic methodologies for derivatization and 2) characterizing JadX, a protein of undocumented function in jadomycin biosynthesis. The steps required to accomplish these goals are presented:

Jadomycin Production

1. Investigate *S. venezuelae* ISP5230 VS1099 jadomycin biosynthesis in the presence of diamino acids (L-ornithine, D-ornithine and L-lysine).
2. Isolate and characterize natural products from these growths.

3. Determine the appropriate amino acid configuration of these molecules using NMR spectroscopy.
4. Synthesize a series of succinimidyl esters to selectively alkylate the free amine containing jadomycins to create a small library of jadomycin amide analogues.
5. Assess the biological activity of these compounds through collaboration.

JadX Studies

1. Compare the natural product profiles of a series of *S. venezuelae* ISP5230 disruption mutants, including a *jadX*-disruption mutant, to identify any potential function of JadX.
2. Clone and amplify *jadX* from *S. venezuelae* ISP5230 genomic DNA.
3. Create a pET28a(+)::*jadX* plasmid for overexpression of JadX in *E. coli*.
4. Overexpress and purify JadX for protein-ligand binding experiments.
5. Identify and quantitate binding of ligands to JadX by ligand observed NMR spectroscopic methods.
6. Overexpress and purify ^{15}N-labeled JadX.
7. Quantitate ligand binding by protein observed chemical shift perturbation methods.

CHAPTER 2: RESULTS AND DISCUSSION PART 1

2.1. Exploiting Jadomycin Biosynthesis

Excerpts of this section were taken from: Robertson, A. W.; Martinez-Farina, C. F.; Smithen, D. A.; Yin, H.; Monro, S.; Thompson, A.; McFarland, S. A.; Syvitski, R. T.; Jakeman, D. L. *J. Am. Chem. Soc.* **2015**, *DOI: 10.1021/ja5114672*.[86] All work presented here, with the exception of the biological activities was performed by the first author, Andrew W. Robertson.

The isolation of new scaffolds and the generation of diverse libraries remains one of the major goals associated with natural products research in an effort to identify unique or enhanced bioactivity for clinical treatment of disease. As mentioned previously, JadG has been identified as the enzyme responsible for the B-ring opening in the jadomycin biosynthetic pathway.[51, 53] The C-C cleavage proceeds via a Baeyer-Villiger oxidation producing a reactive aldehyde that couples in a non-enzymatic fashion to a singular amino acid in the culture media, forming an imine intermediate that cyclizes into the jadomycin backbone (Scheme 7).[57, 77, 78, 81, 82] If this biosynthetic step could be exploited to react with an amine other than the α-amine of an amino acid, it could yield a unique opportunity to expand the structural diversity of these natural products. One group of amino acids that had yet to be studied were the diamino acids. These were of particular interest as we hypothesized that either amino group could act as a nucleophile forming imine intermediates, and potentially undergo spontaneous cyclization with the free carboxylic acid forming either the typical five-membered oxazolone ring, or a new class of large heterocyclic ring containing jadomycins. A small group of diamino acids including L-ornithine (**54**), D-ornithine (**55**) and L-lysine (**56**) was selected for testing in jadomycin precursor directed fermentations (Figure 6).

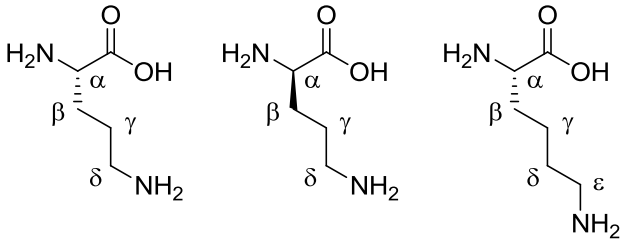

Figure 6. Structures of four amino acids used in *S. venezuelae* ISP5230 VS1099 growths for jadomycin production: L-ornithine (**54**), D-ornithine (**55**), and L-lysine (**56**).

L-Ornithine was the first of the amino acids tested. Since it contains both α- and δ- amino groups, we hypothesized that either could act as a nucleophile, forming either a five-membered (jadomycin Orn, **57**), or eight-membered (jadomycin Oct, **58**) heterocyclic ring (Scheme 9). Initial cultures of *S. venezuelae* ISP5230 VS1099 were, therefore, grown with L-ornithine (as outline in Chapter 4.2.) as the sole nitrogen source and the characterization of the major structural isomer commenced.

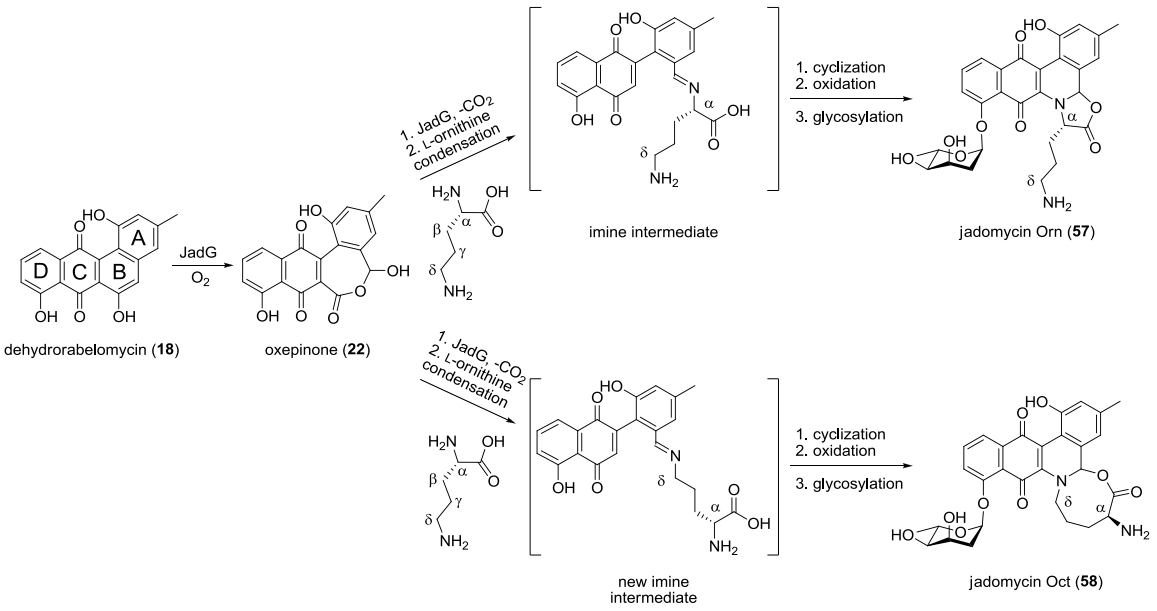

Scheme 9. Possible L-ornithine incorporation into the jadomycin backbone.

2.1.1. Derivatization of Jadomycin Oct

Purification of the jadomycin proved difficult with significant breakdown occurring during workup. Similar stability issues were experienced during the purification of jadomycin OPS (**45**) by Jakeman and coworkers, who opted to treat crude extracts of **45** with excess azide-analogues to derivatize the compound in an effort to improve stability and improve yields.[81] Insufficient isolable yields of **57** or **58** and the instability of the material necessitated derivatization of crude extracts for in depth structural characterization purposes. With a reactive handle present, chemo-selective derivatization of the free amino-functionality using *N*-hydroxy succinimide activated carboxylic acids was chosen to create a small library of jadomycin amides. Growths of *S. venezuelae* ISP5230 VS1099 in the presence of L-ornithine (60 mM) as the sole nitrogen source[69]

were extracted using reversed-phased Si-phenyl columns and H_2O:EtOAc extractions (as outlined in Chapter 4.2.2.) to yield ~100 mgL^{-1} crude extract used for all derivatizations.

Bioconjugation techniques using succinimidyl esters are well established in the literature, primarily for biolabeling of proteins,[87] and allow for very selective amine reactivity under mild conditions.[87] As such, a series of activated succinimidyl esters **59-64** were purchased or prepared *via* coupling of *N*-hydroxysuccinimide to the corresponding carboxylic acid or acid chloride using modified literature precedent[88-91] in order to protect the free amine of the incorporated L-ornithine (Scheme 10).

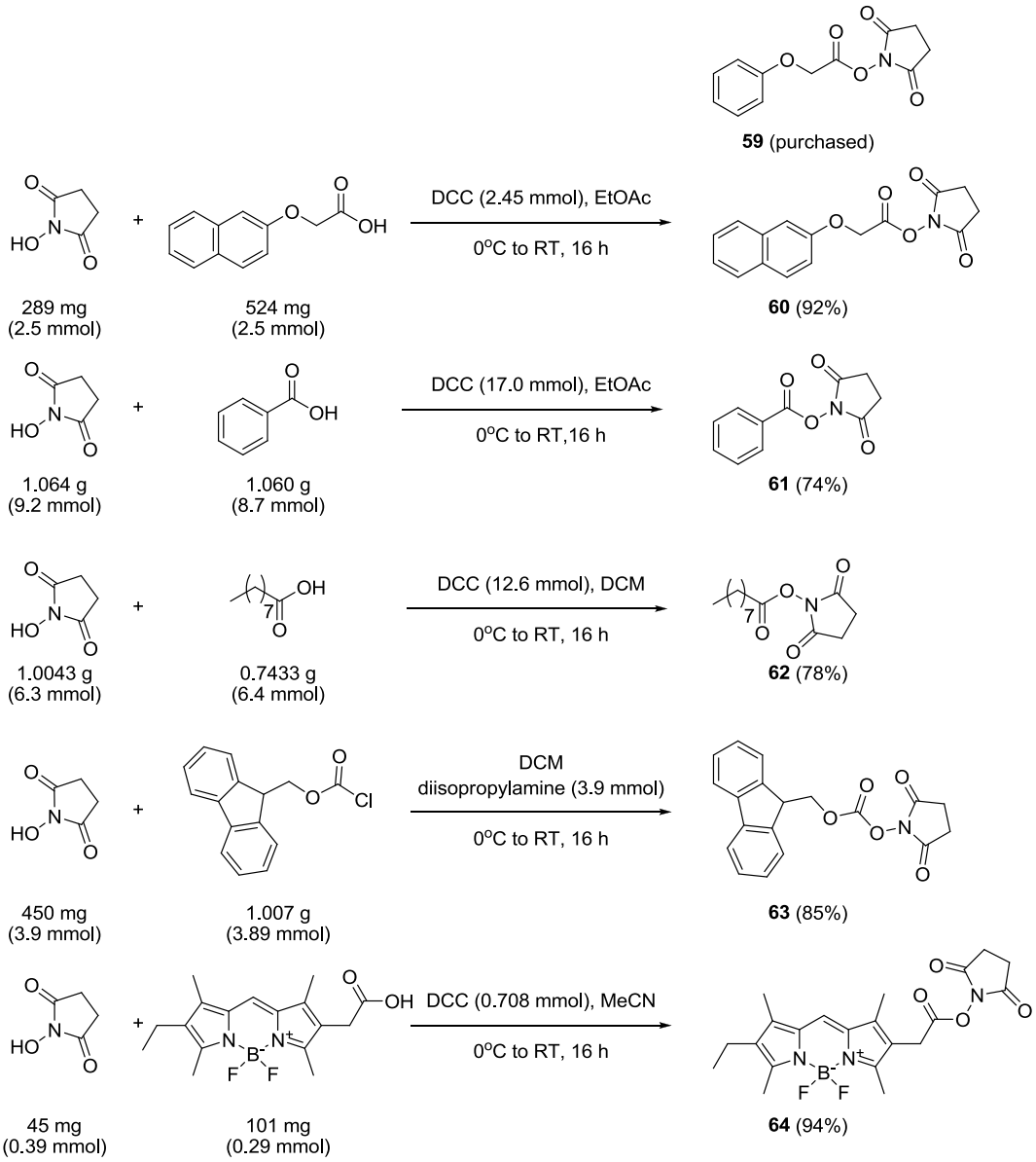

Scheme 10. Synthesis of activated succinimidyl esters (**59-64**).

Solvent selection proved very important for the coupling reactions. The crude growth extract was found to be water soluble with little to no solubility in most organic solvents (with the exception of methanol), whereas succinimidyl esters **59-64** were mainly soluble in organic solvents with little to no water solubility. It has been shown that aprotic organic solvents in the presence of a basic buffer can be effective in facilitating reactions involving succinimidyl esters,[92] and that as the pH is increased amine reactivity also increases.[93] Unfortunately, under basic conditions, jadomycins have been shown to undergo a ring opening event producing an aldehyde intermediate (Scheme 11). Many jadomycins exist as a mixture of two diastereomers in a dynamic equilibrium as a result of this ring opening event.[94] It was believed that this intermediate could potentially react with the free amine of L-ornithine forming undesired imine side products.[94]

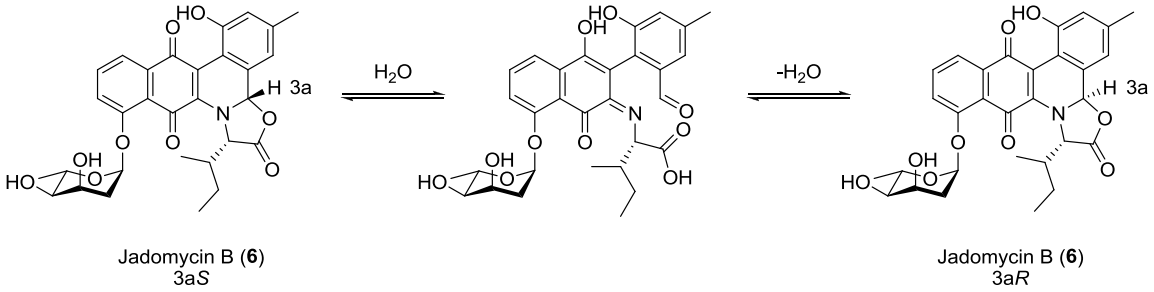

Scheme 11. Proposed interconversion of jadomycin diastereomers. Scheme adapted from Syvitski *et al*.[94]

To prevent this, a near physiological pH was selected. It was found that a 1:1 mixture of CH_3CN and phosphate buffered saline (PBS, pH 7.6) allowed for the best solubility and stability of both the crude extract and the activated acids. Crude extracts (~100 mg) were treated with excess succinimidyl esters for 3-6 h at room temperature (Scheme 12), and the reaction progress was monitored using TLC and (Chapter 4.4). Production of the desired mono-derivatized compounds was confirmed by analysis of the reaction mixtures using liquid chromatography-tandem mass spectrometry (LC-MS/MS), showing the characteristic jadomycin fragmentation patterns in each case (Figure 7*B*).

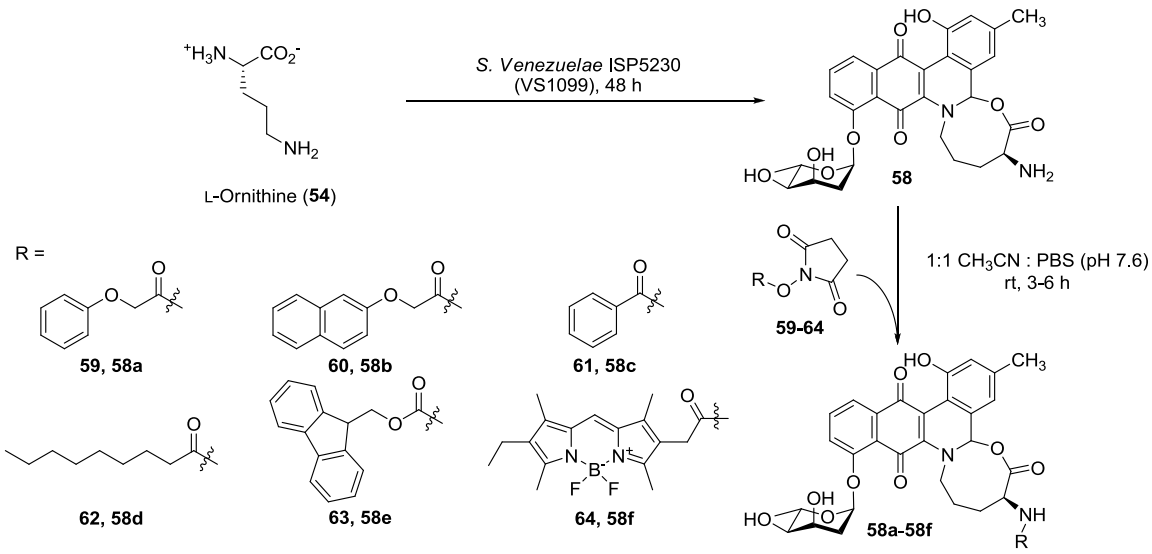

Scheme 12. Semi-synthetic derivatization of jadomycin Oct (**58**).

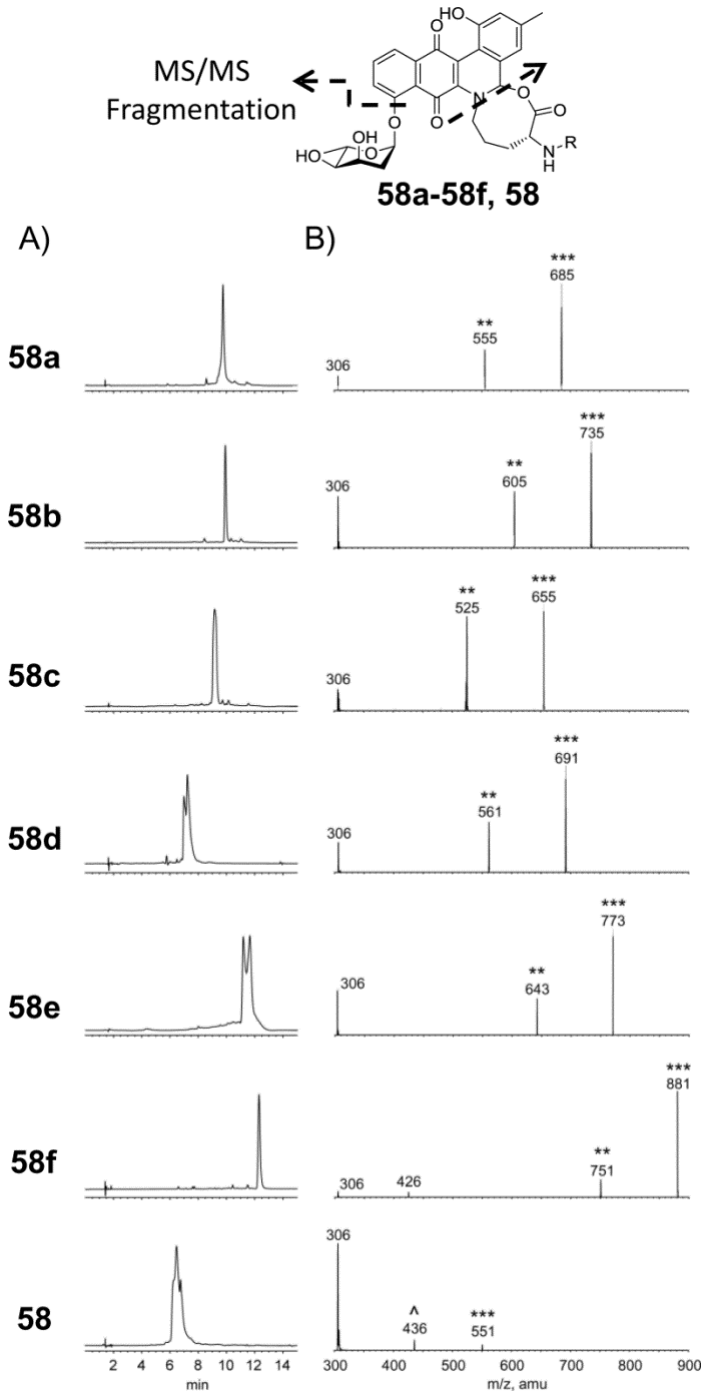

Figure 7. HPLC traces and LC-MS/MS fragmentations of **58a**-**58f** and **58**. (*A*) HPLC traces of **58a**-**58f** and **58**. Compound **58d** required alternative HPLC conditions (see Chapter 4.1.2.). Diastereomers are readily observed for **58d** and **58e** by HPLC; (*B*) LC-MS/MS fragmentation of **58a**-**58f** and **58**, illustrating $[M+H]^+$ (***), cleavage of the sugar $[M + H – digitoxose]^+$ (**) and the amino acid groups $[M + H – digitoxose – R]^+$ (*m*/*z* 306). Compound **58** showed loss of amino acid group first $[M+H–R]^+$ (^).

Compounds **58a-58f,** with the exception of **58e,** proved more stable compared to **58**, and thus were more amenable to purification. Isolated yields of the derivatives ranged from 1.5-14 mgL^{-1} (Table 1). Compounds **58a-58f** were isolated using liquid-liquid extractions and solid-phase methodologies (as outlined in Chapter 4.4.) as dark purple or red solids consisting of two diastereomers by NMR, in a ratio of ~5:4 in all cases (Table 1). High-resolution mass spectrometry (HRMS) analysis of the purified compounds confirmed the presence of the appropriate *m/z* for each analogue (Table 1).

Table 1. Diastereomeric ratios, isolated yields and HRMS *m/z* of jadomycin amides **58a-58f** and **58**.

Compound	Mj : Mn[a]	Yield (mgL^{-1})	HRMS Found[b]	HRMS Expected
58a	100 : 80	14	685.2383	685.2392
58b	100 : 74	11	735.2517	735.2548
58c	100 : 81	13	707.2202[c]	707.2211
58d	100 : 81	9	691.3194	691.3225
58e	100 : 75	1.5	803.2838[d]	803.2821
58f	100 : 70	12	881.3698	881.3739
58	100 : 82	1.5	573.1834[e]	573.1844

[a]Ratios of diastereomers [major diastereomer (Mj), minor diastereomer (Mn)] were determined by ^{1}H-NMR integrations; [b]all HRMS *m/z* values reported are $[M + H]^+$ unless otherwise stated; [c]*m/z* of **58c** corresponds to $[M + Na]^+$; [d]*m/z* of **58e** corresponds to $[M + MeOH - H]^-$; [e]*m/z* of **58** corresponds to $[M + Na]^+$.

2.1.2. Structural Characterization of 58a-58f

In order to identify the major structural isomer as either an eight-membered or five-membered ring system, characterization of derivatives **58a-58f** was carried out using NMR spectroscopy. ^{1}H-NMR spectra and ^{1}H-^{1}H COSY analysis of **58a-58f** identified the expected jadomycin spin systems (C4 to C6, C9 to C11, and C1″ to C5″-CH_3) associated with the intact A, D, and sugar rings respectively (Figure 8). HMBC correlation between the anomeric H1″ (δ_H = ~6 ppm) and C12 (δ_C = ~155 ppm) confirmed glycosylation at the 12-position of the D-ring. HMBC correlations between the protons of the A and D rings

identified the intact C-ring quinone and the appropriate connectivity of the polyaromatic backbone (Figure 8). The ^{1}H-^{1}H COSY experiment also successfully identified the C1 to C3′ spin system of the incorporated L-ornithine (Figure 8); an edited-HSQC was analyzed to assign the L-ornithine methylene linkers. The ^{1}H-NMR spectra were confounded by two sets of signals, each from an individual diastereomer associated with the different stereochemistry at the 3a position (Figure 8). The H1′- H3′ protons were particularly challenging to identify since they were found to be diastereotopic leading to four signals for each methylene group, denoted either as $H1'_{Mj}$-$H3'_{Mj}$ for the major diastereomer, or as $H1'_{Mn}$-$H3'_{Mn}$ for the minor diastereomer. This spectral property turned out to be paramount in the characterization of the major structural isomer.

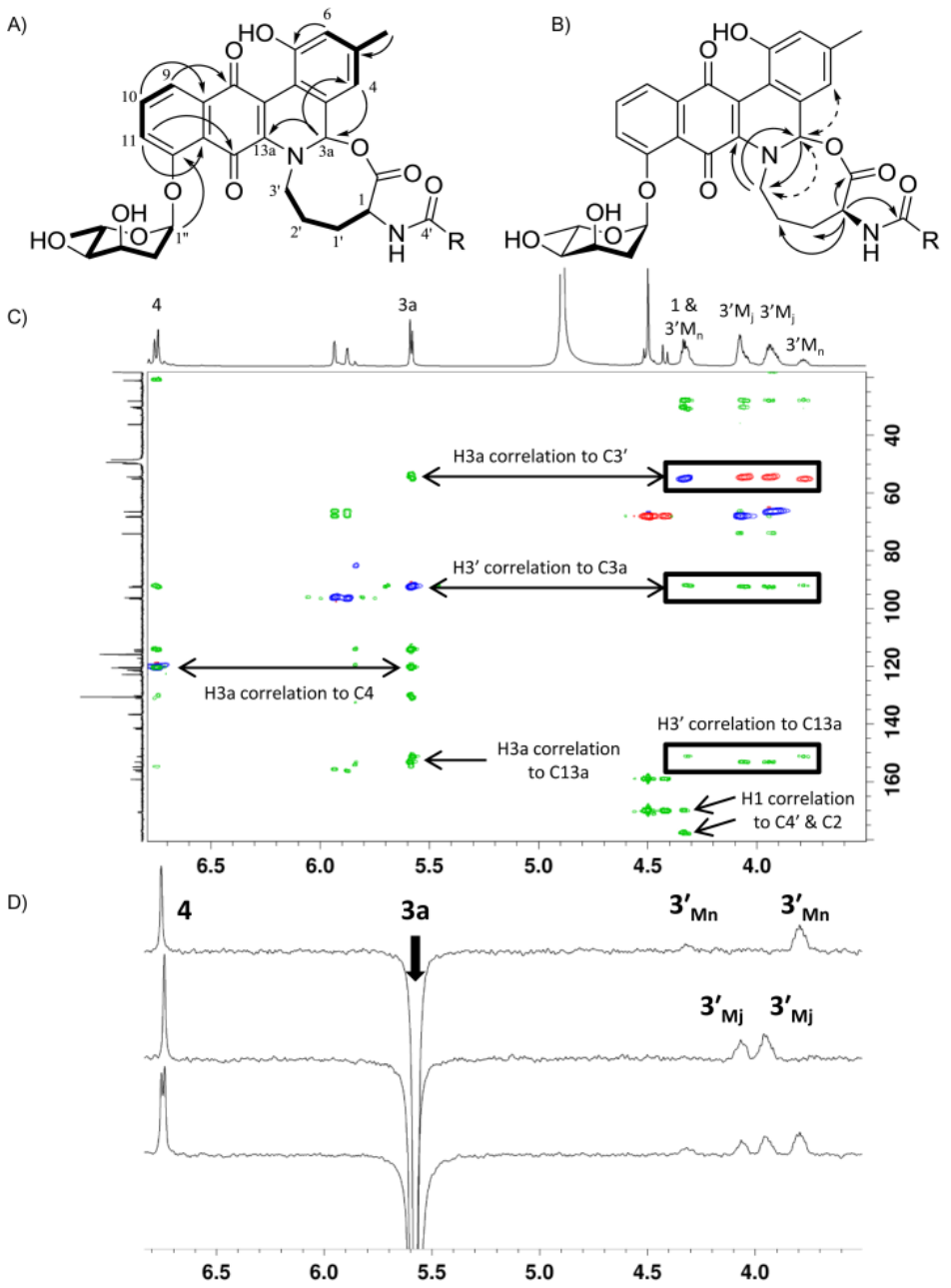

Figure 8. Key NMR correlations for characterization of **58a**-**58f**. (*A*) Observed ^{1}H-^{1}H COSY (bold) and HMBC (solid arrows) correlations of compounds **58a**-**58f** illustrating intact A, B, C, D, and sugar rings; (*B*) observed HMBC (solid arrows) and ROESY (dashed arrows) correlations of **58a**-**58f** identifying the configuration of the incorporated L-ornithine; (*C*) overlaid edited-HSQC and HMBC spectra of **58a**. Edited-HSQC data is represented in blue (-CH- or -CH_3) and red (-CH_2-), and HMBC correlations are represented in green (^{2}J-^{4}J coupling); (*D*) selective ROESY spectra of **58a**, selectively irradiating H3a of the minor diastereomer (top), H3a of the major diastereomer (middle) and both simultaneously (bottom).

The edited-HSQC gave ^{1}J ^{1}H-^{13}C correlations, and also provided multiplicity information in which -CH- and -CH_3 groups are phased opposite to -CH_2- groups. This data alongside the ^{1}H-^{1}H COSY experiment, allowed for identification of the appropriate ^{1}H-^{1}H geminal coupling and ^{3}J coupling of the C1 to C3′ spin system, allowing assignment of the connectivity within the L-ornithine side chain. ^{1}H-NMR spectra and ^{1}H-^{1}H COSY analyses of **58a-58f** identified the appropriate signals and spin systems associated with the presence of each R functionality. The ^{1}H-NMR (integration) and HSQC (phasing) identified H3a as a -CH- group. The ^{1}H-^{1}H COSY also showed the H3a in its own spin system with no coupling to adjacent protons, consistent with other jadomycins at the 3a position. The ^{13}C-NMR chemical shifts of the C3a atoms were within the typical range for most jadomycins (δ_C ~ 90-96 ppm, in MeOD-d_4) in which the 3a position is surrounded by nitrogen, an aromatic ring carbon, and an oxygen atom. The masses identified by HRMS were also consistent with cyclized products. The HMBC experiments enabled us to assign the connectivity of L-ornithine within the structures. HMBC correlations, in all cases, were observed from H3a to C3′ (Figure 8*C*). If the configurations of **58a-58f** contained five-membered oxazolone rings then the observed HMBC correlations between H3a and C3′ would represent unlikely ^{6}J couplings. In contrast, these correlations would represent much more likely ^{3}J couplings within eight-membered heterocycles. The H3′ protons, in all cases, also showed HMBC correlations back to C3a as well as C13a of the quinone ring system, identifying the close through bond proximity of the 3′ position to the B ring. These correlations were readily identified as all four H3′ signals showed these correlations (Figure 8). It is important to note in the presented HSQC spectrum (Figure 8), the absence of a ^{1}J ^{1}H-^{13}C correlation (red) corresponding to one of the H3′$_{Mn}$ protons at ~4.35 ppm. This is due to coincidental overlap of the ^{1}H-^{13}C correlations associated with the 1 and 3′$_{Mn}$ positions. In the edited-HSQC these two signals phase oppositely, with the more intense signal, in this case the -CH- phased positively (blue), phasing out the less intense ^{1}H-^{13}C correlation associated with the -CH_2- of the 3′$_{Mn}$ position.

The unique diastereotopic nature of the 3′ position also aided in ROESY analysis. Selective ROESY spectra identified rOe correlations between the H3a and H3′ further substantiating the structures as the eight-membered ring containing configuration (Figure

8*D*). ROESY experiments were also performed irradiating each of the $H3a_{Mj}$ or $H3a_{Mn}$ separately. Correlations were observed between the appropriate H4 and H3′ of the major and minor diastereomers. The rOe correlations of $H3a_{Mj}$ to the $H3'_{Mj}$ protons were of approximate equal intensity suggesting a similar distance through space between the protons. The rOe correlations of $H3a_{Mn}$ to the $H3'_{Mn}$ protons showed different intensities also suggesting differences in the 3a stereochemistry between the major and minor diastereomers. As a final confirmation of the structure, HMBC correlations between H1 and C4′ of the amide side chain (^3J) were observed indicating selective coupling of the α-amino group of L-ornithine to the succinimidyl esters confirming the proposed eight-membered ring configuration (Figure 8*C*).

2.1.3. Characterization of 58

With the structural characterization of **58a**-**58f** confirmed, investigation shifted back to the isolation and characterization of **58** to ensure that the L-ornithine configuration was conserved through the chemo-selective derivatization. Compound **58** was produced and isolated using liquid-liquid extractions and solid phase methodologies in a time-sensitive manner (as outlined in Chapter 4.4.7.) yielding a dark purple solid (1.5 mgL^{-1}), consisting of a mixture of two diastereomers in a ratio of 100:82. The diastereomeric ratios of **58a**-**58f** were consistent with **58**, suggesting reaction conditions did not facilitate ring opening. LC-MS/MS and HRMS data identified the appropriate fragmentation pattern and *m/z* expected for **58** (Figure 7 and Table 1). Structural characterization by NMR analysis showed many of the same correlations as **58a**-**58f**, excluding the chemo-selectively derivatized groups (Chapter 4.4.7.), confirming **58** as an eight-membered heterocyclic ring containing jadomycin (Figure 9).

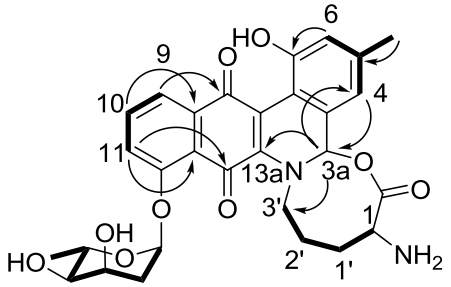

58

Figure 9. Observed ^1H-^1H COSY (bold) and HMBC (arrows) correlations of **58.**

Concurrently with our investigation, Yang and co-workers described the growth and isolation of a natural product from *S. venezuelae* ISP5230 growths with L-ornithine.[78] They proposed the five-membered oxazolone ring containing structure **57** in contrast to our eight-membered derivative, although NMR data were incomplete making comparison to our material impossible.[78] Interestingly, in our hands, **58** was identified as the major product in the growth media, with no direct evidence of **57**.[78] The isolation of **58** may provide insight into the substrate specificity of the glycosyltransferase, JadS, involved in jadomycin biosynthesis. If glycosylation occurs after amino acid incorporation, it illustrates that JadS is able to accommodate structural divergence of the glycosyl-acceptor beyond the hydroxy-quinone functionality, not only accepting five-membered ring-containing oxazolones,[76] but also eight-membered ring containing derivatives.

2.1.4. Deprotection of 58e

As a potential method for enhanced isolation and purification of **58**, a removable fluorenylmethyloxycarbonyl (Fmoc) protecting group was introduced in the case of **58e**. We had anticipated **58e** would prove more stable compared to **58** allowing for easier purification in higher yields. Counterintuitively, the stability of **58e** was poor and purification was challenging with a great deal of material degrading during this process (Chapter 4.4.5.). Nevertheless, **58e** was treated with 1,8-diazabicycloundec-7-ene (DBU) and SiliaBond® Piperazine in a buffered organic solvent system (Scheme 13). This was followed by workup providing **58** (1.3 mg, 61% yield). The identity of **58** was confirmed by HPLC, LC-MS/MS, TLC and ^{1}H-NMR.

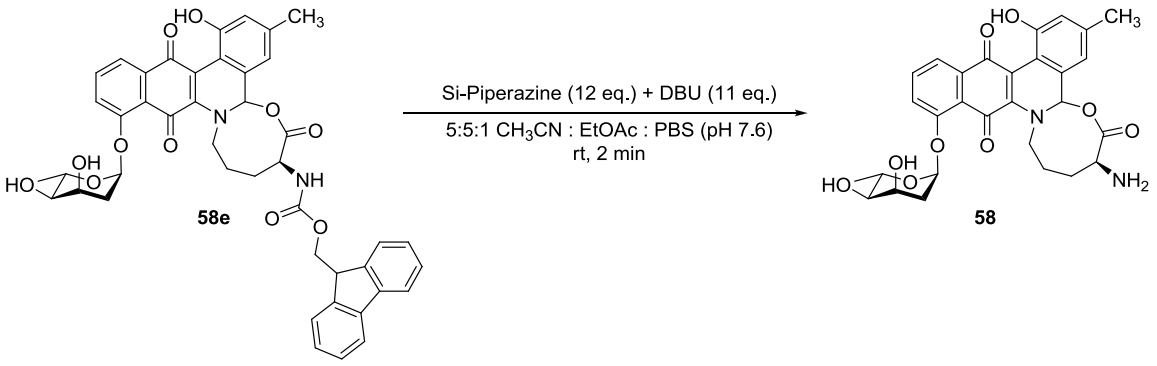

Scheme 13. Deprotection of **58e** as an alternative purification route to **58**.

2.2. Probing Structural Diversity

To expand the scope of this study, and isolate new eight-membered ring containing jadomycins, *S. venezuelae* ISP5230 VS1099 was grown in the presence of either **55** (60 mM) or 5-aminovaleric acid (**65**) (60 mM). Based on the results obtained with L-ornithine, incorporation of D-ornithine was also predicted to produce the eight-membered ring containing compound jadomycin DOct (**66**) (Figure 10). Likewise, given that **65** only has a δ-amino group, incorporation into the jadomycin backbone was anticipated to produce the eight-membered ring containing derivative, jadomycin AVA (**67**) (Figure 10).

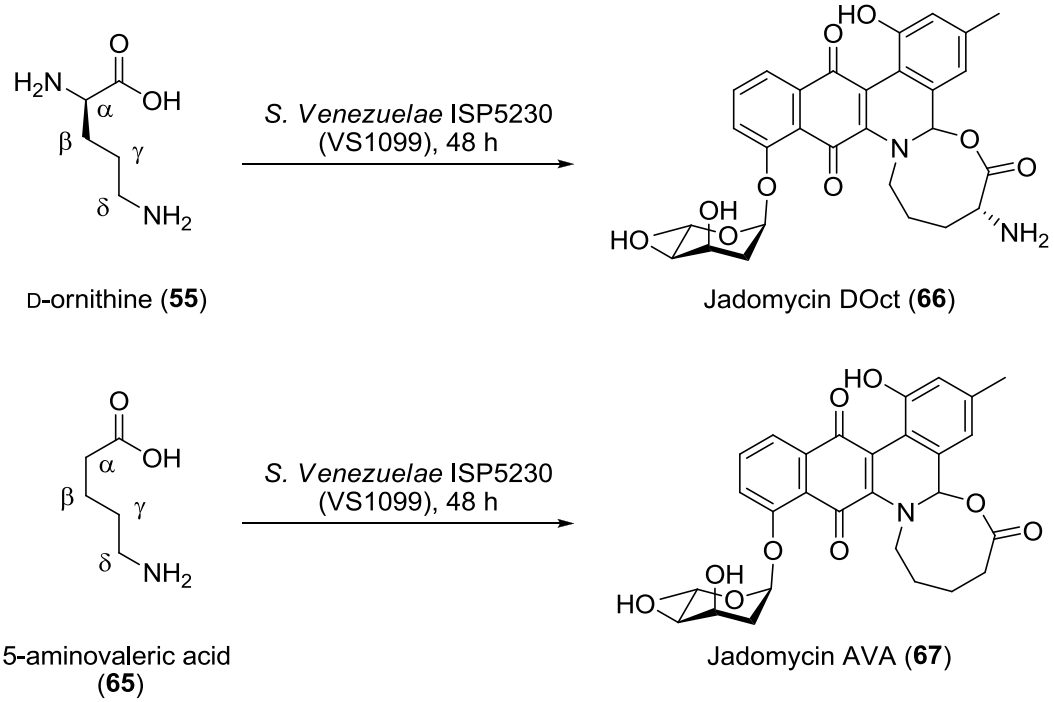

D-ornithine (**55**)

Jadomycin DOct (**66**)

5-aminovaleric acid (**65**)

Jadomycin AVA (**67**)

Figure 10. Structures of D-ornithine (**55**), 5-aminovaleric acid (**65**), and the structures of the analogues incorporating these amino acids, jadomycin DOct (**66**) and jadomycin AVA (**67**).

2.2.1. Attempted Isolation of Jadomycin DOct (66) and the Derivative (66a)

S. venezuelae ISP5230 VS1099 fermentations with **55** were conducted on a reduced scale (200 mL) compared to growths with **54** (2 L) due to limited amino acid availability. Bacterial growth and production of coloured compounds were significantly reduced

compared to fermentations with **54** or **65** (Chapter 4.2). Only 5 mg of crude material was isolated from the growth, nevertheless, compound **66** was identified via LC-MS/MS analysis (Figure 11*B*). Due to the instability and low yield of **66**, purification and characterization were not attempted. Instead we opted to use our developed methodology to derivatize **66** using succinimidyl ester **59** (Figure 11*A*). Production of **66a** was confirmed via LC-MS/MS analysis of the reaction mixture (Figure 11*C*), and the material was purified. Compound **66a** was isolated in limited quantity (< 1 mg) with significant impurities. MS/MS fragmentation of **66a** was entirely consistent with the data for **58a**, and the ^{1}H-NMR spectra of both compounds were also similar (Appendix 3), suggesting the presence of an eight-membered ring containing derivative. Due to limited yields, full structural characterization of **66a** was not accomplished.

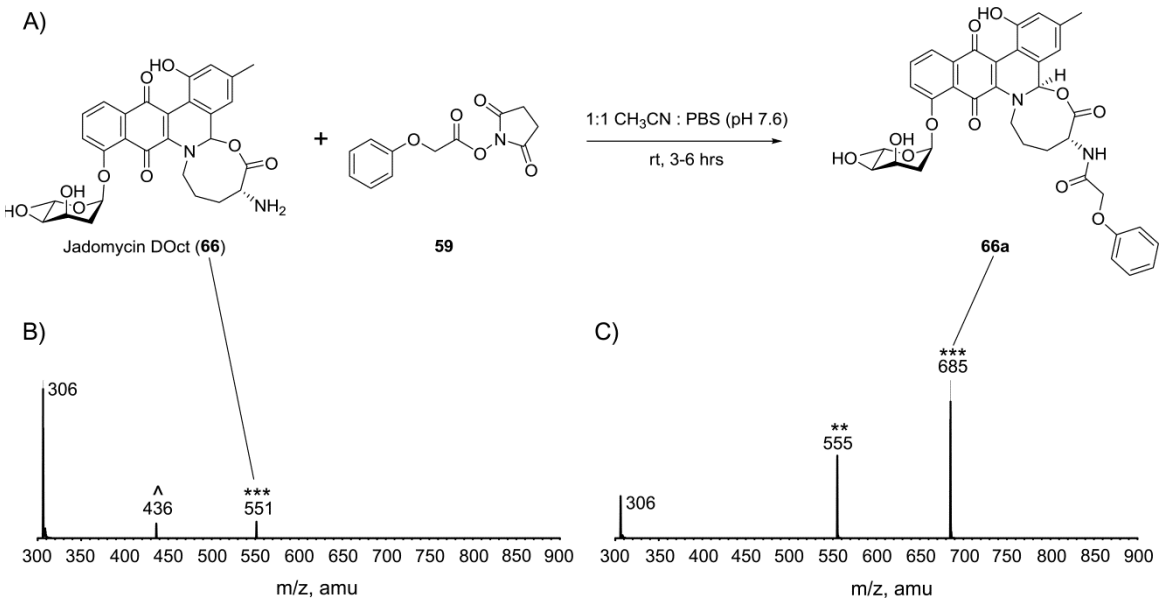

Figure 11. Attempted derivatization of jadomycin DOct (**66**). (*A*) Semi-synthetic derivatization of jadomycin DOct (**66**) with the succinimidyl ester **59** to produce **66a**; (*B*) LC-MS/MS fragmentation of **66** and (*C*) LC-MS/MS fragmentation of **66a** illustrating $[M+H]^+$ (***), cleavage of the sugar $[M + H - \text{digitoxose}]^+$ (**) and the amino acid groups $[M + H - \text{digitoxose} - R]^+$ (*m*/*z* 306). Compound **66** showed loss of amino acid group first $[M+H-R]^+$ (^).

2.2.2. Isolation and Characterization of Jadomycin AVA (67)

When *S. venezuelae* ISP5230 VS1099 was grown in the presence of **65**, surprisingly, bacterial growth and production of coloured material was comparable to fermentations

with **54** (Chapter 4.2). The major natural product, compound **67**, was isolated in a yield of 10 mgL^{-1} as a mixture of diastereomers (Mj:Mn 100:67). LC-MS/MS analysis showed the expected fragmentation pattern (Figure 12*A*) and HRMS confirmed the presence of the expected *m/z*. NMR spectroscopic analysis showed patterns and correlations similar to those observed for **58** and its derivatives, specifically, the HMBC correlations from H3a to C3′ and H3′ to C3a (Figure 12*B*-*C*) were identified. In addition, correlations from both the H3a and H3′ to C13a were observed illustrating the close through bond proximity of these positions to the quinone B ring (Figure 12*B*-*C*). Finally, nOe correlation between the H3a and H3′ protons were observed, thereby confirming the expected eight-membered ring system (Figure 12*C*).

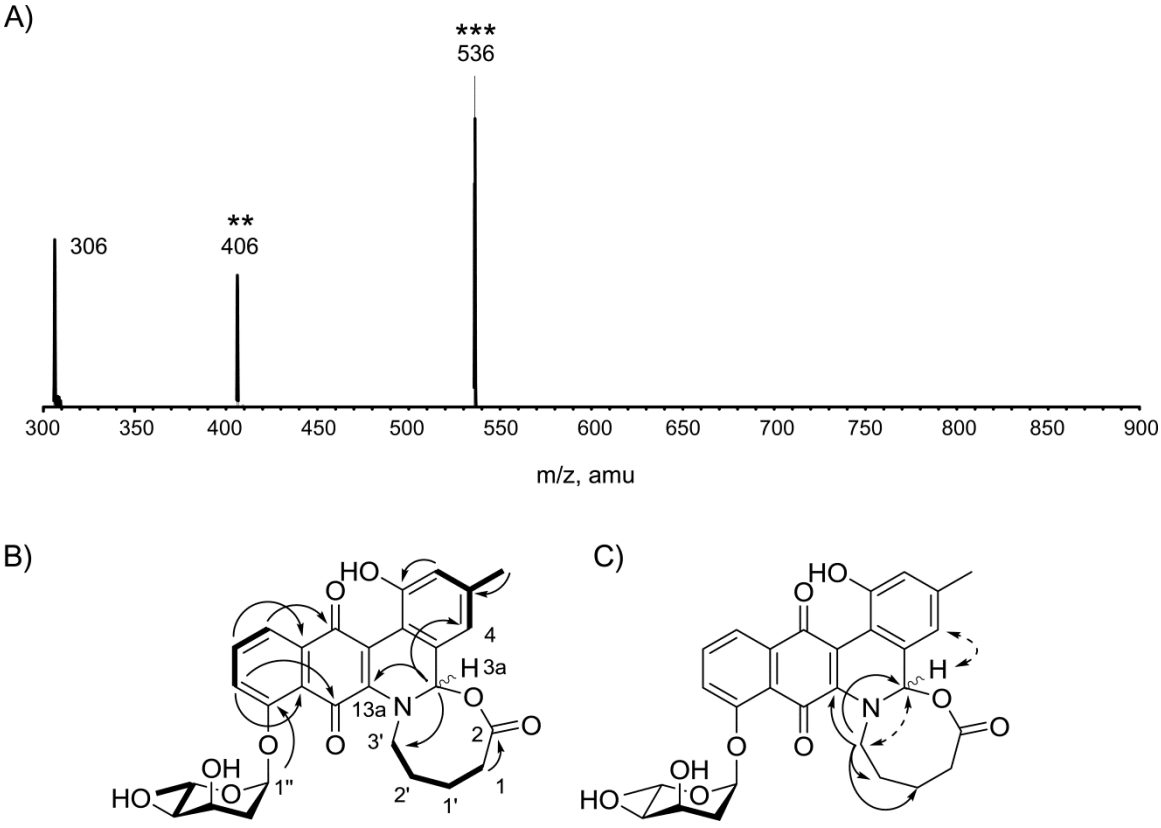

Figure 12. Structural characterization of jadomycin AVA (**67**); (*A*) LC-MS/MS fragmentation of **67**, illustrating $[M+H]^+$ (***), cleavage of the sugar $[M + H - digitoxose]^+$ (**) and the amino acid groups $[M + H - digitoxose - R]^+$ (*m/z* 306); (*B*) observed ^1H-^1H COSY (bold) and HMBC (solid arrows) correlations of compound **67** illustrating intact A, B, C, D, and sugar rings; (*C*) key observed HMBC (solid arrows) and NOESY (dashed arrows) correlations of **67** identifying the configuration of the incorporated 5-aminovaleric acid.

2.3. Biological Activity of Jadomycin Amides

All biological studies discussed in this section are results of collaborative efforts. Anticancer drug screening was performed by the National Cancer Institute (NCI) in the USA. DNA cleavage and antimicrobial studies were performed in the laboratory of Dr. Sherri McFarland at Acadia University, Wolfville, NS Canada. This data is presented to supplement the discussion and outline the significance of the isolation of these novel compounds.

Compounds **58a**, **58c**, **58d** and **58f** were selected by the NCI for testing against their 60 DTP human tumor cell line one-dose screen. In contrast to the previous jadomycins bearing five-membered oxazolone rings, cytotoxicity of the compounds was limited despite their ability to invoke Cu(II)-mediated DNA damage (Chapter 4.5). This suggests the importance of the five-membered oxazolone ring for antitumor bioactivity over the new eight-membered ring system.[77] The expanded ring system also led to changes in the antimicrobial properties associated with the oxazolone ring containing jadomycins. Lack of cytotoxicity under ambient conditions is desirable for photodynamic applications that employ light-responsive agents, so compounds **58a**-**58d** were tested for their light induced antibacterial activity against *Streptococcus mutans*. All four compounds exhibited photodynamic inactivation (PDI) of bacteria, with **58a** as the most potent compound. However, they do not appear to act via a DNA photodamaging mechanism, given that gel electrophoretic mobility-shift assays showed minimal DNA photocleavage under similar conditions (Chapter 4.5). This unexpected PDI activity is a unique feature of these eight-membered ring jadomycins.

2.4. L-Lysine (56) Fermentations

With the successful isolation of **58** and **67**,[86] in an effort to isolate a jadomycin incorporating L-lysine (**56**), where we anticipated formation of either a five- (**68**) or nine-membered (**69**) heterocyclic ring, *S. venezuelae* fermentations in the presence of **56** were undertaken (Scheme 14).

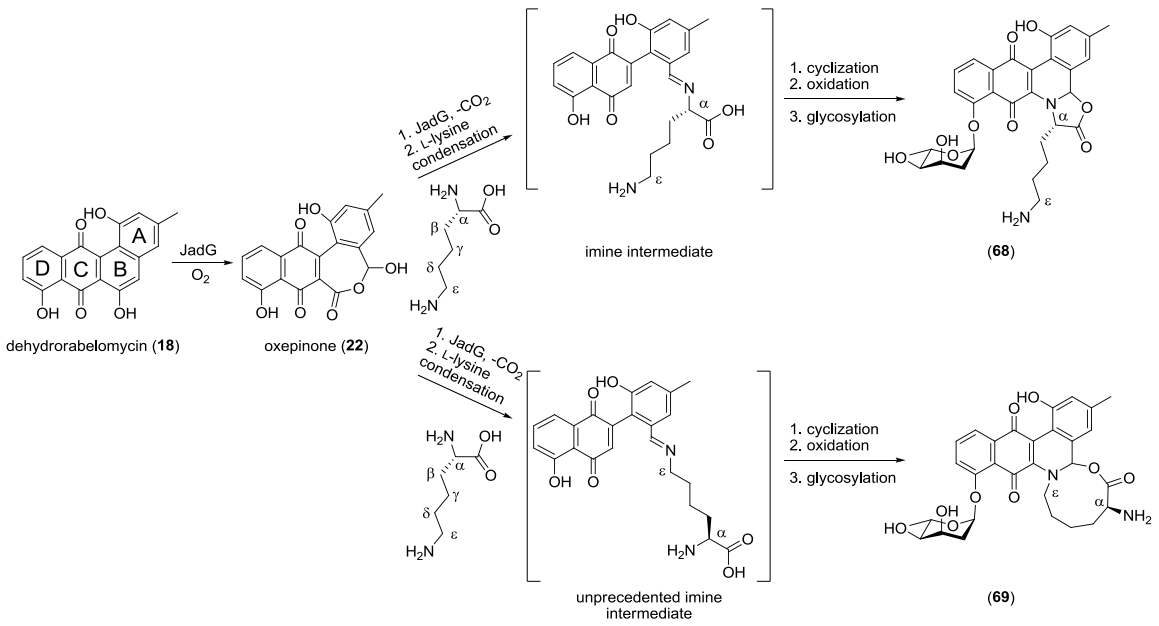

Scheme 14. Possible L-lysine (**56**) incorporation into the jadomycin backbone.

S. venezuelae ISP5230 VS1099 was grown using typical conditions for jadomycin production with **56** (60 mM) as the sole nitrogen source.[69] The fermentation was allowed to proceed for 48 h while monitoring by absorption spectroscopy for cell growth at 600 nm (OD_{600}) and the production of coloured natural products at 526 nm (Abs_{526}) (Chapter 4.2). After 48 h, the growth media was reddish-purple indicating jadomycin production. Although production of a jadomycin analogue with the appropriate *m/z* for L-lysine incorporation was confirmed by LC-MS/MS analysis of the crude growth media (Figure 13*A*-*B*), attempts to isolate the product using standard methodologies employed for other jadomycins were unsuccessful due to compound instability. These results were in agreement with the work of Yang and co-workers who described difficulties in the isolation of the L-lysine containing jadomycin analogue.[78] They proposed the five-membered oxazolone ring containing structure **68**, but NMR data were very incomplete making this structural assignment impossible to confirm.[78] Chemical derivatization of the crude growth media was also attempted using succinimidyl ester **59**, and the formation of the appropriate product *m/z* was observed by LC-MS/MS; unfortunately, attempts to isolate this product were also unsuccessful.

2.4.1. ^{15}N-Labeled L-Lysine

With LC-MS/MS data suggesting the presence of either **68** or **69** in the crude growth media, our interest shifted to determining whether the five-membered or nine-membered ring was preferentially formed. As such, *S. venezuelae* ISP5230 VS1099 growths were conducted in the presence of ε-^{15}N-L-lysine (60 mM) or α-^{15}N-L-lysine (45 mM). We hypothesized that the MS/MS fragmentation pattern of the labeled jadomycins would determine which amino group, α or ε, is incorporated into the jadomycin backbone. Specifically, if ^{15}N was incorporated into the polyaromatic backbone, the typical 306 *m/z* phenanthroviridin aglycone fragment would be shifted by one mass unit fragmenting to 307 *m/z*. LC-MS/MS analysis of both the α-^{15}N and ε-^{15}N-L-lysine labeled jadomycin identified the appropriate parent ion peak at 566 *m/z* $[^{15}NM + H]^+$ illustrating successful incorporation of each isotopically labeled ^{15}N-L-lysine Figure (13*C* and *E*). In addition, when scanning growth media for the non-isotopically labeled parent ion 565 *m/z* $[M + H]^+$, signals were not observed. The ε-^{15}N-L-lysine labeled jadomycin showed a loss of 130 to a fragment *m/z* of 436 *m/z*, corresponding to either the loss of the ^{15}N-amino acid $[M + H - C_6H_{11}{}^{15}NO_2]^+$ or the loss of L-digitoxose $[M + H - \text{digitoxose}]^+$ (Figure 13*C*). This was followed by a second loss of 130 forming the typical 306 *m*/*z* fragment (Figure 13*D*), illustrating the absence of the ^{15}N-label in the polyaromatic backbone. In contrast, the α-^{15}N-L-lysine labeled jadomycin fragmentation pattern showed the loss of 129 corresponding to the loss of the amino acid side chain forming the ^{15}N-L-digitoxosyl phenanthroviridin fragment $[^{15}NM + H - C_6H_{11}NO_2]^+$ (Figure 13*E*), followed by a loss of 130 corresponding to the cleavage of the L-digitoxose moiety, giving an atypical 307 *m*/*z* fragment (Figure 13*F*). These fragmentation patterns illustrate that the α-nitrogen of L-lysine is the primary nitrogen incorporated into the jadomycin backbone. This finding suggests that the hypothesized nine-membered ring containing jadomycin **69** may not form due to preferential nucleophilic attack by the α-amino group of L-lysine to form the imine intermediate during jadomycin biosynthesis, or **69** is unstable and breaks down quickly upon formation. These data suggest that the oxazolone ring containing jadomycin **68** is preferentially formed.

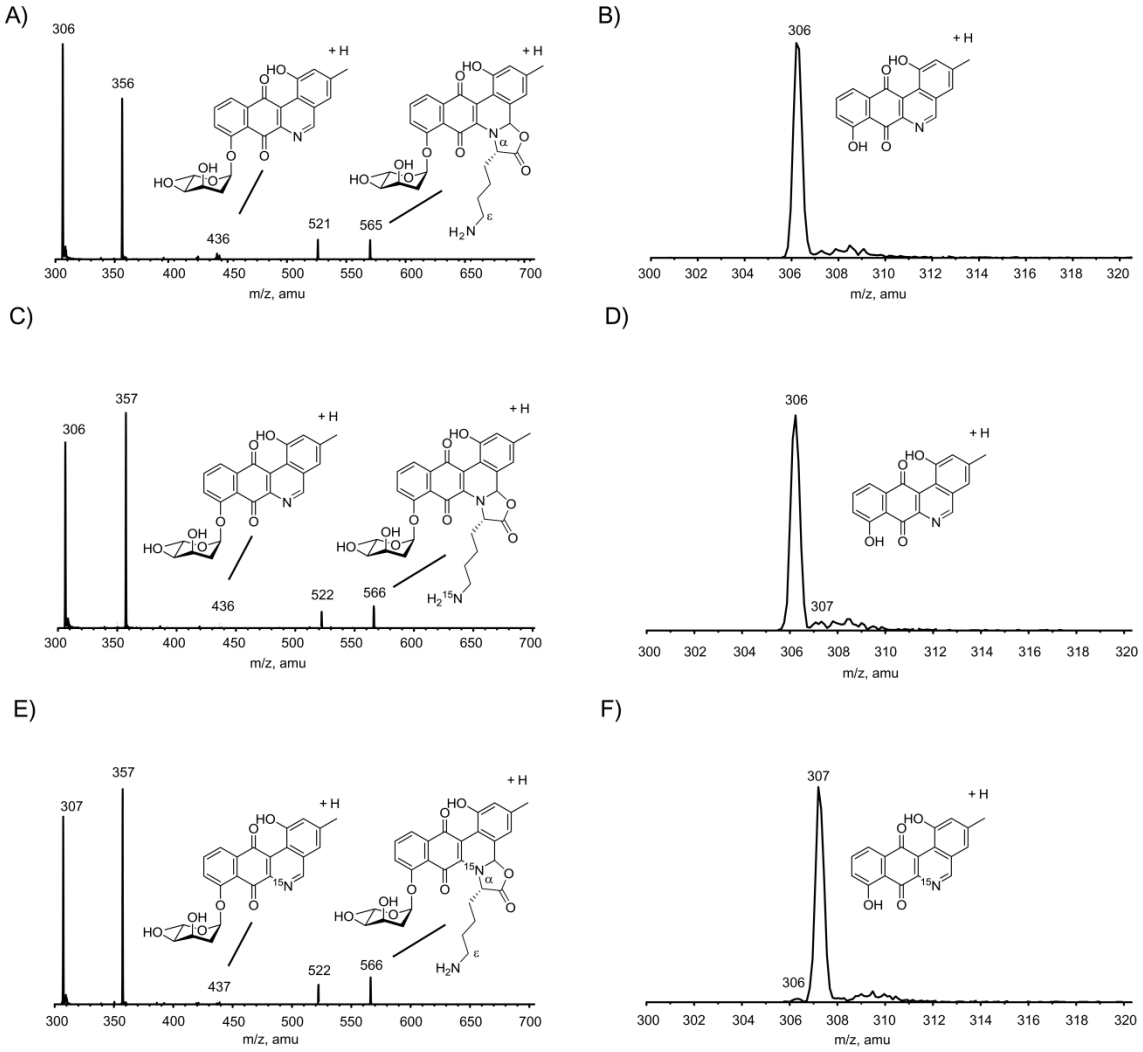

Figure 13. Comparative LC-MS/MS fragmentation patterns of jadomycin L-lysine, jadomycin ε-^{15}N-L-lysine, and jadomycin α-^{15}N-L-lysine. (*A*) LC-MS/MS fragmentation pattern of jadomycin L-lysine showing parent ion 565 *m/z* [M + H] (*B*) enlarged region of Figure 13*A* (300-320 *m/z*) illustrating the 306 *m/z* fragment [M + H – $C_6H_{11}NO_2$ – digitoxose]$^+$; (*C*) LC-MS/MS fragmentation pattern of jadomycin ε-^{15}N-L-lysine showing parent ion 566 *m/z* [^{15}NM + H]$^+$; (*D*) enlarged region of Figure 13*C* (300-320 *m/z*) illustrating the unlabeled 306 *m/z* fragment [M + H – $C_6H_{11}{}^{15}NO_2$ – digitoxose]$^+$; (E) LC-MS/MS fragmentation pattern of jadomycin α-^{15}N-L-lysine showing parent ion 566 *m/z* [^{15}NM + H]$^+$; (*F*) enlarged region of Figure 13*E* (300-320 *m/z*) illustrating the labeled 307 *m/z* fragment resulting from the cleavage of both the amino acid and L-digitoxose [^{15}NM + H – $C_6H_{11}NO_2$ – digitoxose]$^+$.

2.4.2. Isolation of L-digitoxosyl-phenanthroviridin

After failing to isolate and characterize **68**, isolation of new derivatives from *S. venezuelae* ISP5230 VS1099 growths with unlabeled L-lysine were explored. During

investigation of crude fermentation extracts, we identified an intriguing unknown amber coloured compound by TLC that proved to be sufficiently stable for isolation and characterization. TLC analysis of ethyl acetate extracts revealed that a yellow compound was the predominant natural product in the mixture. Preparative TLC was performed on the material, yielding 8 mg of the amber-yellow solid (4 mgL^{-1}), of sufficient purity for characterization. The compound was identified as a new phenanthroviridin analogue, L-digitoxosyl-phenanthroviridin (**70**). The isolation of the phenanthroviridin aglycone (**71**) has been reported previously from cultures of *S. venezuelae* ISP5230 (Figure 14). Compound **71** was simultaneously identified during the first isolation of **5**.[23] However, the glycosylated analogue **70** had not been reported.

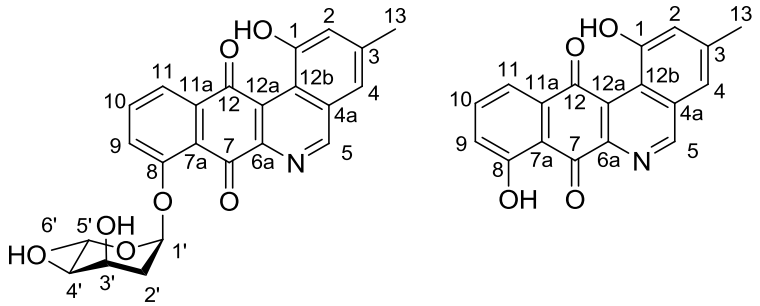

Figure 14. Structures of L-digitoxosyl-phenanthroviridin (**70**) and phenanthroviridin aglycone (**71**).[23]

2.4.3. Structural Elucidation of 70

HRMS identified a molecular formula of $C_{24}H_{21}NO_7$. LC-MS/MS analysis scanning for $[M + H]^+$ identified an *m/z* of 436, with fragmentation to *m/z* of 306, corresponding to a loss of 130. This fragmentation pattern is typical of jadomycin-like molecules and represents the loss of L-digitoxose, identifying a glycosylation of the unknown compound (Figure 15).[95]

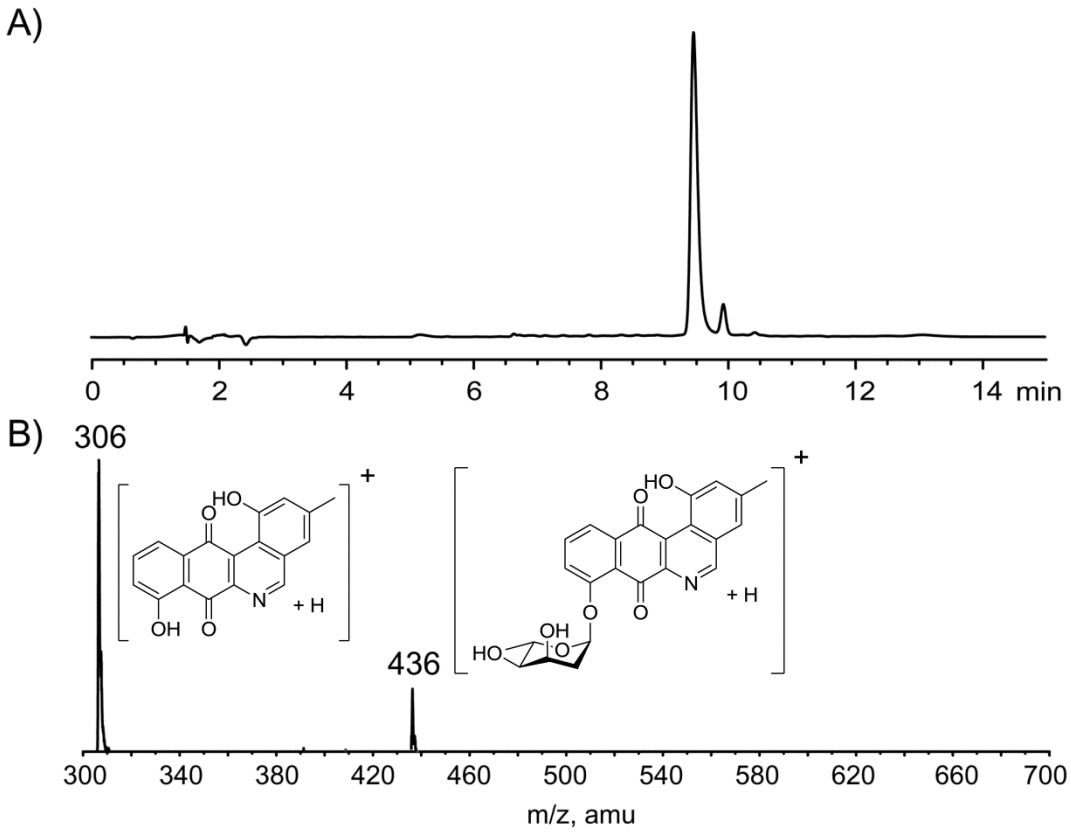

Figure 15. HPLC and LC-MS/MS analysis of **70**; (*A*) HPLC trace of **70** (R_t = 9.47 min); (*B*) LC-MS/MS fragmentation of **70**, showing parent ion $[M + H]^+$ (436), and fragmentation resulting from the cleavage of L-digitoxose $[M + H - \text{digitoxose}]^+$ (*m*/*z* 306).

Structural characterization was accomplished using a combination of ^1H, ^{13}C, COSY, edited-HSQC, HMBC, and NOESY NMR spectroscopy experiments. The ^1H-NMR and COSY experiments confirmed the presence of the L-digitoxose spin system (C1′ through C6′). In addition, the characteristic jadomycin A-ring (C2, C4, and C13) and D-ring (C9 through C11) spin systems were observed. An exchangeable singlet (observed in CD_2Cl_2 but not in MeOD-d_4) at δ_H = 11.84 ppm was also present, corresponding to the 1-OH proton. HMBC data provided core connectivity typical of a jadomycin (Figure 16). An additional non-exchangeable CH proton at δ_H = 9.42 ppm in the ^1H-NMR with an HSQC correlation to a carbon at δ_C = 160.9 ppm was observed. This relatively downfield chemical shift suggested a distinct heteroaromatic chemical environment resembling that of the phenanthroviridin aglycone at C5, as opposed to L-digitoxosyl-dehydrorabelomycin which lacks the heteroaromatic ring (Figure 16). HMBC and

NOESY correlations from H5 to C4 and H4, respectively, confirmed the proximity of the proton to the A-ring; HMBC analysis also identified a correlation to the C6a position of the B-ring. Glycosylation at the 8-position was confirmed by NOESY correlations between H9 of the D-ring and H1′ of the L-digitoxose moiety. These data are consistent with our proposed structure of **70** as a functionalized benzo[*b*]phenanthridine framework glycosylated with L-digitoxose.

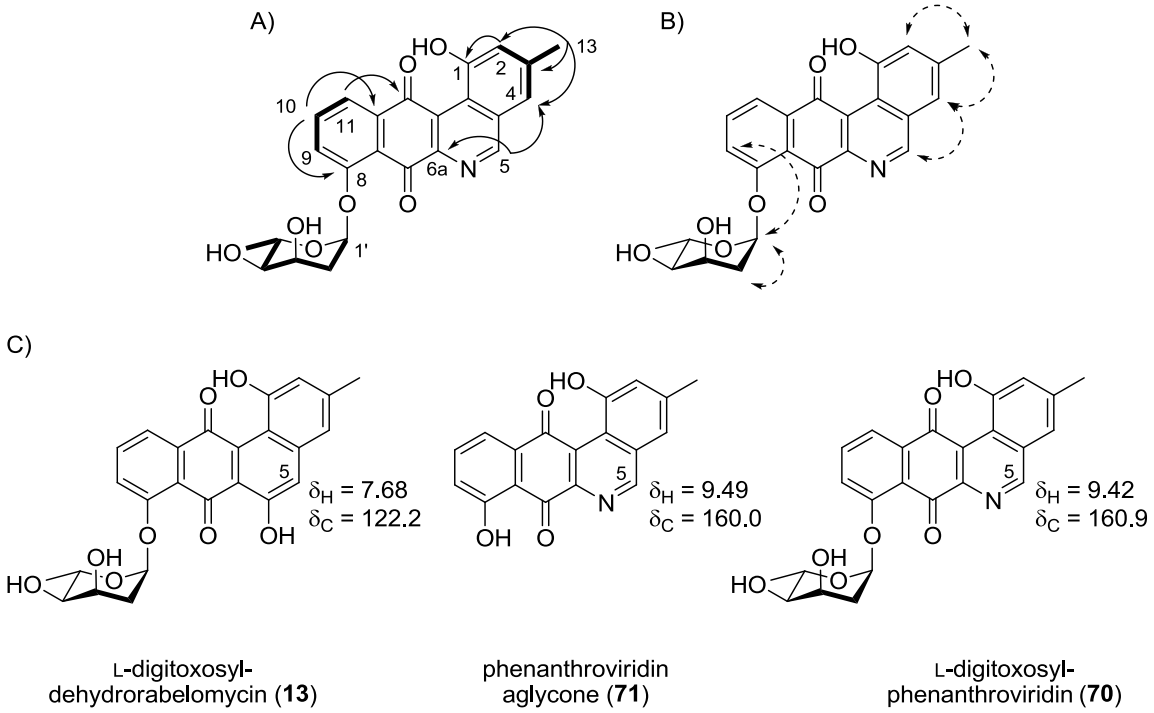

Figure 16. Structural elucidation and comparison of **70**; (*A*) Key ^{1}H-^{1}H COSY (bold) and HMBC (solid arrows) correlations in **70**; (*B*) key NOESY (dashed arrows) correlations of **70**; (*C*) δ_H and δ_C values of H5 and C5 associated with the compounds **13**,[49] **71**,[23] and **70**.

Our difficulties in isolation of the jadomycin L-lysine derivative paralleled work by Yang and co-workers, who attempted purification of the compound but were hampered by product instability and low yields resulting in incomplete structural characterization.[78] Compound **70** is proposed to be a stable degradation product of the L-lysine analogue. Although speculative at this time, a mechanism for degradation is proposed to occur through a series of base-catalyzed events starting with delocalization of the lone pair of electrons on nitrogen to form an alkylated pyridinium ion intermediate (Scheme 15). This is followed by deprotonation of the α-position to form an iminium ion. Addition of water or hydroxide to the iminium carbon results in the formation of a

tetrahedral intermediate which, upon deprotonation of the hydroxyl group, results in the elimination of an L-digitoxosyl-phenanthroviridin hydroquinone intermediate accompanied with the formation of an α-keto acid. This hydroquinone could then undergo spontaneous oxidation yielding the final product **70** (Scheme 15).[50]

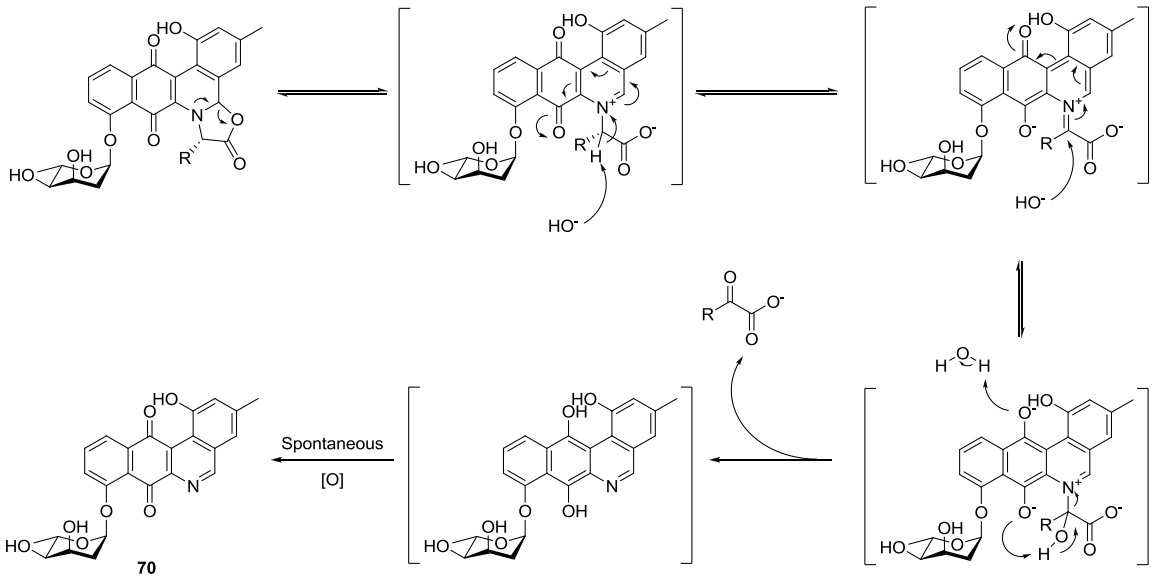

Scheme 15. Proposed jadomycin degradation pathway forming **70**.

2.4.4. Cytotoxic Activity of 70

Isolation of **70** presented an opportunity to test the bioactivity of a unique jadomycin-like analogue, and to probe the structure activity relationship (SAR) associated with the oxazolone ring system. Compound **70** was evaluated against the National Cancer Institutes (NCI) 60 DTP Human Tumor Cell Line Screen. All screening was carried out according to the NCI protocol with the exception that ethanol was substituted for dimethyl sulfoxide due to compound stability. Initial single dose screening (10 μM) identified sufficient cytotoxicity for further testing in a five-dose assay (10 nM- 100 μM) using $\log_{10}$ concentration intervals. Percent growth was plotted as a function of the concentration of **70** giving dose response curves for each tumor cell line (Appendix D). From these curves the GI_{50} (growth inhibition of 50%), TGI (drug concentration resulting in total growth inhibition), and LC_{50} (drug concentration resulting in 50% tumor death)

were calculated. Compound **70** showed respectable cytotoxicity resulting, in many cases, complete or near complete tumor death at higher concentrations (100 μM) (Appendix D).

Direct comparison of the GI_{50}, TGI, and LC_{50} values between **70** and other jadomycin derivatives previously isolated in the Jakeman lab revealed that despite lacking an amino acid side chain and an oxazolone ring, **70** had comparable bioactivity when compared to this small library of natural and semi-synthetic jadomycins. These data are summarized in Table 2.

Table 2. Summary of NCI 60 cancer cell line screen GI_{50}, TGI, and LC_{50} values of **70**, compared to a small library of jadomycin analogues.

		GI_{50} (μM)		TGI (μM)		LC_{50} (μM)	
Compound[a]	concentration range (nM-μM)[b]	median (range)	*n*	median (range)	*n*	median (range)	*n*
70	10-100	2.14 (0.27-16.6)	57	5.75 (1.4-48)	56	18.2 (4.7-96)	41
Jadomycin G (**72**)	10-100	1.68 (0.20-21.4)	54	9.6 (0.40-85)	54	38.5 (0.78-96)	42
Jadomycin L (**35**)	10-100	1.82 (0.28-11.2)	58	4.1 (0.76-85)	51	9.3 (4.0-79)	43
Jadomycin DNV (**39**)	3.2-32	4.79 (0.59-9.1)	59	10 (1.23-31)	57	19 (2.4-32)	42
Jadomycin DNL (**40**)	3.2-32	3.89 (0.47-9.3)	59	8.7 (0.91-26)	56	18 (1.8-32)	44
Jadomycin T (**44**)	10-100	1.35 (0.17-2.6)	59	3.02 (0.48-8.9)	58	6.5 (1.4-41)	48
52	1.6-16	3.5 (0.45-16.6)	54	7.2 (1.3-14.9)	40	11.8 (7.7-16.3)	17
47	2.5-25	6.1 (0.7-23.6)	51	11.9 (2.6-4.6)	28	14.9 (13-21.4)	10
50	1.6-16	3.1 (0.6-10)	55	6.8 (2.3-15.1)	46	11.6 (8.2-16.3)	25
53	1.6-16	3.7 (0.5-9.3)	54	6.6 (1.6-15.6)	42	10.9 (8.3-15)	19
51	1.6-16	3.1 (0.5-15.6)	57	6.3 (2.1-16)	51	9.8 (1.0-16.5)	26

[a]Compound list includes jadomycin G (**72**) (incorporated amino acid is glycine),[82] jadomycin L (**35**),[77] jadomycin DNV (**39**),[95] jadomycin DNL (**40**),[95] and jadomycin T (**44**).[82] Compounds **47**, and **51-53** are a series of semisynthetic jadomycin triazoles (Figure 18).[81] [b]All values are expressed as median (range), where n = the number of cancer cell lines in which GI_{50}, TGI, or LC_{50} were quantifiable below the maximal concentrations used in each experiment.

In an effort to probe the mechanism of action of **70**, a standard COMPARE[96, 97] analysis screening against the NCI-standard agents database, using GI_{50}, TGI, and LC_{50} values was performed. The COMPARE analysis identifies and evaluates similarities between the screened compounds cytotoxicity profiles and known anticancer agents in

the NCI databases. The screen identified weak to moderate correlation (Pearson correlation coefficient (PCC) < 0.58) between **70** and the standard agents database, a library of 171 known cytotoxic compounds, when compared to GI_{50}, TGI and LC_{50} values. Results showed correlations to a wide variety of compounds (**10**, **73**-**85**) including known antimitotic agents, alkylating agents, topoisomerase II inhibitors and a series of compounds with listed unknown function (Figure 17). The highest correlation obtained was associated with trimethyltrimethylolmelamine (**82**) (PCC = 0.573) while comparing LC_{50} data (Figure 17). This correlation, together with a GI_{50} correlation to pancratiastatin (**73**) (PCC = 0.467) has been reported previously for structurally similar naphthoquinone moiety containing compounds.[98]

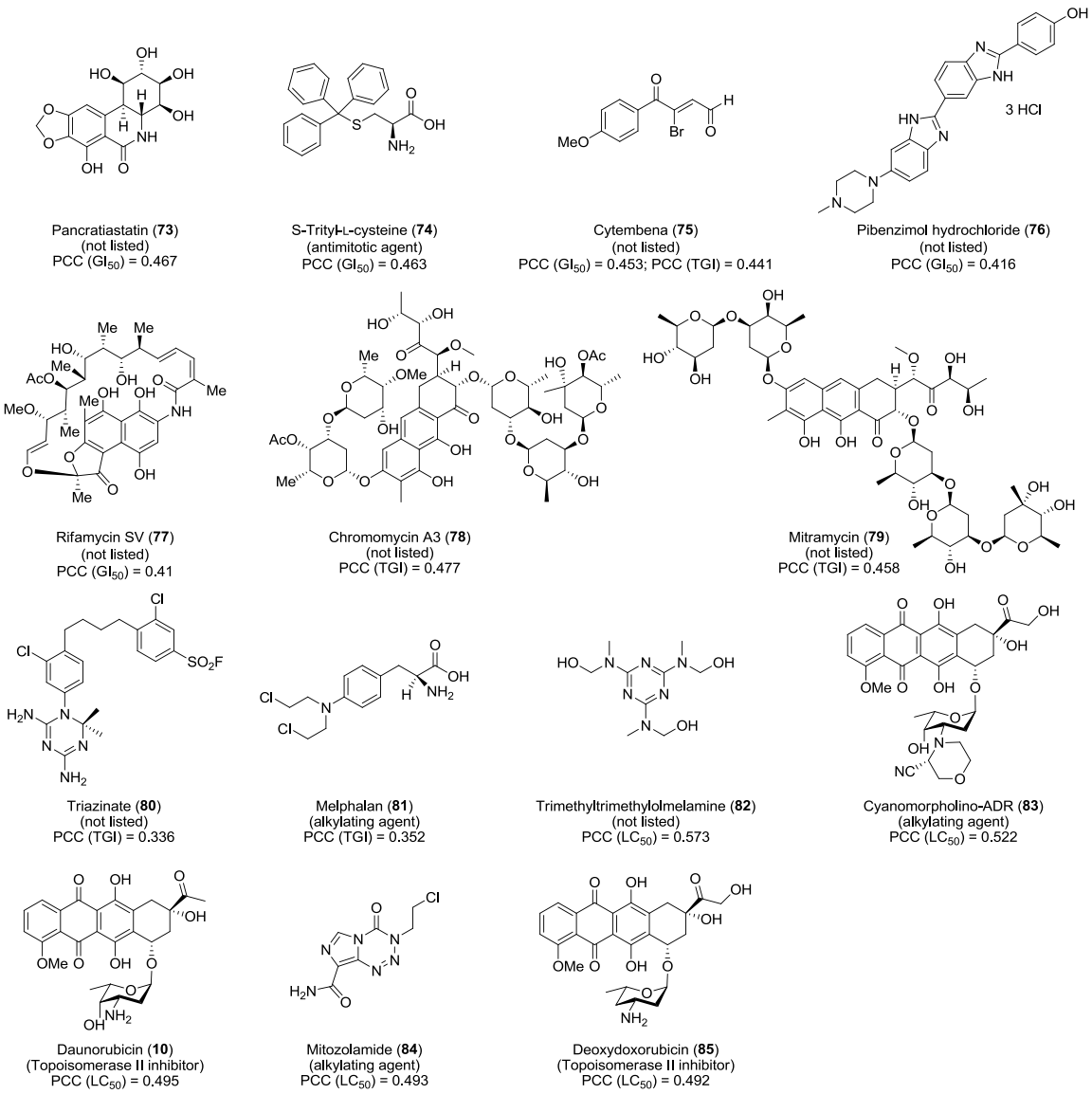

Figure 17. Top identified compounds by COMPARE analysis for each GI_{50}, TGI and LC_{50} correlations with **70** comparing against the NCI Standard Agents Database. Proposed functions according to the NCI website are given underneath each compound in parentheses. Pearson correlation coefficient (PCC) values are listed with the appropriate parameter (GI_{50}, TGI, or LC_{50}) in parentheses (http://dtp.nci.nih.gov/docs/cancer/searches/standard_agent_table.html).

Correlations, although moderate, between **70** and the anthracyclines daunorubicin (**10**) (PCC = 0.495), deoxydoxorubicin (**85**) (PCC = 0.492), and cyanomorpholino-ADR (**83**) (PCC = 0.522) were observed when comparing LC_{50} values. These clinically used anthracyclines exhibit potent anti-tumor properties. They impart cytotoxicity *via* intercalation into DNA, allowing the formation of a stable complex with topoisomerase

II, inhibiting the enzymes ability to effectively cut DNA during replication, disrupting tumor proliferation.[99, 100] The jadomycin family of natural products shares structural similarities to these compounds, and jadomycin inhibition of topoisomerase II has been speculated in the past.[101] This may suggest a similar mode of action for **70** and other jadomycins.

When compared to the synthetic compound database (>40,000 compounds including synthetic compounds and natural products of known structure) strong correlations between **70** and a number of jadomycins (**35**, **47**, **50**-**53** and **72**) previously isolated in our lab were observed (correlations ~0.7-0.8), in addition to 3 non-jadomycin compounds (**86**-**88**) (Figure 18). Thus, it can be concluded that **70** has a similar mode of action to oxazolone ring containing jadomycins and that cytotoxic effect may not be strongly dependent on the incorporated amino acid. Rather, the amino acid functionality may tune other physiochemical properties of the natural product. This discovery illustrates the opportunity to direct efforts towards modifying the sugar moiety or derivatizing the polyaromatic backbone in order to identify new analogues with improved or altered bioactivity, while concurrently varying the amino acid incorporated into the jadomycin scaffold to adjust physicochemical properties.

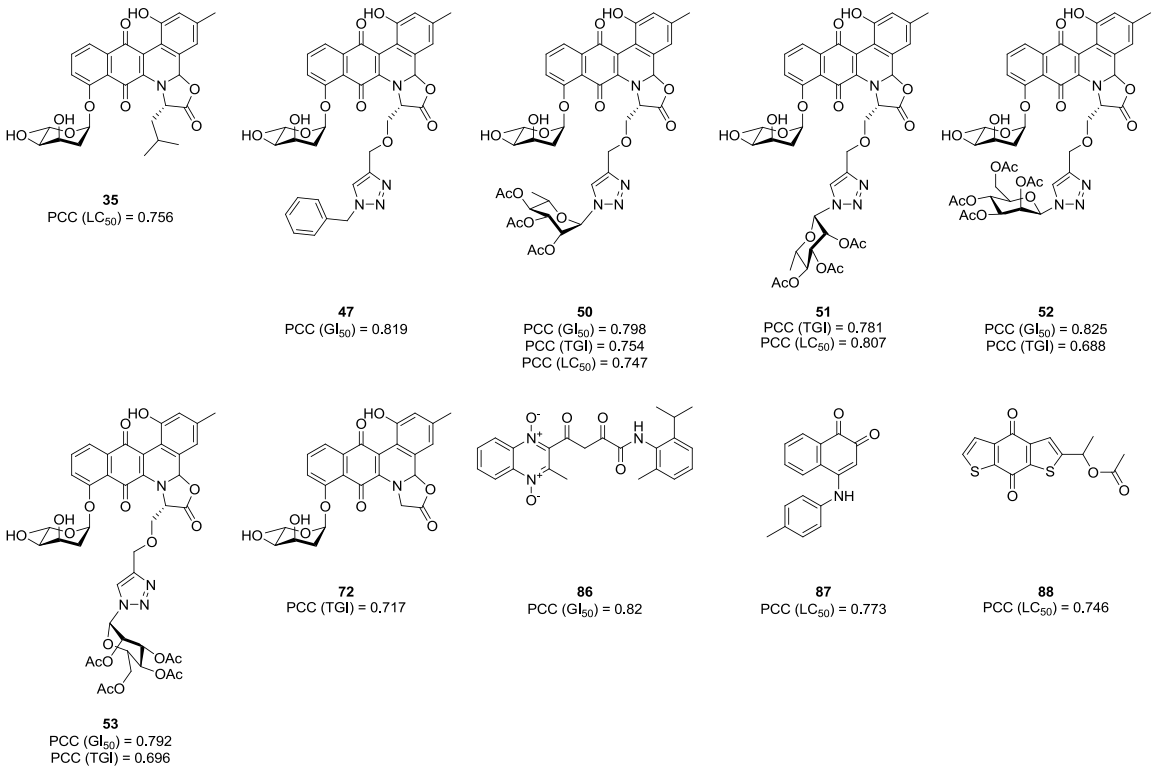

Figure 18. Structures of compounds from the NCI synthetic compounds database (synthetic compounds and natural products of known structure) showing highest correlations to **70** for each GI_{50}, TGI and LC_{50}. Pearson correlation coefficient (PCC) values are listed with the appropriate parameter (GI_{50}, TGI, or LC_{50}) in parentheses.

CHAPTER 3: RESULTS AND DISCUSSION PART 2

3.1. Regulation in Jadomycin Biosynthesis

As previously stated, the Actinobacteria genus *Streptomyces* is one of the largest producers of bioactive secondary metabolites, and as such, is also a rich source of diverse enzymatic and protein activity.[14, 17, 18, 102] Biosynthetic pathways producing natural products require enzymes and regulatory proteins to work cooperatively to furnish complex stereospecific structures important in improving the molecule's bioactivity in order to out-compete other organisms in an ecological setting. Genes essential for individual secondary metabolite production are often found in gene clusters with genes localized in close proximity to one another.[20, 21] The biosynthesis of these natural products is often subject to complex regulation, controlled by one or more regulatory proteins coded for within their respective biosynthetic gene clusters.[103-105] Many strains of *Streptomyces* are capable of producing multiple secondary natural products. In addition, there is a growing body of evidence that the production of many of these compounds are further regulated *via* complex cross-regulation, in which cluster-situated regulatory proteins from one pathway affect gene expression in other secondary metabolite pathways.[21, 103-105] Examples of this multi-natural product cross-regulation can be found in the model organism *S. coelicolor*, regulating production of undecylprodigiosin (**89**) and actinorhodin (**90**) (Figure 19),[106] and more recently, *S. venezuelae* ISP5230, regulating jadomycin and chloramphenicol (**3**) biosyntheses.[107, 108]

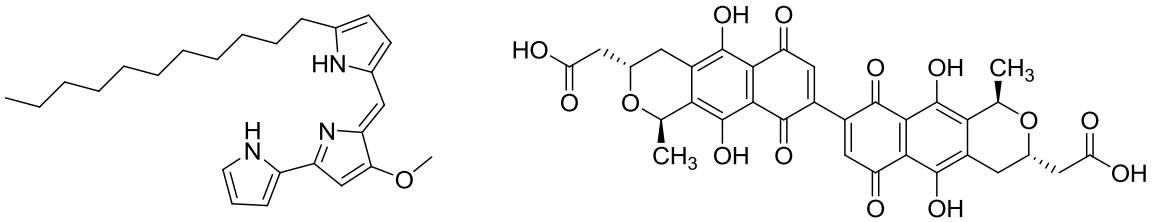

undecylprodigiosin (**89**) actinorhodin (**90**)

Figure 19. Structures of the *Streptomyces coelicolor* produced natural products undecylprodigiosin (**89**) and actinorhodin (**90**).

It was reported by Tan and coworkers that JadR2 is responsible for repressing jadomycin production by inhibiting the transcription of *jadR1*, whose gene product is responsible for activation of jadomycin production.[107, 108] There are a number of regulatory genes within the jadomycin biosynthetic gene cluster, but none in the gene cluster of **3**.[108, 109] Tan and coworkers identified that regulation of biosynthesis of **3** is accomplished by jadomycin cluster-situated regulators JadR1 and JadR2 via cross-regulation between the pathways. JadR2 has also been shown to bind both end products **3** and **6** further substantiating the cross talk between these pathways.[108] Cross-regulation of natural product biosynthetic pathways may also occur at an interspecies level. Yang and coworkers have recently shown jadomycin to be involved in a complex modulation of other exogenous natural product biosynthetic gene clusters, specifically in *S. coelicolor*.[110] It is rare that a secondary metabolite biosynthetic pathway is completely elucidated, and despite extensive research conducted towards the mapping of jadomycin biosynthesis, many of the gene products involved only have putatively assigned function, or have yet to have any function ascribed to them.[67] Despite the wealth of genomic data available, assignment of function *via* homology, especially in complex biosynthetic pathways, can lead to misrepresentation of function.[111] This problem is compounded when little or no known homology is identified, or a protein exists in a family of structurally similar proteins with diverse functions.[112] Characterization of these proteins remains one of the most challenging problems associated with mapping biochemical processes. Identification of ligands for these proteins is a very important first step for identifying function, but requires fast, reliable, efficient screens for potential ligands. For secondary metabolite biosynthetic systems, a sensitive, non-destructive method is beneficial to avoid loss of valuable, often difficult to purify, natural products. The ability to observe binding in the presence of impurities or other compounds is also highly advantageous. NMR spectroscopic methodologies for examining binding offer these desired experimental parameters, and have been used extensively in drug design,[113-115] and more recently the functional assignment of putatively characterized proteins.[111] This methodology could offer a powerful tool for streamlining ligand screening as an initial step to aid in the characterization of proteins of unknown function.

3.1.1 JadX Homology Studies

The *jad*X gene was identified by Vining and coworkers immediately upstream of the dideoxysugar tailoring region of the jadomycin biosynthetic gene cluster (Figure 20).[67] A BLASTP search identified that JadX is included in the NTF2-like superfamily. This superfamily represents a large group of proteins all containing a similar fold, but very dispersive functions, making putative functional analysis by homology difficult.[112]

Figure 20. Genetic organization of *S. venezuelae* ISP5230 jadomycin gene cluster showing predicted promotor regions and ORFs coding for: regulatory proteins (diagonal stripes), predicted promotor regions (white), PKS structural enzymes (black), dideoxysugar enzymes (checkered), efflux protein (horizontal stripes) JadL, the FMN/FAD reductase JadY (wavy stripes) and JadX (grey).

A BLASTP search identified a series of similar proteins coded for in other secondary metabolite biosynthetic pathways including azicemicin (**91**),[116] kinamycin A (**92**),[117] herbimycin A (**93**),[118] geldanamycin (**94**),[119] and methylenomycin A (**95**) (Figure 21).[120, 121] A full sequence alignment of all proteins compared to JadX can be found in Appendix E. All of these natural products are polyketide derived natural products, except methylenomycin. Compounds **91** and **92** are, together with the jadomycins, angucyclines. The putative function of these proteins is either described as unknown or "JadX-like". It can be postulated that the reoccurrence of these JadX-like proteins coded for in many secondary metabolite gene clusters suggests an important role within their respective pathways.

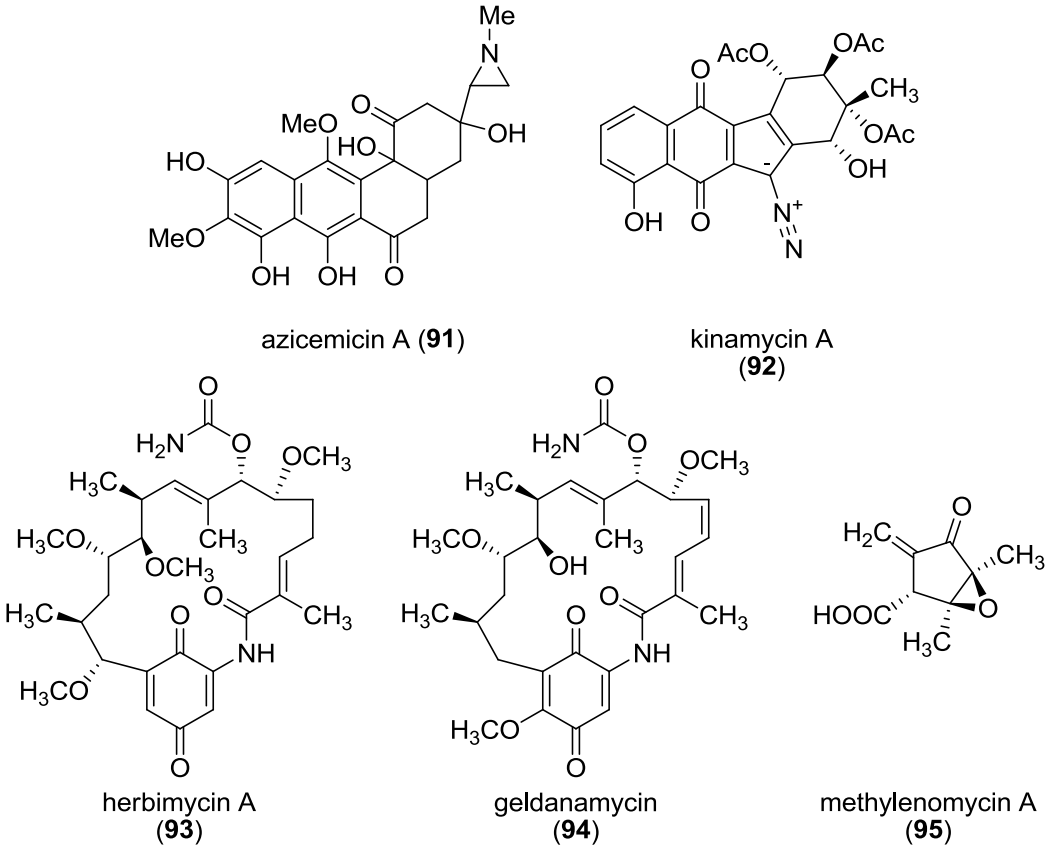

Figure 21. Structures of the natural products azicemicin (**91**), kinamycin A (**92**), herbimycin A (**93**), geldanamycin (**94**), and methylenomycin A (**95**) whose biosynthetic gene clusters code for a JadX homolog.

3.1.2. JadX Disruption Shifts *S. venezuelae* Natural Product Profile

To test the importance of *jadX* for production of jadomycin, comparative jadomycin production growths were conducted for *S. venezuelae* ISP5230 (WT), and *S. venezuelae* VS1085 disruption-mutant (Δ*jadX*), a mutant strain in which *jadX* is disrupted *via* insertion of an apramycin resistance cassette.[67] The disruption-mutant strain *S. venezuelae* ISP5230 VS1099 (Δ*jadW2*), in which *jadW2* is disrupted with an apramycin resistance cassette, was selected as a positive jadomycin control. *jadW2* is a regulatory gene involved in the regulation of jadomycin production.[122] This mutant shows an increase in jadomycin production by a factor of 2-5 compared to the WT and has been successfully utilized as a production strain to increase yields of several jadomycin analogues.[69, 76, 77, 81, 82, 86] To aid in both the analysis of the growth media and NMR-based binding studies, growths were carried out in the presence of D-serine (60 mM) as the sole nitrogen source. It is well established in the literature that growing *S. venezuelae* in the

presence of serine (D, L, or DL) as the sole nitrogen source, slows cellular growth while facilitating higher natural product production, especially with respect to **3**.[123-125] When subjected to shock conditions (ethanol), the bacteria switches natural product production from **3** to production of jadomycins.[82] The use of D-serine as the nitrogen source facilitates production of jadomycin DS (**96**) (Figure 22).

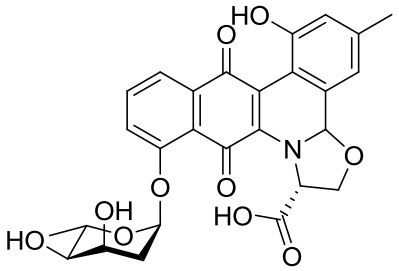

Jadomycin DS
(**96**)

Figure 22. Structure of jadomycin DS (**96**).

It has been found that this compound is produced at higher levels compared to **6**, allowing for straightforward detection using LC-MS/MS. All 3 strains could utilize the D-serine minimal media as a nutrient source, growing to a similar OD_{600} value (Figure 23*A*). This suggested that any changes in natural product profiles were not a result of differences in cell proliferation. Abs_{526} values indicated a significant reduction in the production of coloured compounds from Δ*jadX* compared to the Δ*jadW2* and WT strains (Figure 23*B*), suggesting a drop in the production of **96**. LC-MS/MS analysis of the growth media after 48 h revealed that media concentrations of **96** were highest for Δ*jadW2* (~64 μM) followed by the WT strain (~25 μM) (Figure 23*C* and *F*). The Δ*jadX* mutant produced concentrations of **96** below the limit of accurate detection by LC-MS/MS analysis (~2 μM). Upon concentration of growth media 5-10×, the presence of **96** was not clearly observed. These results were re-examined using L-isoleucine as the nitrogen source, and a similar loss in production of **6** was found (Appendix E).

To determine whether the natural product HPLC profile of the Δ*jadX* strain was altered, a crude purification was performed by passing clarified growth media through a reversed-phase phenyl matrix to trap the natural products. These natural products were

eluted with methanol and analyzed using HPLC (Figure 23*D*). Both the Δ*jadW2* and WT showed a peak corresponding to **96** at 9 min. As expected, based on the LC-MS/MS analysis, the Δ*jad*X HPLC profile showed an absence of **96**, but a new signal appeared at 6.5 min (Figure 23*D*). This peak was identified as **3** via HPLC-spiking experiments (Figure 23*E*) and LC-MS/MS analysis. LC-MS/MS analysis quantifying **3** production was performed with crude media of each strain. It was found that neither the WT nor Δ*jadW2* strains produced quantifiable amounts of **3**. The Δ*jadX* mutant produced **3** to a final concentration of 23 μM after 48 h (Figure 23*F*). This value is similar to reported production of **3** by *S. venezuelae* ISP5230 in similar media.[126] The complete loss of production of **96** and **6** illustrates the importance of JadX for jadomycin biosynthesis. Production of **3** by the Δ*jadX* mutant may be explained by the loss of production of jadomycin. The two antibiotics are heavily cross-regulated; it is believed that this regulation is antagonistic in fashion, with jadomycin production eliminating biosynthesis of **3** and *vice versa*.[108] This may account for the shift in the natural product profile of the Δ*jadX* mutant, further illustrating the complex cross-regulation of these compounds.

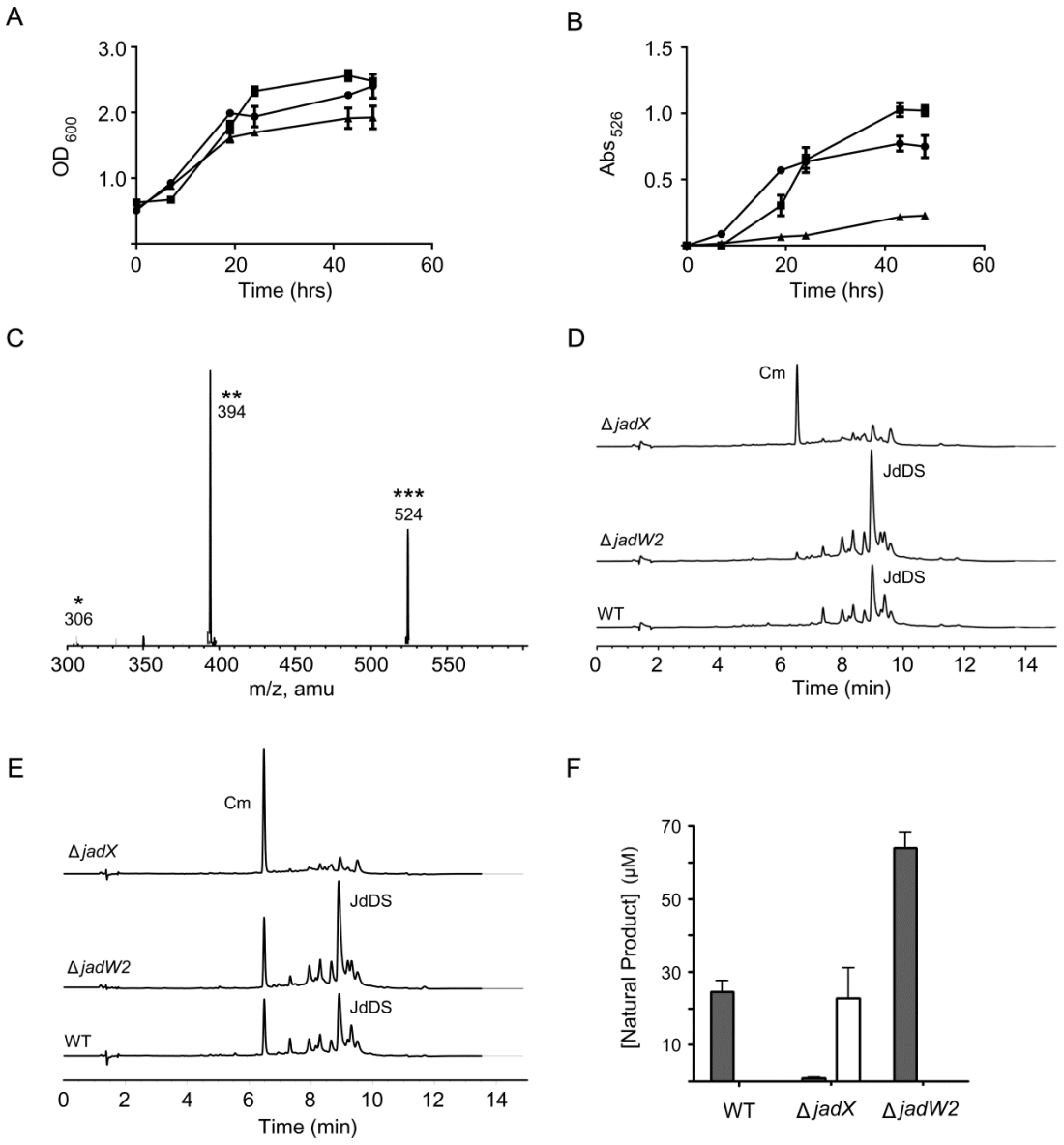

Figure 23. *S. venezuelae* ISP5230 comparative growths of wild-type and gene-disruption mutants Δ*jadX* and Δ*jadW2*. (*A*) Cellular growth curves (OD_{600}) of *S. venezuelae* ISP5230 WT (●), *S. venezuelae* ISP5230 VS1099 (■), and *S. venezuelae* ISP5230 VS1085 (▲). (*B*) Absorbance of clarified growth media at λ = 526 nm (Abs_{526}), estimating coloured compound production of *S. venezuelae* ISP5230 WT (●), *S. venezuelae* ISP5230 VS1099 (■), and *S. venezuelae* ISP5230 VS1085 (▲). (*C*) LC-MS/MS fragmentation pattern of **96**, illustrating $[M+H]^+$ (***), cleavage of the sugar $[M + H – digitoxose]^+$ (**), and the amino acid group $[M + H – digitoxose – R]^+$ (*). (*D*) HPLC traces of reversed-phase phenyl column growth media extracts after 48 h. (*E*) HPLC traces of reversed-phase phenyl column growth media extracts after 48 h spiked with 100 μM **3**. (*F*) Final **96** (grey bars) and **3** (white bars) concentrations from strains after 48 h growth.

3.2. Ligand Observed NMR Binding: JadX Binds Jadomycins and Chloramphenicol

In an effort to provide further insight into the function of JadX, protein-ligand binding using NMR-based methodologies was conducted. The *jadX* gene was cloned and recombinantly expressed in *E. coli* BL21(DE3) and purified (Chapter 4.7) for use in these studies. The two ligand-observed NMR methods that were tested for their screening capabilities were saturation transfer difference (STD) NMR[127, 128] and water ligand-observed *via* gradient spectroscopy (WaterLOGSY) NMR[129], methods previously utilized in the Jakeman lab.[130, 131] WaterLOGSY proved to be a more sensitive method compared to STD-NMR, and as such was used extensively for this study. WaterLOGSY NMR is a 1D nOe experiment in which the bulk water is irradiated, facilitating magnetization transfer from water in the active-site of the enzyme/protein to bound ligands *via* the enzyme-ligand complex.[113] Compounds that experience binding will maintain a perturbed magnetic state when released back into solution and produce an opposite sign nOe relative to non-binding compounds. This gives the WaterLOGSY experiment the added benefit of being able to directly observe both non-binding (phased negatively) and binding compounds (phased positively) simultaneously in a simple 1D-spectrum, allowing for the inclusion of non-binding controls to aid in data interpretation. Several small molecules were screened as potential JadX ligands, but the only compounds found to bind JadX were jadomycins and **3** (Figure 24).

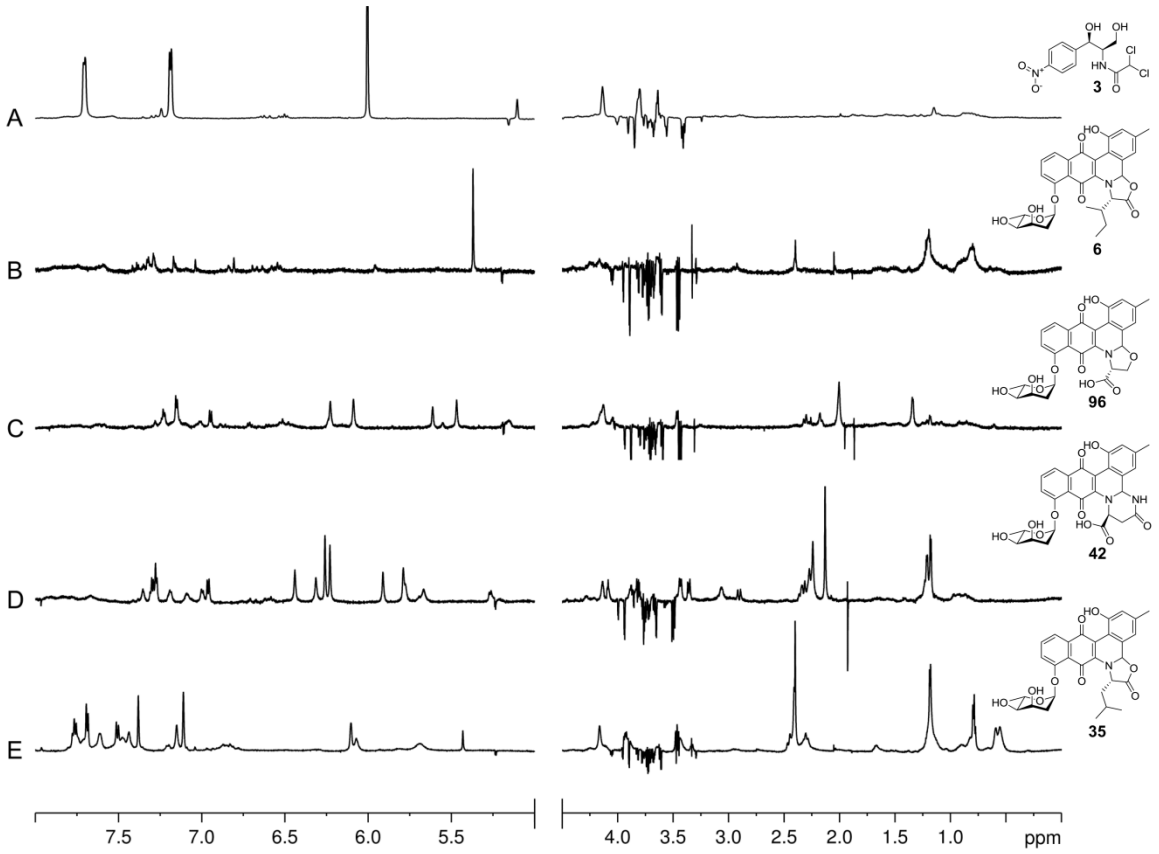

Figure 24. Selective JadX-jadomycin binding by WaterLOGSY NMR. (*A*-*E*) Stacked WaterLOGSY spectra (700 MHz, 1:9 dPBS/PBS, pH 7.6), with JadX (0.05 mM) in the presence of the non-binding standard D-galactose (2 mM) phased negatively in each case, and (*A*) **3** (2 mM); (*B*) **6** (500 μM); (*C*) **96** (750 μM); (*D*) **42** (750 μM); (*E*) **35** (1 mM).

It was found that JadX was capable of binding a diverse series of jadomycins. Both typical oxazolone ring containing jadomycin (**6** and **35**) and differentially cyclized jadomycins (**96** and **42**) showed interactions with JadX (Figure 24*B*-*E*). Compound **96** possessed excellent water solubility, was easily purified, and was used for all subsequent binding studies. We were confident that the JadX-**96** interaction was specific due to the ability for JadX to bind the selection of jadomycins. Additionally, JadX does not bind benzoic acid, illustrating that the interaction was not dominated by the carboxylic acid present on **96** (Figure 25*B*). More interesting was the unexpected result that JadX bound the disparate antibiotic **3** (Figure 24*A*). To test the specificity of this interaction WaterLOGSY experiments were conducted with JadX in the presence of **3** and a series of other small molecules. In the presence of known non-binders, D-galactose and benzoic acid, JadX showed selective binding to **3** (Figure 24*A* and Figure 25*B*). Even in the

presence of a structural mimic 4-nitrophenyl α-D-glucopyranoside, JadX bound **3** preferentially (Figure 25*C*).

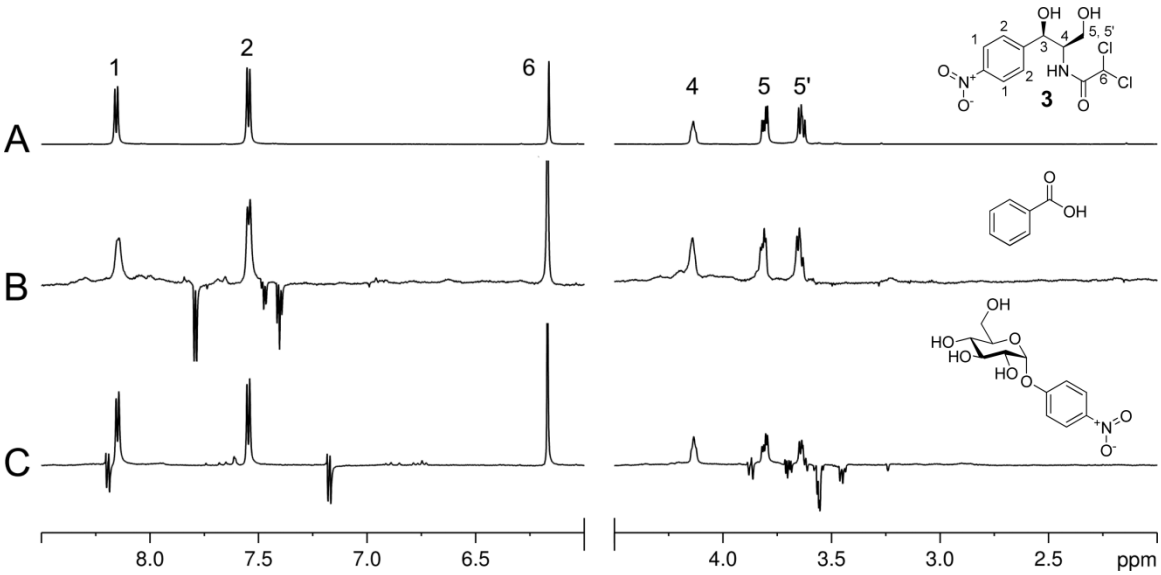

Figure 25. Selective JadX-chloramphenicol (**3**) binding by WaterLOGSY NMR. (*A*) ^{1}H-NMR standard of **3** (2 mM); (*B*-*C*) Stacked WaterLOGSY NMR spectra (700 MHz, 1:9 dPBS/PBS, pH 7.6) with JadX (0.1 mM) illustrating JadX-**3** (2 mM) binding (positive phasing) in the presence of nonbinding compounds (negative phasing) (*B*) benzoic acid (2 mM); (*C*) 4-nitrophenyl α-D-glucopyranoside (2 mM).

This illustrated that the JadX-**3** interaction is specific, and is not dictated by the presence of the para-nitrophenyl group. It also suggests the chlorinated amide "tail" may play an important role in binding. Tan and coworkers have previously shown the jadomycin regulator JadR2 to interact with **3**, **5**, and **6**, resulting in release from the jadomycin gene cluster promoter, up regulating the transcription of *jadR1*.[108] The *jadR1* gene product then goes on to directly inhibit production of **3** by binding a promoter within the **3** gene cluster. The cross-regulation of secondary metabolite biosyntheses in *Streptomyces* is becoming a well-established phenomenon. Since JadX has no documented catalytic activity, is capable of binding the two end product secondary metabolites, and a loss of jadomycin production with an increase in production of **3** is observed with the Δ*jad*X mutant, it suggests an important regulatory or signal receptor function involved in the biosynthetic coordination of these two pathways. This work is the first to identify JadX, and likely other JadX-like homologs, as a new class of antibiotic-receptor proteins involved in the modulation of natural product biosynthesis.

3.2.1 Quantification of JadX-Ligand Binding

With the discovery of **3** and **96** as JadX ligands, focus shifted to measuring ligand affinity. WaterLOGSY is not only a qualitative screening tool for protein-ligand interactions, but can also be implemented to determine dissociation constants (K_D) of protein-ligand systems.[115, 132] This is accomplished through a series of experiments keeping protein concentration constant while varying ligand concentration. Signal intensity can be plotted versus ligand concentration giving a hyperbolic-like curve. Control experiments for ligand in the absence of protein must also be generated to correct the loss of signal intensity associated with free ligand. Taking the difference of these experiments produces a typical dose-response curve (Figure 26*C*) that can be fitted using non-linear regression estimating K_D.[115] Equation 1 is fitted to the data:

$$I = \frac{-I_{max}}{1+(\frac{L}{K_D})} + I_{max} \quad (1)$$

where I_{max} is the maximum intensity of the WaterLOGSY signal, K_D is the dissociation constant being calculated, L is the free ligand concentration, and I is the measured intensity.[115] This equation assumes a single site binding model. Individual peak intensities can be plotted as a function of ligand concentration giving a series of K_D values associated with individual protons.

Signal intensities of **96** and **3** were measured over a range of concentrations in the presence and absence of JadX. Due to solubility issues with both ligands, NMR samples were supplemented with 5% (v/v) DMSO-d_6 to improve natural product solubility. DMSO-d_6 also acted as a non-binding control, phasing in the opposite orientation compared to binding molecules in the resultant spectra (Figure 26*A* and 27*A*). This allowed for easier interpretation of the results as the DMSO-d_6 peak always phased negatively in the presence or absence of JadX. ^{1}H-signals for both natural products that produced acceptable dose response curves were analyzed (Figure 26*C* and 27*C*). For multiplets (doublets and triplets) each peak was analyzed separately, and the listed K_D values represent the average of all peaks within a given multiplet (Figure 26*B* and 27*B*). Calculated values for **96**, ranged from 503 to 2277 μM, with an average value of 1217 μM (Figure 26*B*-*C*). The majority of these values were associated with protons on the polyaromatic backbone. Unfortunately, not all signals could be used. Peaks close to the

HOD had inconsistent signal intensities, in addition, the observed signals are nOes and the changes in intensities were not large enough to accurately generate dose response curves, this may also explain the spread of the K_D values. Many of the sugar proton signals suffered from poor nOe intensities. This may illustrate JadX binding selectively to the aromatic moieties while the L-digitoxose sugar may not be directly involved. Impurities associated with the samples of **96** also consistently phased negatively in the presence and absence of JadX, further illustrating selective protein-ligand interaction (Figure 26*A*). For **3**, all signals, with the exception of H3 and H4 (too close to HOD signal), were suitable for K_D quantification. Values ranged from 897 to 1670 μM with an average of 1181 μM (Figure 27*A*-*C*). These values are similar to the K_D values of **96**, suggesting JadX has similar affinity for both natural products.

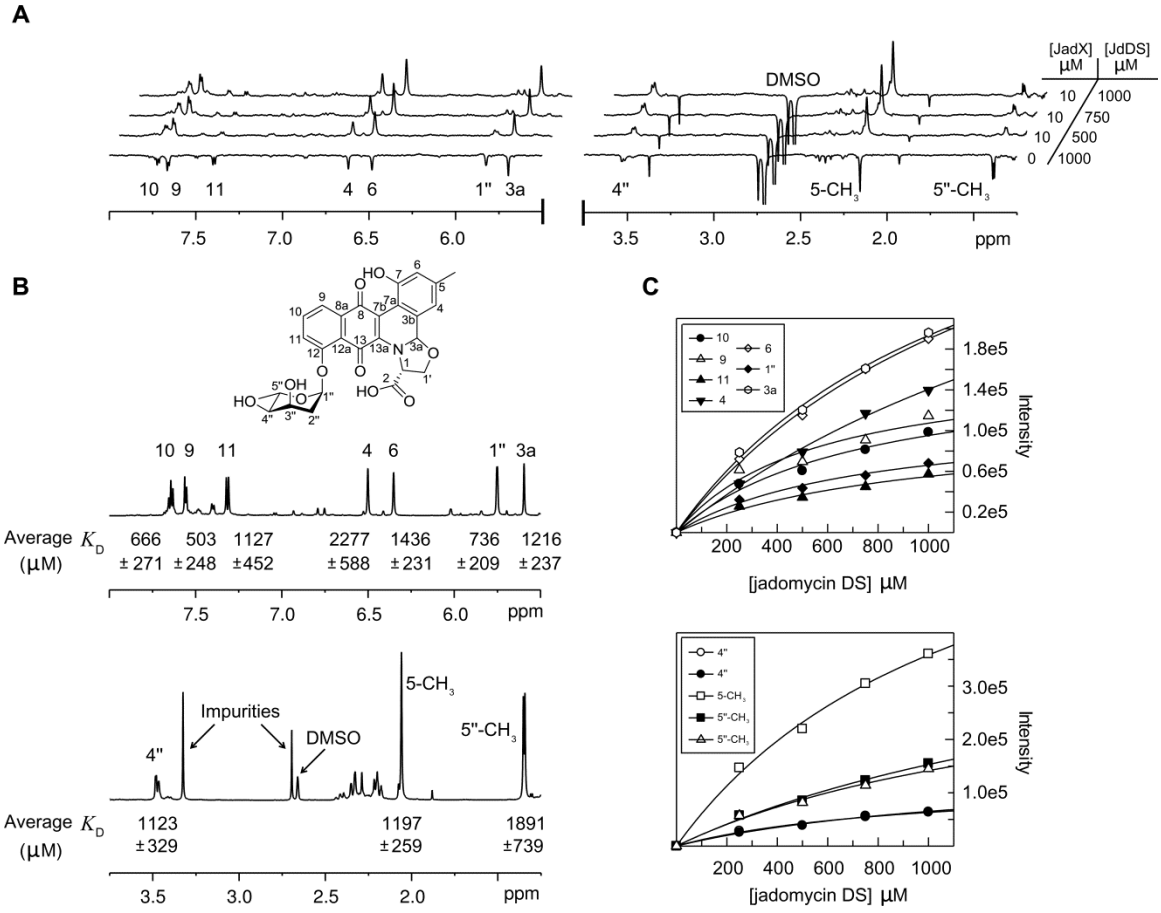

Figure 26. JadX-**96** WaterLOGSY spectra and dose response curves: (*A*) Labeled overlaid WaterLOGSY NMR spectra of varying **96** concentrations in the absence of and presence of JadX. Concentrations are listed to the right of each spectrum. Non-binding compounds are phased negatively and binding compounds are phased positively. (*B*) Labelled structure of **96**, and labeled ^{1}H-NMR spectrum of **96** with the average K_D values associated with each signal listed below. K_D values of doublets and triplets are an average of the K_D values associated with each individual peak. Errors associated with each K_D are listed below. (*C*) Select dose response curves including best fit curves (solid lines) used to calculate K_D values.

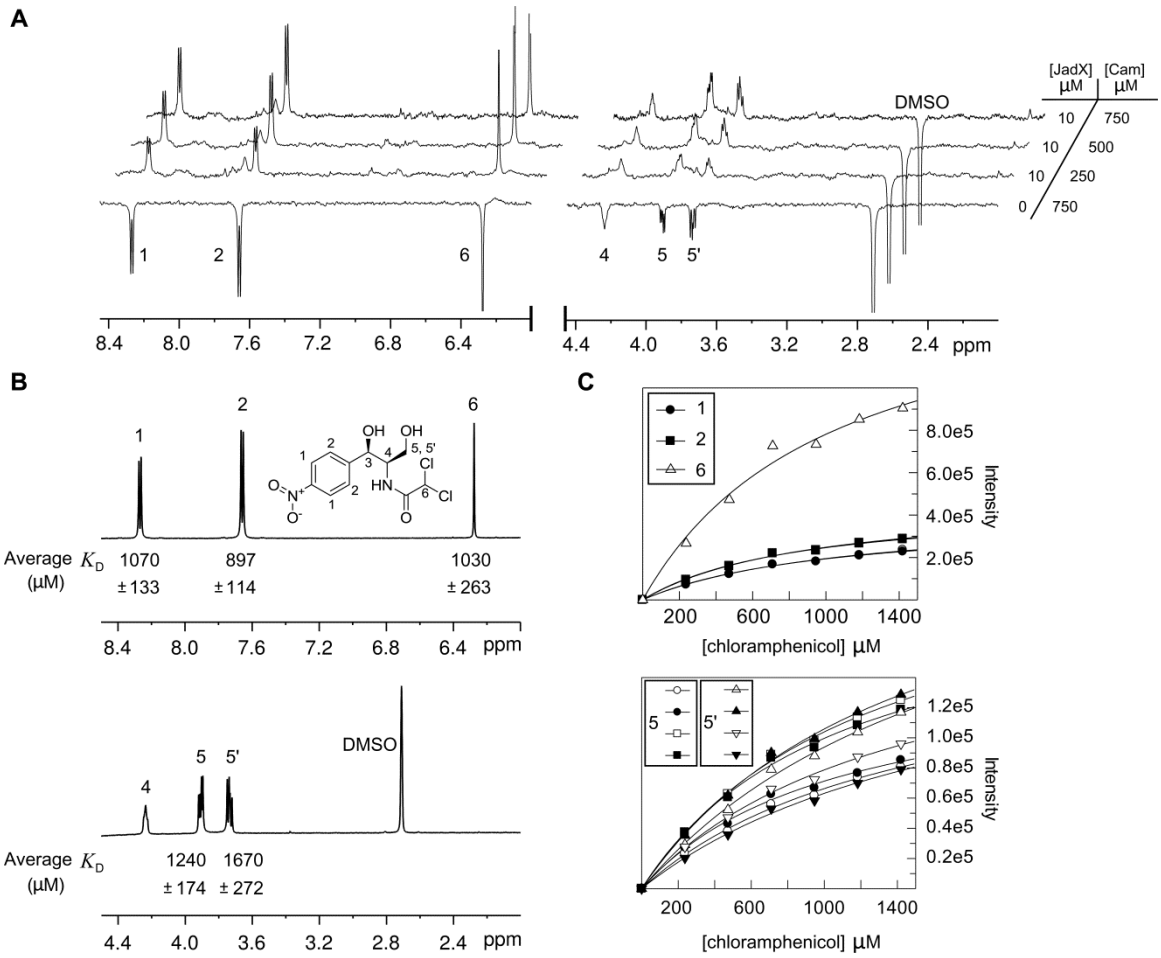

Figure 27. JadX-**3** WaterLOGSY spectra and dose response curves: (*A*) Labeled overlaid WaterLOGSY NMR spectra of varying **3** concentrations in the absence of and presence of JadX. Concentrations are listed to the right of each spectrum. Non-binding compounds are phased negatively and binding compounds are phased positively. (*B*) Labelled structure of **3**, and labeled ^{1}H-NMR spectrum of **3** with the average K_D values associated with each peak listed below. K_D values of doublets and triplets are an average of the K_D values associated with each individual signal. Errors associated with each K_D are listed below. (*C*) Select dose response curves including best fit curves (solid lines) used to determine K_D values.

3.2.2. Competitive Binding Experiments

To test whether **96** and **3** bound in a competitive fashion, JadX WaterLOGSY experiments in the presence of both **96** and **3** were conducted. By keeping one ligand at a high constant concentration while varying the other in the presence of JadX, K_D values can be estimated and compared to values in the absence of the other ligand. If a known binder phases negatively in the presence of high concentrations of another ligand, it

illustrates a competitive binding interaction where both ligands are competing for the same binding site. For both sets of experiments, both natural products appeared to simultaneously bind, with signals from each compound phasing positive in the WaterLOGSY spectra (Appendix 5). Monitoring the signal intensities of the natural product at lower concentrations resulted in typical dose-response curves. For both sets of experiments, K_d values were marginally higher than the single ligand systems suggesting poorer affinity (Table 3).

Table 3. Quantitative comparison of JadX binding.

3 ^{1}H-signal	**3** K_D (μM)	**3** K_D (μM) with **96**[a]	**96** ^{1}H-signal	**96** K_D (μM)	**96** K_D (μM) with **3**[b]
Total Avg.[c]	1181 ± 161	N/A	**Total Avg.**	1217 ± 395	N/A
1	1070 ± 133	1649 ± 405	**3a**	1216 ± 237	2262 ± 1232
2	897 ± 114	1323 ± 312	**6**	1436 ± 231	2534 ± 973
5′	1240 ± 272	1359 ± 306	**4**	2277 ± 588	5441 ± 4082
6	1670 ± 263	1374 ± 270	**5-CH$_3$**	1197 ± 259	2810 ± 1558
Avg.[d]	1219 ± 208	1426 ± 327	**Avg.**	1532 ± 361	3262 ± 2321

[a]K_D values associated with JadX binding **3** in the presence of **96** (1500 μM); [b]K_D values associated with JadX binding **96** in the presence of **3** (2000 μM); [c]Total Avg. represents the average K_D values calculated for the individual ligands; [d]Avg. K_D values calculated from the usable peaks listed in the competitive experiments.

The fact that both ligands appear to bind JadX simultaneously may be explained using a non-competitive binding model in which each ligand has a distinct binding site and binding is independent of one another. The dual binding may also be an artifact of the NMR experiment. The first natural product could bind, receive the magnetization transfer from the protein, then leave the binding pocket opening the site for the second natural product, resulting in both phasing positively. Unfortunately, this ligand-observed binding approach does not conclusively determine the presence of several binding sites or identify if ligands interact with different residues on the protein.

3.3. Protein Observed Binding

To complement the WaterLOGSY data, and to identify if **3** and **96** interact differentially with JadX, K_D determinations using ^{1}H-^{15}N HSQC chemical shift perturbations were examined. Labeled ^{15}N-JadX-His$_6$ was prepared and purified according to literature precedent.[133] At pH 7.6 there were few ^{1}H-^{15}N HSQC cross peaks. To address this, the pH of the PBS was dropped to pH 6.6 to slow H-D exchange. To ensure no appreciable loss

in binding affinity associated with the pH change, ^{15}N-JadX-**3** WaterLOGSY binding experiments were conducted at both pH values. It was found that ^{15}N-JadX bound **3** at both pHs, with minimal loss in signal intensities (Figure 28).

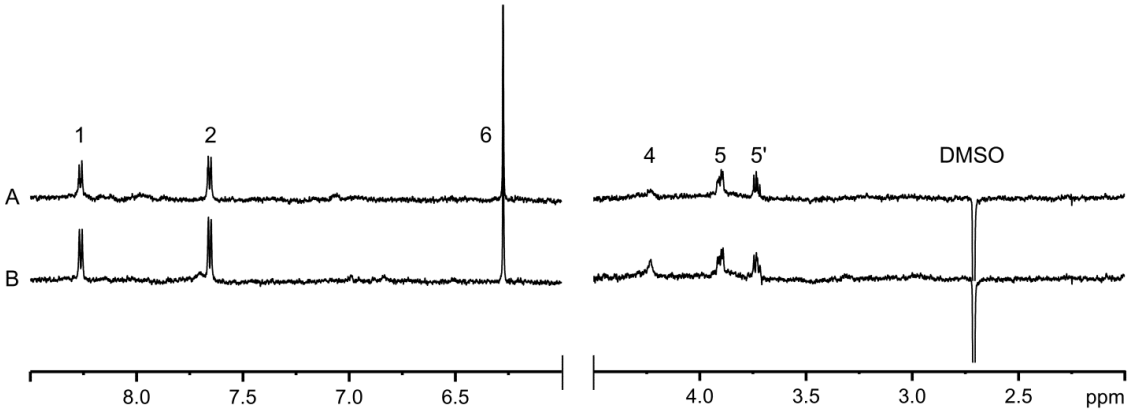

Figure 28. Comparing JadX-**3** binding at different pH; WaterLOGSY NMR spectra (10% dPBS, 85% PBS, 5% DMSO-d_6) of **3** (750 μM) in the presence of JadX (10 μM) showing similar signal intensities at (A) pH 6.6 and (B) pH 7.6.

With WaterLOGSY results similar at pH 6.6 and pH 7.6, a series of ^{1}H-^{15}N HSQC titration experiments were recorded with ^{15}N-JadX in the presence of increasing concentrations of **3** or **96**. In both series of HSQC titrations, different ^{1}H-^{15}N-JadX cross-peaks were observed to shift. Thus, the cross peaks that shifted in the presence **96** were different to those associated with **3** binding (Figure 29*A*-B). Unfortunately, none of the induced chemical shift perturbations associated with **3** were large enough to accurately measure K_D values (Figure 29*A*). Varying the **96** concentration resulted in a more pronounced shift in the observed cross peaks (Figure 29*B*), with one signal (Figure 29*C*) undergoing a significant chemical shift change of 30-40 Hz between the no ligand control and the maximum ligand:protein (3:1) ratio (Figure 29*B*). Plotting the $\Delta\delta_{obs}$ as a function of ligand concentration gave a typical protein-ligand binding saturation curve which was fit using non-linear regression (Figure 29*D*) to equation 2:

$$\Delta\delta_{\mathrm{obs}} = \Delta\delta_{\mathrm{max}} \frac{([P]_t+[L]_t+K_D)-[([P]_t+[L]_t+K_D)^2-4[P]_t[L]_t]^{1/2}}{2[P]_t} \quad (2)$$

where $\Delta\delta_{obs}$ is the observed change in chemical shift, $\Delta\delta_{max}$ is the maximum shift change, $[P]_t$ is the total protein concentration, $[L]_t$ is the total ligand concentration, and K_D is the dissociation constant.[134]

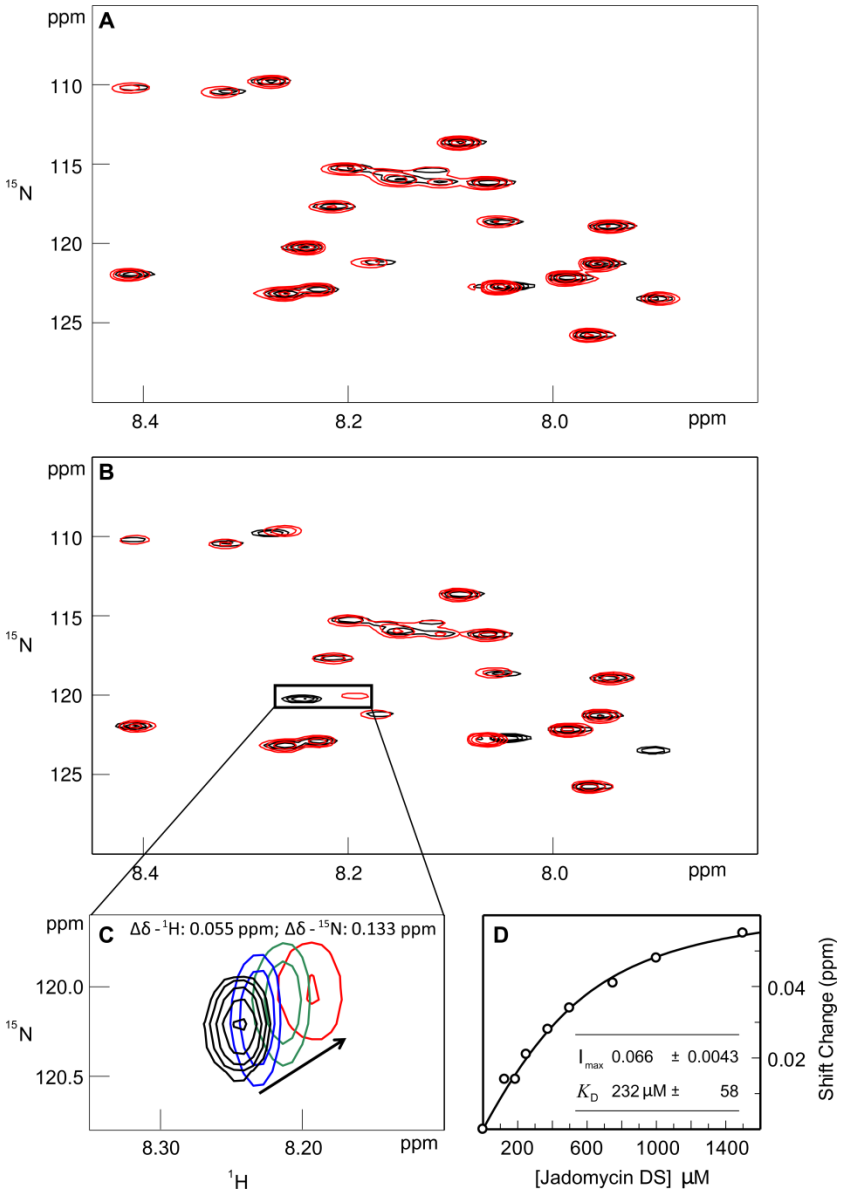

Figure 29. JadX-ligand binding by protein observed chemical shift perturbation: (*A*) Overlaid ^{15}N-^{1}H HSQC of ^{15}N-JadX (500 µM), pH 6.6, in the absence (black) and presence (red) of **3** (2000 µM). (*B*) Overlaid ^{15}N-^{1}H HSQC of ^{15}N-JadX (500 µM), pH 6.6, in the absence (black) and presence (red) of **96** (1500 µM). (*C*) Overlaid ^{15}N-^{1}H HSQC of ^{15}N-JadX (500 µM) in the presence of varying concentrations of **96**: 0 µM (black), 187.5 µM (blue), 500 µM (green), and 1500 µM (red). The maximum ^{1}H and ^{15}N Δδ values are shown. (*D*) Representative dose response curve with best-fit curve (solid line). The estimated K_D and maximum Δδ (I_{max}) are shown.

The measured K_D value of 232 μM was lower than that observed with the WaterLOGSY methodology. K_D values determined by WaterLOGSY have been reported to underestimate affinity due to experimental variables.[135, 136] Additionally, pH differences between the two experiments may have affected the apparent K_D values.

3.4. Further Discussion

Functional characterization of proteins involved in natural product biosynthesis with little or no sequence homology to current protein sequence databases remains a challenging functional scientific problem. Modeling of these pathways is very important from an industrial perspective as strong understanding of the enzymatic and regulatory systems in a biosynthetic pathway facilitates bioengineering approaches to improve yields, shift production from one natural product to another, or biosynthesize new derivatives. Finding that *jadX* disruption led to a complete loss of production of **96** suggests a more important role for JadX in jadomycin biosynthesis than previously established.[67] A similar finding associated with the JadX homologue MmyY, coded for in the methylenomycin gene cluster has been observed. A disruption of *mmyY* with an apramycin resistance cassette (Δ*mmyY::aac(3)IV*) resulted in complete loss of production of methyleneomycin.[121] This further illustrates that these "JadX-like" homologs play vital roles in their respective biosynthetic pathways. Disruption of *jadX* also led to a switch in natural product biosynthesis from **96** to **3** suggesting a role in regulation of both natural products. Using NMR binding methodologies, JadX-ligand binding was identified and quantified. JadX was found to selectively bind both the jadomycins and **3**.

There are 6 known regulatory genes in jadomycin biosynthesis (*jadW1*, *W2*, *W3*, *R1*, *R2, R3,* and *R**) located at the beginning and end of the jadomycin gene cluster.[67, 122, 137-139] The cluster-situated regulatory gene products of *jadR1* and *jadR2* are involved in cross-regulation of jadomycin and **3** biosynthesis and are located upstream of the polyketide synthase structural genes.[108, 140] The *jadX* gene, located upstream of the sugar biosynthetic genes, likely codes for a key biosynthetic regulatory or signalling protein.

CHAPTER 4: EXPERIMENTAL

4.1. General Methods

All reagents were purchased from commercial sources and used without further purification. Solvents used for all reactions and chromatographic methods were HPLC grade unless otherwise stated. Flash chromatography was performed using a SP1™ unit (Biotage®) using pre-packed normal phase silica columns (40 g or 80 g) from SiliCycle®. Glass-backed thin layer chromatography (TLC) plates (SiliCycle®) layered with 250 μm silica were used to monitor reaction progress and assess purity of compounds. Jadomycin and boron-dipyrromethene (BODIPY) analogues required no visualization reagents or ultraviolet (UV) light as the compounds were highly colored. Compounds **59-61** and **63** were visualized under 254 nm and 365 nm UV-light. All other compounds were visualized using potassium permanganate dip (1.5 g $KMnO_4$, 10 g K_2CO_3, 125 mg NaOH, 200 mL H_2O) followed by heating. All reported R_f values were determined using 250 μm silica TLC plates. Preparative TLC was performed using 20 × 20 cm glass-backed plates (SiliCycle®) layered with 1000 μm or 2000 μm silica. Using the appropriate solvent mixture, the TLC plates were developed, then allowed to dry, then developed and dried again. This process was repeated until good separation was observed (~2-4 cycles). Bands of interest were scraped off the glass backing and eluted using the same solvent used for development. Size-exclusion chromatography was accomplished using Sephadex™ LH-20 (GE Healthcare) resin. All compounds were characterized by liquid chromatography tandem-mass spectrometry (LC-MS/MS), high resolution mass spectrometry (HRMS), and 1D- and 2D-nuclear magnetic resonance (NMR) spectroscopy. Low resolution LC-MS/MS spectra were obtained on an Applied Biosystems hybrid triple quadrupole linear ion trap (2000Qtrap) mass spectrometer using an electrospray ionization (ESI) source. This was coupled with an Agilent 1100 high performance liquid chromatography (HPLC) instrument with a Phenomenex Kinetex 2.6 μm Hilic column (150 mm × 2.10 mm). Samples were prepared in methanol and 5 μL aliquots were injected onto the column, unless otherwise stated. Elution of compounds was accomplished using an isocratic gradient of (7:3) CH_3CN : 2 mM ammonium acetate in water (pH 5.5) with a flow rate of 120 μL min^{-1} for 10 min. For all jadomycins, the

instrument was used in positive mode (ESI+). Enhanced product ionization (EPI) was performed with a capillary voltage of +4500 kV, declustering potential +80 V, and curtain gas 10 arbitrary units. Enhanced product ionization (EPI) scans were conducted over a range of 300-900 *m/z* scanning for $[M+H]^+$ and the appropriate jadomycin fragmentation. Scans were conducted using two steps, 300 amu to 320 amu (0.005 s) and 300 amu to 900 amu (0.150 s). Spectra were analyzed using Analyst software version 1.4.1 (Applied Biosystems). HRMS traces of all jadomycins were recorded on a Bruker Daltonics MicroTOF Focus Mass Spectrometer using an ESI+ source, with the exception of **58e** which required ESI-. All ultra-violet-visible (UV-vis) spectroscopy was carried out on a SpectraMax Plus Microplate Reader (Molecular Devices), and analyzed using SoftMax® Pro Version 4.8 Software. Samples were dissolved in methanol placed in a quartz cuvette (1 cm path length) and scanned over a range of 280-700 nm using 1 nm intervals. Two separate dilutions were used in each case (concentrations are listed with the appropriate characterization data) to calculate a series of extinction coefficients (ε) from several maximal absorbance wavelengths (λ_{max}). NMR analyses of activated acids **59-64** and selective rotating frame nuclear Overhauser effect spectroscopy (ROESY) of **58a-58f** were performed on a Bruker AV 500 MHz Spectrometer (^{1}H: 500 MHz, ^{13}C: 125 MHz) equipped with an auto-tune and match (ATMA) broadband observe (BBFO) SmartProbe located at the Nuclear Magnetic Resonance Research Resource (NMR-3) facility (Dalhousie University) unless otherwise stated. NMR spectra of all jadomycin analogues were recorded using a Bruker AV-III 700 MHz Spectrometer (^{1}H: 700 MHz, ^{13}C: 150 MHz) equipped with an ATMA 5 mm TCI cryoprobe located at the Canadian National Research Council Institute for Marine Biosciences (NRC-IMB) in Halifax, Nova Scotia. All spectra were recorded in MeOD-d_4, $CDCl_3$, or CD_2Cl_2. Appropriate solvents used in each case can be found with the accompanying supplemental NMR-spectra. Chemical shifts (δ) were given in ppm, and calibrated to residual solvent peaks (MeOD: 3.31 ppm; $CDCl_3$: 7.24 ppm; CD_2Cl_2: 5.32 ppm). Structural characterization and signal assignments were accomplished using ^{1}H-NMR chemical shifts and multiplicities, and ^{13}C-NMR chemical shifts. In addition, ^{1}H-^{1}H correlated spectroscopy (COSY), ^{1}H-^{13}C heteronuclear single quantum coherence (HQSC) NMR, ^{1}H-^{13}C heteronuclear multiple

bond correlation (HMBC) NMR, and ^{1}H-^{1}H ROESY experiments were used in the NMR analyses.

4.1.1. HPLC Method #1

HPLC analyses of all UV active compounds, with the exception of **58d**, were performed on a Hewlett Packard Series 1050 instrument with an Agilent Zorbax 5 μm Rx-C18 column (4.6 × 150 mm). Elution of the compounds was monitored at an absorbance of 254 nm using an isocratic gradient of 9:1 (A:B) over 0.5 min followed by an increasing linear gradient from 9:1 (A:B) to 4:6 (A:B) over 7.5 min, followed by an isocratic gradient of 4:6 (A:B) for an additional 2 min. This was then followed by a decreasing linear gradient from 4:6 (A:B) to 9:1 (A:B) over 1 min, ending with an isocratic gradient of 9:1 (A:B) over 4 min (total time 15 min; flow rate of 1 ml/min). Buffer A was an aqueous buffer comprised of 12 mM Bu_4NBr, 10 mM KH_2PO_4, and 5% HPLC grade CH_3CN (pH 4.0) and B was HPLC grade CH_3CN.

4.1.2. HPLC Method #2: Compound 58d

HPLC of jadomycin analogue **58d** was performed on a Hewlett Packard Series 1050 instrument with an Agilent Zorbax 5 μm Rx-C18 column (4.6 × 150 mm). Elution of the compound was monitored at an absorbance of 254 nm using an isocratic gradient of 9:1 (A:B) over 0.5 min followed by an increasing linear gradient from 9:1 (A:B) to 2:8 (A:B) over 4.5 min, followed by an isocratic gradient of 2:8 (A:B) for an additional 15 min. This was then followed by a decreasing linear gradient from 2:8 (A:B) to 9:1 (A:B) over 1 min, ending with an isocratic gradient of 9:1 (A:B) over 9 min (total time 30 min; flow rate of 1 ml/min). Buffer A was an aqueous buffer comprised of 12 mM Bu_4NBr, 10 mM KH_2PO_4, and 5% HPLC grade CH_3CN (pH 4.0) and B was HPLC grade CH_3CN.

4.2. *S. venezuelae* ISP5230 VS1099 Media and Growth Conditions

All media was prepared with distilled water and autoclaved at 120 °C for 20 minutes prior to use unless otherwise stated. Two hundred fifity (250) mL fractions of broth solutions were prepared into 1 L glass Erlenmeyer flasks. Twenty five (25) mL fractions of broth solutions were prepared in 125 mL Erlenmeyer flasks. One hundred twenty five

(125) mL fractions of MYM agar were prepared in 250 mL glass Erlenmeyer flasks. Agar solutions were supplemented with 50 μgmL^{-1} apramycin sulfate before being poured into standard petri dishes while molten. All media was adjusted to pH 7 or 7.5 with 5 M NaOH or 5 M HCl as required.

All jadomycin fermentations were carried out using modified conditions for production previously established in the Jakeman laboratory.[69] *S. venezuelae* ISP5230 VS1099 was maintained in 20% glycerol stock solution stored at -70 °C. Colonies were grown on MYM agar [maltose (4 g/L), yeast extract (4 g/L), malt extract (10 g/L), agar 15 (g/L), pH 7.0] at 30 °C for a period of 1-3 weeks before use in jadomycin productions. Fresh MYM liquid media [maltose 4 g/L, yeast extract 4 g/L, malt extract 10 g/L, (pH 7.0)] was inoculated with a 1 cm^2 lawn of surface growth from the MYM agar plates. Growths were incubated at 30 °C for 16-20 hrs at 250 RPM. The cells were centrifuged at 4 °C (3750 RPM) for ~30 min. The supernatant was decanted and the cell pellets were washed twice with 20 mL MSM, re-pelleting in between each wash. MSM media was comprised of (per litre): $MgSO_4$ (0.4 g), MOPS (1.9 g), salt solution (9 mL of 1% w/v NaCl and 1% w/v $CaCl_2$), $FeSO_4 \bullet 7H_2O$ (4.5 mL of 0.2% w/v) and trace mineral solution (4.5 mL). The trace mineral solution contained (per litre): $ZnSO_4 \bullet 7H_2O$ (880 mg), $CuSO_4 \bullet 5H_2O$ (39 mg), $MnSO_4 \bullet 4H_2O$ (6.1 mg), H_3BO_3 (5.7 mg) and $(NH_4)_6Mo_7O_{24} \bullet 4H_2O$ (3.7 mg). The cell pellet was re-suspended in 10-15 mL MSM. This cell solution was added to the production media (MSM-amino acid solution) to an OD_{600} of ~0.6. Production media consisted of MSM media supplemented with an amino acid (L-ornithine, D-ornithine, or L-lysine) as the sole nitrogen source to a final concentration of 60 mM. The amino acid was dissolved in the MSM media and the pH was adjusted to 7.5 with NaOH and autoclaved. Stock glucose (30% w/v) and phosphate (9 mM, 10.5 g K_2HPO_4, 4.5 g KH_2PO_4 per litre) solutions were prepared and sterilized separately to avoid precipitation. Stock solutions were added aseptically to the MSM production media to final concentrations of glucose 33 mM, and phosphate 0.1 mM. For jadomycin AVA (**67**) growths, MSM without amino acid (3 × 66 mL in 250 mL flasks) was supplemented with glucose (33 mM) and phosphate (50 μM) and a 6 M filter sterilized solution of 5-aminovaleric acid to a final concentration of 60 mM before being inoculated with the pre-growth *S. venezuelae* ISP5230 VS1099 cell suspension to an initial OD_{600} of 0.6. The 5-

aminovaleric acid solution was prepared in MSM without amino acid to a concentration of 6 M and pH was adjusted to pH 7.5 prior to filter sterilization. Growths were immediately ethanol shocked with 100% ethanol (3% v/v) and incubated at 30 °C with agitation (250 RPM) for 48 hours. After 24 hours, the pH of the media was readjusted to a pH of 7.5. Bacterial growths were monitored by absorbance at 600 nm (OD_{600}), jadomycin and colored natural product production was monitored by absorbance of clarified growth media at 526 nm. Absorbance and optical density values greater than 1.0 were recorded by appropriately diluting solutions to values between 0.1 and 0.9 to assure accuracy.

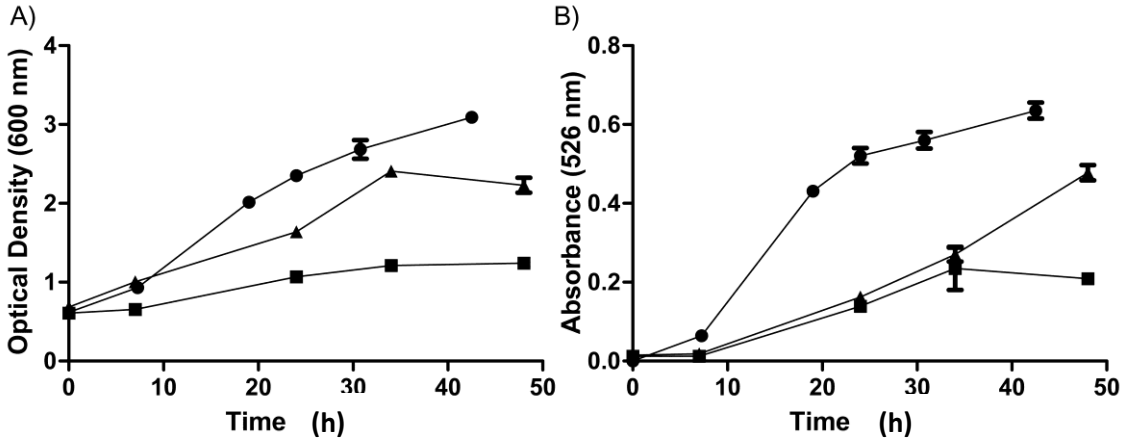

Figure 30. Absorbance plots of *S. venezuelae* ISP5230 VS1099 growths using **54**, **55** and **65** at 60 mM. (*A*) *S. venezuelae* ISP5230 VS1099 growth curves measured at 600 nm (OD_{600}) in the presence of L-ornithine (●), D-ornithine (■), and 5-aminovaleric acid (▲) as the sole nitrogen sources; (*B*) *S. venezuelae* ISP5230 VS1099 growth curves measured at 526 nm (Abs_{526}) estimating production of colored compounds in the presence of L-ornithine (●), D-ornithine (■), and 5-aminovaleric acid (▲) as the sole nitrogen sources.

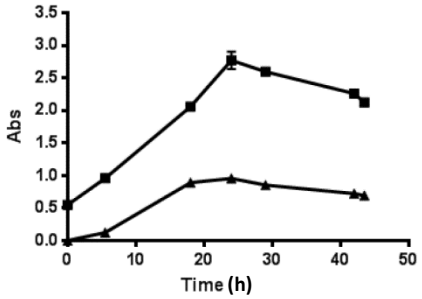

Figure 31. Absorbance plots of *S. venezuelae* ISP5230 VS1099 growths using **56** at 60 mM. Cell density measured at 600 nm (OD_{600}) (■), and jadomycin production at 526 nm (Abs_{526}) (▲).

4.2.1. Labeled ^{15}N-L-lysine growths

S. venezuelae ISP5230 VS1099 was grown as previously described. MSM (25 mL) was supplemented with 1 mL filter sterilized solutions of either ε-^{15}N-L-lysine (1 M) or α-^{15}N-L-lysine (750 mM) in MSM (pH 7.5) to final concentrations of 60 mM and 45 mM respectively, prior to inoculation and ethanol shock. After the typical 48 hour growth period, cells were filtered from the solution and samples of the clarified growth media were used without further purification for all LC-MS/MS analyses.

4.2.2. Crude Growth Purification

Bacterial cells were removed via suction filtration through Whatman No. 5 filter paper, followed by 0.45 μm then 0.22 μm Millipore Durapore® membrane filters. The clear media was passed through a reversed-phase SiliCycle® phenyl column (70 g for large scale growth of compounds **58** and **70** or 2 g for small scale growths of **66** and **67**), and washed with distilled water until flow through was colorless [~4-8 L (70 g column) or ~500-1000 mL (2 g column)] to remove all water soluble material. Remaining material was eluted with 100% methanol and dried *in vacuo*. No further extractions were performed on **67**, methodology for purification can be found with the accompanying compound information. For **58, 66**, and **70** the crude mixtures were dissolved in minimal H_2O and extracted with equal volumes of EtOAc three times. For **58**, the aqueous layer was fractioned into 4 equal aliquots (corresponding to ~ 500 mL of growth solution each) and dried *in vacuo* yielding an aqueous extract of ~100 mgL^{-1}. For purposes of derivatization of **58**, the aqueous layer was not purified further. For purposes of characterizing **58** the crude extracts were purified further. Methodology for purification can be found with the accompanying compound information. For **66**, the aqueous layer was dried *in vacuo* yielding an aqueous extract of ~20 mgL^{-1}. For purposes of derivatization of **66**, the aqueous layer was not purified further. For **70**, the organic layer layer was dried in *vacuo* yielding an organic extract of ~40 mgL^{-1}. For purposes of characterizing **58** the crude extracts were purified further, methodology for purification can be found with the accompanying compound information.

4.3. Succinimidyl Ester Preparation (Compounds 59-64)

4.3.1. Phenoxyacetic acid *N*-hydroxysuccinimide ester (59)

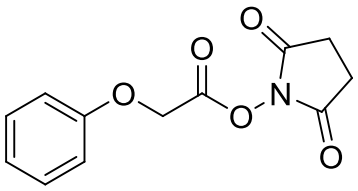

Compound **59** was purchased and used without further purification.

4.3.2. (2-Naphthoxy)acetic acid *N*-hydroxysuccinimide ester (60)

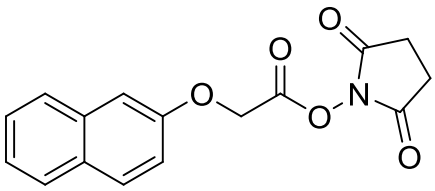

Compound **60** was synthesized using modified literature methodology.[88] *N*-hydroxysuccinimide (289 mg, 2.51 mmol) was added to a 50 mL round bottom flask with a stir bar, and placed under an N_2 atmosphere. (2-naphthoxy)acetic acid (524 mg, 2.59 mmol) was dissolved in 10 mL of anhydrous EtOAc under an N_2 atmosphere and added, with gentle stirring, to the flask containing *N*-hydroxysuccinimide and cooled to 0 °C. A solution of *N*,*N*′-dicyclohexylcarbodiimide (DCC) (506 mg, 2.45 mmol) dissolved in 10 mL anhydrous EtOAc was then added drop-wise to the mixture with gentle stirring. Upon complete addition of DCC, the reaction flask was removed from the ice bath and the reaction was allowed to proceed for 16 h. The reaction mixture was filtered through #5 Whatman filter paper to remove 1,3-dicyclohexylurea (DCU) precipitate, and the filtrate was dried. The residue was then suspended in 50 mL of anhydrous ether, filtered, and washed with an additional 75 mL of ether (3 × 25 mL). The material was dried, yielding **60** as a white powder (688 mg, 92% yield). The pure material was stored at 4 °C under desiccation and used without further purification. ^{1}H NMR ($CDCl_3$, 700 MHz) δ: 7.80-7.78 (m, 3 × CH), 7.47 (t, *J* = 7.49 Hz), 7.38 (t, *J* =7.49 Hz), 7.23 (dd, *J* = 9.0 Hz, 2.5 Hz), 7.19 (d, *J* = 2.5 Hz), 5.10 (s), 2.85 (bs); ^{13}C NMR ($CDCl_3$, 176 MHz) δ: 168.8, 164.7, 155.2, 134.3, 130.1, 129.8, 127.8, 127.3, 126.8, 124.6, 118.4, 107.6, 63.4, 25.7 ppm. These data are consistent with literature values.[88]

4.3.3. Benzoic acid *N*-hydroxysuccinimide ester (61)

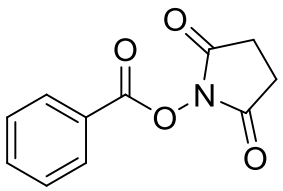

Compound **61** was synthesized using modified literature methodology.[88] *N*-hydroxysuccinimide (1.064 g, 9.2 mmol) was added to a 50 mL round bottom flask with a stir bar, and placed under an N_2 atmosphere. Benzoic acid (1.060 g, 8.7 mmol) was dissolved in 15 mL of anhydrous EtOAc under an N_2 atmosphere and added, with gentle stirring, to the flask containing the *N*-hydroxysuccinimide and cooled to 0 °C. A solution of DCC (3.586, 17.0 mmol) dissolved in 15 mL anhydrous EtOAc was added drop-wise to the mixture with gentle stirring. Upon complete addition of DCC, the reaction flask was removed from the ice bath and the reaction was allowed to proceed for 16 h. The reaction mixture was filtered through #5 Whatman filter paper to remove DCU precipitate, and the filtrate was dried. The residue was suspended in 50 mL of anhydrous ether, filtered, and washed with an additional 75 mL of ether (3 × 25 mL). The material was dried, yielding **61** as a white powder (1.413 g, 74% yield). The material was stored at 4 °C under desiccation and used without further purification. ^{1}H NMR ($CDCl_3$, 700 MHz) δ: 8.14 (d, J = 8.3 Hz,), 7.68 (t, J = 7.4 Hz), 7.52 (t, J = 8.3 Hz), 2.91 (bs); ^{13}C NMR ($CDCl_3$, 176 MHz) δ: 169.4, 162.0, 135.1, 130.7, 129.0, 128.7, 125.2, 25.8 ppm. These data are consistent with literature values.[88]

4.3.4. Nonoic acid *N*-hydroxysuccinimide ester (62)

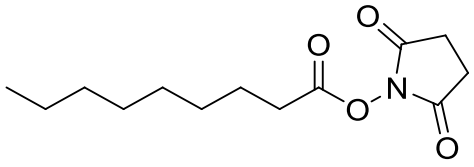

Compound **62** was synthesized using modified literature methodology.[90] *N*-hydroxysuccinimide (0.7433, 6.4 mmol) was added to a 50 mL round bottom flask with a stir bar, and placed under an N_2 atmosphere. Nonoic acid (1.043 g, 6.3 mmol) was dissolved in 20 mL of DCM under an N_2 atmosphere and added, with gentle stirring, to the flask containing the *N*-hydroxysuccinimide and cooled to 0 °C. A solution of DCC

(2.59 g, 12.6 mmol) dissolved in 20 mL anhydrous CH_3CN was added drop-wise to the mixture with gentle stirring. Upon complete addition of the DCC, the reaction flask was removed from the ice bath and the reaction was allowed to proceed for 16 h. The reaction mixture was filtered through #5 Whatman filter paper to remove DCU precipitate, and the filtrate was dried. The reaction mixture was brought up in minimal DCM (~ 2 mL) and loaded onto a 40 g pre-packed normal phase silica column (SiliCycle®), conditioned with 100% hexanes. Material was eluted with a flow rate of 25 mL/min collecting 9 mL fractions. Purification was accomplished using a gradient system, first washing with 1 CV of 100% hexanes followed by a linear gradient from 0% to 50% EtOAc in hexanes over 5 CV, followed finally by an isocratic gradient of 50% EtOAc in hexanes over 5 CV. Fractions were checked by TLC for purity and combined yielding **62** as a white powder (1.255 g, 78% yield). The pure material was stored at 4 °C under desiccation and used without further purification. R_f: 0.67 (1:1 EtOAc:Hexanes), ^{1}H NMR ($CDCl_3$, 700 MHz) δ: 2.83 (bd, J = 13 Hz), 2.59 (t, J = 7.5 Hz), 1.74 (p, J = 7.5 Hz), 1.40 (p, J = 7.5 Hz), 1.33-1.22 (bm, 4 × CH_2), 0.87 (t, 7.0 J = Hz); ^{13}C NMR ($CDCl_3$, 125 MHz) δ: 169.4, 168.9, 31.9, 31.1, 29.2, 29.1, 28.9, 25.7, 24.7, 22.8, 14.2 ppm. These data are consistent with literature values.[90]

4.3.5. SuO-Fmoc (63)

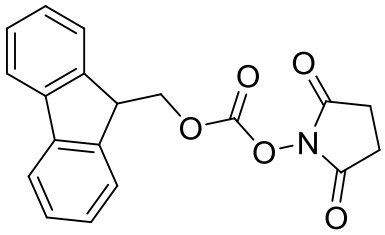

Compound **63** was synthesized using modified literature methodology.[89] *N*-hydroxysuccinimide (450 mg, 3.90 mmol) and diisopropylamine (550 µL, 4 mmol) were dissolved in anhydrous dichloromethane (5 mL) under N_2 at room temperature. The mixture was added drop wise to a solution of Fmoc chloride (1.007 g, 3.89 mmol) in anhydrous dichloromethane (5 mL) under N_2 at 0 °C with stirring over a period of 5 min. Upon completion, the flask was allowed to warm to room temperature, and the reaction mixture was stirred under N_2 for 16 h. The solution was filtered, and the precipitate was washed with 20 mL dichloromethane. The filtrate and washings were combined and

washed with, in order, 15 mL of 10% (w/v) citric acid in distilled water, 15 mL of 10% sodium bicarbonate (w/v) in distilled water, and 3 × 15 mL of distilled water. The organic layer was dried with anhydrous magnesium sulfate and filtered. The dichloromethane was removed *in vacuo* to give compound **63** (1.115 g, 85% yield) as a light yellow powder. The pure material was stored at 4 °C under desiccation and used without further purification. ^{1}H NMR ($CDCl_3$, 500 MHz) δ 7.78 (d, 2H, *J* = 7.6 Hz), 7.63 (d, 2H, *J* = 7.6 Hz), 7.44 (t, 2H, *J* =7.5 Hz), 7.35 (dt, 2H, *J* = 7.5 Hz, 1.0 Hz), 4.58 (d,2H, *J* = 7.5 Hz), 4.35 (t, 1H, *J* = 7.4 Hz), 2.81 (bs, 4H); ^{13}C NMR ($CDCl_3$, 126 MHz) δ 168.6, 151.7, 142.6, 141.5, 128.4, 127.6, 125.4, 120.3, 73.1, 46.5, 25.6 ppm. These data are consistent with literature values.[89]

4.3.6. Synthesis of SuO-F-BODIPY (64)

The boron-dipyrromethene (BODIPY) carboxylic acid (**97**) was synthesized by Dr. Deborah A. Smithen according to Scheme 16. The full synthetic methodology can be found in the literature.[86, 141] For the scope of this document, only the final coupling step producing **64** will be discussed.

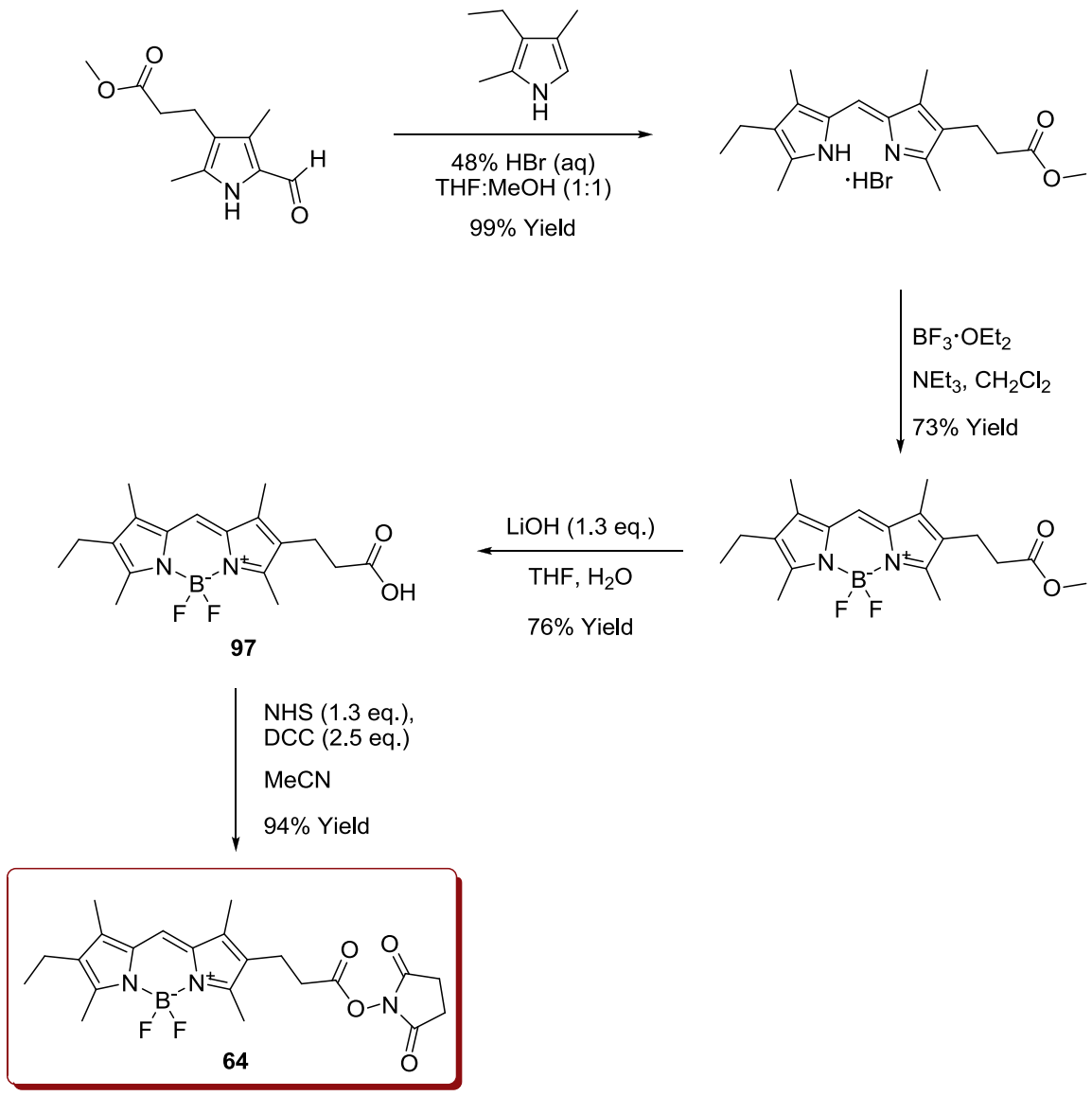

Scheme 16. Synthesis of **64**.

4.3.7. 4,4-Difluoro-1,3,5,7-tetramethyl-2-ethyl-6-(3-propanoic acid)-8-H-4-bora-3a,4a-diaza-s-indacene N-hydroxysuccinimide ester (64)

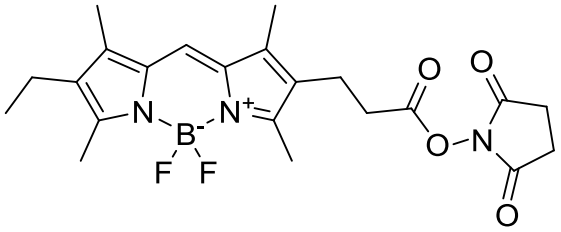

Compound **64** was synthesized using modified literature methodology for similar compounds.[91] An anhydrous solution of *N*-hydroxysuccinimide (45 mg, 0.388 mmol) in CH_3CN (5 mL) was added to a 100 mL round bottom flask containing an anhydrous solution of the **97** (101 mg, 0.287 mmol) in CH_3CN (5 mL) with gentle stirring under an N_2 atmosphere at 0 °C in an ice bath. An anhydrous solution of DCC (146 mg, 0.708 mmols) in CH_3CN (10 mL) was then added drop-wise to the mixture. Upon the complete addition, the flask was taken from the ice bath and allowed to warm to room temperature with gentle stirring for 16 h. The reaction mixture was filtered through a #5 Whatman filter paper disk to remove DCU and the filtrate was dried *in vacuo*. The crude reaction mixture was brought up in minimal DCM (~ 2 mL) and loaded onto a 25 g pre-packed normal phase silica column. Material was eluted with a flow rate of 25 mL/min collecting 9 mL fractions. Purification was accomplished using a gradient system, first washing with 1 CV of 100% DCM followed by a linear increasing gradient from 0% to 20% EtOAc in DCM over 10 CV, followed finally by an isocratic gradient of 20% EtOAc in DCM over 5 CV. Fractions were checked by TLC for purity and combined yielding **64** (120 mg, 94% yield) as a solid red powder. TLC R_f = 0.8 (1:4 EtOAc:DCM); ^{1}H NMR ($CDCl_3$, 500 MHz) δ 6.98 (s), 2.86 (bs), 2.84 (bs), 2.82 (t, *J* = 8.0 Hz), 2.72 (t, *J* = 8.0 Hz), 2.51 (s, 2 × CH_3), 2.38 (q, *J* = 7.6 Hz), 2.20 (s), 2.17 (s), 1.06 (t, 7.6 *J* = Hz); ^{13}C NMR ($CDCl_3$, 125 MHz) δ 169.2, 167.9, 157.0, 153.2, 137.9, 133.3, 132.7, 132.0, 126.0, 119.2, 31.4, 25.7, 19.4, 17.4, 14.6, 12.9, 12.7, 9.8, 9.6 ppm; ^{11}B NMR ($CDCl_3$, 160 MHz) δ 0.87 (t, *J* = 33.4 Hz); ^{19}F NMR ($CDCl_3$, 282 MHz) δ -146.2 (q, *J* = 33.1 Hz) LRMS: 446.4 $(M+H)^+$; HRMS: 468.1882 Found, 468.1867 Calculated for $C_{22}H_{26}BF_2N_3NaO_4$.

4.4. Jadomycin Amide Syntheses, Purification, and Characterization (58a-58f, and 66a)

4.4.1. Jadomycin Oct Phenoxyacetylamide (58a)

Crude **58** (68.2 mg) was dissolved in 15 mL of a 1:1 mixture of CH_3CN:PBS buffer (pH 7.6), and added to compound **59** (63 mg, 0.253 mmol) in a 25 mL round bottom flask drop-wise with gentle stirring. The flask was corked and protected from light, and the reaction was allowed to proceed for 6 h. The reaction mixture was diluted with 15 mL PBS, and extracted with dichloromethane (3 × 50 mL). By TLC analysis, the organic fractions contained the new purple compound of interest. The organic fractions were pooled and dried *in vacuo*. The reaction mixture was brought up in minimal DCM (~ 3 mL) and filtered. Filtrate was applied to a 40 g silica column preconditioned with a 1:1 EtOAc:CH_3CN solution. Material was eluted with a flow rate of 35 mL/min collecting 9 mL fractions. Purification was accomplished using a gradient system comprised of solvent A (1:1 EtOAc:CH_3CN), and solvent B (5:5:1 EtOAc:CH_3CN:H_2O). To start, an initial isocratic gradient step using solvent A (1 CV) was performed. This was followed by a linear increasing gradient from 0% to 100% B over 10 CV, followed finally by an isocratic gradient of 100% B over 7.5 CV. Fractions were checked by TLC for the presence of the compound of interest, combined, and dried yielding 15.2 mg of crude **58a**. Prep TLC was performed twice using the same 5:5:1 EtOAc:CH_3CN:H_2O solvent system yielding 12.6 mg. Final purification was accomplished by size exclusion chromatography (LH-20 resin). Material was eluted using 5:5:1 EtOAc:CH_3CN:H_2O and dried yielding **58a** as a reddish-purple solid (7.0 mg) as a mixture of diastereomers (M_j/M_n = 5/4) by NMR. TLC R_f: 0.46 (5:5:1 EtOAc:CH_3CN:H_2O); HPLC R_t = 9.73 min; NMR data to follow, for labeling scheme see **58a** NMR data table; UV-Vis (4×10^{-4} and 5×10^{-5} M, MeOH): λ_{max} (ε) = 312 (14820), 375 (2943), 523 (1875); LRMS (ESI^+): MS/MS (685) found 685 $[M+H]^+$, 555 $[M+H-digitoxose]^+$, 306 $[M+H-digitoxose-C_{13}H_{15}NO_4]^+$; HRMS ($ESI^+$): 685.2383 Found, 685.2392 Calculated for $C_{37}H_{37}N_2O_{11}$.

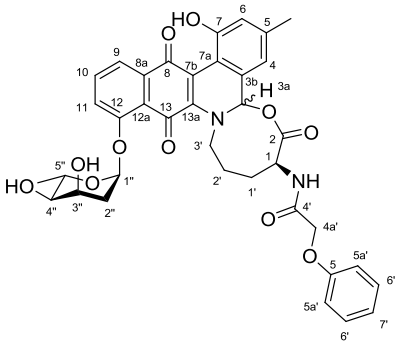

Figure 32. Atom-labeled structure of compound **58a**.

Table 4. Jadomycin Oct phenoxyacetylamide (**58a**) $3a_{Mj}$ diastereomer NMR data.

Position	δ ^{1}H (ppm)	Multiplicity (J(Hz))	δ ^{13}C (ppm)	COSY	HMBC
1	4.39	bs	54.5	1'	3b, 7b
2			176.8		
3a	5.58 (s)	s	92.6	None	1, 4, 7a, 7b, 13, 13a, 3'
3b			115.0		
4	6.74 (s)	s	120.4	5-CH_3, 6	3a, 5-CH_3, 6, 7a
5			141.3		
5-CH_3	2.34 (s)	s	21.1	4, 6	4, 5, 6
6	6.82 (s)	s	120.6	4, 5-CH_3	3b, 5-CH_3, 7, 7a, 7b
7			154.8		
7-OH					
7a			114.4		
7b			130.2		
8			183.3		
8a			136.7		
9	7.82	d (7.6)	121.4	10	8, 8a, 10
10	7.71	t (8.0)	136.7	9, 11	8a, 9, 11, 12
11	7.52	d (8.2)	120.6	10	9, 10, 12, 13
12			155.8		
12a			120.6		
13			185.7		
13a			153.1		
1'	1.81, 2.01	bm	30.5	2'	none
2'	1.69, 1.74	bm	28.3	1', 3'	none
3'	3.90, 3.94	bm	54.5	2'	3a, 13a
4'			170.4		
4a'	4.51	s	68.3	none	4', 5'
5'			159.1		
5a'	6.92	d (8.2)	115.9	6'	5', 5a', 7'
6'	7.14	t (8.2)	130.6	5a', 7'	5', 6'
7'	6.84	t (7.3)	122.9	6'	5a'
1''	5.94	d (3.0)	96.3	2''	3'', 5''
2''	2.19	dd (15.2, 3.9)	36.3	1'', 3''	3'', 4''
2''	2.42	bt (13.2)	36.3	1'', 3''	3'', 4''
3''	4.08	m	68.2	2'', 4''	none
3''-OH					
4''	3.94	m	74.1	3'', 5''	none
4''-OH					
5''	3.28	obscured	66.6	4'', 5''-CH_3	none
5''-CH_3	1.22	d (6.8)	18.2	5''	4'', 5''

Table 5. Jadomycin Oct phenoxyacetylamide (**58a**) $3a_{Mn}$ diastereomer NMR data.

Position	δ ^{1}H (ppm)	Multiplicity (J(Hz))	δ ^{13}C (ppm)	COSY	HMBC
1	4.39 (bs)	bs	54.5	1'	3b, 7b
2			176.8		
3a	5.57 (s)	s	92.3	None	1, 4, 7a, 7b, 13, 13a, 3'
3b			118.9		
4	6.75 (s)	s	120.4	5-CH_3, 6	3a, 5-CH_3, 6, 7a
5			141.7		
5-CH_3	2.34 (s)	s	21.1	4, 6	4, 5, 6
6	6.82 (s)	s	120.6	4, 5-CH_3	3b, 5-CH_3, 7, 7a, 7b
7			154.8		
7-OH					
7a			114.2		
7b			131.1		
8			184.0		
8a			136.7		
9	7.82	d (7.6)	121.4	10	8, 8a, 10
10	7.70	t (8.0)	136.7	9, 11	8a, 9, 11, 12
11	7.51	d (8.2)	121.3	10	9, 10, 12, 13
12			156.4		
12a			120.7		
13			184.1		
13a			151.3		
1'	1.74, 1.89	bm	30.8	2'	none
2'	1.69, 1.74	bm	28.2	1', 3'	none
3'	3.79, 4.29	bm	55.2	2'	3a, 13a
4'			170.5		
4a'	4.51	s	68.3	none	4', 5'
5'			159.1		
5a'	6.91	d (8.2)	115.9	6'	5', 5a', 7'
6'	7.16	t (8.2)	130.6	5a', 7'	5', 6'
7'	6.86	t (7.3)	122.8	6'	5a'
1''	5.89	d (3.0)	96.6	2''	3'', 5''
2''	2.19	dd (15.2, 3.9)	36.3	1'', 3''	3'', 4''
2''	2.42	bt (13.2)	36.3	1'', 3''	3'', 4''
3''	4.08	m	68.2	2'', 4''	none
3''-OH					
4''	3.9	m	74.1	3'', 5''	none
4''-OH					
5''	3.28	obscured	66.5	4'', 5''-CH_3	none
5''-CH_3	1.21	d (6.8)	18.2	5''	4'', 5''

4.4.2. Jadomycin Oct Naphthoxyacetylamide (58b)

Crude **58** (80 mg) was dissolved in 20 mL of a 1:1 mixture of CH_3CN:PBS buffer (pH 7.6), and added to solid compound **60** (92 mg, 0.308 mmol) in a 25 mL round bottom flask drop-wise with gentle stirring. The flask was corked and protected from light, and the reaction was allowed to proceed for 8 h. The reaction mixture was diluted with 15 mL PBS, and extracted with dichloromethane (3 × 50 mL). The organic fractions were pooled and dried *in vacuo*. The reaction mixture was brought up in minimal DCM (~ 4 mL) and filtered. Filtrate was then applied to a 40 g silica column preconditioned with a 1:1 EtOAc:CH_3CN solution. Material was eluted with a flow rate of 35 mL/min collecting 9 mL fractions. Purification was accomplished using a gradient system comprised of solvent A (1:1 EtOAc:CH_3CN), and solvent B (5:5:1 EtOAc:CH_3CN:H_2O). To start, an initial isocratic gradient step using solvent A (1 CV) was performed. This was followed by a linear increasing gradient from 0% to 100% B over 10 CV, followed finally by an isocratic gradient of 100% B over 7.5 CV. Fractions were checked by TLC for the presence of the compound of interest, and combined and dried yielding 21 mg of crude **58b**. Prep TLC was then performed three times using the same 5:5:1 EtOAc:CH_3CN:H_2O solvent system yielding 14 mg. Final purification was accomplished by size exclusion chromatography (LH-20 resin). Material was dissolved and eluted using 5:5:1 EtOAc:CH_3CN:H_2O. This process was repeated twice more (total = 3 ×) and dried yielding **58b** as a reddish-purple solid (11 mg) as a mixture of diastereomers (M_j/M_n = 50/37) by NMR. TLC R_f: 0.45 (5:5:1 EtOAc:CH_3CN:H_2O), HPLC R_t = 9.92 min, NMR data to follow, for labeling scheme see **58b** NMR data table, UV-Vis (5.10×10^{-4} and 6.38×10^{-5} M, MeOH): λ_{max} (ε) = 312 (12774), 389 (2496), 520 (1727); LRMS (ESI^+): MS/MS (735) found 735 $[M+H]^+$, 605 $[M+H-digitoxose]^+$, 306 $[M+H-digitoxose-C_{17}H_{17}NO_4]^+$, HRMS ($ESI^+$): 735.2517 Found, 735.2548 Calculated for $C_{41}H_{39}N_2O_{11}$.

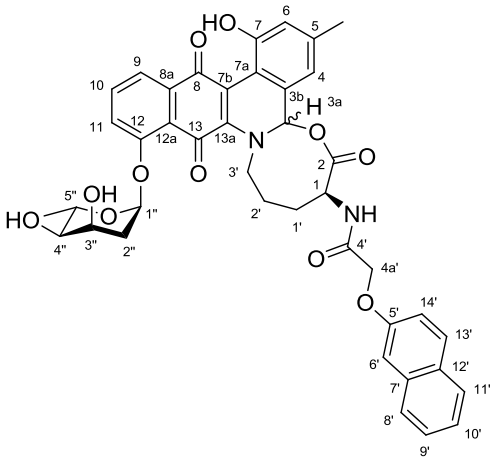

Figure 33. Atom-labeled structure of compound **58b**.

Table 6. Jadomycin Oct naphthoxyacetylamide (**58b**) $3a_{Mj}$ diastereomer NMR data.

Position	δ ^{1}H (ppm)	Multiplicity (J(Hz))	δ ^{13}C (ppm)	COSY	HMBC
1	4.38	bm	55.3	1'	2, 1', 2'
2			177.6		
3a	5.52	s	92.4	None	3b, 4, 7a, 13a, 3'
3b			130.1		
4	6.72	s	120.4	5-CH_3, 6	3a, 5-CH_3, 6, 7a
5			141.2		
5-CH_3	2.34	s	21.1	4, 6	4, 5, 6
6	6.84	s	120.6	4, 5-CH_3	4, 5-CH_3, 7, 7a
7			154.8		
7-OH					
7a			114.2		
7b*			127.9		
8			183.2		
8a*			127.3		
9	7.78	d (7.4)	121.3	10	8
10	7.66	Obscured	136.5	9, 11	Obscured
11	7.47	d (8.5)	120.4	10	12
12			155.7		
12a*			120.6		
13			185.3		
13a			153.0		
1'	1.81	bm	30.5	2'	1
1'	2.02	bm	30.5	2'	1, 2
2'	1.65	bm	28.1	1', 3'	None
2'	1.72	bm	28.1	1', 3'	None
3'	3.87	bm	54.6	2'	3a, 13a, 2'
3'	3.91	bm	54.6	2'	3a, 13a, 2'
4'			170.1		
4a'	4.65, 4.68	d (14.9)	68.4	4a'	4', 5'
5'			156.9		
6'	7.22	Obscured	108.7	None	13', 14'
7'			135.7		
8'	7.59-7.68	Obscured	130.7	9'	Obscured
9'	7.14-7.25	Obscured	124.9 or 127.4	8', 10'	Obscured
10'	7.14-7.26	Obscured	124.9 or 127.5	9', 11'	Obscured
11'	7.59-7.71	Obscured	128.6	10'	Obscured
12'			127.1		
13'	7.56	Obscured	130.7	14'	7', 11'
14'	7.19	Obscured	119.5	13'	12', 13'
1''	5.89	d (3.1)	96.3	2''	3''
2''	2.19	bm	36.4	1'', 3''	None
2''	2.37	dd (15.1, 2.6)	36.4	1'', 3''	None
3''	4.07	bd (3.1)	68.0	2'', 4''	None
3''-OH					
4''	3.27	dd (9.9, 3.2)	74.2	3'', 5''	None
4''-OH					
5''	3.96	dq (12.1, 5.3)	66.6	4'', 5''-CH_3	None
5''-CH_3	1.24	d (6.2)	18.3	5''	4'', 5''

(*) ^{13}C shifts were assigned by ^{13}C-NMR only and may be interchanged

Table 7. Jadomycin Oct naphthoxyacetylamide (**58b**) $3a_{Mn}$ diastereomer NMR data.

Position	δ ^{1}H (ppm)	Multiplicity (J(Hz))	δ ^{13}C (ppm)	COSY	HMBC
1	4.38	bm	55.1	1'	2, 1', 2'
2			177.6		
3a	5.54	s	92.2	None	3b, 4, 7a, 13a, 3'
3b			130.8		
4	6.72	s	120.4	5-CH_3, 6	3a, 5-CH_3, 6, 7a
5			141.6		
5-CH_3	2.34	s	21.1	4, 6	4, 5, 6
6	6.82	s	120.6	4, 5-CH_3	4, 5-CH_3, 7, 7a
7			154.8		
7-OH					
7a			114.2		
7b*			127.8		
8			183.6		
8a*			127.5		
9	7.78	d (7.4)	121.5	10	8
10	7.66	Obscured	136.4	9, 11	Obscured
11	7.44	d (8.5)	121.3	10	12
12			155.7		
12a*			120.6		
13			183.9		
13a			151.5		
1'	1.9	bm	30.8	2'	None
1'	1.73	bm	30.8	2'	None
2'	1.65	bm	28.2	1', 3'	None
2'	1.72	bm	28.2	1', 3'	None
3'	3.7	bm	55.3	2'	None
3'	4.2	bm	55.3	2'	None
4'			170.2		
4a'	4.55, 4.68	d (14.9)	68.2	4a'	4', 5'
5'			157		
6'	7.14	Obscured	108.5	None	13', 14'
7'			135.7		
8'	7.59-7.68	Obscured	130.7	9'	Obscured
9'	7.14-7.25	Obscured	124.9 or 127.4	8', 10'	Obscured
10'	7.14-7.26	Obscured	124.9 or 127.5	9', 11'	Obscured
11'	7.59-7.71	Obscured	128.5	10'	Obscured
12'			127.1		
13'	7.66	Obscured	130.6	14'	7', 11'
14'	7.19	Obscured	119.5	13'	12', 13'
1''	5.85	d (3.1)	96.5	2''	3''
2''	2.17	bm	36.3	1'', 3''	None
2''	2.42	dd (15.1, 2.6)	36.3	1'', 3''	None
3''	4.09	bd (3.1)	68	2'', 4''	None
3''-OH					
4''	3.24	dd (9.9, 3.2)	74.2	3'', 5''	None
4''-OH					
5''	3.87	Obscured	66.5	4'', 5''-CH_3	None
5''-CH_3	1.19	d (6.2)	18.2	5''	4'', 5''

(*) ^{13}C shifts were assigned by ^{13}C-NMR only and may be interchanged

4.4.3. Jadomycin Oct Benzoylamide (58c)

Crude **58** (82 mg) was dissolved in 20 mL of a 1:1 mixture of CH_3CN:PBS buffer (pH 7.6), and added to a 50 mL round bottom flask containing **61** (67 mg, 0.306 mmol) drop-wise with gentle stirring. The flask was corked and protected from light, and the reaction was allowed to proceed for 16 h. After 16 h the reaction had not proceeded to completion as observed by the presence of **58** by TLC analysis. Another 36 mg (0.164 mmol) of **61** was dissolved in 5 mL of a 1:1 (CH_3CN:PBS) solution and added to the reaction flask. The reaction was allowed to proceed for an additional 2 h until complete. The reaction mixture was diluted with 25 mL PBS, and extracted with dichloromethane (3 × 50 mL). The organic fractions were pooled and dried *in vacuo*. The reaction mixture was brought up in minimal DCM (~ 3 mL) and filtered. Filtrate was then applied to a 40 g silica column preconditioned with a 1:1 EtOAc:CH_3CN solution. Material was eluted with a flow rate of 35 mL/min collecting 9 mL fractions. Purification was accomplished using a gradient system comprised of solvent A (1:1 EtOAc:CH_3CN), and solvent B (5:5:1 EtOAc:CH_3CN:H_2O). To start, an initial isocratic gradient step using solvent A (1 CV) was performed. This was followed by a linear increasing gradient from 0% to 100% B over 10 CV, followed finally by an isocratic gradient of 100% B over 7.5 CV. Fractions were checked by TLC for the presence of the compound of interest, and combined and dried yielding 21 mg of crude **58c**. Prep TLC was then performed twice using the same 5:5:1 EtOAc:CH_3CN:H_2O solvent system yielding 15 mg. Final purification was accomplished by size exclusion chromatography (LH-20 resin). Material was eluted using 5:5:1 EtOAc:CH_3CN:H_2O and dried yielding **58c** as a purple solid (13 mg) as a mixture of diastereomers (M_j/M_n = 100/81) by NMR. TLC R_f: 0.43 (5:5:1 EtOAc:CH_3CN:H_2O), HPLC R_t = 9.13 min, NMR data to follow, for labeling scheme see **58c** NMR data table, UV-Vis (4.58×10^{-4} 5.73×10^{-5} M, MeOH): λ_{max} (ε) = 300 (13000), 388 (2647), 527 (1798); LRMS (ESI^+): MS/MS (655) found 655 $[M+H]^+$, 525 $[M+H-digitoxose]^+$, 306 $[M+H-digitoxose-C_{12}H_{13}NO_3]^+$, HRMS ($ESI^+$): 707.2202 Found, 707.2211 Calculated for $C_{37}H_{36}N_2NaO_{11}$.

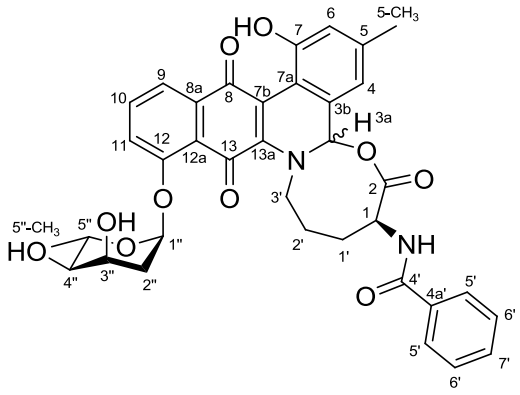

Figure 34. Atom-labeled structure of compound **58c**.

Table 8. Jadomycin Oct benzoylamide (**58c**) $3a_{Mj}$ diastereomer NMR data.

Position	δ ^{1}H (ppm)	Multiplicity (J(Hz))	δ ^{13}C (ppm)	COSY	HMBC
1	4.5	bs	55.1	1'	None
2			177.3		
3a	5.61	s	92.7	None	3b, 4, 7b, 13a, 3'
3b			130.1		
4	6.75	s	120.4	5-CH_3, 6	3a, 3b, 5-CH_3, 6, 7a
5			141.4		
5-CH_3	2.33	s	21.1	4, 6	4, 5, 6
6	6.81	s	120.6	4, 5-CH3	4, 5-CH_3, 7, 7a
7			154.8		
7-OH					
7a			114.3		
7b			136.7		
8			183.4		
8a			136.7		
9	7.79	d (7.5)	121.3	10	8, 11
10	7.70	t (8.1)	136.6	9, 11	8a, 9, 11, 12
11	7.49	Obscured	120.6	10	9, 12, 12a, 13
12			155.7		
12a			121.6		
13			185.8		
13a			153.3		
1'	1.86	Broad Multiplet	30.7	1, 1', 2'	None
1'	2.05	Broad Multiplet	30.7	1, 1', 2'	None
2'	1.87	Broad Multiplet	28.9	1', 2', 3'	1
2'	1.95	Broad Multiplet	28.9	1', 2', 3'	1
3'	4.08-4.14	Broad Multiplet	54.4	2', 3'	3a, 13a, 1', 2'
3'	4.08-4.15	Broad Multiplet	54.4	2', 3'	3a, 13a, 1', 2'
4'			169.6		
4a'			135.7		
5'	7.83	d (7.4)	128.4	6'	4', 5', 7'
6'	7.44	Obscured	129.6	5', 7'	4a', 5', 6'
7'	7.51	Obscured	132.7	6'	5'
1''	5.89	d (3.1)	96.3	2''	3'', 5'', 12
2''	2.18 (bm)	Broad Multiplet	36.3	1'', 3''	1'', 3'', 4''
2''	2.34 (bm)	Broad Multiplet	36.3	1'', 3''	1'', 3'', 4''
3''	4.03	bd (2.7)	68.4	2'', 4''	none
3''-OH					
4''	3.26	t (2.4)	74.1	3'', 5''	5'', 5''-CH_3
4''-OH					
5''	3.89	bm	66.5	4'', 5''-CH_3	1'', 3'', 4''
5''-CH3	1.19	d (6.0)	18.2	5''	4'', 5''

Table 9. Jadomycin Oct benzoylamide (**58c**) $3a_{Mn}$ diastereomer NMR data.

Position	δ ^{1}H (ppm)	Multiplicity (J(Hz))	δ ^{13}C (ppm)	COSY	HMBC
1	4.5	bs	55.1	1'	None
2			177.3		
3a	5.59	s	92.2	None	3b, 4, 7b, 13a, 3'
3b			131.0		
4	6.68	s	120.3	5-CH_3, 6	3a, 3b, 5-CH_3, 6, 7a
5			141.7		
5-CH_3	2.28	s	21.1	4, 6	4, 5, 6
6	6.79	s	120.6	4, 5-CH3	4, 5-CH_3, 7, 7a
7			154.8		
7-OH					
7a			114.1		
7b			136.7		
8			184.1		
8a			136.7		
9	7.80	d (7.5)	121.3	10	8, 11
10	7.70	t (8.1)	136.6	9, 10	8a, 9, 11, 12
11	7.49	Obscured	120.6	10	9, 12, 12a, 13
12			156.3		
12a			121.6		
13			184.1		
13a			151.5		
1'	1.79	Broad Multiplet	30.7	1, 1', 2'	None
1'	2.00	Broad Multiplet	30.7	1, 1', 2'	None
2'	1.79	Broad Multiplet	28.5	1', 2', 3'	None
2'	1.90	Broad Multiplet	28.5	1', 2', 3'	None
3'	3.88-3.91	Obscured	54.8	2', 3'	3a, 13a, 1'
3'	4.33-4.37	Broad Multiplet	54.8	2', 3'	3a, 13a, 1'
4'			169.6		
4a'			135.7		
5'	7.85	d (7.4)	128.4	6'	4', 5', 7'
6'	7.44	Obscured	129.6	5', 7'	4a', 5', 6'
7'	7.51	Obscured	132.7	6'	5'
1''	5.90	d (3.1)	96.5	2''	3'', 5'', 12
2''	2.16 (bm)	Broad Multiplet	36.3	1'', 3''	1'', 3'', 4''
2''	2.37 (bm)	Broad Multiplet	36.3	1'', 3''	1'', 3'', 4''
3''	4.05	bd (2.7)	68.1	2'', 4''	none
3''-OH					
4''	3.25	t (2.4)	74.1	3'', 5''	5'', 5''-CH_3
4''-OH					
5''	3.89	bm	66.5	4'', 5''-CH_3	1'', 3'', 4''
5''-CH3	1.21	d (6.0)	18.2	5''	4'', 5''

4.4.4. Jadomycin Oct Nonoylamide (58d)

Crude **58** (98.7 mg) was dissolved in 20 mL of a 1:1 mixture of CH_3CN:PBS buffer (pH 7.6), and added to a 50 mL round bottom flask containing **62** (103 mg, 0.40 mmol) with gentle stirring at room temperature. The flask was corked and protected from light, and the reaction was allowed to proceed for 7 h. The reaction mixture was diluted with 20 mL PBS, and extracted with dichloromethane (3 × 50 mL). The organic fractions were pooled and dried *in vacuo*. The reaction mixture was brought up in minimal DCM (~ 4 mL) and filtered. Filtrate was then applied to a 40 g silica column preconditioned with a 1:1 EtOAc:CH_3CN solution. Material was eluted with a flow rate of 35 mL/min collecting 9 mL fractions. Purification was accomplished using a gradient system comprised of solvent A (1:1 EtOAc:CH_3CN), and solvent B (5:5:1 EtOAc:CH_3CN:H_2O). To start, an initial isocratic gradient step using solvent A (1 CV) was performed. This was followed by a linear increasing gradient from 0% to 100% B over 10 CV, followed finally by an isocratic gradient of 100% B over 7.5 CV. Fractions were checked by TLC for the presence of the compound of interest, combined, and dried yielding 28 mg of crude **58d**. Prep TLC was then performed three times using the same 5:5:1 EtOAc:CH_3CN:H_2O solvent system yielding 13 mg. Final purification was accomplished by size exclusion chromatography (LH-20 resin). Material was dissolved and eluted using 5:5:1 EtOAc:CH_3CN:H_2O, this process was then repeated a second time. Compound **58d** was then dried *in vacuo*, re-dissolved in 10 mL of 1:1 H_2O:CH_3CN, and extracted with 3 × 10 mL of hexanes. The H_2O:CH_3CN layer was dried yielding **58d** as a purple solid (9 mg) as a mixture of diastereomers (M_j/M_n = 100/81) by NMR. TLC R_f: 0.52 (5:5:1 EtOAc:CH_3CN:H_2O); HPLC R_t = 6.95 and 7.19 min; NMR data to follow, for labeling scheme see **58d** NMR data table; UV-Vis (4.7×10^{-4} and 5.8×10^{-5} M, MeOH): λ_{max} (ε) = 312 (11745), 383 (2440), 527 (1474); LRMS (ESI^+): MS/MS (691) found 691 $[M+H]^+$, 561 $[M+H-\text{digitoxose}]^+$, 306 $[M+H-\text{digitoxose}-C_{14}H_{25}NO_3]^+$; HRMS ($ESI^+$): Found 691.3194, Calculated 691.3225 for $C_{41}H_{39}N_2O_{11}$.

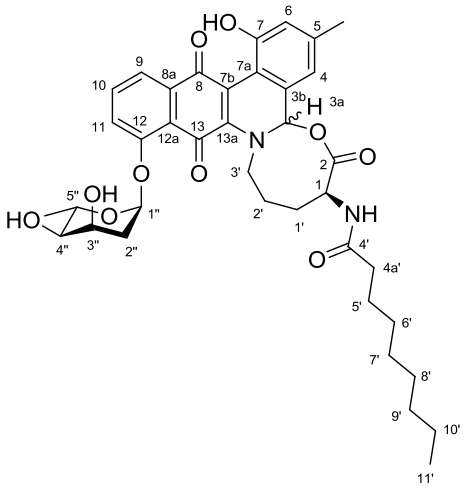

Figure 35. Atom-labeled structure of compound **58d**.

Table 10. Jadomycin Oct nonoylamide (**58d**) $3a_{Mj}$ diastereomer NMR data.

Position	δ ^{1}H (ppm)	Multiplicity (J(Hz))	δ ^{13}C (ppm)	COSY	HMBC
1	4.33	bs	54.3	None	None
2			Unobserved		
3a	5.6	s	92.5	None	4, 7a, 7b, 13a, 3'
3b			115.4		
4	6.76	s	120.4	5-CH_3, 6	3a, 5-CH_3, 6, 7a, 7b
5			141.4		
5-CH_3	2.36	s	21.1	4, 6	4, 5, 6
6	6.82	s	120.6	5-CH_3, 6	4, 5-CH_3, 7, 7a
7			154.8		
7-OH					
7a			114.3		
7b			130.3		
8			183.4		
8a			136.7		
9	7.82	d (7.5)	121.4	10	8, 10, 11
10	7.72	t (8.1)	136.7	9, 11	8a, 9, 11, 12
11	7.55	d (8.4)	120.6	10	9, 10, 12, 12a, 13
12			155.9		
12a			120.5		
13			185.6		
13a			152.8		
1'	1.80, 1.86	bm	30.4	1', 1', 2'	Not assignable
2'	1.73, 1.93	bm	28.6	1', 3'	Not assignable
3'	3.82, 4.22	bm	54.6	2'	Not assignable
4'			176.1		
4a'	2.23	bm	37.2	5'	4'
5'	1.58	bm	27.1	4a', 6'	4'
6'	1.2-1.7	bm	23.7, 30.4, 33.0	Obscured	Obscured
7'	1.2-1.7	bm	23.7, 30.4, 33.1	Obscured	Obscured
8'	1.2-1.7	bm	23.7, 30.4, 33.2	Obscured	Obscured
9'	1.2-1.7	bm	23.7, 30.4, 33.3	Obscured	Obscured
10'	1.2-1.7	bm	23.7, 30.4, 33.4	Obscured	Obscured
11'	0.84	t (7.0)	14.4	10'	Alkyl chain
1''	5.99	bs	96.2	2''	3'', 5''
2''	2.41	bm	36.3	1'', 3''	None
2''	2.23	bm	36.3	1'', 3''	None
3''	4.11	bm	68.2	2'', 4''	None
3''-OH					
4''	3.3	Obscured	74.1	3'', 5''	None
4''-OH					
5''	3.95	bm	66.6	4'', 5''-CH_3	None
5''-CH_3	1.22	d (5.8)	18.2	5''	None

Table 11. Jadomycin Oct nonoylamide (**58d**) $3a_{Mn}$ diastereomer NMR data.

Position	δ ^{1}H (ppm)	Multiplicity (J(Hz))	δ ^{13}C (ppm)	COSY	HMBC
1	4.33	bs	54.3	None	None
2			Unobserved		
3a	5.6	s	92.1	None	4, 7a, 7b, 13a, 3'
3b			116.3		
4	6.76	s	120.3	5-CH_3, 6	3a, 5-CH_3, 6, 7a, 7b
5			141.5		
5-CH_3	2.36	s	21.1	4, 6	4, 5, 6
6	6.82	s	120.6	5-CH_3, 6	4, 5-CH_3, 6, 7, 7a
7			154.8		
7-OH					
7a			114.3		
7b			130.7		
8			183.7		
8a			136.7		
9	7.82 (d, 7.5)	d (7.5)	121.4	10	8, 10, 11
10	7.72 (t, 8.1)	t (8.1)	136.7	9, 11	8a, 9, 11, 12
11	7.54 (d, 8.4)	d (8.4)	120.6	10	9, 10, 12, 12a, 13
12			156.3		
12a			120.5		
13			184.1		
13a			152.1		
1'	1.73, 1.90	bm	30.5	1, 1', 2'	Not assignable
2'	1.67, 1.87	bm	28.3	1', 3'	Not assignable
3'	3.94, 4.16	bm	55.1	2'	Not assignable
4'			176.1		
4a'	2.23	bm	37.2	5'	4'
5'	1.58	bm	27.1	4a', 6'	4'
6'	1.2-1.7	bm	23.7, 30.4, 33.0	Obscured	Obscured
7'	1.2-1.7	bm	23.7, 30.4, 33.1	Obscured	Obscured
8'	1.2-1.7	bm	23.7, 30.4, 33.2	Obscured	Obscured
9'	1.2-1.7	bm	23.7, 30.4, 33.3	Obscured	Obscured
10'	1.2-1.7	bm	23.7, 30.4, 33.4	Obscured	Obscured
11'	0.81	t (7.0)	14.4	10'	Alkyl chain
1''	5.98	bs	96.3	2''	3'', 5''
2''	2.41	bm	36.3	1'', 3''	None
2''	2.23	bm	36.3	1'', 3''	None
3''	4.11	bm	68.9	2'', 4''	None
3''-OH					
4''	3.3	Obscured	74.1	3'', 5''	None
4''-OH					
5''	3.9	bm	66.6	4'', 5''-CH_3	None
5''-CH_3	1.22	d (5.8)	18.2	5''	None

4.4.5. Jadomycin Oct Fmoc amide (58e)

Crude **58** (171 mg) was dissolved in 20 mL of CH_3CN:PBS (1:1) and added to a 50 mL round bottom flask containing **63** (215 mg, 637 μmol) and stirred gently at room temperature. The reaction was determined to be complete after 3 h by TLC analysis. The reaction was diluted with 10 mL PBS and extracted with ethyl acetate (3 × 50 mL). The combined organic layers were combined and dried *in vacuo*, giving an impure reddish-purple solid (120 mg). The material was brought up in minimal (5:5:1) EtOAc:CH_3CN:PBS (pH 7.6) solvent and loaded onto an LH-20 column and eluted using the same solvent system at room temperature, collecting ~3 mL fractions. To each fraction, ~3 mL of PBS was added, resulting in the EtOAc to separate from the rest of the solution. All colour was contained within the EtOAc layer. The fractions were concentrated down and analyzed by HPLC. Pure fractions were combined and dried. Impure fractions containing the compound of interest were pooled and dried *in vacuo*, and the process was repeated 4 more times (5 × LH-20 columns total). Pure material was brought up in ethyl acetate, filtered to remove any residual salt, and dried down yielding **58e** as a purple solid (3.2 mg) as a mixture of diastereomers (M_j/M_n = 4/3) by NMR. TLC R_f = 0.64 (5:5:1 EtOAc:CH_3CN:H_2O); HPLC R_t = 11.18 min & 11.63 min; NMR data to follow, for labeling scheme see **58e** NMR data table; UV-Vis (5.8×10^{-6} M and 7.3×10^{-8} M, MeOH): λ_{max} (ε) = 320 (12570), 386 (2638), 530 (1660); LRMS (ESI^+): Q1 found ; LC-MS/MS of 773 found 773 $[M+H]^+$, 643 $[M+H-L-digitoxose]^+$, 306 $[M+H-C_{26}H_{29}NO_7]^+$; HRMS (ESI-) for $C_{45}H_{43}N_2O_{12}$ $[M-H+MeOH]^-$: found 803.2838; calculated 803.2821 for $C_{45}H_{43}N_2O_{12}$.

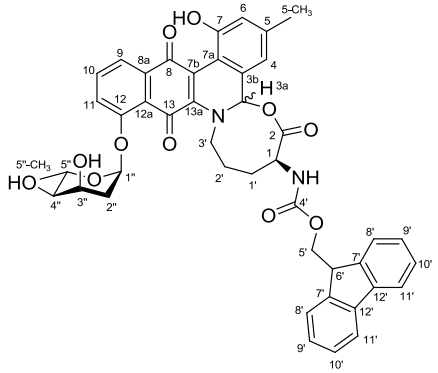

Figure 36. Atom-labeled structure of compound **58e**.

Table 12. Jadomycin Oct Fmoc amide (**58e**) $3a_{Mj}$ diastereomer NMR data.

Position	δ ^{1}H (ppm)	Multiplicity (J(Hz))	δ ^{13}C (ppm)	COSY	HMBC
1	4.07	Obscured	57.3	1'	2, 1', 2'
2			178.6		
3a	5.61	s	92.6	None	3b, 4, 7a, 13, 13a, 3'
3b			130.3		
4	6.74	s	120.4	5-CH_3, 6	3a, 3b, 5-CH3, 6, 7, 7a
5			141.3		
5-CH_3	2.33	s	21.1	4, 6	4, 5, 6
6	6.83	s	120.6	4, 5-CH_3	4, 5-CH3, 7, 7a
7			154.8		
7-OH					
7a			114.3		
7b			136.6		
8			183.4		
8a			136.6		
9	7.8	d (7.2)	121.3	10	8, 10, 11, 12a
10	7.67	Obscured	136.6	9, 11	8a, 9, 11, 12, 12a
11	7.45	d (8.5)	120.8	10	9, 10, 11, 13
12			156.4		
12a			120.8		
13			185.6		
13a			152.9		
1'	1.83	Broad Multiplet	28.6	2'	None Observed
1'	1.83	Broad Multiplet	28.6	2'	None Observed
2'	1.74	Broad Multiplet	30.9	1', 3'	None Observed
2'	2.00	Broad Multiplet	30.9	1', 3'	None Observed
3'	4.01	Obscured	54.8	2'	3a, 13a, 1', 2'
3'	4.07	Obscured	54.8	2'	3a, 13a, 1', 2'
4'			158		
5'	4.21	Obscured	67.8	6'	4', 6', 7'
5'	4.34	dd (9.9, 6.9)	67.8	6'	4', 6', 7'
6'	4.2	Obscured	48.4	5'	5', 7', 12'
7'			145.5		
8'	7.59	d (7.4)	126.3	9'	6', 10', 12'
9'	7.21	Obscured	128.1	8', 10'	7', 11'
10'	7.31	Obscured	128.7	9', 11'	8', 12'
11'	7.71	d (7.6)	121	10'	7', 8', 9', 12'
12'			142.5		
1''	5.87	d, 3.2	96.4	2''	12, 3'', 5''
2''	2.15	dt (11.2, 3.6)	36.3	1'', 3''	1'', 3'', 4''
2''	2.36	Obscured	36.3	1'', 3''	1'', 3'', 4''
3''	4.06	Obscured	68.2	2'', 4''	Obs
3''-OH					
4''	3.25	dd (7.4, 3.4)	74.2	3'', 5''	5'', 5''-CH3
4''-OH					
5''	3.87	Obscured	66.6	4'', 5''-CH_3	5''-CH_3
5''-CH_3	1.19	d (6.2)	18.2	5''	4'', 5''

Table 13. Jadomycin Oct Fmoc amide (**58e**) $3a_{Mn}$ diastereomer NMR data.

Position	δ ^{1}H (ppm)	Multiplicity (J(Hz))	δ ^{13}C (ppm)	COSY	HMBC
1	4.02	Obscured	57.1	1'	2, 1', 2'
2			178.6		
3a	5.58	s	92.2	None	3b, 4, 7a, 13, 13a, 3'
3b			130.9		
4	6.73	s	120.4	5-CH_3, 6	3a, 3b, 5-CH3, 6, 7, 7a
5			141.6		
5-CH_3	2.3	s	21.1	4, 6	4, 5, 6
6	6.81	s	120.5	4, 5-CH_3	4, 5-CH3, 7, 7a
7			154.8		
7-OH					
7a			114.2		
7b			136.6		
8			183.9		
8a			136.6		
9	7.79	d (7.2)	121.5	10	8, 10, 11, 12a
10	7.67	Obscured	136.6	9, 11	8a, 9, 11, 12, 12a
11	7.47	d (8.5)	121.3	10	9, 10, 11, 13
12			155.9		
12a			120.8		
13			183.9		
13a			151.7		
1'	1.73	Broad Multiplet	28.2	2'	None Observed
1'	1.73	Broad Multiplet	28.2	2'	None Observed
2'	1.7	Broad Multiplet	31.2	1', 3'	None Observed
2'	1.86	Broad Multiplet	31.2	1', 3'	None Observed
3'	3.78	Broad Multiplet	55.5	2'	3a, 13a, 1', 2'
3'	4.23	Obscured	55.5	2'	3a, 13a, 1', 2'
4'			158.1		
5'	4.11 (obs)	Obscured	67.4	6'	4', 6', 7'
5'	4.45	dd (10.7, 6.9)	67.4	6'	4', 6', 7'
6'	4.13 (obs)	Obscured	48.5	5'	5', 7', 12'
7'			145.2		
8'	7.63	Obscured	126.3	9'	6', 10', 12'
9'	7.19	Obscured	128.1	8', 10'	7', 11'
10'	7.27	Obscured	128.7	9', 11'	8', 12'
11'	7.66	Obscured	121	10'	7', 8', 9', 12'
12'			142.5		
1''	5.82	d (3.2)	96.6	2''	12, 3'', 5''
2''	2.14	dt (11.2, 3.6)	36.3	1'', 3''	1'', 3'', 4''
2''	2.36	Obscured	36.3	1'', 3''	1'', 3'', 4''
3''	4.06	Obscured	68	2'', 4''	Obs
3''-OH					
4''	3.23	dd (7.4, 3.4)	74.1	3'', 5''	5'', 5''-CH3
4''-OH					
5''	3.82	Obscured	66.6	4'', 5''-CH_3	5''-CH_3
5''-CH_3	1.12	d (6.2)	18.2	5''	4'', 5''

4.4.6. Jadomycin Oct BODIPY amide (58f)

Compound **64** (35 mg, 0.80 mmol) was dissolved in 10 mL CH_3CN with gentle stirring. Crude **58** (42 mg) was brought up in 10 mL PBS buffer (pH 7.6), and added to the solution of **64** drop-wise. The reaction flask was protected from light and the reaction was allowed to proceed for 5 h. After 5 h the reaction had not proceeded to completion as observed by the presence of **58** by TLC analysis. Another 16 mg (0.035 mmol) of **64** was dissolved in 5 mL of a 1:1 (CH_3CN:PBS) solution and added to the reaction flask. The reaction was allowed to proceed for an additional 2 h until complete. The reaction mixture was diluted with 25 mL PBS, and extracted with dichloromethane (3 × 50 mL). The organic fractions were pooled and dried *in vacuo*. The reaction mixture was brought up in minimal DCM (~ 5 mL) and filtered. Filtrate was then applied to a 40 g silica column preconditioned with a 1:1 EtOAc:CH_3CN solution. Material was eluted with a flow rate of 30 mL/min collecting 9 mL fractions. Purification was accomplished using a gradient system comprised of solvent A (1:1 EtOAc:CH_3CN), and solvent B (5:5:1 EtOAc:CH_3CN:H_2O). To start, an initial isocratic gradient of 100% A (1 CV) was performed. This was followed by a linear increasing gradient from 0% to 100% B over 10 CV, followed by an isocratic gradient of 100% B over 5 CV. Fractions were checked by TLC for the presence of the compound of interest, and combined and dried yielding crude **58f** (22 mg). Prep TLC was then performed using the same 5:5:1 EtOAc:CH_3CN:H_2O solvent system yielding 11 mg of partially pure **58f**. Final purification was accomplished by size exclusion chromatography (LH-20 resin). Material was eluted using 5:5:1 EtOAc:CH_3CN:H_2O and dried yielding 6 mg of **58f** as a solid pink-red compound. TLC R_f: 0.41 (5:5:1 EtOAc:CH_3CN:H_2O); HPLC R_t = 12.3 min; NMR data to follow, for labeling scheme see **58f** NMR data table; UV-Vis (7.8×10^{-6} and 1.95×10^{-6} M, MeOH): λ_{max} (ε) = 285 (13128), 319 (14333), 377 (8038), 495 (23487), 526 (49538); LRMS (ESI^+): MS/MS (881) found 881 $[M+H]^+$, 751 $[M+H-digitoxose]^+$, 306 $[M+H-digitoxose-C_{23}H_{30}BF_2N_3O_3]^+$; HRMS ($ESI^+$): Found 881.3698 $[M+H]^+$, Calculated 881.3739 $[M+H]^+$ for $C_{47}H_{52}BF_2N_4O_{10}$.

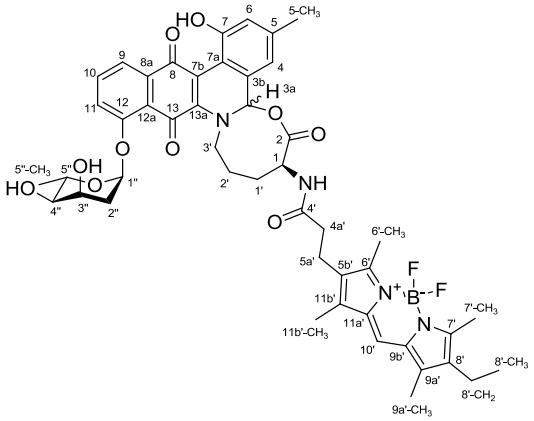

Figure 37. Atom-labeled structure of compound **58f**.

Table 14. Jadomycin Oct BODIPY amide (**58f**) $3a_{Mj}$ diastereomer NMR data.

Position	δ ^{1}H (ppm)	Multiplicity (J(Hz))	δ ^{13}C (ppm)	COSY	HMBC
1	4.28	bs	55.2	1'	2, 1', 2', 4'
2			178.1		
3a	5.47	s	91.7	None	3b, 4, 7a, 13a, 3'
3b			129.9		
4	6.68	s	120.4	5-CH3, 6	3a, 5, 5-CH_3, 6, 7a
5			141.1		
5-CH_3	2.35	s	21.1	4, 6	4, 5, 6
6	6.80	s	120.7	4, 5-CH3	4, 5-CH_3, 6, 7, 7a
7			154.8		
7-OH					
7a			114.4		
7b			120.5		
8			183.0		
8a			137.0		
9	7.77	d (7.6)	121.5	10	8, 8a, 11
10	7.67	t (8.2)	136.5	9, 11	8a, 12
11	7.49	d (8.6)	120.4	10	9, 12, 13
12			155.9		
12a			120.7		
13			183.1		
13a			153.2		
1'	1.71, 1.83	m	30.8	1, 2'	None
2'	1.60, 1.84	m	27.1	1', 3'	None
3'	3.60, 3.85	m	55.0	2'	3a, 1', 2'
4'			174.9		
4a'	2.36, 2.60	m	37.0	5a'	4', 5a', 5b'
5a'	2.66, 2.81	m	21.1	4a'	4', 4a', 5b' 6', 11b'
5b'			129.3		
6'			155.1		
6'-CH_3	2.39	s	12.8	None	5b', 6'
7'			156.0		
7'-CH_3	2.17	s	12.4	None	7', 8'
8'			132.9		
8'-CH_2	2. 28, 2.35	obscured	18.0	8'-CH3	7', 8', 8'-CH_3, 9a'
8'-CH_3	1.01	t (7.5)	14.8	8'-CH2	8', 8'-CH_2
9a'			138.6		
9a'-CH_3	1.88	s	9.2	None	8', 9a', 9b'
9b'			133.9		
10'	6.99	s	120.5	None	9a', 9b', 11a'
11a'			133.8		
11b'			139.3		
11b'-CH_3	2.21	s	9.9	None	5b', 11a', 11b'
1''	6.06	d (2.5)	95.7	2''	3'', 5''
2''	2.24	obscured	36.1	1'', 2'', 3''	1'', 3'', 4''
2''	2.46	obscured	36.1	1'', 2'', 3''	1'', 3'', 4''
3''	4.13	q (3.1)	68.2	2'', 4''	None
3''-OH					
4''	3.23	m	74.4	3'', 5''	None
4''-OH					
5''	3.81	m	66.7	4'', 5''-CH3	None
5''-CH_3	1.18	d (6.2)	18.3	5''	4'', 5''

Table 15. Jadomycin Oct BODIPY amide (**58f**) $3a_{Mn}$ diastereomer NMR data.

Position	δ ^{1}H (ppm)	Multiplicity (J(Hz))	δ ^{13}C (ppm)	COSY	HMBC
1	4.29	bs	55.4	1'	1', 2, 2'
2			177.8		
3a	5.49	s	92.3	None	3b, 4, 7a, 13a, 3'
3b			130.3		
4	6.73	s	120.4	5-CH3, 6	3a, 5, 5-CH_3, 6, 7a
5			141.4		
5-CH_3	2.34	s	21.1	4, 6	4, 5, 6
6	6.81	s	120.7	4, 5-CH3	4, 5-CH_3, 6, 7, 7a
7			154.9		
7-OH					
7a			114.1		
7b			120.5		
8			183.9		
8a			136.4		
9	7.73	d (7.6)	121.3	10	8, 11
10	7.65	t (8.2)	136.4	9, 11	8a, 12
11	7.47	d (8.6)	120.4	10	9, 12, 13
12			155.9		
12a			120.7		
13			184.7		
13a			152.1		
1'	1.71, 1.83	m	30.4	1, 2'	None
2'	1.60, 1.84	m	27.1	1', 3'	None
3'	3.60, 3.85	m	55.0	2'	3a, 1', 2'
4'			174.8		
4a'	2.36, 2.60	m	37.4	5a'	4', 5a', 5b'
5a'	2.66, 2.81	m	21.4	4a'	4', 4a', 5b' 6', 11b'
5b'			129.7		
6'			155.3		
6'-CH_3	2.44	s	12.8	None	5b', 6'
7'			155.9		
7'-CH_3	2.30	s	12.6	None	7', 8'
8'			133.0		
8'-CH_2	2. 28, 2.35	obscured	18.0	8'-CH3	7', 8', 8'-CH_3, 9a'
8'-CH_3	0.97	t (7.5)	14.8	8'-CH2	8', 8'-CH_2
9a'			138.9		
9a'-CH_3	2.05	s	9.3	None	8', 9a', 9b'
9b'			134.0		
10'	7.16	s	120.9	None	9b', 11a'
11a'			133.8		
11b'			139.3		
11b'-CH_3	2.18	s	9.7	None	5b', 11a', 11b'
1''	5.95	d (2.5)	96.0	2''	3'', 5''
2''	2.18	obscured	36.3	1'', 2'', 3''	None
2''	2.36	obscured	36.3	1'', 2'', 3''	None
3''	4.08	q (3.1)	68.3	2'', 4''	None
3''-OH					
4''	3.25	m	74.2	3'', 5''	None
4''-OH					
5''	3.87	m	66.5	4'', 5''-CH3	None
5''-CH_3	1.18	d (6.2)	18.2	5''	4'', 5''

4.4.7. Jadomycin Oct (58) Purification and Characterization

Growth and crude purification of **58** was accomplished as previously described. Crude aqueous extract containing **58** (208 mg) was dissolved in minimal methanol, filtered, absorbed onto Isolute® HM-N, and dried *in vacuo*. The isolute containing crude **58** was then applied to an 80 g silica column preconditioned with dichloromethane. Material was eluted with a flow rate of 50 mL/min collecting 9 mL fractions. Purification was accomplished using a gradient system comprised of solvent A (dichloromethane), and solvent B (methanol). To start, an initial isocratic gradient step using solvent A (1 CV) was performed. This was followed by a linear increasing gradient from 0% to 100% B over 10 CV. Fractions were checked by TLC for the presence of the compound of interest, combined and dried, yielding 46 mg of crude **58**. Prep TLC was then performed three times, first using a 9:1 (dichloromethane:methanol) solvent system, followed by two more prep TLCs using the 5:5:1 (EtOAc:CH_3CN:H_2O) solvent system yielding 12 mg. Final purification was accomplished by size exclusion chromatography (LH-20 resin). Material was eluted using 100% methanol. The compound was then dried *in vacuo*, yielding **58** as a purple solid (3 mg) as a mixture of diastereomers (M_j/M_n = 100/82) by NMR. Compound **58** proved to be very unstable, with significant breakdown occurring over time (within hours). TLC R_f: 0.074 (5:5:1 EtOAc:CH_3CN:H_2O); HPLC R_t = 6.47 and 6.76 min (broad peaks); NMR data to follow, for labeling scheme see **58** NMR data table; UV-Vis (8.17×10^{-4} and 1.02×10^{-4} M, MeOH): λ_{max} (ε) = 319 (8941), 388 (1850), 541 (1218) ; LRMS (ESI+): MS/MS (551) found 551 $[M+H]^+$, 436 $[M+H-C_5H_9NO_2]^+$, 306 $[M+H-\text{digitoxose}-C_{12}H_{13}NO_3]^+$; HRMS (ESI+): found 573.1834, calculated 573.1844 for $C_{37}H_{36}N_2NaO_{11}$.

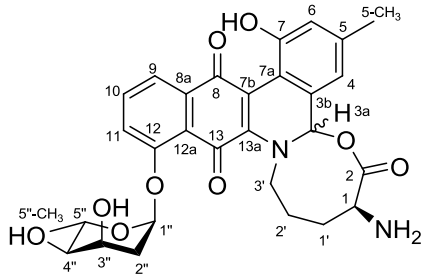

Figure 38. Atom-labeled structure of compound **58**.

Table 16. Jadomycin Oct (**58**) $3a_{Mj}$ diastereomer NMR data.

Position	δ ^{1}H (ppm)	Multiplicity (J(Hz))	δ ^{13}C (ppm)	COSY	HMBC
1	3.78	bm	55.1	1'	None
2			Unobserved		
3a	5.66	s	92.1	None	3b, 4, 7a, 13a, 3'
3b			129.8		
4	6.77	d (1.5)	120.4	5-CH_3, 6	3a, 5-CH3, 6, 7a
5			141.5		
5-CH_3	2.36	s	20.9	None	4, 5, 6
6	6.83	d (1.5)	120.6	4, 5-CH_3	4, 5-CH3, 7, 7a
7			154.6		
7-OH					
7a			114.3		
7b			Unobserved		
8			183.1		
8a			136.2		
9	7.83	dd (7.6, 0.9)	121.3	10	8, 11
10	7.73	t (8.1)	135.3	9, 11	8a, 12
11	7.55	bd (7.6)	120.5	10	9, 12a
12			155.4		
12a			120.1		
13			Unobserved		
13a			153.0		
1'	1.82-2.03	bm	28.9	1, 1', 2'	None
2'	1.82-2.04	bm	26.5	1', 2' 3'	None
3'	3.80, 4.20	dd (10.7, 3.6)	55.2	2', 3'	None
1''	6.03	d (3.1)	96.0	2''	3'', 5''
2''	2.23	m	36.0	1'', 3''	None
2''	2.39	dd (obscured)	36.0	1'', 3''	None
3''	4.10	m (obscured)	68.5	2'', 4''	None
3''-OH					
4''	3.33	Obscured	73.8	3'', 5''	None
4''-OH					
5''	3.92	m	66.5	4'', 5''-CH_3	None
5''-CH_3	1.21	d (6.2)	18.3	5''	4'', 5''

Table 17. Jadomycin Oct (**58**) $3a_{Mn}$ diastereomer NMR data.

Position	δ ^{1}H (ppm)	Multiplicity (J(Hz))	δ ^{13}C (ppm)	COSY	HMBC
1	3.72	bm	55.4	1'	None
2			Unobserved		
3a	5.55	s	92.5	None	3b, 4, 7a, 13a, 3'
3b			130.6		
4	6.77	d (1.5)	120.4	5-CH_3, 6	3a, 5-CH_3, 6, 7a
5			141.5		
5-CH_3	2.36	s	20.9	None	4, 5, 6
6	6.84	d (1.5)	120.6	4, 5-CH_3	4, 5-CH_3, 7
7			Unobserved		
7-OH					
7a			113.8		
7b			Unobserved		
8			184.2		
8a			136.2		
9	7.84	dd (7.6, 0.9)	121.3	10	8, 11
10	7.72	t (8.1)	135.3	9, 11	8a, 12
11	7.54	bd (7.6)	120.5	10	9, 12a
12			155.4		
12a			120.1		
13			Unobserved		
13a			149.7		
1'	1.82-2.03	bm	28.9	1, 1', 2'	None
2'	1.82-2.04	bm	26.5	1', 2' 3'	None
3'	3.70, 4.12	Obscured	54.4	2', 3'	None
1''	5.98	d (3.1)	95.8	2''	3'', 5''
2''	2.23	m	36.0	1'', 3''	None
2''	2.39	Obscured	36.0	1'', 3''	None
3''	4.12	m (obscured)	68.5	2'', 4''	None
3''-OH					
4''	3.3	Obscured	74.0	3'', 5''	None
4''-OH					
5''	3.86	m	66.4	4'', 5''-CH_3	None
5''-CH_3	1.2	d (6.2)	18.3	5''	4'', 5''

4.4.8. Deprotection of 58e

SiliaBond® Piperazine (Si-PPZ) was purchased from SiliCycle® as a 0.91 mmol g^{-1} molecular loaded resin. The Si-PPZ was used in the deprotection of **58e** as a heterogeneous Fmoc scavenger. Compound **58e** (3 mg, 3.9 μmol) was dissolved in 1 mL (5:5:1) EtOAc:CH_3CN:PBS (pH 7.6). The solution of **58e** was added to a vial containing 51 mg of Si-PPZ resin (46 μmol, 11.6 equivalents) with gentle stirring. To this solution 500 μL of a 1.5% (v/v) 1,8-diazabicycloundec-7-ene solution (45 μmol, 11 equivalents) in 5:5:1 (EtOAc:CH_3CN:PBS) was added. The reaction flask was protected from light and the reaction was allowed to proceed for 3 min. The reaction mixture was centrifuged at 13000 RPM (4 °C) for 5 min, and the supernatant was removed from the Si-PPZ. The resin was washed twice with 0.5 mL of 5:5:1 (EtOAc:CH_3CN:PBS) and centrifuged after each wash to ensure removal of all resin. Supernatant fractions were pooled (~ 2.5 mL), filtered and loaded onto an LH-20 resin size exclusion column preconditioned in 5:5:1 (EtOAc:CH_3CN:H_2O). Elution was accomplished using the same 5:5:1 (EtOAc:CH_3CN:H_2O) solvent system. Fractions were checked by TLC and HPLC for the presence of the compound of **58**, combined and dried yielding **58 (**1.3 mg, 61% yield). R_f: 0.074 (5:5:1 EtOAc:CH_3CN:H_2O); HPLC R_t = 6.47 and 6.76 min (broad peaks); LRMS (ESI^+): MS/MS (551) found 551 $[M+H]^+$, 436 $[M+H-C_5H_9NO_2]^+$, 306 $[M+H-\text{digitoxose}-C_{12}H_{13}NO_3]^+$.

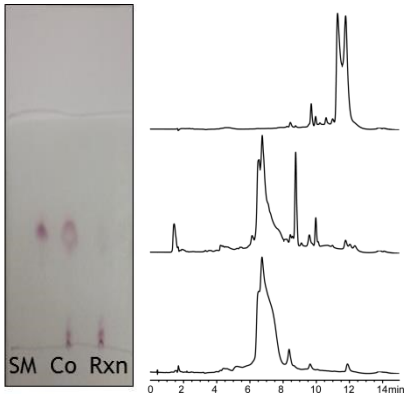

Figure 39. Deprotection of **58e**. (Left) Normal phase silica TLC (5:5:1, EtOAc:CH_3CN:H_2O) comparison of **58e** starting material (SM), the reaction mixture after 2 minutes (Rxn), and the co-spot of both (Co); and HPLC comparison of starting material **58e** (top), reaction mixture after 3 min (middle) showing the formation of **58**, and the purified reaction mixture containing **58** (bottom).

4.4.9. Jadomycin AVA (67) Purification and Characterization

Crude **67** (16.4 mg) was purified using prep TLC using 15% MeOH in DCM as the elution system yielding 15.2 mg. This material was further purified using prep TLC using 1:1 EtOAc:CH_3CN followed by 5:5:1 EtOAc:CH_3CN:H_2O as the elution system, with drying in between, yielding 5.2 mg. Final purification was accomplished using prep TLC using 15% MeOH in DCM as the elution system yielding **67** as a reddish-purple solid (2 mg) as a mixture of diastereomers (Mj/Mn = 100:67) by NMR. TLC R_f: 0.54 (10% MeOH in DCM); HPLC R_t = 8.57 min; NMR data to follow, for labeling scheme see **67** NMR data table; UV-Vis (3 x 10^{-4} and 3 x 10^{-5} M, MeOH): λ_{max} (ε) = 311 (10087), 522 (1167); LRMS (ESI+): MS/MS (536) found 536 $[M+H]^+$, 406 $[M+H\text{-digitoxose}]^+$, 306 $[M+H\text{-digitoxose-C5H10O2}]^+$; HRMS (ESI+): 558.1753 found, 558.1735 calculated for $C_{29}H_{29}NNaO_9$.

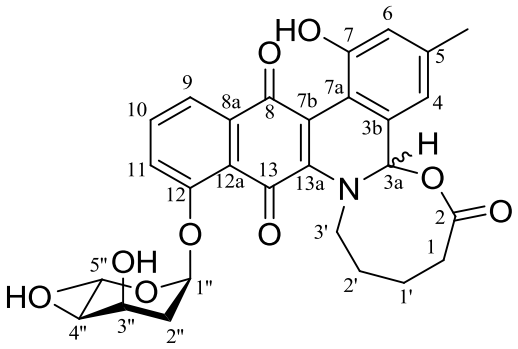

Figure 40. Atom-labeled structure of compound **67**.

Table 18. Jadomycin AVA (**67**) $3a_{Mj}$ diastereomer NMR data.

Position	δ ^{1}H (ppm)	Multiplicity (J(Hz))	δ ^{13}C (ppm)	COSY	HMBC
1	2.16 - 2.21	obscured	38.2	1'	2
2			182.0		
3a	5.64	s	92.6		3', 4, 7a, 7b, 13, 13a
3b					
4	6.77	s	120.4	5-CH_3, 6	3a, 5-CH_3, 6, 7a, 7b
5			141.3		
5-CH_3	2.36	s	21.1	4, 6	4, 5, 6
6	6.82	s	120.6	4, 5-CH_3	4, 5-CH_3, 7, 7a
7			154.8		
7-OH					
7a			114.3		
7b			129.9		
8			183.0		
8a			136.8		
9	7.81	d(7.5)	121.3	10	8, 8a, 10, 11
10	7.72	t(8.1)	136.7	9, 11	8a, 9, 11, 12
11	7.54	d(8.1)	120.6	10	9, 10, 12, 12a, 13
12			155.8		
12a			121.6		
13			185.8		
13a			154.0		
1'	1.16 - 1.68	bm	24.5	1, 2'	1, 2, 2', 3'
2'	1.72	obscured	32.2	1', 3'	1, 1', 3'
3'	3.98, 4.11	obscured	54.8	2', 3'	1', 2', 3a, 13a
1''	5.95	d(2.9)	96.5	2''	2'', 3'', 5'', 12
2''	2.22	bm	36.4	1'', 2'', 3''	
2''	2.41	bm	36.4	1'', 2'', 3''	
3''	4.08	obscured	68.4	5''-CH_3, 2'', 4', 5''	
3''OH					
4''	3.28	obscured	74.1	3'', 5''	5'', 5''-CH_3
4''-OH					
5''	3.93	bm	66.4	4'', 3'', 5''-CH_3	
5''-CH_3	1.22	d(6.2)	18.2	3'', 5''	4'', 5''
MeOH	3.31		49.0		

Table 19. Jadomycin AVA (**67**) $3a_{Mn}$ diastereomer NMR data.

Position	δ ^{1}H (ppm)	Multiplicity (J(Hz))	δ ^{13}C (ppm)	COSY	HMBC
1	2.16 - 2.21	obscured	38.2	1'	2
2			182.0		
3a	5.61	s	92.2		3', 4, 7a, 7b, 13, 13a
3b					
4	6.78	s	120.4	5-CH_3, 6	3a, 5-CH_3, 6, 7a, 7b
5			141.7		
5-CH_3	2.36	s	20.9	4, 6	4, 5, 6
6	6.82	s	120.6	4, 5-CH_3	4, 5-CH_3, 7, 7a
7			154.8		
7-OH					
7a			114.2		
7b			131.3		
8			184.0		
8a			136.8		
9	7.85	d(7.5)	121.6	10	8, 8a, 10, 11
10	7.72	t(8.1)	136.7	9, 11	8a, 9, 11, 12
11	7.56	d(8.1)	121.3	10	9, 10, 12, 12a, 13
12			156.4		
12a			121.0		
13			184.2		
13a			151.3		
1'	1.16 - 1.68	bm	24.5	1, 2'	1, 2, 2', 3'
2'	1.68 - 1.86	obscured	32.0	1', 3'	1, 1', 3'
3'	3.80, 4.36	bm	55.6	2', 3'	1', 2', 3a, 13a
1''	5.93	d(2.9)	96.8	2''	2'', 3'', 5'', 12
2''	2.22	bm	36.4	1'', 2'', 3''	
2''	2.41	bm	36.4	1'', 2'', 3''	
3''	4.08	obscured	68.1	5''-CH_3, 2'', 4', 5''	
3''OH					
4''	3.28	obscured	74.1	3'', 5''	5'', 5''-CH_3
4''-OH					
5''	3.93	bm	66.5	4'', 3'', 5''-CH_3	
5''-CH_3	1.22	d(6.2)	18.2	3'', 5''	4'', 5''
MeOH	3.31		49.0		

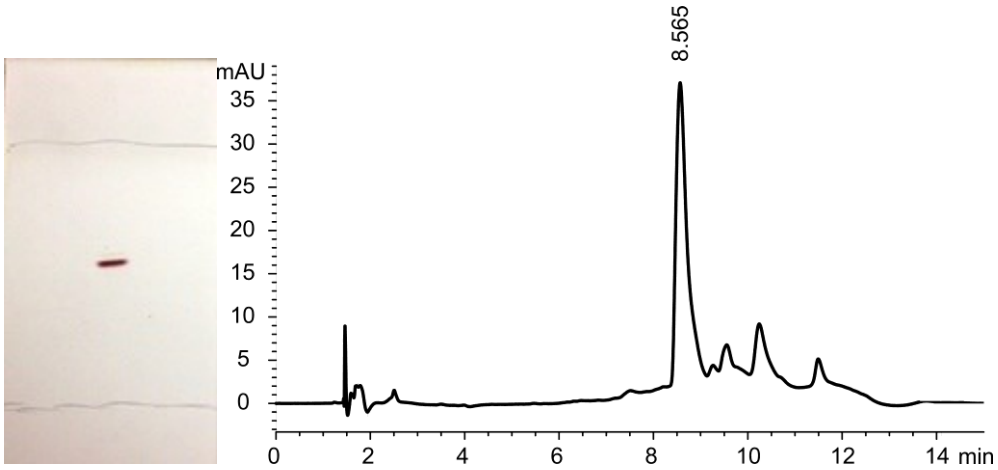

Figure 41. TLC and HPLC analysis of **67**. (Left) Normal phase silica TLC (9:1, DCM:MeOH) of purified 67; and (right) HPLC of purified **67**.

4.4.10. Jadomycin DOct (66) Crude Isolation

Due to a lack of material (5 mg crude extract), purification of compound **66** was not attempted. LC-MS/MS performed on the crude extract used for further derivatization showed the same fragmentation pattern observed for compound **58**, suggesting similar chemical properties (Figure 42). For crude extraction procedure see Chapter 4.2.

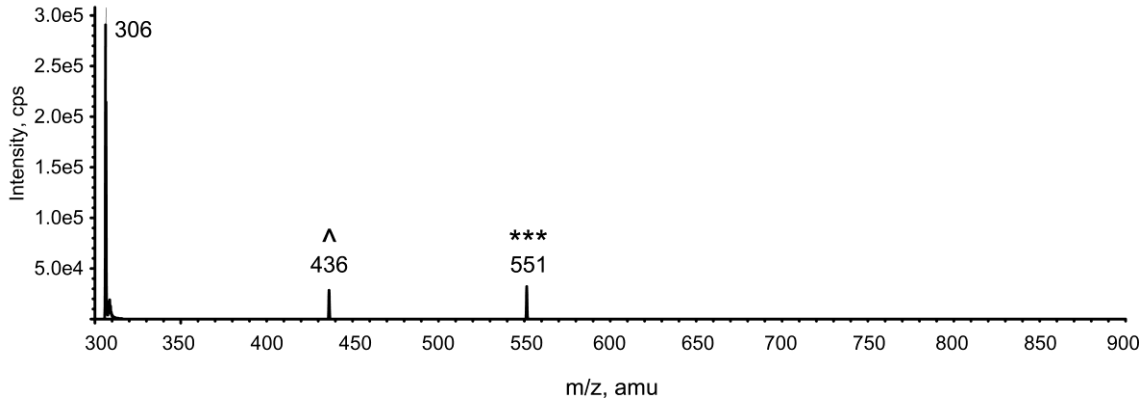

Figure 42. LC-MS/MS fragmentation of **66** illustrating $[M+H]^+$ (***),of amino acid group first $[M+H–R]^+$ (^) and cleavage of the sugar $[M + H – \text{digitoxose} – R]^+$ (*m/z* 306).

4.4.11. Jadomycin DOct Phenoxyacetylamide (66a)

Crude **66** (5 mg) was dissolved in 5 mL of a 1:1 mixture of CH_3CN:PBS buffer (pH 7.6), and added to solid compound **59** (9 mg, 18 μmol) in a 25 mL round bottom flask drop-

wise with gentle stirring. The flask was corked and protected from light, and the reaction was allowed to proceed for 2 h. After 2 h the reaction had not proceeded to completion as observed by the presence of **66** by TLC analysis. Another 5 mg (9 μmol) of **59** was dissolved in 1 mL of a 1:1 (CH_3CN:PBS) solution and added to the reaction flask. The reaction was allowed to proceed for an additional 2 h until complete. The reaction mixture was dried *in vacuo*. The reaction mixture was brought up in minimal DCM (~ 1 mL), loaded onto prep TLC plate a developed 3× using a 5:5:1 EtOAc:CH_3CN:H_2O solvent system. The band of interest was scraped from the plate and the compound was eluted with 100% methanol. Final purification was accomplished by size exclusion chromatography (LH-20 resin). Material was eluted using 5:5:1 EtOAc:CH_3CN:H_2O and dried yielding >1 mg of the purple solid **66a** as as a mixture of diastereomers (M_j/M_n = 100:65) by NMR. TLC R_f: 0.36 (5:5:1 EtOAc:CH_3CN:H_2O), HPLC R_t = 8.90 min; LRMS (ESI^+): MS/MS (685) found 685 $[M+H]^+$, 555 $[M+H-\text{digitoxose}]^+$, 306 $[M+H-\text{digitoxose}-C_{13}H_{15}NO_4]^+$.

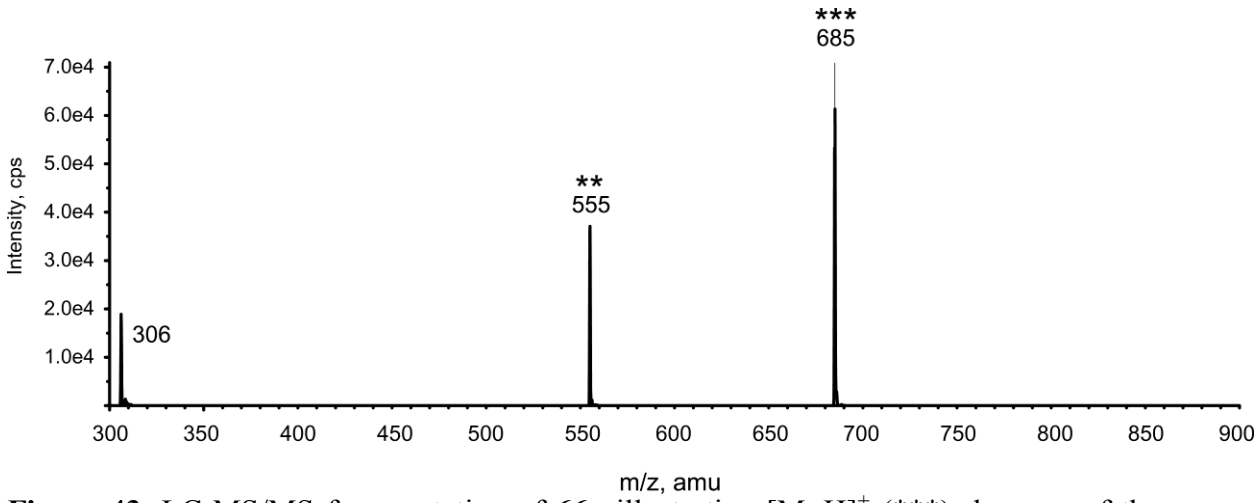

Figure 43. LC-MS/MS fragmentation of **66a** illustrating $[M+H]^+$ (***),cleavage of the sugar $[M + H - \text{digitoxose}]^+$ (**) and the amino acid groups $[M + H - \text{digitoxose} - R]^+$ (*m*/*z* 306).

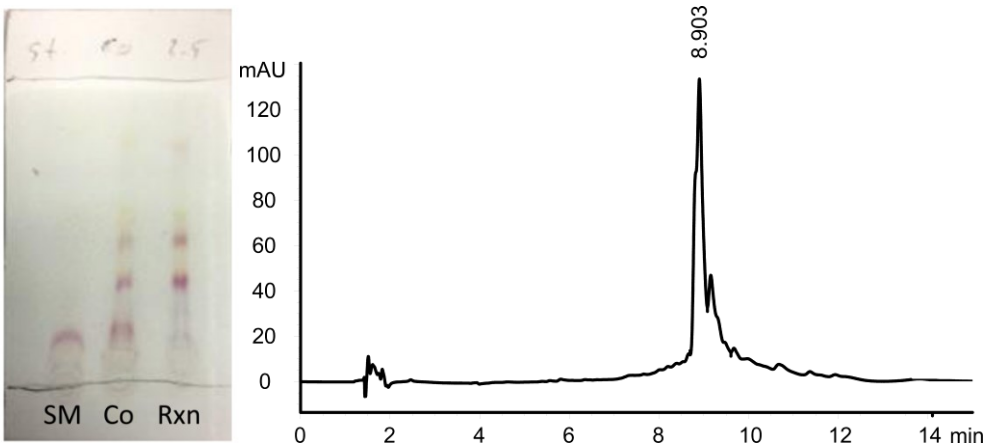

Figure 44. TLC and HPLC analysis of **66a** (Left) Normal phase silica TLC (5:5:1, EtOAc:CH_3CN:H_2O) comparison of crude **66** starting material (SM), the reaction mixture of **66** and **59** after 2.5 hours (Rxn), and the co-spot of both (Co); and (right) HPLC of purified **66a**.

4.4.12. L-digitoxosyl-phenanthroviridin (70)

Crude ethyl acetate extract was dissolved in minimal CH_2Cl_2 and loaded onto preparatory TLC plates. The plates were developed 3× with 5% methanol in CH_2Cl_2 and the band of interest was scraped from the glass backing and eluted with 100% methanol yielding 16 mg of material. Final purification was accomplished by preparatory TLC using a 1:1 EtOAc:CH_3CN solvent system and developing the plate twice to ensure separation. The band of interest was scraped from the glass backing and eluted with 100% methanol and dried *in vacuo*. Dry material was brought up in CH_2Cl_2 and filtered to remove any residual silica and dried yielding 8 mg of **70** (4 mgL^{-1}) as an amber yellow solid as a single diastereomer by NMR. TLC R_f: 0.46 (9:1 CH_2Cl_2:MeOH); HPLC R_t = 9.47 min; NMR data to follow, for labeling scheme see **70** NMR data table; UV-Vis (2.25 x 10^{-4} M, MeOH): λ_{max} (ε) = 303 (3911), 369 (1444); LRMS (ESI^+): MS/MS (436) found 436 $[M+H]^+$, 306 $[M+H\text{-digitoxose}]^+$; HRMS ($ESI^+$): 458.1192 Found, 458.1216 Calculated for $C_{24}H_{21}NNaO_7$.

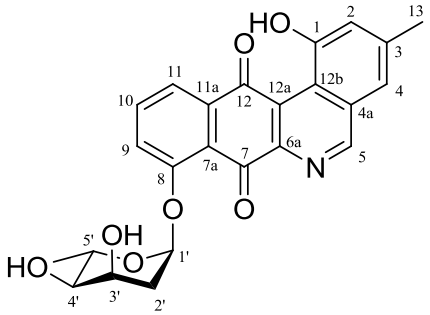

Figure 45. Atom-labeled structure of compound **70**.

Table 20. L-digitoxosyl-phenanthroviridin (**70**) NMR data.

position	δ ^{1}H (ppm)	Multiplicity (**J**(Hz))	δ ^{13}C (ppm)	COSY	HMBC	NOESY
1			155.3			
1-OH	11.84	s (br)				
2	7.32	d(1.4)	123.6	4, 13	1, 4, 13	13
3			144.2			
4	7.46	s	121.5	2, 13	2, 4a, 5, 13	5, 13
4a			132.8			
5	9.42	s	160.9	none	4, 4a, 6a, 12b	4
6a			147.4			
7			181.5			
7a			120.1			
8			156.2			
9	7.63	d(8.5)	121.9	10	7a, 11	1', 10
10	7.76	t(8.1)	136.2	9, 11	8, 11a	9, 11
11	8.00	d(7.6)	122.7	10	7a, 9, 12	10
11a			136.3			
12			191.1			
12a			126.9			
12b			120.6			
13	2.55	s	21.7	2, 4	2, 3, 4	4
1'	5.96	d(3.2)	95.2	2'$_{ax}$, 2'$_{eq}$	3'	9, 2'
2'$_{ax}$	2.24	dt(15.1, 3.7)	35.6	1', 2'eq, 3'	none	2'$_{eq}$
2'$_{eq}$	2.52	ddd(15.1, 2.8, 0.9)	35.6	1', 2'ax, 3'	3', 4'	2'$_{ax}$
3'	4.11	bm	66.5	2'$_{ax}$, 2'$_{eq}$, 3'-OH, 4'	none	2', 4'
3'-OH	5.2	brd(10.6)		3'		
4'	3.24	bm	72.9	3', 5'	none	6'
4'-OH	2.89	s (br)		4'		
5'	3.79	dq (10.1, 6.2)	66.6	4', 6'	none	6'
6'	1.22	d (6.2)	18.1	5'	4', 5'	4', 5'

4.5. Biological Activity Evaluation

All procedures and data presented in section 4.5 were carried out in collaboration with the laboratory of Dr. Sherri McFarland at Acadia University, Wolfville, NS Canada. This work was not conducted by the author, but acts as a supplement to the results and discussions presented.

4.5.1. Photo-mediated DNA cleavage assays

Supercoiled plasmid (form I) was prepared by transformation of NovaBlue cells (Novagen) followed by purification using the QIAprep Spin miniprep kit (Qiagen) to

yield approximately 30 μg of plasmid DNA per 20 mL culture. Jadomycins **58a-58d** were dissolved in 99% ethanol, and subsequent dilutions were made with distilled water, where the final assay tubes contained <1% ethanol. Reaction mixtures (20 μL total volume) were prepared in 0.5 mL sterile microcentrifuge tubes. Transformed pUC19 plasmid (final concentration 130 ng, or 20 μM bases, >95% form I) was delivered to the assay tubes as a solution in 10 mM Tris-Cl (pH 8.5) and diluted with Tris (pH 7.4, final concentration 5 mM) and NaCl (final concentration 50 mM). Solutions of jadomycins were added to give the final concentrations (10, 25, 50, 75, 100 μM) and the reaction mixtures were diluted to a final volume of 20 μL with ultrapure water. Sample tubes were kept at 37 °C in the dark, or irradiated with white light in a photoreactor (Luzchem LZC-4X, 7.72 mW cm^{-2}) for 30 min in order to yield an energy density of approximately 14 J cm^{-2}. After treatment, all samples (dark and light) were quenched by the addition of 4 μL gel loading buffer (0.025% bromophenol blue, 40% glycerol), loaded onto 1% agarose gels cast with 1 × TAE (40 mM Tris-acetate, 1 mM EDTA, pH 8.2) containing ethidium bromide (0.75 μg mL^{-1}) and electrophoresed for 30 min at 80 V cm^{-1} in 1 × TAE. The bands were visualized with UV-transillumination (UVP transilluminator) and processed using the Gel Doc-It Imaging System (UVP).

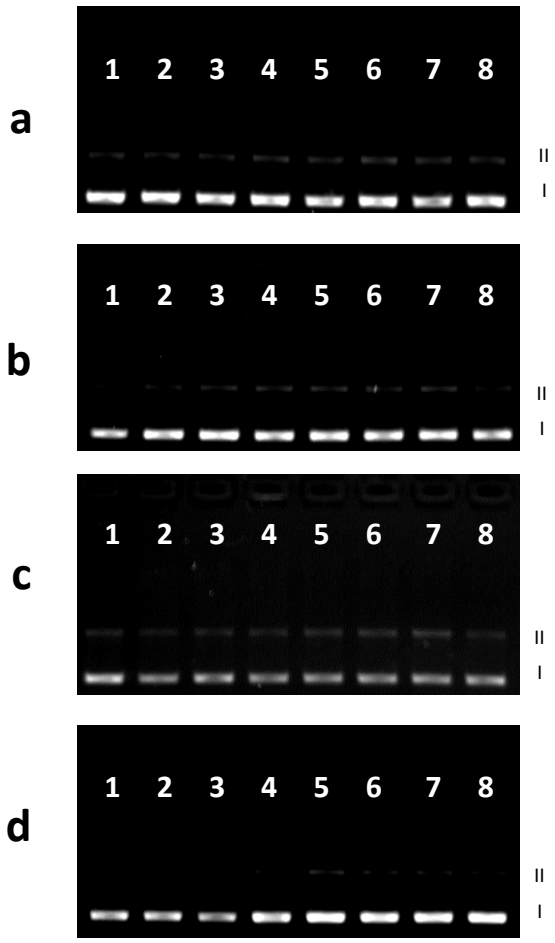

Figure 46. Photo-mediated DNA cleavage assay with jadomycins **58a-58d**. Gel electrophoresis analysis of pUC19 DNA (20 μM bases) in a photocleavage assay, performed in 1% agarose gel, 1X TAE, 8V cm^{-1}, 30 min photoreactor with vis bulbs (14 J cm^{-2}), in the presence of jadomycin compounds **58a** (*a*), **58b** (*b*), **58c** (*c*), **58d** (*d*). Lane 1, DNA alone dark; lane 2-7 different concentrations of jadomycin compounds: (2) 0 μM, hν; (3) 10 μM, hν; (4) 25 μM, hν; (5) 50 μM, hν; (6) 75 μM, hν; (7) 100 μM, hν; lane (8) 100 μM, dark. Form I (supercoiled) and form II (nicked) plasmid DNA are indicated.

4.5.2. Copper-mediated DNA cleavage assays

Plasmid DNA cleavage assays were prepared as above for compounds **58a - 58d** at 100 μM, in 20 μL reaction volumes, with and without the addition of 100 μM cupric acetate. The reaction tubes were incubated at 37 °C for 24 hr. The samples were then quenched by the addition of 4 μL gel loading buffer (0.025% bromophenol blue, 40% glycerol), loaded onto 1% agarose gels cast with 1 × TAE (40 mM Tris-acetate, 1 mM EDTA, pH 8.2) containing ethidium bromide (0.75 μg mL^{-1}) and electrophoresed for 30

min at 80 V cm^{-1} in 1 × TAE. The bands were visualized with UV-transillumination (UVP transilluminator) and processed using the Gel Doc-It Imaging System (UVP).

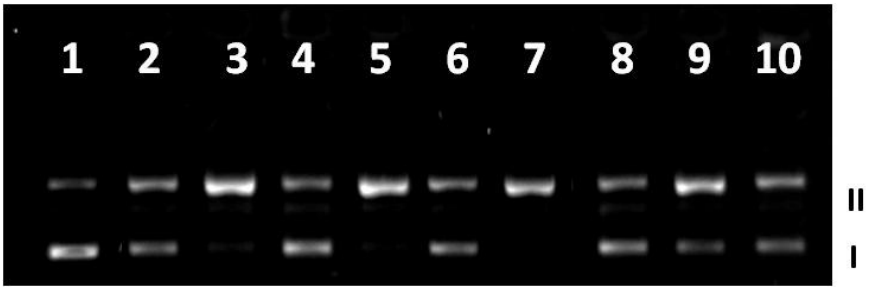

Figure 47. Copper-mediated DNA cleavage by jadomycins **58a**-**58d**. Gel electrophoresis analysis of pUC19 DNA (20 μM bases) in a DNA cleavage assay, performed in 1% agarose gel containing 0.75 μg mL^{-1} ethidium bromide, 1 × TAE, 8 V cm^{-1}, overnight dark incubation, in the presence of 4 jadomycin compounds with/without cupric acetate. Lane 1, DNA alone ; Lane 2, **58a**, 100 μM; Lane 3, **58a** and Cu^{2+}, 100 μM; Lane 4, **58b**, 100 μM; Lane 5, **58b** and Cu^{2+}, 100 μM; Lane 6, **58c**, 100 μM; Lane 7, **58c** and Cu^{2+}, 100 μM; Lane 8, **58d**, 100 μM; Lane 9, **58d** and Cu^{2+}, 100 μM; Lane 10, Cu^{2+} only, 100 μM. Form I (supercoiled) and form II (nicked) plasmid DNA are indicated.

4.5.3. Bacterial culture

Using aseptic technique, a vial of *Streptococcus mutans* (*S. mutans* Clarke, NCTC 10449) was propagated by transferring half of the freeze-dried pellet, using a sterile loop, to a culture tube containing 2 mL Brain Heart Infusion media (BHI, Oxoid), and gently mixed by swirling. The tube was capped loosely and placed in a 37 °C incubator for 24 hr. The following day, 10 serial dilutions were made (10^{-1} to 10^{-8}), then 0.1 mL aliquots from each dilution were spread on to fresh BHI agar plates (3.8% BHI) using sterile loops, allowed to dry with lids askew, then placed upside down in 37 °C incubator overnight. Purity of the colony growth was verified, and then the bacterial culture tube was subcultured by centrifuging (5000 rpm, 5 min), carefully pouring off the supernatant to waste, and replacing with 5 mL fresh media. A frozen stock of *S. mutans* was prepared by transferring 500 μL aliquots of *S. mutans* culture to sterile 1.5 mL microcentrifuge tubes containing 500 μL sterile 70% glycerol/water. The tubes were mixed by vortexing briefly and subsequently stored in a -80 °C freezer. Primary growth colony plates were prepared by transferring 50 μL frozen *S. mutans* to a sterile microcentrifuge tube

containing 500 µL tryptic soy broth (TSB, Fluka 22092) and the solution was mixed well by vortexing. An aliquot of 50 µL was applied, using a quadrant streak method, to a TSA plate (3% TSB in agar), allowed to dry with the lid askew, and incubated overnight. The following morning the purities of the primary growth cultures were verified, then 1-2 colonies were transferred to a sterile microfuge tube containing 500 µL TSB and mixed well by pipetting up and down and vortexing. A secondary growth colony plate was prepared by transferring 50 µL of this mixture to a warmed TSA plate, quadrant streaked, allowed to dry as before, then incubated overnight. The next morning the purities of the secondary growth cultures were again verified and subsequently used for agar well diffusion assays. All experiments using *S. mutans* were made from freshly made (less than one week old) secondary growth colony plates.

4.5.4. Agar well diffusion assays

The agar well diffusion method was used as an antibacterial screening test for jadomycins **58a-58d**. Under aseptic conditions, an inoculum of *S. mutans* was prepared by transferring colonies from a secondary growth plate to a sterile 15 mL conical tube (VWR, Canada) containing 5 mL sterile distilled water and the contents were mixed well by vortexing. A 500 µL aliquot of the inoculum was applied to each of 4 TSA plates and was spread evenly, using sterile loops, to allow uniform growth of a bacterial lawn. The plates were given time to completely dry, with lids askew, for about 30 min. Using sterile glass Pasteur pipettes, bored holes of about 6 cm were made in 4 quadrants of each TSA plate. Ethanolic stock solutions of jadomycins (5 mM) were diluted to 300 µM in water (final concentration of ethanol 6%) and 50 µL aliquots were added to duplicate wells along with a 6% ethanol solvent control, for dark and light treatments. The dark plates were kept in a dark drawer, covered in foil, and the light plates were irradiated with white light in a photoreactor (Luzchem LZC-4X, 7.72 mW cm^{-2}) for 60 min in order to yield an energy density of approximately 28 J cm^{-2}. The bacterial growth inhibition zones were measured in mm using vernier calipers (Bel-Art, USA).

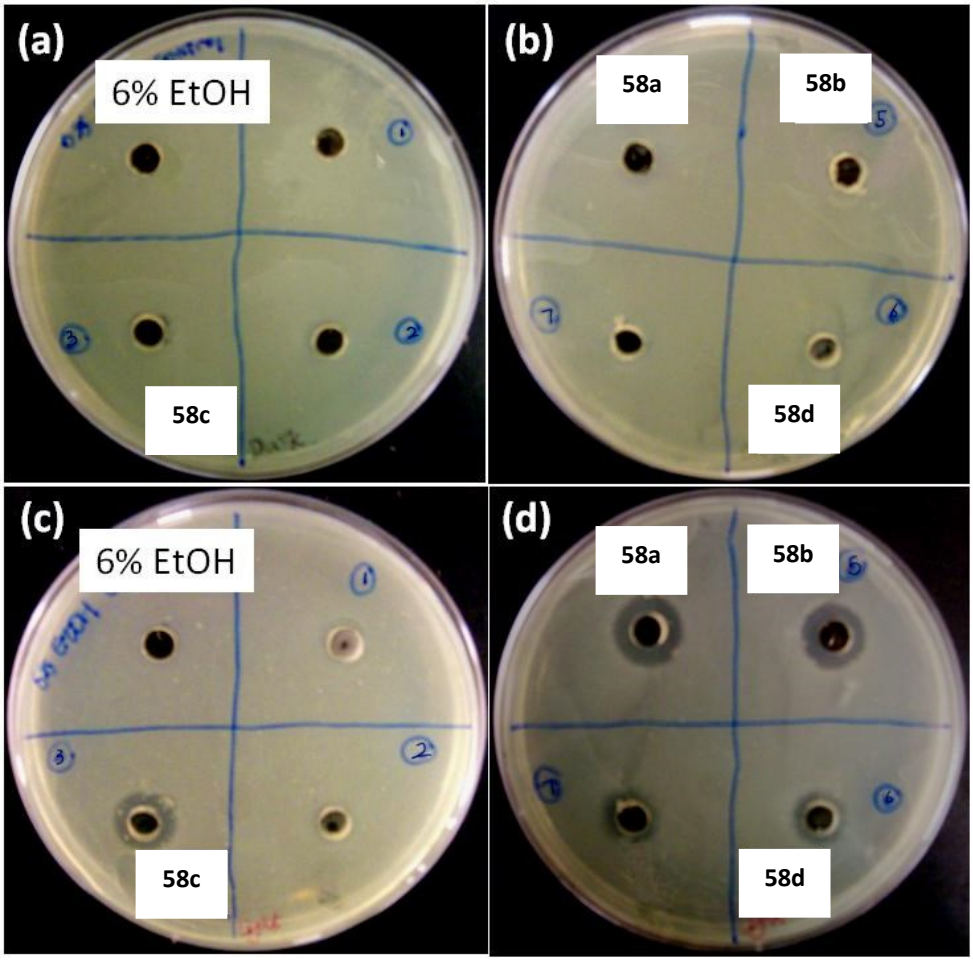

Figure 48. *Streptococcus mutans* growth plates and agar well diffusion inhibition zones from jadomycins **58a-58d** (300 μM), in the dark (a, b) and light (c, d).

Table 21. Agar well diffusion tabulated results for bacterial growth inhibition by jadomycins **58a-58d**.

Jadomycin	Dark Inhibition Zone (mm)	Light Inhibition Zone (mm)
58a	6.0	11.3
1b	6.0	10.5
58c	6.0	10.0
58d	6.0	7.3
Control (6% EtOH)	6.0	6.0

Inhibition zones (mm) given as the diameter of the inhibition halo, including the 6 mm sample well

4.6 General Methods for JadX NMR Binding Studies

4.6.1. Buffers and Growth Media

A complete list of buffers and growth media used for this study can be found in Appendix E.

4.6.2. HPLC Analysis

For HPLC analyses of growth media, 20 mL of growth media from the WT, Δ*jadW2* or Δ*jadX* growths were passed down 2 g phenyl columns preconditioned with methanol. Columns were washed with 100 mL H_2O and material was eluted with 100% methanol. Eluent was dried down and dissolved in 4 mL methanol. This crude extract was then injected (20 μL) into the system. HPLC analyses were performed as previously described. Samples were compared to a standard of pure jadomycin DS (**96)**. Chloramphenicol (**3**) spiking experiments were accomplished by spiking with purchased **3** to a final concentration of 100 μM **3**.

4.6.3. LC-MS/MS Analysis

Low-resolution liquid chromatography mass spectrometry was performed using the system previously described. Clarified growth media was lyophilized. Samples were dissolved appropriately (to ensure a concentration of jadomycin or **3** that was within the

linear detectable range of the instrument) in methanol (Appendix E), filtered and 5 μL aliquots were injected onto the column. Elution of compounds was accomplished as previously described. For the jadomycins, the instrument was used in positive mode (ESI+) scanning 524 *m/z* $[M+H]^+$ for **96**, and 550 *m/z* $[M+H]^+$ for **6**. For **3**, the instrument was used in negative mode (ESI-) scanning for 321 $[M-H]^-$. Enhanced product ionization (EPI) was conducted over a range of 300-900 *m/z* scanning for the appropriate $[M+H]^+$ or $[M-H]^-$ and the appropriate fragmentation. Peaks representing total ion count were integrated and integrals were compared to standard curves generated from pure samples to determine concentrations in media. All measurements were performed in triplicate.

4.6.4. NMR Methodologies.

All NMR spectra were recorded using a Bruker AV-III 700 MHz Spectrometer (^{1}H: 700 MHz, ^{13}C: 150 MHz) equipped with an ATMA 5 mm or 1.7 mm TCI cryoprobe, located at the Canadian National Research Council Institute for Marine Biosciences (NRC-IMB) in Halifax, Nova Scotia unless otherwise stated. All experiments were run at 293.2 K. To prepare dPBS buffer, PBS buffer of the appropriate pH was lyophilized and dissolved in an equal volume of D_2O. All STD-NMR spectra were recorded in dPBS (pH 7.6) buffer. All initial WaterLOGSY NMR spectra used for ligand screening purposes were recorded in 90% PBS, 10% dPBS (pH 7.6) buffer. All WaterLOGSY and ^{15}N-^{1}H HSQC experiments used for K_D estimations were recorded in 85% PBS, 10% dPBS, 5% DMSO-d_6 (pH 7.6 and 6.6 respectively). Appropriate solvents used in each case can be found with the accompanying NMR-spectra (Appendix E). Chemical shifts (δ) were given in ppm, and calibrated to residual solvent peaks (HOD 4.79 ppm or DMSO in water 2.71 ppm).[142]

4.7. pET28a(+)::*jadX* Plasmid Construction

4.7.1. Genomic DNA Isolation (Kirby Mix Procedure)

S. venezuelae ISP5230 WT and *S. venezuelae* ISP5230 VS1085 (Δ*jadX*) mutant genomic DNA were isolated using the Kirby mix procedure. *S. venezuelae* ISP5230 WT and *S. venezuelae* ISP5230 VS1085 were grown in 25 mL MYM media overnight at 30 °C (250 RPM). Bacterial growths were centrifuged at 3750 RPM (4 °C) for 30 min. Supernatant

was decanted and the cell pellet was washed with TE25S buffer. Cells were re-pelleted by centrifugation and supernatant was decanted. Cell pellets were re-suspended in 3 mL TE25S buffer, and 100 µL of a lysozyme solution (60 mg/mL) was added. The mixtures were incubated at 37 °C for 60 min. Four (4) mL of 2 × Kirby mix was added and the solutions were agitated for 1 min by vortexing. Eight (8) mL of a phenol:chloroform:isoamyl alcohol mix (50:50:1) was added and the solutions were agitated for 15 seconds by vortexing. Solutions were centrifuged at 3750 RPM (4 °C) for 10 min. The top aqueous layers were removed and added to 3 mL of a fresh phenol:chloroform:isoamyl alcohol mix (50:50:1) containing 600 µL of an unbuffered 3 M sodium acetate solution. The mixtures were vortexed for 1 min and centrifuged at 3750 RPM (4 °C) for 10 min. Isopropanol was added to the solution (~0.6 vol.) and mixed thoroughly. DNA was spooled onto a sealed Pasteur pipette and washed with 5 mL of a 70% ethanol solution. The DNA solution was dried overnight and dissolved in 1 mL distilled deionized water at 50 °C.

4.7.2. *jadX* Cloning and Amplification

jadX was amplified by polymerase chain reaction (PCR) from DNA isolated from *S. venezuelae* ISP5230 WT *via* the Kirby mix procedure. For amplification, the primers *jadX2mR* 5'-GGTGGTAAGCTTTCAGGAGTGGCCCTTCGCGCCGGGGGCCTCGCCGGCGTTC-3' and *jadX3mF* 5'-GGTGGTCATATGACCACCACCGACCTCACCGCCGTGACCACCACCG ACGGA-3' were used. *jadX2mR* and *jadX3mF* introduced HindIII and NdeI restriction sites respectively (sites underlined). Amplification was accomplished using Finnzymes Phusion® High-Fidelity DNA Polyemerase system. The PCR reaction mixture for *jadX* amplification was as follows:

PCR Reaction Set Up

Component	Volume (µL)	Company
Distilled deionized water	13.5	
5 × Phusion Buffer (HF)	10	New England Biolabs
10 mM dNTPs	1	New England Biolabs
Primer A (*jadX*2mR, 5 mM)	5	New England Biolabs
Primer B (*jadX*3mF, 5 mM)	5	New England Biolabs
Genomic DNA	10	
DMSO	5	Sigma
Phusion Polymerase (2 U/µL)	0.5	New England Biolabs

The reaction mixture was gently centrifuged and placed into a BIOMETRA TPersonal thermocycler. The PCR procedure was a touchdown-like procedure and was carried out as follows:

Step	Temperature	Time	Repeats
(1) Initial Denaturing	95 °C	2 min	None
(2) Denaturing	95 °C	30 sec	Steps 2-4 Repeated × 14 (15 cycles total)
(3) Annealing	82.6 °C (1 °C drop per cycle)	30 sec	Steps 2-4 Repeated × 14 (15 cycles total)
(4) Extension	72 °C	1 min	Steps 2-4 Repeated × 14 (15 cycles total)
(5) Denaturing	95 °C	30 sec	Steps 5-7 Repeated × 19 (20 cycles total)
(6) Annealing	55 °C	30 sec	Steps 5-7 Repeated × 19 (20 cycles total)
(7) Extension	72 °C	1 min	Steps 5-7 Repeated × 19 (20 cycles total)
(8) Final Extension	72 °C	5 min	None
(9) Storage	4 °C		None

Amplification was confirmed by ethidium bromide (EtBr) DNA gel electrophoresis (1% agarose gel). A strong UV active band at approximately 520 base pairs (estimated size of *jadX*) (Figure 49) was observed. The UV active band was compared to a 0.5 μg of 100 bp DNA ladder (New England Biolabs). The amplified *jadX* solution was run on a 1% agarose gel, cut from the gel, and purified with a QIAquick gel extraction kit. DNA from the *S. venezuelae* ISP5230 VS1085 (Δ*jadX*) mutant was also isolated, and the *jadX* gene was amplified to ensure presence of the disrupting apramycin resistance cassette (Figure 49).

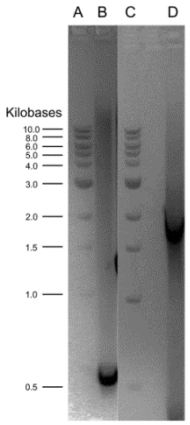

Figure 49. 1% agarose gel comparing cloned amplified *jadX* from *S. venezuelae* ISP5230 WT and *S. venezuelae* ISP5230 VS1085; (*A*) a 1 kb DNA ladder, (*B*) amplified *jadX* from *S. venezuelae* ISP5230 WT, (*C*) a 1 kb DNA ladder, and (*D*) amplified *jadX* disrupted with an apramycin resistance cassette from *S. venezuelae* ISP5230 VS1085 (Δ*jadX*).

4.7.3. pET28a(+) Plasmid Preparation

E. coli DH5α™ was transformed with the pET28a(+) plasmid *via* heat shock. One hundred (100) µL of the transformed *E. coli* was plated on LB agar supplemented with kanamycin (50 µg ml^{-1}) (LB_{Kan}), and grown at 37 °C overnight. One colony was randomly selected and streaked onto new LB_{Kan} agar and grown overnight. A colony from the second plate was selected and grown in 25 mL LB_{Kan} at 37 °C with agitation (250 RPM) overnight. Four 2 mL samples were drawn and centrifuged at 13,000 RPM for 10 min at 4 °C. The supernatant was discarded and the pellets stored at -70 °C. The plasmid was extracted and purified from the pellets utilizing a QIAprep Spin Miniprep Kit. The concentration of the resultant purified plasmid solution was determined to be approximately 30 ng/µL.

4.7.4. pET28a(+) and *jadX* Digestion

The pET28a(+) from the plasmid preparation was doubly digested by treatment with HindIII and NdeI.

Plasmid Digestion Reaction

Component	Volume (µL)	Company
pET28a(+) solution from plasmid prep	49	
10 × Buffer #2	7	NEB
HindIII (20000 U/mL)	7	NEB
NdeI (20000 U/mL)	7	NEB

The reaction mixture was incubated at 37 °C for 1 hr. The mixture was gently centrifuged, and 7 µL of calf intestinal alkaline phosphatase (10000 U/mL, NEB) was added, and the reaction mixture was incubated for an additional 45 min. The double digested pET28a(+) was purified using a QIAquick PCR Purification Kit (QIAGEN). The amplified *jadX* was then doubly digested by treatment with HindIII and NdeI.

jadX Digestion Reaction

Component	Volume (µL)	Company
jadX solution	20	
10 × Buffer #2	3	NEB
HindIII (20000 U/mL)	3	NEB
NdeI (20000 U/mL)	3	NEB
Distilled deionized water	1	

The reaction was mixed and incubated at 37 °C for 1 h. The digestion reaction was purified using a QIAquick PCR Purification Kit (QIAGEN). Concentrations of doubly digested pET28a(+) and *jadX* were determined by comparative agarose gel electrophoresis, comparing ethidium bromide stained band intensities of the digested fragments to known DNA standards. Digestions yielded concentrations of 11 ng/µL digested pET28a(+), and 18 ng/µL digested *jadX*. Ratios of *jadX*-insert to linearized pET28a(+) for ligation were determined using the formula:

X ng of insert = (3)(bp insert)(50 ng linearized plasmid) / (bp of linearized plasmid)

The *jadX*-insert was 521 bp in size, and the linearized plasmid was 5304 bp. Ligation was accomplished using T4 DNA ligase (NEB).

Ligation Reaction

Component	Volume (µL)	Company
Digested *jadX* insert (18 ng/µL)	1	
Digested pET28a(+) (11 ng/µL)	5	
Distilled deionized water	11	
10 × Ligation buffer	3	NEB
T4 DNA Ligase	1	NEB

The reaction was mixed and incubated at room temperature for 15 min. A 5 µL aliquot of the ligation mixture was mixed with a 100 µL aliquot of of *E. coli* DH5-α competent cells, and transformed into the cells via heat shock. One hundred (100) µL of the mixture was plated onto a LB_{Kan} agar plate, and grown overnight at 37 °C. Approximately 25 bacterial colonies grew. Five (5) colonies were randomly selected for analysis. Colonies were inoculated and grown in 25 mL LB_{Kan} at 37 °C with agitation (250 RPM) overnight.

Samples were fractioned (12 × 2 mL) and centrifuged at 13000 RPM (4 °C) for 45 min. The supernatant was decanted and pellets were stored at -70 °C. Plasmids from each colony were extracted and purified from the pellets utilizing a QIAprep Spin Miniprep Kit. Plasmid digestion was performed on each of the purified plasmids using HindIII and NdeI to test for the presence of the *jadX*-insert.

pET28a(+)::*jadX* Plasmid Digestion Reactions

Component	Volume (µL)	Company
Plasmid	7	
10 × Buffer #2	1	NEB
HindIII (20000 U/mL)	1	NEB
NdeI (20000 U/mL)	1	NEB

Reactions were mixed and incubated at 37 °C for 1 h. Digestion was visualized by agarose gel electrophoresis. All plasmids showed the appropriate digestion pattern suggesting the successful ligation of the *jadX*-insert into the plasmid.

4.7.5. Overexpression and Purification of JadX

The plasmid was then introduced into *E. coli* BL21(λDE3). Transformed cells were grown overnight on LB-agar plates supplemented with kanamycin (50 µg ml^{-1}). Transformants were grown overnight in LB media supplemented with kanamycin (50 µg ml^{-1}) on a rotary shaker (250 rpm) at 30 °C. A 2.5 mL aliquot of inoculum from the overnight culture was added to 250 mL LB media supplemented with kanamycin (50 µg ml^{-1}). Growths were performed on a 2 L scale (8 × 250 mL in 1 L flasks). Bacteria were grown in the fresh media at 30 °C until an OD_{600} of ~0.6 was reached. A 250 µL aliquot of a 1 M IPTG stock solution was added to the media to a final concentration of 1 mM. Cultures were cooled to 17 °C and incubated at that temperature for 20 hr. The cells were pelleted by centrifugation (4000 × g, 4 °C, 60 min) and the supernatant was decanted. Cells were suspended in 20 mL of lysis buffer (lysis buffer: 3 mL sterile glycerol, 1 mL 10% 100× Triton, 16 mL of binding buffer [300mM NaCl; 20mM Tris•HCl, 25 mM imidazole; pH= 8.0]) per 1 L of growth media. Lysozyme (0.5 mg/mL) and DNase (1 µg/mL) were added, and the solution was mixed on ice for 30 minutes followed by sonication (5 x 5s pulses; amplitude 50%; Autotune High Intensity Ultrasonic Processor,

750 W). The crude lysate was centrifuged at 13,000 RPM for 15 minutes at 4 °C. The supernatant then loaded onto a HiTrap 5 ml Chelating HP NTA-Ni^{2+} affinity column (Amersham Biosciences) and purified at 4 °C using a Fast Protein Liquid Chromatography (FPLC) (AKTA purifier 10). A step-wise gradient of imidazole (25–250 mM) was applied and elution of the protein was monitored by UV absorbance 280 nm. The presence of JadX was determined by sodium dodecyl sulfate polyacrylamide gel (SDS-PAGE) analysis of the fractions. Those containing JadX were pooled and concentrated to ~2.5 mL by ultrafiltration (3000 × g at 4 °C, in Vivaspin-20, 10,000 MWCO tubes, VivaScience Sartorious group). Buffer exchange was then performed into PBS buffer (pH 7.6) using a PD-10 desalting column (GE Healthcare). The solution was concentrated again to 2.5 mL by ultrafiltration and desalted again into PBS buffer (pH 7.6) to ensure removal of all Tris contamination. For ^{1}H-^{15}N HSQC studies, buffer exchange was performed into PBS buffer (pH 6.6). Protein concentrations were determined using spectrophotometeric analysis (ε_{280}= 22460 $M^{-1}cm^{-1}$). The protein was further identified by MS/MS analysis.

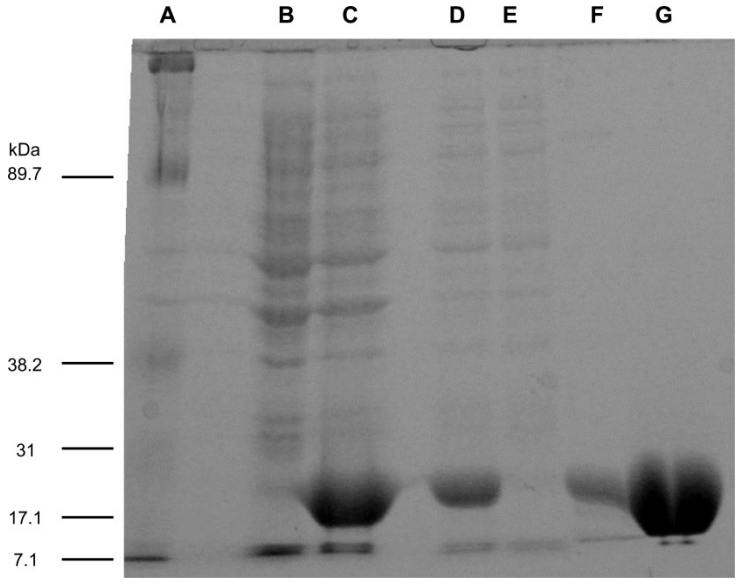

Figure 50. SDS-PAGE gel (15%) of JadX purification showing (*A*) Broad Range Prestained Protein Marker 7-175 kDa (NEB); (*B*) cells before IPTG induction; (*C*) cells after IPTG induction; (*D*) clear lysate before Ni^{2+}-NTA column; (*E*) clear lysate after Ni^{2+}-NTA column; (*F*-*G*) FPLC fractions showing purified JadX.

4.7.6. Overexpression and Purification of ^{15}N-JadX

Growth conditions used for the ^{15}N-labeling of JadX were taken from optimal conditions laid out by Marley and associates.[133] For a list of all buffers and media compositions, see Appendix E. Four (4) flasks containing 25 mL LB-liquid media supplemented with 50 μg/ml kanamycin were inoculated with single transformed colonies (pET28a(+)::*jadX*) and incubated overnight at 37 °C (250 RPM). The overnight growths were combined and centrifuged at 4 °C, 8,500 RPM for 30 minutes. The resultant pellet was washed with 10 mL of the 2× M9 solution without a nitrogen source. The cells were centrifuged, and the supernatant decanted, and re-suspended in 20 mL of minimal growth media. One (1) mL of cell solution per 250 mL minimal media was inoculated into the minimal media containing $^{15}NH_4Cl$, and allowed to grow at 37 °C, 250 RPM until OD_{600} reached between 0.5-0.7. Protein expression was induced with 250 μL per 250 mL of growth solution using a 1 M IPTG solution (final concentration of ~1 mM). Growth was allowed to continue for an additional 11 h (overnight) at 25 °C, 250 RPM. Purification and concentration was performed in the same manner as previously described with native JadX-His_6.

4.8. Jadomycin Growths and Purification

4.8.1. Bacterial Strains and Growth Conditions

S. venezuelae ISP5230 WT, *S. venezuelae* ISP5230 VS1099 (Δ*jadW2*), and *S. venezuelae* ISP5230 VS1085 (Δ*jadX*) were maintained in 20% glycerol stock solutions at -70 °C, and grown on MYM agar at 30 °C for a period of 1-3 weeks before use in jadomycin production.[76] Jadomycin productions were carried out as previously described.

4.8.2. Jadomycin DS Production, Isolation and Characterization

S. venezuelae ISP5230 VS1099 was grown under standard conditions previously developed in the Jakeman lab in MSM minimal media supplemented with D-serine (60 mM) in 2 L batches.[69] Production of **96** was initiated by ethanol shock, and growths were monitored spectrophotometrically over a 48 h incubation period as described.[69] After 24 h, the pH of the media was readjusted to pH 7.5. Cells were removed via filtration through Whatman No. 5 filter paper, followed by 0.45 mm then 0.22 mm Millipore

Durapore® membrane filters. The clarified growth media was passed through a reversed-phase SiliCycle® phenyl column (70 g), and washed with distilled water until flow through was colorless. The remaining material was eluted with 100% methanol and dried *in vacuo*. The crude mixture was purified using an 80 g silica column pre-conditioned with dichloromethane (DCM). The material was eluted using a 30 mL/min flow rate collecting 9 mL fractions. Purification was accomplished using a linear gradient system from 0% to 100 % methanol in DCM over 50 CV. The fractions containing **96** pooled and dried *in vacuo*. The sample was dissolved in minimal 10% methanol in DCM and loaded onto a preparatory TLC plate and developed in the same solvent system. Silica containing **96** was scraped from the plate and the compound was eluted using 10% methanol in DCM and dried *in vacuo*. A second preparative TLC was run on the crude natural product (5:5:1 CH_3CN:EtOAc:H_2O). Solvent was then removed *in vacuo* to yield the purified **96** as a purple solid in a yield of 51 mg/L. The compound was successfully characterized by NMR spectroscopy and LC-MS/MS. Pure samples were prepared and served as standards for NMR-binding studies and for LC-MS/MS production curves. NMR data in dPBS can be found in Table 22, for labeling scheme see Figure 51.

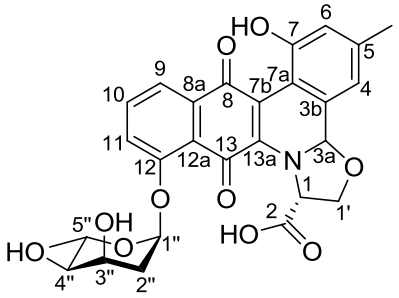

Figure 51. Atom-labeled structure of jadomycin DS (**96**).

Table 22. Jadomycin DS (**96**) NMR data recorded in dPBS.

Position	δ ^{1}H (ppm)	Multiplicity (J(Hz))	δ ^{13}C (ppm)	COSY	HMBC
1	5.22	t (7.7)	63.2	1'	2, 3a, 1'
2			175.6		
3a	5.54	s	89.1	None	4
3b			Unobserved		
4	6.44	s	115.9	5-CH_3, 6	3a, 5-CH_3, 6, 7a
5			141.8		
5-CH_3	2.01	s	21.8	4, 6	4, 5, 6
6	6.26	s	120.0	4, 5-CH_3	4, 5-CH_3, 7, 7a
7			152.4		
7-OH					
7a			111.7		
7b			Unobserved		
8			180.7		
8a			Unobserved		
9	7.63	d (7.6)	121.8	10	8, 11, 12a
10	7.60	t (8.1)	137.3	9, 11	11, 12
11	7.28	bd (8.5)	120.0	10	9, 10, 12, 12a, 13
12			155.9		
12a			118.8		
13			183.0		
13a			Unobserved		
1'	4.05	t (7.8)	71.5	1, 1'	1, 2, 3a
1'	4.91	t (8.4)	71.5	1, 1'	1, 2, 3a
1''	5.71	d (2.5)	97.2	2''	12, 3'', 5''
2''	2.18	dt (15.1, 3.3)	36.0	1'', 3''	None
2''	2.33	dd (15.1, 2.8)	36.0	1'', 3''	3'', 4''
3''	4.14	m	67.9	2'', 4''	1''
3''-OH					
4''	3.47	dd (10.0, 3.0)	73.7	3'', 5''	5'', 5''-CH_3
4''-OH					
5''	4.18	m	66.4	4'', 5''-CH_3	None
5''-CH_3	1.36	d (6.2)	18.7	5''	4'', 5''

CHAPTER 5: CONCLUSIONS

5.1. Precursor Directed Biosynthesis and Semi-synthesis of Novel Jadomycins

In conclusion, the amine containing jadomycin Oct (**58**) was successfully isolated, characterized and identified as having L-ornithine incorporated as a unique eight-membered ring system. This demonstrates promiscuity of the spontaneous amino acid incorporation step of jadomycin biosynthesis, and exemplifies how it could be further exploited. Additionally, a group of activated carboxylic acids were prepared and successfully utilized to semi-synthetically derivatize the free amine of **58**, producing a small library of jadomycin amides that act as antimicrobial phototoxins (**58a**-**58f**), all containing the unique eight-membered ring scaffold. These compounds are the first examples of jadomycins containing eight-membered heterocyclic rings. The knowledge that the spontaneous amino acid incorporation step of jadomycin biosynthesis could facilitate formation of large heterocycles led to the isolation and characterization of jadomycin AVA (**67**). The structural characterization of this compound unequivocally confirmed the presence of the eight-membered rings in **58** and its derivatives. The ability to form fully cyclized compounds using amino groups other than the α-amino group of amino acids suggests the structural diversity associated with the jadomycins may be much larger than previously established. By utilizing a unique non-enzymatic process within the jadomycin biosynthetic pathway, *S. venezuelae* likely produces many jadomycin analogues under stress conditions in an ecological setting.

In an attempt to isolate nine-membered ring containing jadomycins, *S. venezuelae* ISP5230 VS1099 growths using L-lysine were attempted. Unfortunately the L-lysine derivative was not successfully isolated due to product instability. An LC-MS/MS fragmentation analysis of *S. venezuelae* growths using singly labeled α- or ε-^{15}N-L-lysine supported the findings and demonstrated that the nine-membered ring was likely not formed at all. Upon further examination of crude growth extracts, the novel compound, L-digitoxosyl-phenanthroviridin (**70**) was isolated and characterized. Evaluation of **70** against the U.S.A. National Cancer Institutes (NCI) 60 DTP Human Tumor Cell Line Screen identified comparable bioactivity to a library of previously screened oxazolone-

ring containing jadomycin analogues. This suggested that cytotoxicity may not be affected by the incorporated amino acid as much as previously believed.

5.2. Functional Characterization of JadX

JadX-ligand binding was explored using two NMR approaches, ligand and protein observed NMR binding. Ligand observed NMR binding methodologies qualitatively identified jadomycin DS (**96**) and chloramphenicol (**3**) as JadX ligands with specific binding. WaterLOGSY methodologies were used to quantify K_d values of these protein-ligand interactions, and showed JadX to have similar affinity to these structurally diverse natural products. Protein observed binding was also demonstrated using ^{15}N-JadX titration data to support the WaterLOGSY results. Both the competitive binding and ^{1}H-^{15}N HSQC experiments identified a likely non-competitive model for the two ligands with separate JadX binding sites. The data also highlights the complex cross-regulation of these two disparate natural products. The data presented illuminates the function of JadX as a new class of nuclear transport factor 2-like (NTF2-like) protein involved in binding multiple secondary metabolites and likely involved in the complex cross-regulation of jadomycin and chloramphenicol (**3**) biosynthesis, acting by responding to endogenous natural product signals to elicit a physiological response. Reoccurrence of these "JadX-like" proteins, which are coded for in many secondary metabolite gene clusters, suggests a role in the biosynthesis of a wide array of natural products. It is likely that other JadX-like gene products play similar cross-regulatory roles. The research emphasizes that protein-ligand binding by NMR spectroscopy can be applied to biosynthetic proteins of unknown function to aid in characterization.

REFERENCES

(1) Kingston, D. G. I. *J. Nat. Prod.* **2011**, *74*, 496-511.

(2) Butler, M. S. *J. Nat. Prod.* **2004**, *67*, 2141-2153.

(3) Newman, D. J.; Cragg, G. M.; Snader, K. M. *Nat. Prod. Rep.* **2000**, *17*, 215-234.

(4) Fleming, A. *Br. J. Exp. Pathol.* **1929**, *10*, 226-236.

(5) Drews, J. *Science* **2000**, *287*, 1960-1964.

(6) Chain, E.; Florey, H. W.; Gardner, A. D.; Heatley, N. G.; Jennings, M. A.; Orr-Ewing, J.; Sanders, A. G. *Lancet* **1940**, *2*, 226-228.

(7) Schatz, A.; Bugle, E.; Waksman, S. A. *Exp. Biol. Med.* **1944**, *55*, 66-69.

(8) Jukes, T. H. *Rev. Infect. Dis.* **1985**, *7*, 702-707.

(9) Bartz, Q. R. *J. Biol. Chem.* **1948**, *172*, 445-450.

(10) Glazko, A. J.; Dill, W. A.; Resbstock, M. C. *J. Biol. Chem.* **1950**, *183*, 679-691.

(11) Levine, D. P. *Clin. Infect. Dis.* **2006**, *42*, S5-S12.

(12) Camp, D.; Davis, R. A.; Campitelli, M.; Ebdon, J.; Quinn, R. J. *J. Nat. Prod.* **2012**, *75*, 72-81.

(13) Newman, D. J.; Cragg, G. M. *J. Nat. Prod.* **2012**, *75*, 311-335.

(14) Butler, M. S.; Robertson, A. A. B.; Cooper, M. A. *Nat. Prod. Rep.* **2014**, *31*, 1612-1661.

(15) Wang, Y.; Chen, Y.; Zhou, Q.; Huang, S.; Ning, K.; Xu, J.; Kalin, R. M.; Rolfe, S.; Huang, W. E. *PLoS One* **2012**, *7*, e47530.

(16) Chater, K. F. *Philos. T. Roy. Soc. B* **2006**, *361*, 761-768.

(17) Berdy, J. *J. Antibiot.* **2005**, *58*, 1-26.

(18) Scherlach, K.; Hertweck, C. *Org. Biomol. Chem.* **2009**, *7*, 1753-1760.

(19) Ruiz, B.; Chavez, A.; Forero, A.; Garcia-Huante, Y.; Romero, A.; Sanchez, M.; Rocha, D.; Sanchez, B.; Rodriguez-Sanoja, R.; Sanchez, S.; Langley, E. *Crit. Rev. Microbiol.* **2010**, *36*, 146-167.

(20) Lawrence, J. *Curr. Opin. Genet. Dev.* **1999**, *9*, 642-648.

(21) Liu, G.; Chater, K. F.; Chandra, G.; Niu, G.; Tan, H. *Microbiol. Mol. Biol. Rev.* **2013**, *77*, 112-143.

(22) Chatterjee, S.; Vining, L. C.; Westlake, D. W. S. *Can. J. Microbiol.* **1983**, *29*, 247-253.

(23) Ayer, S. W.; McInnes, A. G.; Thibault, P.; Wang, L.; Doull, J. L.; Parnell, T.; Vining, L. C. *Tetrahedron Lett.* **1991**, *32*, 6301-6304.

(24) Doull, J. L.; Ayer, S. W.; Singh, A. K.; Thibault, P. *J. Antibiot.* **1993**, *46*, 869-871.

(25) Doull, J. L.; Singh, A. K.; Hoare, M.; Ayer, S. W. *J. Ind. Microbiol.* **1994**, *13*, 120-125.

(26) Shen, B. *Curr. Opin. Chem. Biol.* **2003**, *7*, 285-295.

(27) Khosla, C.; Herschlag, D.; Cane, D. E.; Walsh, C. T. *Biochemistry* **2014**, *53*, 2875-2883.

(28) Olano, C.; Mendez, C.; Salas, J. A. *Nat. Prod. Rep.* **2010**, *27*, 571-616.

(29) Zhang, H.; Wang, Y.; Wu, J.; Skalina, K.; Pfeifer, B. A. *Chem. Biol.* **2010**, *17*, 1232-1240.

(30) Kittendorf, J. D.; Sherman, D. H. *Bioorg. Med. Chem.* **2008**, *17*, 2137-2146.

(31) Hertweck, C.; Luzhetskyy, A.; Rebets, Y.; Bechthold, A. *Nat. Prod. Rep.* **2007**, *24*, 162-190.

(32) Ames, B. D.; Lee, M.; Moody, C.; Zhang, W.; Tang, Y.; Tsai, S. *Biochemistry* **2011**, *50*, 8392-8406.

(33) Malla, S.; Prasad Niraula, N.; Singh, B.; Liou, K.; Kyung Sohng, J. *Microbiol. Res.* **2010**, *165*, 427-435.

(34) Yu, D.; Xu, F.; Zeng, J.; Zhan, J. *IUBMB Life* **2012**, *64*, 285-295.

(35) Katsuyama, Y.; Ohnishi, Y. In *Chapter Sixteen - Type III Polyketide Synthases in Microorganisms;* David A. Hopwood, Ed.; Methods in Enzymology; Academic Press: 2012; Vol. 515, pp 359-377.

(36) Abdelfattah, M. S.; Kharel, M. K.; Hitron, J. A.; Baig, I.; Rohr, J. *J. Nat. Prod.* **2008**, *71*, 1569-1573.

(37) Kharel, M. K.; Pahari, P.; Shepherd, M. D.; Tibrewal, N.; Nybo, S. E.; Shaaban, K. A.; Rohr, J. *Nat. Prod. Rep.* **2012**, *29*, 264-325.

(38) Dann, M.; Lefemine, D. V.; Barbatschi, F.; Shu, P.; Kuntsmann, M. P.; Mitscher, L. A.; Bohonos, N. *Antimicrob. Agents Chemother.* **1965**, *5*, 832-835.

(39) Kuntsmann, M. P.; Mitscher, L. A. *J. Org. Chem.* **1966**, *31*, 2920-2925.

(40) Han, L.; Yang, K.; Ramalingam, E.; Mosher, R. H.; Vining, L. C. *Microbiology* **1994**, *140*, 3379-3389.

(41) Han, L.; Yang, K.; Kulowski, K.; Wendt-Pienkowski, E.; Hutchinson, C. R.; Vining, L. C. *Microbiology* **2000**, *146*, 903-910.

(42) Wang, L.; McVey, J.; Vining, L. C. *Microbiology* **2001**, *147*, 1535-1545.

(43) Meurer, G.; Gerlitz, M.; Wendt-Pienkowski, E.; Vining, L. C.; Rohr, J.; Richard Hutchinson, C. *Chem. Biol.* **1997**, *4*, 433-443.

(44) Kulowski, K.; Wendt-Pienkowski, E.; Han, L.; Yang, K. Q.; Vining, L. C.; Hutchinson, C. R. *J. Am. Chem. Soc.* **1999**, *121*, 1786-1794.

(45) Chen, Y. H.; Wang, C. C.; Greenwell, L.; Rix, U.; Hoffmeister, D.; Vining, L. C.; Rohr, J. R.; Yang, K. Q. *J. Biol. Chem.* **2005**, *280*, 22508-22514.

(46) Yang, K.; Han, L.; Ayer, S. W.; Vining, L. C. *Microbiology* **1996**, *142*, 123-132.

(47) McVey, J. Characterization of the Downstream Genes for Jadomycin B Biosynthesis in *Streptomyces venezuelae* ISP5230, MSc thesis, Dalhousie University, Halifax, Nova Scotia, Canada, 1998.

(48) Liu, W. C.; Parker, L.; Slusarchyk, S.; Greenwood, G. L.; Grahm, S. F.; Meyers, E. *J. Antibiot.* **1970**, *23*, 437-441.

(49) Rix, U.; Wang, C. C.; Chen, Y. H.; Lipata, F. M.; Rix, L. L. R.; Greenwell, L. M.; Vining, L. C.; Yang, K. Q.; Rohr, J. *ChemBioChem* **2005**, *6*, 838-845.

(50) Chen, Y.; Fan, K.; He, Y.; Xu, X.; Peng, Y.; Yu, T.; Jia, C.; Yang, K. *ChemBioChem* **2010**, *11*, 1055-1060.

(51) Kharel, M. K.; Rohr, J. *Curr. Opin. Chem. Biol.* **2012**, *16*, 150-161.

(52) Pahari, P.; Kharel, M. K.; Shepherd, M. D.; van Lanen, S. G.; Rohr, J. *Angew. Chem. Int. Ed.* **2012**, *51*, 1216-1220.

(53) Fan, K.; Pan, G.; Peng, X.; Zheng, J.; Gao, W.; Wang, J.; Wang, W.; Li, Y.; Yang, K. *Chem. Biol.* **2012**, *19*, 1381-1390.

(54) Tibrewal, N.; Pahari, P.; Wang, G.; Kharel, M. K.; Morris, C.; Downey, T.; Hou, Y.; Bugni, T. S.; Rohr, J. *J. Am. Chem. Soc.* **2012**, *134*, 18181-18184.

(55) Kharel, M. K.; Zhu, L.; Liu, T.; Rohr, J. *J. Am. Chem. Soc.* **2007**, *129*, 3780-3781.

(56) Gould, S. J. *Chem. Rev.* **1997**, *97*, 2499-2510.

(57) Rix, U.; Zheng, J.; Remsing Rix, L. L.; Greenwell, L.; Yang, K.; Rohr, J. *J. Am. Chem. Soc.* **2004**, *126*, 4496-4497.

(58) Weymouth-Wilson, A. *Nat. Prod. Rep.* **1997**, *14*, 99-110.

(59) Kren, V.; Rezanka, T. *FEMS Microbiol. Rev.* **2008**, *32*, 858-889.

(60) Elshahawi, S. I.; Shaaban, K. A.; Kharel, M. K.; Thorson, J. S. *Chem. Soc. Rev.* **2015**, .

(61) Liu, H.; Thorson, J. S. *Annu. Rev. Microbiol.* **1994**, *48*, 223-256.

(62) de Lederkremer, R. M.; Marino, C. In *Deoxy Sugars: Occurrence and Synthesis;* Derek Horton, Ed.; Advances in Carbohydrate Chemistry and Biochemistry; Academic Press: 2007; Vol. 61, pp 143-216.

(63) Nakashima, T.; Miura, M.; Hara, M. *Cancer Res.* **2000**, *60*, 1229-1235.

(64) Sun, Y.; Hahn, F.; Demydchuk, Y.; Chettle, J.; Tosin, M.; Osada, H.; Leadlay, P. F. *Nat. Chem. Biol.* **2010**, *6*, 99-101.

(65) Fang, J.; Zhang, Y.; Huang, L.; Jia, X.; Zhang, Q.; Zhang, X.; Tang, G.; Liu, W. *J. Bacteriol.* **2008**, *190*, 6014-6025.

(66) Zhang, H.; White-Phillip, J.; Melancon, C. E.; Kwon, H.; Yu, W.; Liu, H. *J. Am. Chem. Soc.* **2007**, *129*, 14670-14683.

(67) Wang, L.; White, R. L.; Vining, L. C. *Microbiology* **2002**, *148*, 1091-1103.

(68) Jakeman, D. L.; Borissow, C. N.; Reid, T. R.; Graham, C. L.; Timmons, S. C.; Syvitski, R. T. *Chem. Commun.* **2006**, *35*, 3738-3740.

(69) Jakeman, D. L.; Graham, C. L.; Young, W.; Vining, L. C. *J. Ind. Microbiol. Biotechnol.* **2006**, *33*, 767-772.

(70) Gantt, R. W.; Peltier-Pain, P.; Thorson, J. S. *Nat. Prod. Rep.* **2011**, *28*, 1811-1853.

(71) Rohr, J. *Chem. Commun.* **1990**, 113-114.

(72) Chatterjee, S.; Vining, L. C. *Can. J. Microbiol.* **1981**, *7*, 639-645.

(73) Jakeman, D. L.; Farrell, S.; Young, W.; Doucet, R. J.; Timmons, S. C. *Bioorg. Med. Chem. Lett.* **2005**, *15*, 1447-1449.

(74) Zheng, J. T.; Rix, U.; Zhao, L.; Mattingly, C.; Adams, V.; Quan, C.; Rohr, J.; Yang, K. Q. *J. Antibiot.* **2005**, *58*, 405-408.

(75) Jakeman, D. L.; Graham, C. L.; Reid, T. R. *Bioorg. Med. Chem. Lett.* **2005**, *15*, 5280-5283.

(76) Borissow, C. N.; Graham, C. L.; Syvitski, R. T.; Reid, T. R.; Blay, J.; Jakeman, D. L. *ChemBioChem* **2007**, *8*, 1198-1203.

(77) Jakeman, D. L.; Dupuis, S. N.; Graham, C. L. *Pure Appl. Chem.* **2009**, *81*, 1041-1049.

(78) Fan, K.; Zhang, X.; Liu, H.; Han, H.; Luo, Y.; Wang, Q.; Geng, M.; Yang, K. *J. Antibiot.* **2012**, *65*, 449-452.

(79) Shan, M.; Sharif, E. U.; O'Doherty, G. A. *Angew. Chem. Int. Ed.* **2010**, *49*, 9492-9495.

(80) Yang, X.; Yu, B. *Chem. Eur. J.* **2013**, *19*, 8431-8434.

(81) Dupuis, S. N.; Robertson, A. W.; Veinot, T.; Monro, S. M. A.; Douglas, S. E.; Syvitski, R. T.; Goralski, K. B.; McFarland, S. A.; Jakeman, D. L. *Chem. Sci.* **2012**, *3*, 1640-1644.

(82) Jakeman, D. L.; Bandi, S.; Graham, C. L.; Reid, T. R.; Wentzell, J. R.; Douglas, S. E. *Antimicrobial Agents and Chemotherapy* **2009**, *53*, 1245-1247.

(83) Issa, M. E.; Hall, S. R.; Dupuis, S. N.; Graham, C. L.; Jakeman, D. L.; Goralski, K. B. *Anticancer Drugs* **2014**, *25*, 255-269.

(84) Fu, D. H.; Jiang, W.; Zheng, J. T.; Zhao, G. Y.; Li, Y.; Yi, H.; Li, Z. R.; Jiang, J. D.; Yang, K. Q.; Wang, Y.; Si, S. Y. *Mol. Cancer Ther.* **2008**, *7*, 2386-2393.

(85) Hall, S. R.; Blundon, H. L.; Ladda, M. A.; Robertson, A. W.; Martinez-Farina, C.; Jakeman, D. L.; Goralski, K. B. *Pharmacol. Res. Perspect.* **2015**, *DOI: 10.1002/prp2.110*.

(86) Robertson, A. W.; Martinez-Farina, C.; Smithen, D. A.; Yin, H.; Monro, S.; Thompson, A.; Mcfarland, S. A.; Syvitski, R. T.; Jakeman, D. L. *J. Am. Chem. Soc.* **2015**, *DOI: 10.1021/ja5114672*.

(87) Hermanson, G. In *Bioconjugate Techniques, (Third Edition)* [Online]; Audet, J., Preap, M., Eds.; Elsevier/Academic Press: San Diego, **2013**; Chapter 3, pp 229-258.

(88) Hankovsky, O. H.; Hideg, K.; Bodi, I.; Frank, L. *J. Med. Chem.* **1986**, *29*, 1138-1152.

(89) Paquet, A. *Can. J. Chem.* **1982**, *60*, 976-980.

(90) Georgiades, S. N.; Clardy, J. *Bioorg. Med. Chem. Lett.* **2008**, *18*, 3117-3121.

(91) Wang, D.; Fan, J.; Gao, X.; Wang, B.; Sun, S.; Peng, X. *J. Org. Chem.* **2009**, *74*, 7675-7683.

(92) Abad, S.; Nolis, P.; Gispert, J. D.; Spengler, J.; Albericio, F.; Rojas, S.; Herance, J. R. *Chem. Commun.* **2012**, *48*, 6118-6120.

(93) Kalkhof, S.; Sinz, A. *Anal. Bioanal. Chem.* **2008**, *392*, 305-312.

(94) Syvitski, R. T.; Borissow, C. N.; Graham, C. L.; Jakeman, D. L. *Org. Lett.* **2006**, *8*, 697-700.

(95) Dupuis, S. N.; Veinot, T.; Monro, S. M. A.; Douglas, S. E.; Syvitski, R. T.; Goralski, K. B.; McFarland, S. A.; Jakeman, D. L. *J. Nat. Prod.* **2011**, *74*, 2420-2424.

(96) Bai, R. L.; Paull, K. D.; Herald, C. L.; Malspeis, L.; Pettit, G. R.; Hamel, E. *J. Biol. Chem.* **1991**, *266*, 15882-15889.

(97) Paull, K. D.; Lin, C. M.; Malspeis, L.; Hamel, E. *Cancer Res.* **1992**, *52*, 3892-3900.

(98) Atamanyuk, D.; Zimenkovsky, B.; Atamanyuk, V.; Nektegayev, I.; Lesyk, R. *Sci. Pharm.* **2013**, *81*, 423-436.

(99) Gewirtz, D. *Biochem. Pharmacol.* **1999**, *57*, 727-741.

(100) Kathiravan, M. K.; Khilare, M. M.; Nikoomanesh, K.; Chothe, A. S.; Jain, K. S. *J. Enzyme Inhib. Med. Chem.* **2013**, *28*, 419-435.

(101) Monro, S. M. A.; Cottreau, K. M.; Spencer, C.; Wentzell, J. R.; Graham, C. L.; Borissow, C. N.; Jakeman, D. L.; McFarland, S. A. *Bioorg. Med. Chem.* **2011**, *19*, 3357-3360.

(102) Nett, M.; Ikeda, H.; Moore, B. S. *Nat. Prod. Rep.* **2009**, *26*, 1362-1384.

(103) Bibb, M. J. *Curr. Opin. Microbiol.* **2005**, *8*, 208-215.

(104) van Wezel, G. P.; McDowall, K. J. *Nat. Prod. Rep.* **2011**, *28*, 1311-1333.

(105) Martin, J.; Liras, P. *Curr. Opin. Microbiol.* **2010**, *13*, 263-273.

(106) Huang, J.; Shi, J.; Molle, V.; Sohlberg, B.; Weaver, D.; Bibb, M. J.; Karoonuthaisiri, N.; Lih, C.; Kao, C. M.; Buttner, M. J.; Cohen, S. N. *Mol. Microbiol.* **2005**, *58*, 1276-1287.

(107) Wang, L.; Tian, X.; Wang, J.; Yang, H.; Fan, K.; Xu, G.; Yang, K.; Tan, H. *Proc. Natl. Acad. Sci. U. S. A.* **2009**, *106*, 8617-8622.

(108) Xu, G. M.; Wang, J. A.; Wang, L. Q.; Tian, X. Y.; Yang, H. H.; Fan, K. Q.; Yang, K. Q.; Tan, H. R. *J. Biol. Chem.* **2010**, *285*, 27440-27448.

(109) Piraee, M.; White, R. L.; Vining, L. C. *Microbiology* **2004**, *150*, 85-94.

(110) Wang, W.; Ji, J.; Li, X.; Wang, J.; Li, S.; Pan, G.; Fan, K.; Yang, K. *Proc. Natl. Acad. Sci. U. S. A.* **2014**, *111*, 5688-5693.

(111) Chen, Y.; Apolinario, E.; Brachova, L.; Kelman, Z.; Li, Z.; Nikolau, B.; Showman, L.; Sowers, K.; Orban, J. *BMC Genomics* **2011**, *12*, S7.

(112) Eberhardt, R.; Chang, Y.; Bateman, A.; Murzin, A.; Axelrod, H.; Hwang, W.; Aravind, L. *BMC Bioinformatics* **2013**, *14*, 327.

(113) Peng, J. W.; Moore, J.; Abdul-Manan, N. *Prog. Nucl. Magn. Reson. Spectrosc.* **2004**, *44*, 225-256.

(114) Skinner, A. L.; Laurence, J. S. *J. Pharm. Sci.* **2008**, *97*, 4670-4695.

(115) Dalvit, C.; Fogliatto, G.; Stewart, A.; Veronesi, M.; Stockman, B. *J. Biomol. NMR* **2001**, *21*, 349-359.

(116) Ogasawara, Y.; Liu, H. *J. Am. Chem. Soc.* **2009**, *131*, 18066-18067.

(117) Rascher, A.; Hu, Z. H.; Viswanathan, N.; Schirmer, A.; Reid, R.; Nierman, W. C.; Lewis, M.; Hutchinson, C. R. *FEMS Microbiol. Lett.* **2003**, *218*, 223-230.

(118) Rascher, A.; Hu, Z. H.; Buchanan, G. O.; Reid, R.; Hutchinson, C. R. *Appl. Environ. Microbiol.* **2005**, *71*, 4862-4871.

(119) Gould, S. J.; Hong, S. T.; Carney, J. R. *J. Antibiot.* **1998**, *51*, 50-57.

(120) Chater, K. F.; Bruton, C. J. *EMBO J.* **1985**, *4*, 1893-1897.

(121) O'Rourke, S.; Wietzorrek, A.; Fowler, K.; Corre, C.; Challis, G. L.; Chater, K. F. *Mol. Microbiol.* **2009**, *71*, 763-778.

(122) Wang, L.; Vining, L. C. *Microbiology* **2003**, *149*, 1991-2004.

(123) Gottlieb, D.; Diamond, L. *Bull. Torey Bot. Club* **1951**, *78*, 56-60.

(124) Gottlieb, D.; Carter, H. E.; Legator, M.; Gallicchio, V. *J. Bacteriol.* **1954**, *68*, 243-251.

(125) Westlake, D. W. S.; Sala, F.; McGrath, R.; Vining, L. C. *Can. J. Microbiol.* **1968**, *14*, 587-593.

(126) Malik, V. S.; Vining, L. C. *Can. J. Microbiol.* **1972**, *18*, 137-143.

(127) Mayer, M.; Meyer, B. *Angew. Chem. Int. Ed.* **1999**, *38*, 1784-1788.

(128) Mayer, M.; Meyer, B. *J. Am. Chem. Soc.* **2001**, *123*, 6108-6117.

(129) Dalvit, C.; Pevarello, P.; Tato, M.; Veronesi, M.; Vulpetti, A.; Sundstrom, M. *J. Biomol. NMR* **2000**, *18*, 65-68.

(130) Sadeghi-Khomami, A.; Lumsden, M. D.; Jakeman, D. L. *Chem. Biol.* **2008**, *15*, 739-749.

(131) Loranger, M. W.; Forget, S. M.; McCormick, N. E.; Syvitski, R. T.; Jakeman, D. L. *J. Org. Chem.* **2013**, *78*, 9822-9833.

(132) Forget, S. M.; Jee, A.; Smithen, D. A.; Jagdhane, R.; Anjum, S.; Beaton, S. A.; Palmer, D. R.; Syvitski, R. T.; Jakeman, D. L. *Org. Biomol. Chem.* **2015**, *13*, 866-875.

(133) Marley, J.; Lu, M.; Bracken, C. *J. Biomol. NMR* **2001**, *20*, 71-75.

(134) Williamson, M. P. *Prog. Nucl. Magn. Reson. Spectrosc.* **2013**, *73*, 1-16.

(135) Fielding, L.; Rutherford, S.; Fletcher, D. *Magn. Reson. Chem.* **2005**, *43*, 463-470.

(136) Fielding, L. *Prog. Nucl. Magn. Reson. Spectrosc.* **2007**, *51*, 219-242.

(137) Zhang, Y.; Pan, G.; Zou, Z.; Fan, K.; Yang, K.; Tan, H. *Mol. Microbiol.* **2013**, *90*, 884-897.

(138) Zhang, Y.; Zou, Z.; Niu, G.; Tan, H. *Sci. China Life Sci.* **2013**, *56*, 584-590.

(139) Zou, Z.; Du, D.; Zhang, Y.; Zhang, J.; Niu, G.; Tan, H. *Mol. Microbiol.* **2014**, *94*, 490-505.

(140) Yang, K.; Han, L.; He, J.; Wang, L.; Vining, L. C. *Gene* **2001**, *279*, 165-173.

(141) Smithen, D. A.; Forrester, A. M.; Corkery, D. P.; Dellaire, G.; Colpitts, J.; McFarland, S. A.; Berman, J. N.; Thompson, A. *Org. Biomol. Chem.* **2013**, *11*, 62-68.

(142) Gottlieb, H. E.; Kotlyar, V.; Nudelman, A. *J. Org. Chem.* **1997**, *62*, 7512-7515.

APPENDIX A: TLC IMAGES FROM COUPLING REACTIONS WITH 58

TLC analysis (5:5:1 EtOAc:CH_3CN:H_2O) for coupling reactions using **58** and the succinimidyl esters **59**-**64**: (SM) = crude **58**; (Co) = co-spot; (Rxn) = reaction mixture.

Reaction of crude **58** with succinimidyl ester **59** after 6 h. 141

Reaction of crude **58** with succinimidyl ester **60** after 8 h. 141

Reaction of crude **58** with succinimidyl ester **61** after 18 h. 141

Reaction of crude **58** with succinimidyl ester **62** after 7 h. 141

Reaction of crude **58** with succinimidyl ester **63** after 3 h. 142

Reaction of crude **58** with succinimidyl ester **64** after 7 h. 142

Reaction of crude **58** with succinimidyl ester **59** after 6 h.

Reaction of crude **58** with succinimidyl ester **60** after 8 h.

Reaction of crude **58** with succinimidyl ester **61** after 18 h.

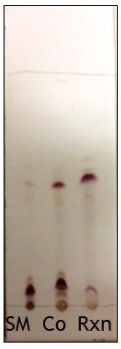

Reaction of crude **58** with succinimidyl ester **62** after 7 h.

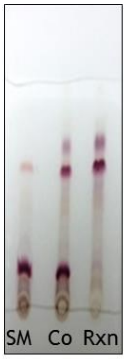

Reaction of crude **58** with succinimidyl ester **63** after 3 h.

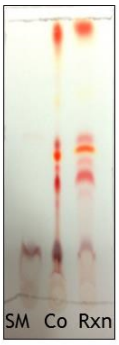

Reaction of crude **58** with succinimidyl ester **64** after 7 h.

APPENDIX B: HRMS DATA

HRMS Spectrum of SuO-BODIPY (**64**). 144
HRMS Spectrum of Jadomycin Oct (**58**). 145
HRMS spectrum of jadomycin Oct phenoxyacetylamide (**58a**). 146
HRMS spectrum of jadomycin Oct naphthoxyacetylamide (**58b**). 147
HRMS spectrum of jadomycin Oct benzoylamide (**58c**). 148
HRMS spectrum jadomycin Oct nonoylamide (**58d**). 149
HRMS spectrum of jadomycin Oct Fmoc (**58e**). 150
HRMS spectrum of jadomycin Oct BODIPY amide (**58f**). 151
HRMS spectrum of jadomycin AVA (**67**) 152
HRMS spectrum of L-digitoxosylphenanthroviridin (**70**) 153

HRMS Spectrum of SuO-BODIPY (**64**).

HRMS Spectrum of Jadomycin Oct (**58**).

HRMS spectrum of jadomycin Oct phenoxyacetylamide (**58a**).

HRMS spectrum of jadomycin Oct naphthoxyacetylamide (**58b**).

HRMS spectrum of jadomycin Oct benzoylamide (**58c**).

HRMS spectrum jadomycin Oct nonoylamide (**58d**).

HRMS spectrum of jadomycin Oct Fmoc (**58e**).

HRMS spectrum of jadomycin Oct BODIPY amide (**58f**).

HRMS spectrum of jadomycin AVA (**67**)

Mass Spectrum Molecular Formula Report

Analysis Info

Analysis Name	D:\Data\Xiao\Jan 13 2015000014.d	Acquisition Date	1/13/2015 10:47:46 AM
Method	xiaofengpos.m	Operator	Administrator
Sample Name	Jadomycin 5-aminovaleric acid	Instrument	micrOTOF 57
Comment			

Acquisition Parameter

Source Type	ESI	Ion Polarity	Positive	Set Corrector Fill	45 V
Scan Range	n/a	Capillary Exit	110.0 V	Set Pulsar Pull	400 V
Scan Begin	50 m/z	Hexapole RF	400.0 V	Set Pulsar Push	400 V
Scan End	3000 m/z	Skimmer 1	50.0 V	Set Reflector	1300 V
		Hexapole 1	23.0 V	Set Flight Tube	9000 V
				Set Detector TOF	2200 V

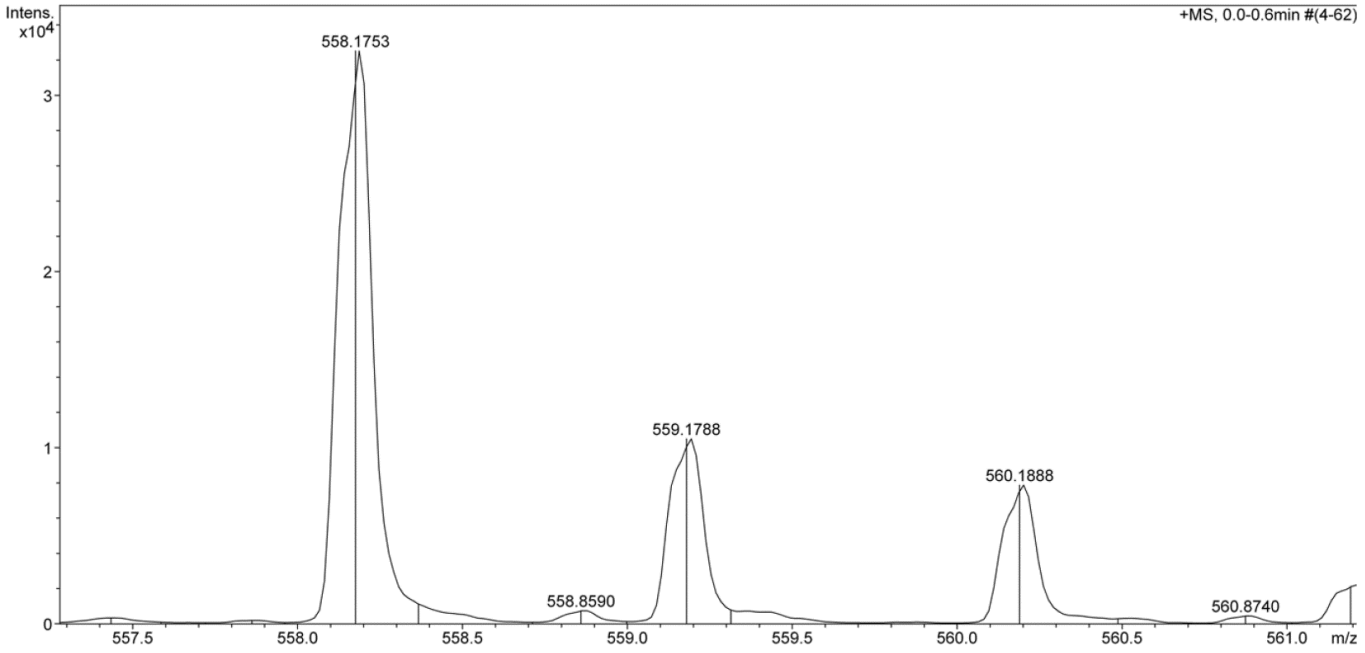

HRMS spectrum of L-digitoxosylphenanthroviridin (**70**)

APPENDIX C: SPECTRAL DATA FOR PURIFIED JADOMYCINS

^{1}H-NMR spectrum of **58a** (diastereomeric mixture) in MeOD-d_4 (^{1}H: 700 MHz). 156

^{13}C-NMR spectrum of **58a** (diastereomeric mixture) in MeOD-d_4 (^{13}C: 176 MHz). 157

COSY (^{1}H-^{1}H) spectrum of **58a** (diastereomeric mixture) in MeOD-d_4 (700 MHz). 158

Edited-HSQC (^{1}H-^{13}C) spectrum of **58a** (diastereomeric mixture) in MeOD-d_4. 159

HMBC (^{1}H-^{13}C) spectrum of **58a** (diastereomeric mixture) in MeOD-d_4..... 160

Overlay of ^{1}H-NMR spectrum of **58**a (top) with ROESY (500 MHz) showing irradiation of H3a_{Mn} (2nd from top), H3a_{Mj} (2nd from bottom), and both H3a_{Mn} and H3a_{Mj} simultaneously, in MeOD-d_4. 161

^{1}H-NMR spectrum of **58b** (diastereomeric mixture) in MeOD-d_4 (^{1}H: 700 MHz). 162

^{13}C-NMR spectrum of **58b** (diastereomeric mixture) in MeOD-d_4 (^{13}C: 176 MHz). 163

COSY (^{1}H-^{1}H) spectrum of **58b** (diastereomeric mixture) in MeOD-d_4 (700 MHz). 164

Edited-HSQC (^{1}H-^{13}C) spectrum of **58b** (diastereomeric mixture) in MeOD-d_4. 165

HMBC (^{1}H-^{13}C) spectrum of **58b** (diastereomeric mixture) in MeOD-d_4. 166

Overlay of ^{1}H-NMR spectrum of **58b** (top) with ROESY (700 MHz) showing irradiation of H3a_{Mn} (middle), and H3a_{Mj} (bottom) in MeOD-d_4. 167

^{1}H-NMR spectrum of **58c** (diastereomeric mixture) in MeOD-d_4 (^{1}H: 700 MHz). 168

^{13}C-NMR spectrum of **58c** (diastereomeric mixture) in MeOD-d_4 (^{13}C: 176 MHz)..... 169

COSY (^{1}H-^{1}H) spectrum of **58c** (diastereomeric mixture) in MeOD-d_4 (700 MHz). 170

Edited-HSQC (^{1}H-^{13}C) spectrum of **58c** (diastereomeric mixture) in MeOD-d_4. 171

HMBC (^{1}H-^{13}C) spectrum of **58c** (diastereomeric mixture) in MeOD-d_4. 172

Overlay of ^{1}H-NMR spectrum of **58c** (top) with ROESY (500 MHz) showing irradiation of both H3a_{Mn} and H3a_{Mj} simultaneously (bottom), in MeOD-d_4. 173

^{1}H-NMR spectrum of **58d** (diastereomeric mixture) in MeOD-d_4 (^{1}H: 700 MHz). 174

DEPTQ spectrum of **58d** (diastereomeric mixture) in MeOD-d_4 (^{13}C: 176 MHz). 175

COSY (^{1}H-^{1}H) spectrum of **58d** (diastereomeric mixture) in MeOD-d_4 (700 MHz). 176

Edited-HSQC (^{1}H-^{13}C) spectrum of **58d** (diastereomeric mixture) in MeOD-d_4. 177

HMBC (^{1}H-^{13}C) spectrum of **58d** (diastereomeric mixture) in MeOD-d_4. 178

^{1}H-NMR spectrum of **58e** (diastereomeric mixture) in MeOD-d_4 (^{1}H: 700 MHz). 179

^{13}C-NMR spectrum of **58e** (diastereomeric mixture) in MeOD-d_4 (^{13}C: 176 MHz)..... 180

COSY (^{1}H-^{1}H) spectrum of **58e** (diastereomeric mixture) in MeOD-d_4 (700 MHz). 181

Edited-HSQC (^{1}H-^{13}C) spectrum of **58e** (diastereomeric mixture) in MeOD-d_4. 182
HMBC (^{1}H-^{13}C) spectrum of **58e** (diastereomeric mixture) in MeOD-d_4. 183
Overlay of ^{1}H-NMR spectrum of **58e** (top) with ROESY (500 MHz) showing irradiation of $H3a_{Mj}$ (middle), and $H3a_{Mn}$ (bottom) in MeOD-d_4. 184
^{1}H-NMR spectrum of **58f** (diastereomeric mixture) in MeOD-d_4 (^{1}H: 700 MHz). 185
^{13}C-NMR spectrum of **58f** (diastereomeric mixture) in MeOD-d_4 (^{13}C: 176 MHz). 186
COSY (^{1}H-^{1}H) spectrum of **58f** (diastereomeric mixture) in MeOD-d_4 (700 MHz). 187
Edited-HSQC (^{1}H-^{13}C) spectrum of **58f** (diastereomeric mixture) in MeOD-d_4. 188
HMBC (^{1}H-^{13}C) spectrum of **58f** (diastereomeric mixture) in MeOD-d_4. 189
Overlay of ^{1}H-NMR spectrum of **58f** (top) with ROESY (700 MHz) showing irradiation of $H3a_{Mn}$ (middle), and $H3a_{Mj}$ (bottom) in MeOD-d_4. 190
^{1}H-NMR spectrum of **58** (diastereomeric mixture) in MeOD-d_4 (^{1}H: 700 MHz)..... 191
COSY (^{1}H-^{1}H) spectrum of **58** (diastereomeric mixture) in MeOD-d_4 (700 MHz). 192
HSQC (^{1}H-^{13}C) spectrum of **58** (diastereomeric mixture) in MeOD-d_4. 193
Edited-HSQC (^{1}H-^{13}C) spectrum of **58** (diastereomeric mixture) in MeOD-d_4. 194
HMBC (^{1}H-^{13}C) spectrum of **58** (diastereomeric mixture) in MeOD-d_4. 195
^{1}H-NMR spectrum of **67** (diastereomeric mixture) in MeOD-d_4 (^{1}H: 500 MHz)..... 196
^{13}C-NMR spectrum of **67** (diastereomeric mixture) in MeOD-d_4 (^{13}C: 176 MHz). 197
COSY (^{1}H-^{1}H) spectrum of **67** (diastereomeric mixture) in MeOD-d_4 (700 MHz). 198
Edited-HSQC (^{1}H-^{13}C) spectrum of **67** (diastereomeric mixture) in MeOD-d_4. 199
HMBC (^{1}H-^{13}C) spectrum of **67** (diastereomeric mixture) in MeOD-d_4. 200
Overlay of ^{1}H-NMR spectrum of **67** (top) with NOESY (500 MHz) showing irradiation of both $H3a_{Mn}$ and $H3a_{Mj}$ simultaneously (bottom), in MeOD-d_4. 201
Overlaid ^{1}H-NMR of **66a**, (top) and **58a** (bottom). 202
^{1}H-NMR spectrum of **70** in CD_2Cl_2 (^{1}H: 500 MHz)..... 203
^{13}C-NMR spectrum of **70** in CD_2Cl_2 (^{13}C: 176 MHz). 204
COSY (^{1}H-^{1}H) spectrum of **70** in CD_2Cl_2 (^{1}H: 700 MHz). 205
Edited-HSQC (^{1}H-^{13}C) spectrum of **70** in CD_2Cl_2 (^{1}H: 700 MHz; ^{13}C: 176 MHz). 206
Edited-HSQC (^{1}H-^{13}C) spectrum of **70** in CD_2Cl_2 (^{1}H: 700 MHz; ^{13}C: 176 MHz) with expanded ^{13}C sweep-width 207
HMBC (^{1}H-^{13}C) spectrum of **70** in CD_2Cl_2 (^{1}H: 700 MHz; ^{13}C: 176 MHz). 208
2D-NOESY (^{1}H-^{1}H) spectrum of **70** in CD_2Cl_2 (^{1}H: 700 MHz). 209

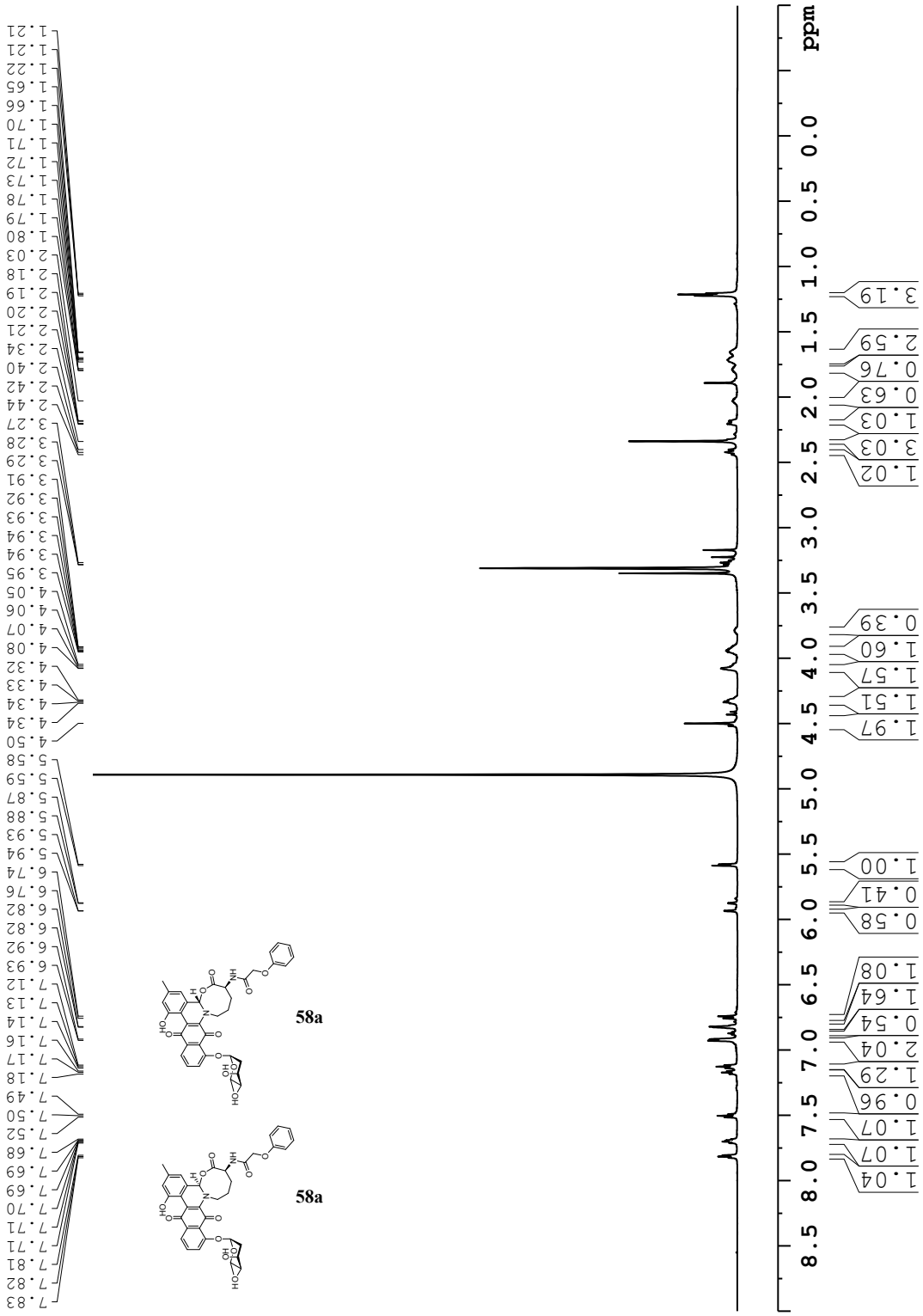

^{1}H-NMR spectrum of **58a** (diastereomeric mixture) in MeOD-d_4 (^{1}H: 700 MHz).

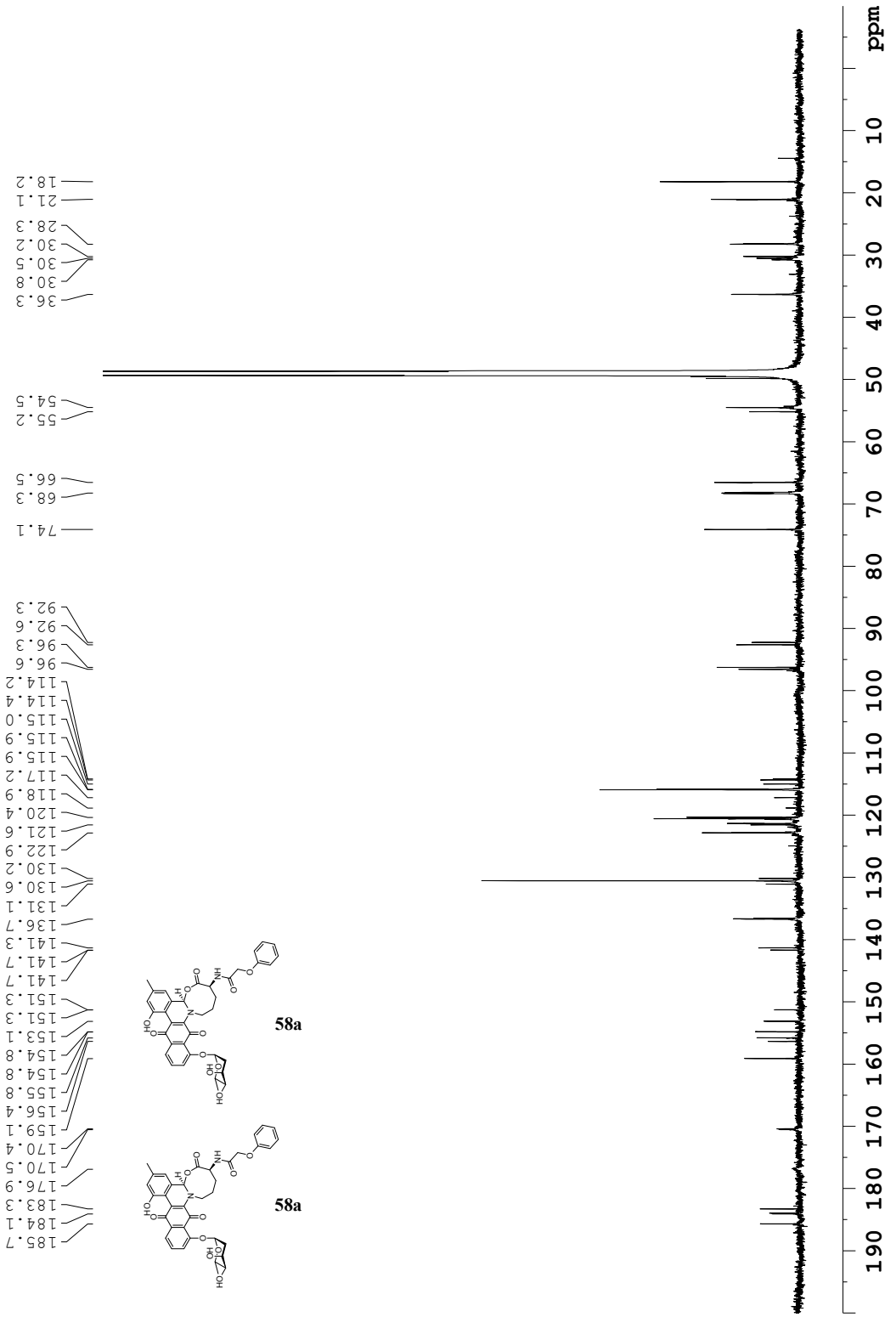

^{13}C-NMR spectrum of **58a** (diastereomeric mixture) in MeOD-d_4 (^{13}C: 176 MHz).

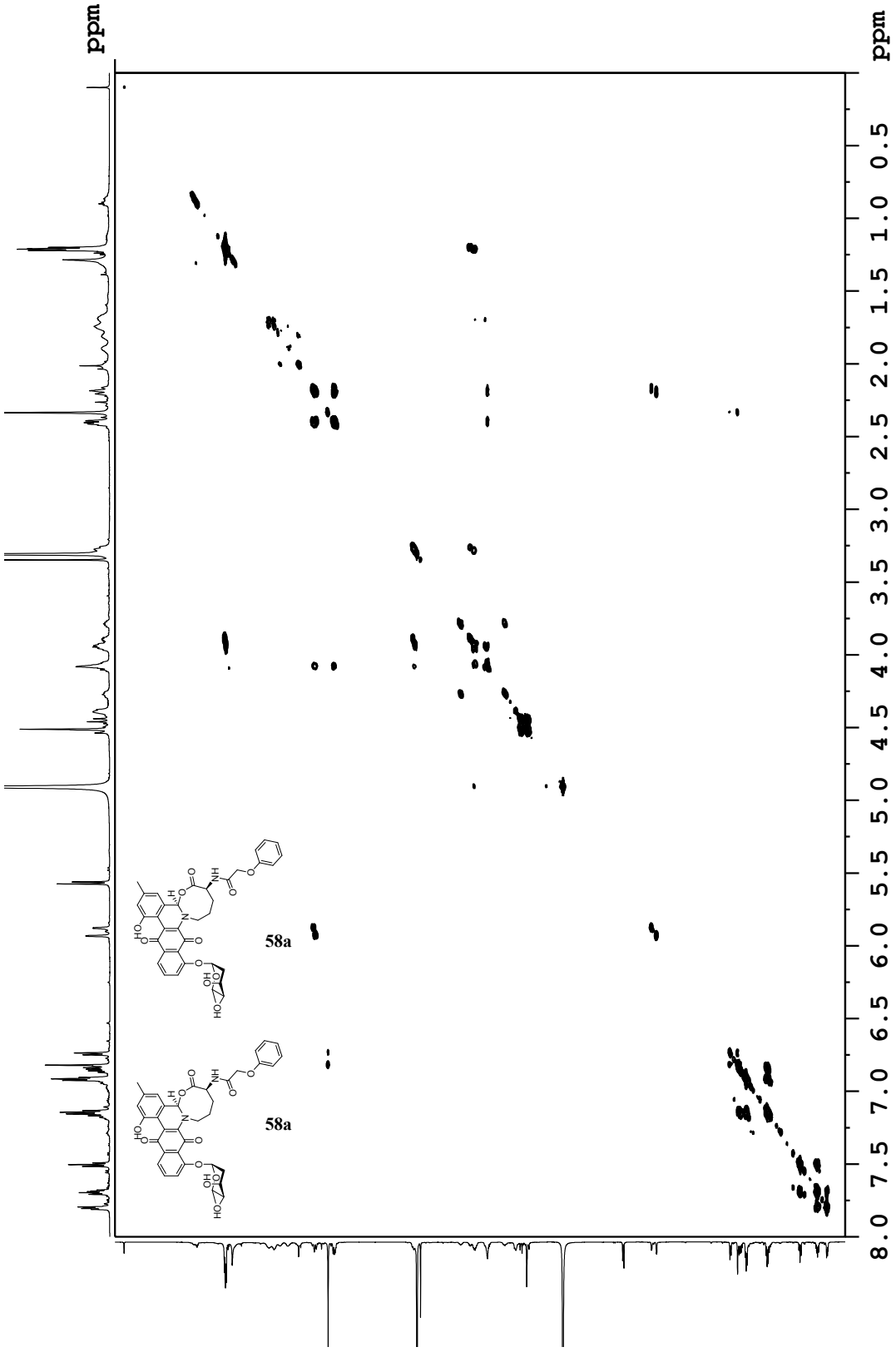

COSY (^{1}H-^{1}H) spectrum of **58a** (diastereomeric mixture) in MeOD-d_4 (700 MHz).

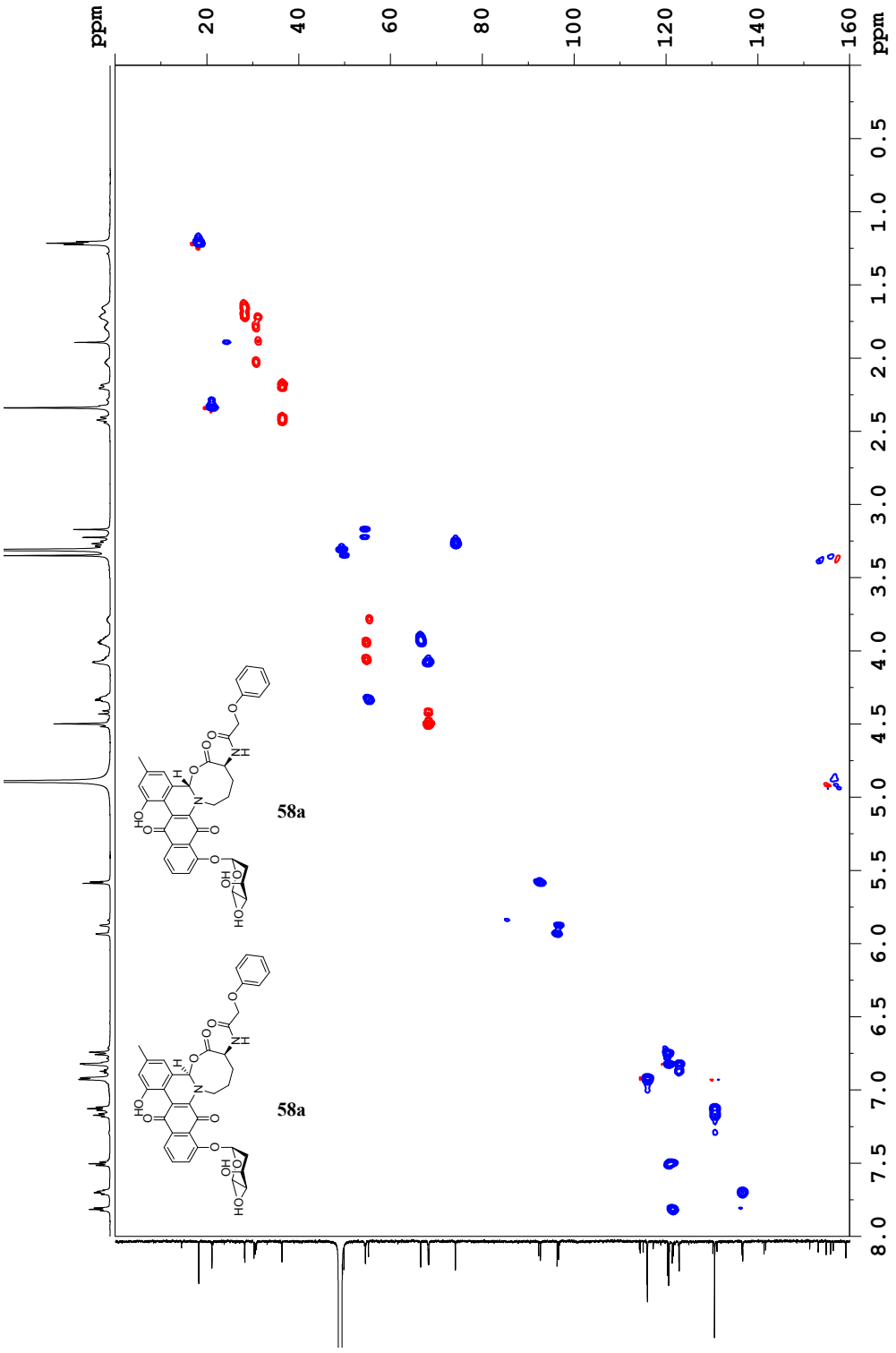

Edited-HSQC (^{1}H-^{13}C) spectrum of **58a** (diastereomeric mixture) in MeOD-d_4. Blue represents CH and CH_3 groups, red represents CH_2 groups.

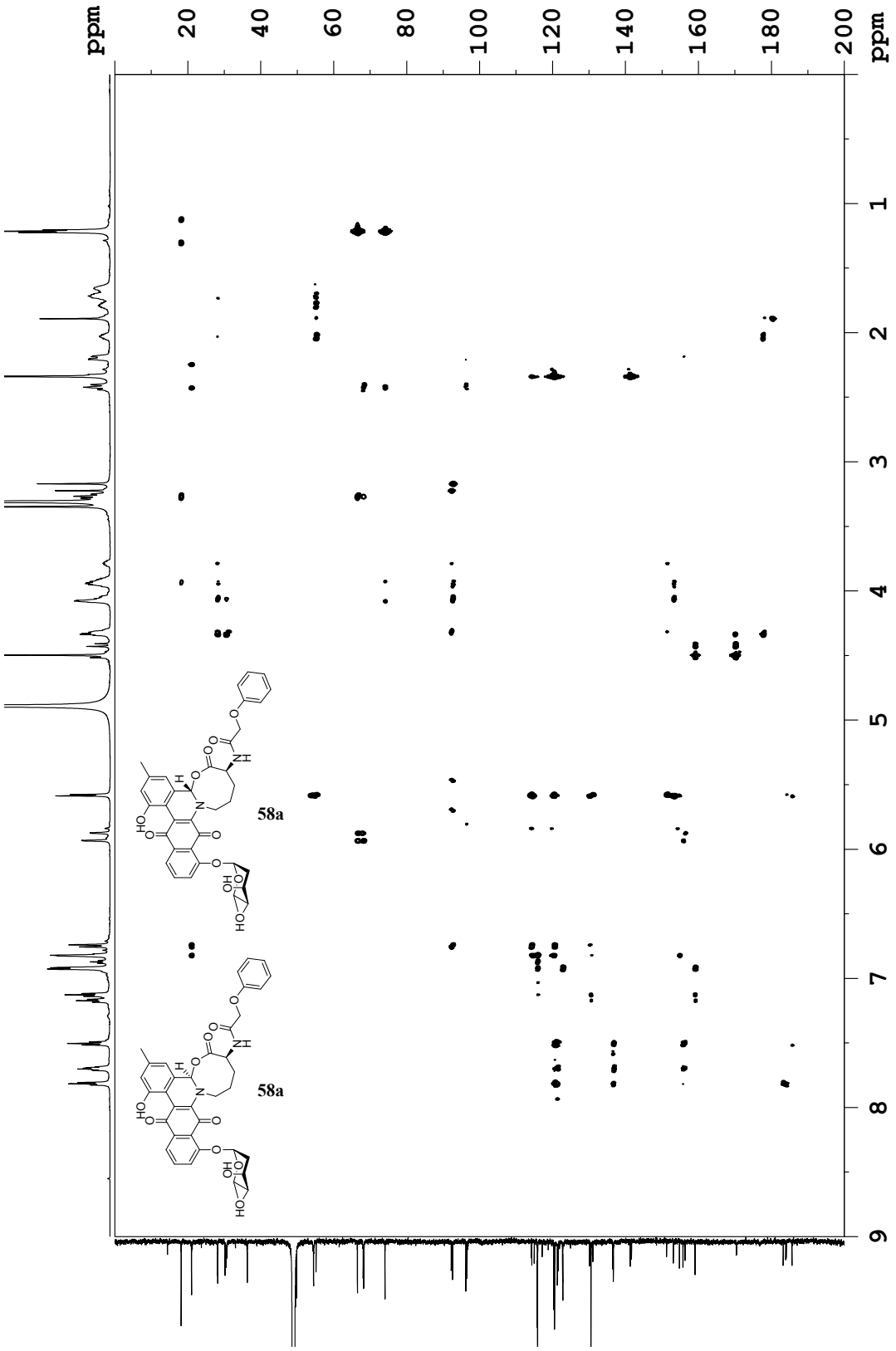

HMBC (^{1}H-^{13}C) spectrum of **58a** (diastereomeric mixture) in MeOD-d_4.

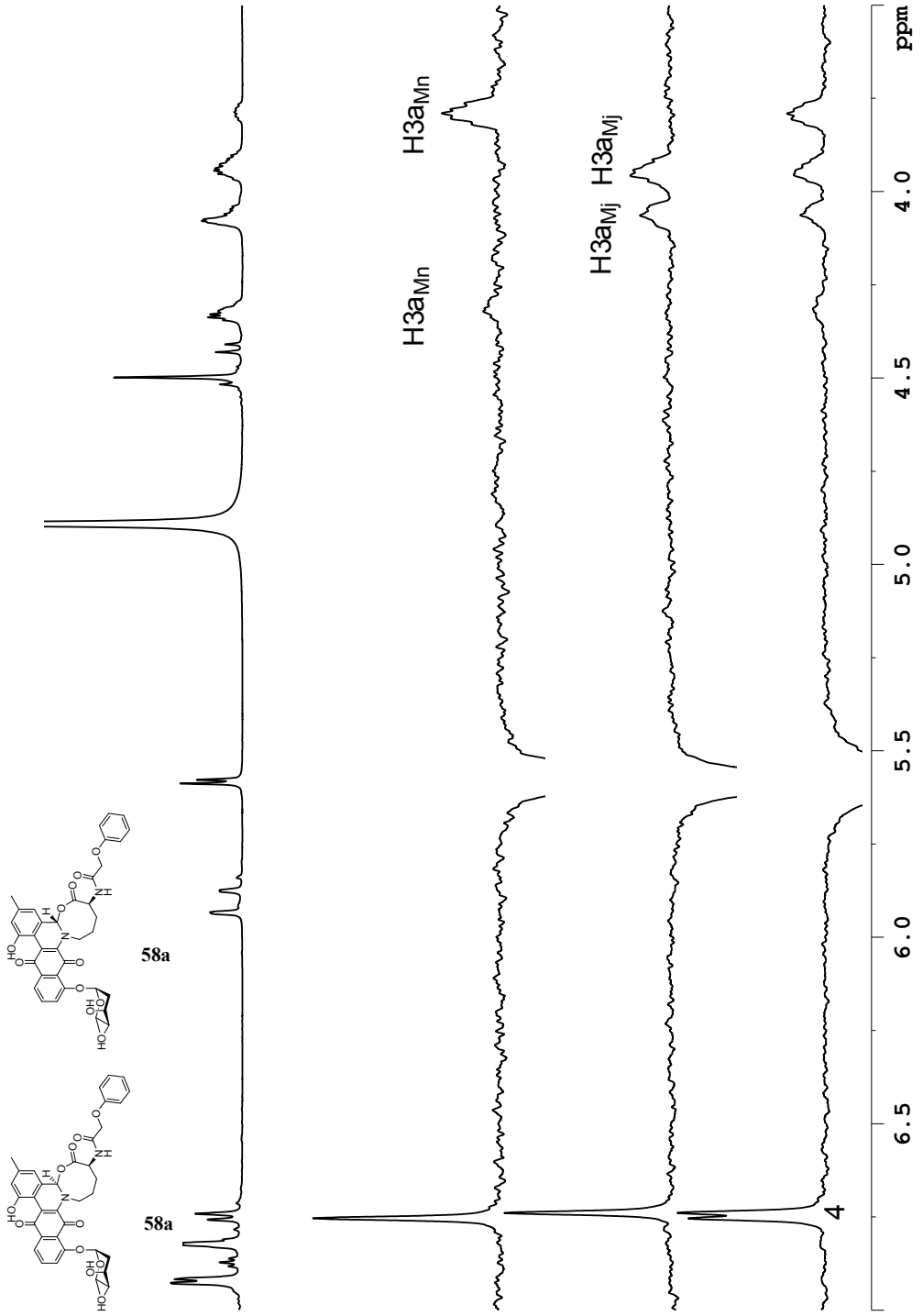

Overlay of ^{1}H-NMR spectrum of **58**a (top) with ROESY (500 MHz) showing irradiation of H3a$_{Mn}$ (2nd from top), H3a$_{Mj}$ (2nd from bottom), and both H3a$_{Mn}$ and H3a$_{Mj}$ simultaneously, in MeOD-d$_4$.

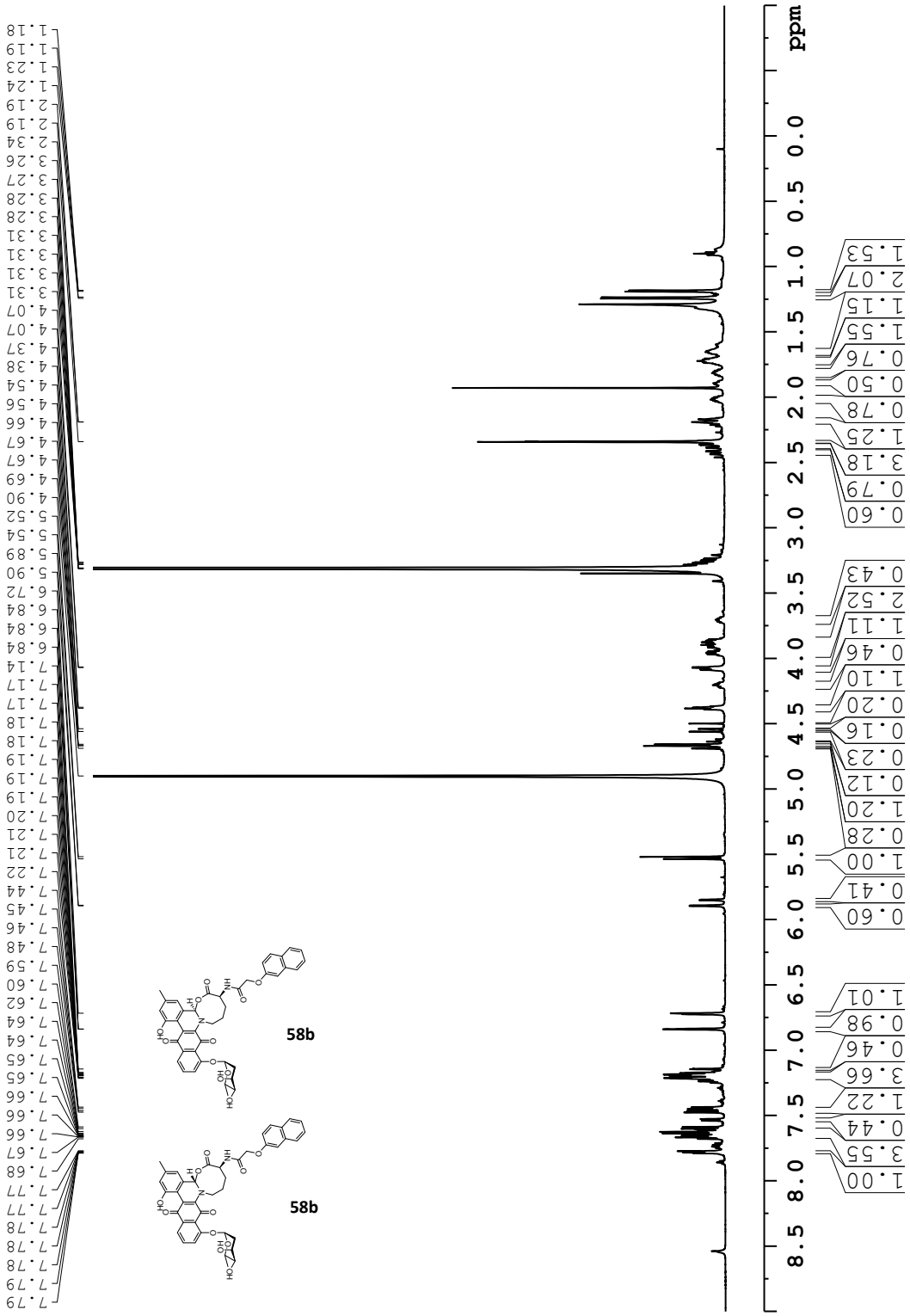

^{1}H-NMR spectrum of **58b** (diastereomeric mixture) in MeOD-d_4 (^{1}H: 700 MHz).

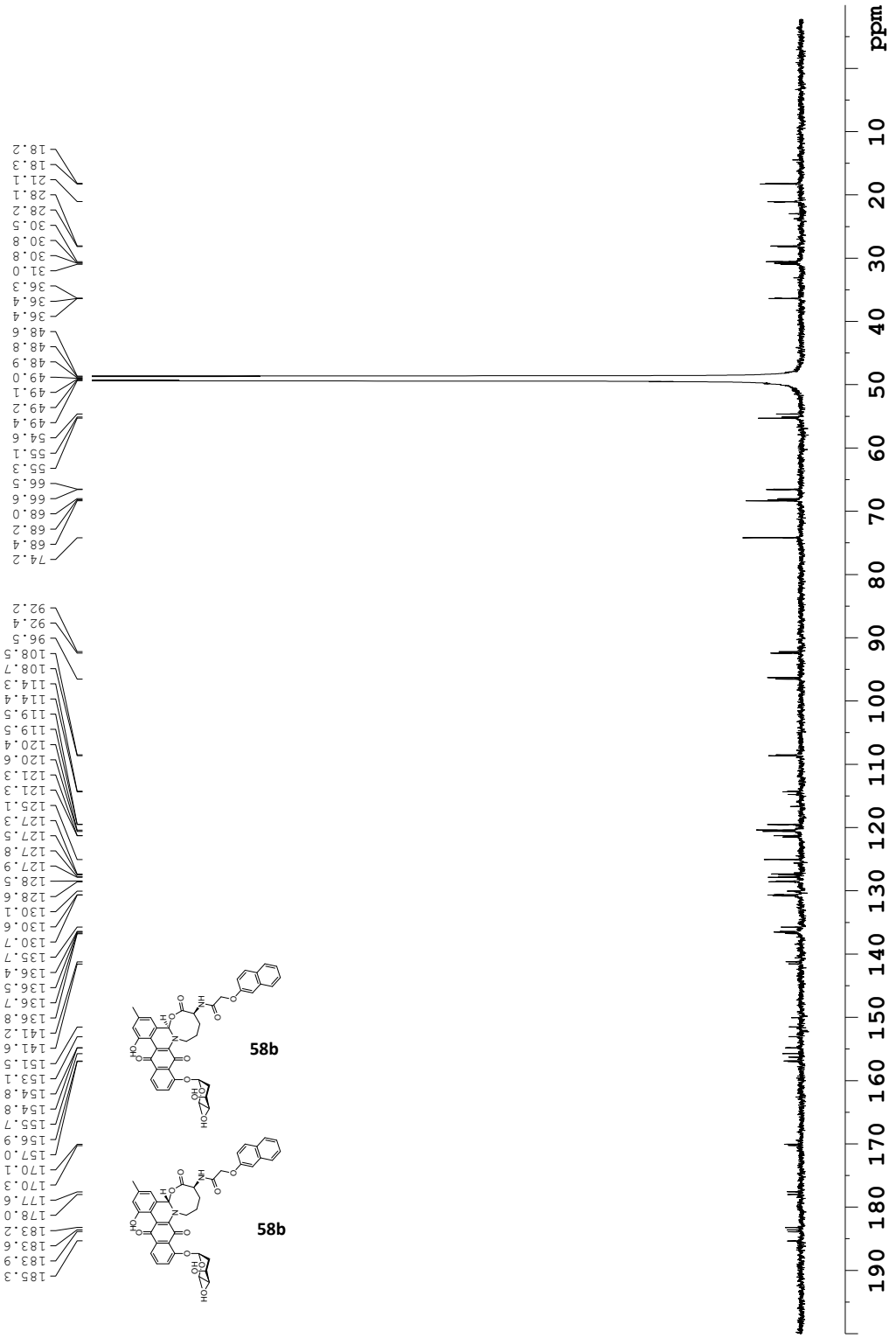

^{13}C-NMR spectrum of **58b** (diastereomeric mixture) in MeOD-d_4 (^{13}C: 176 MHz).

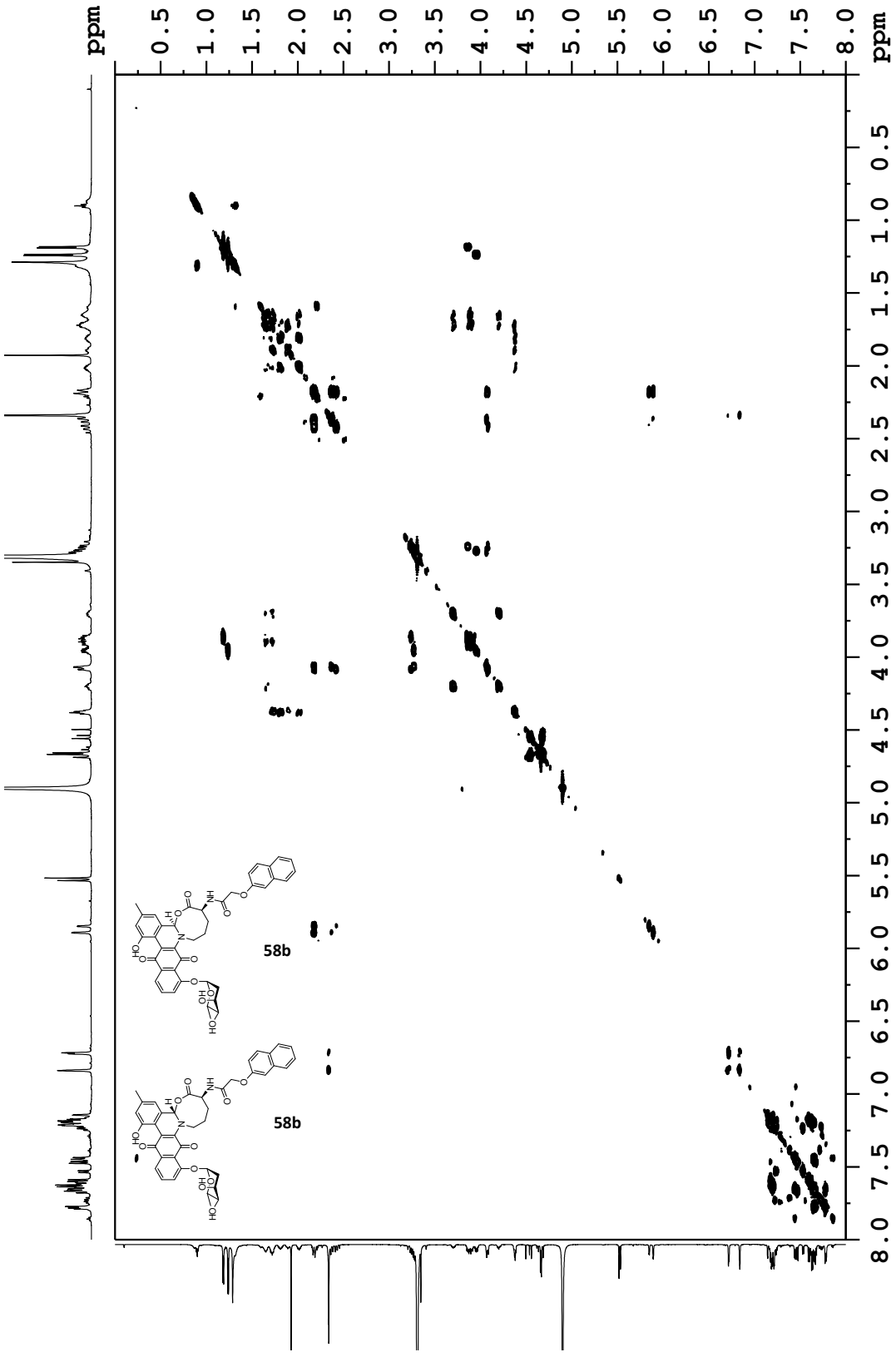

COSY (^{1}H-^{1}H) spectrum of **58b** (diastereomeric mixture) in MeOD-d_4 (700 MHz).

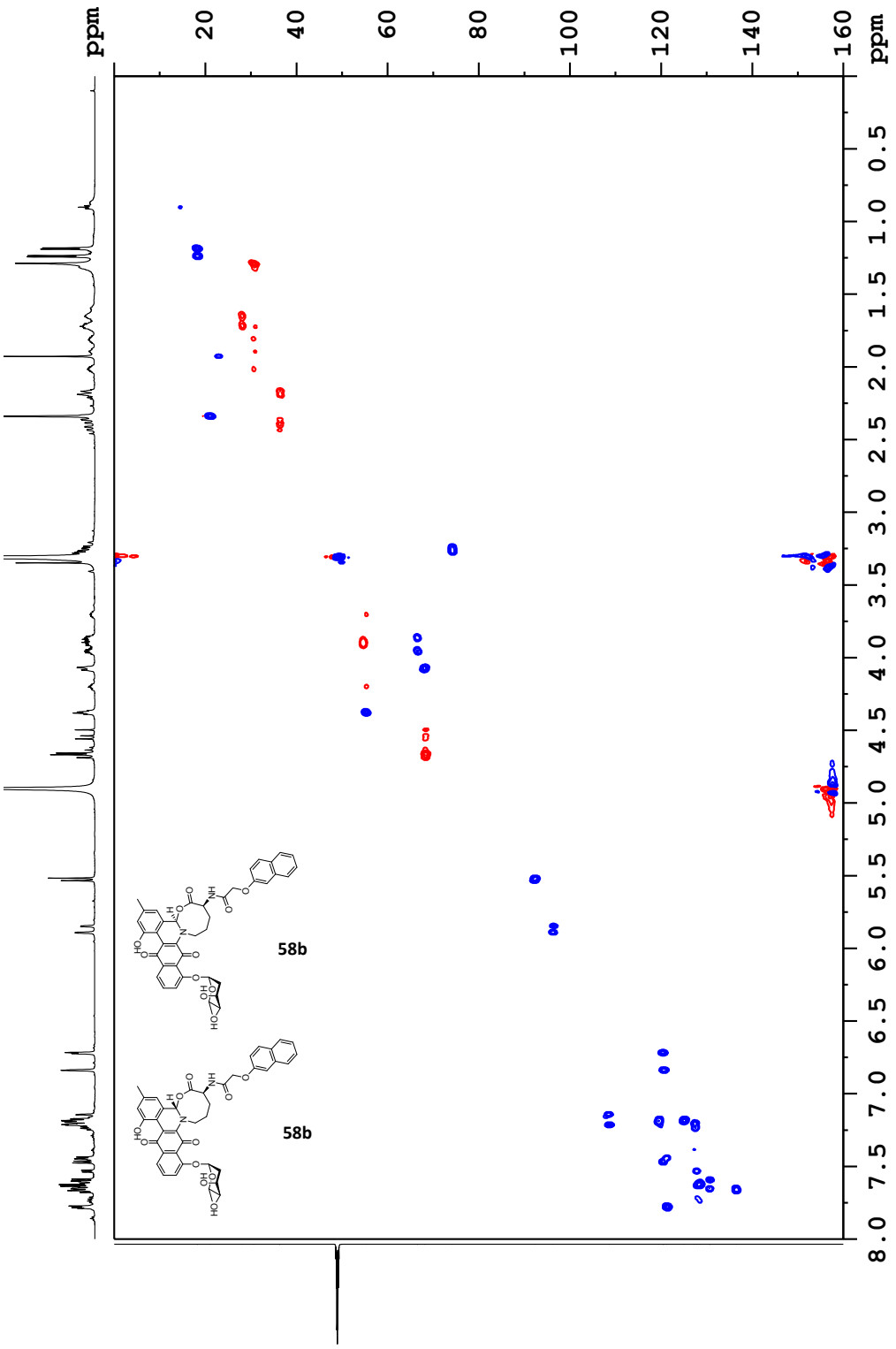

Edited-HSQC (^{1}H-^{13}C) spectrum of **58b** (diastereomeric mixture) in MeOD-d_4. Blue represents CH and CH_3 groups, red represents CH_2 groups.

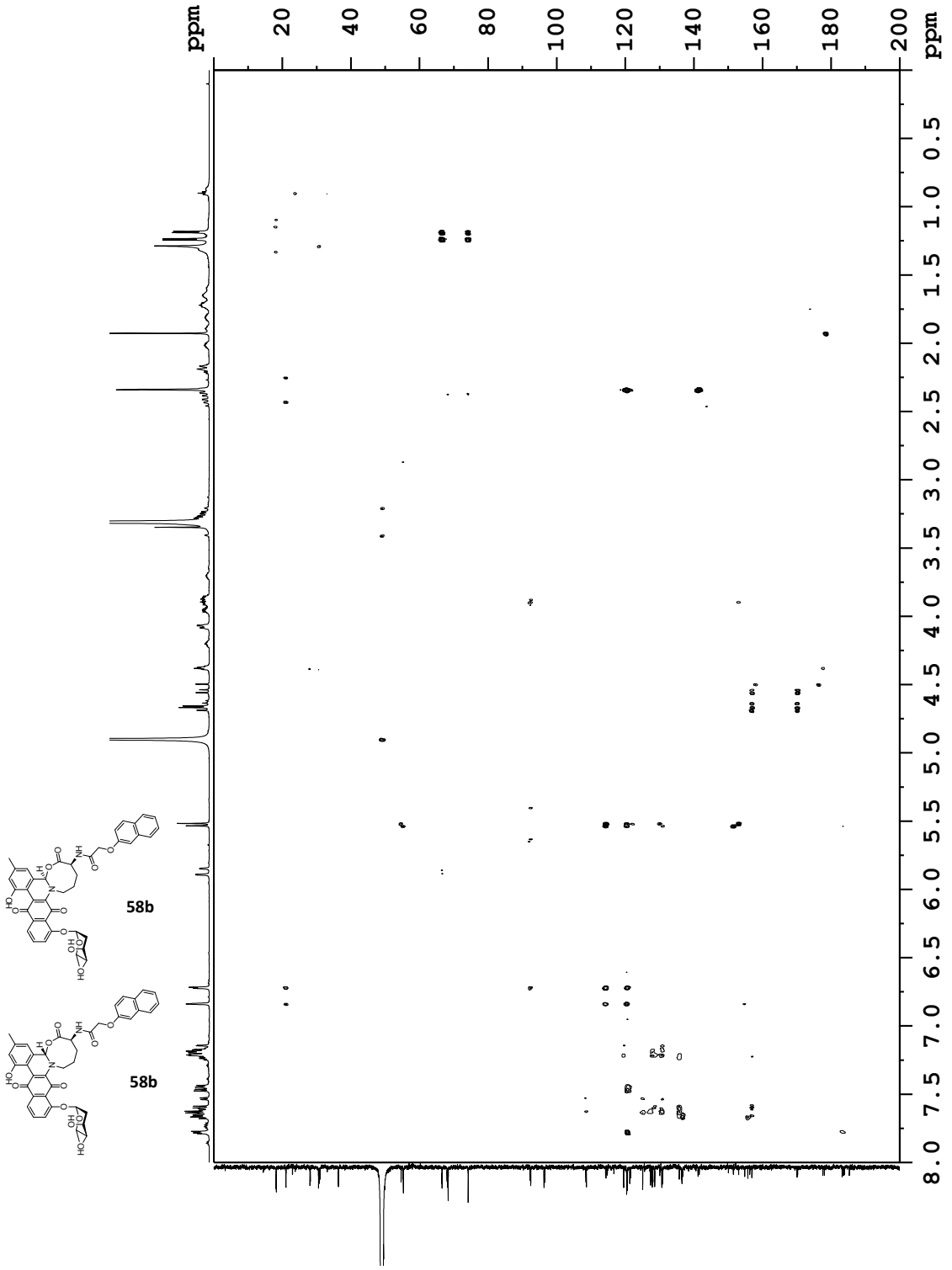

HMBC (^{1}H-^{13}C) spectrum of **58b** (diastereomeric mixture) in MeOD-d_4.

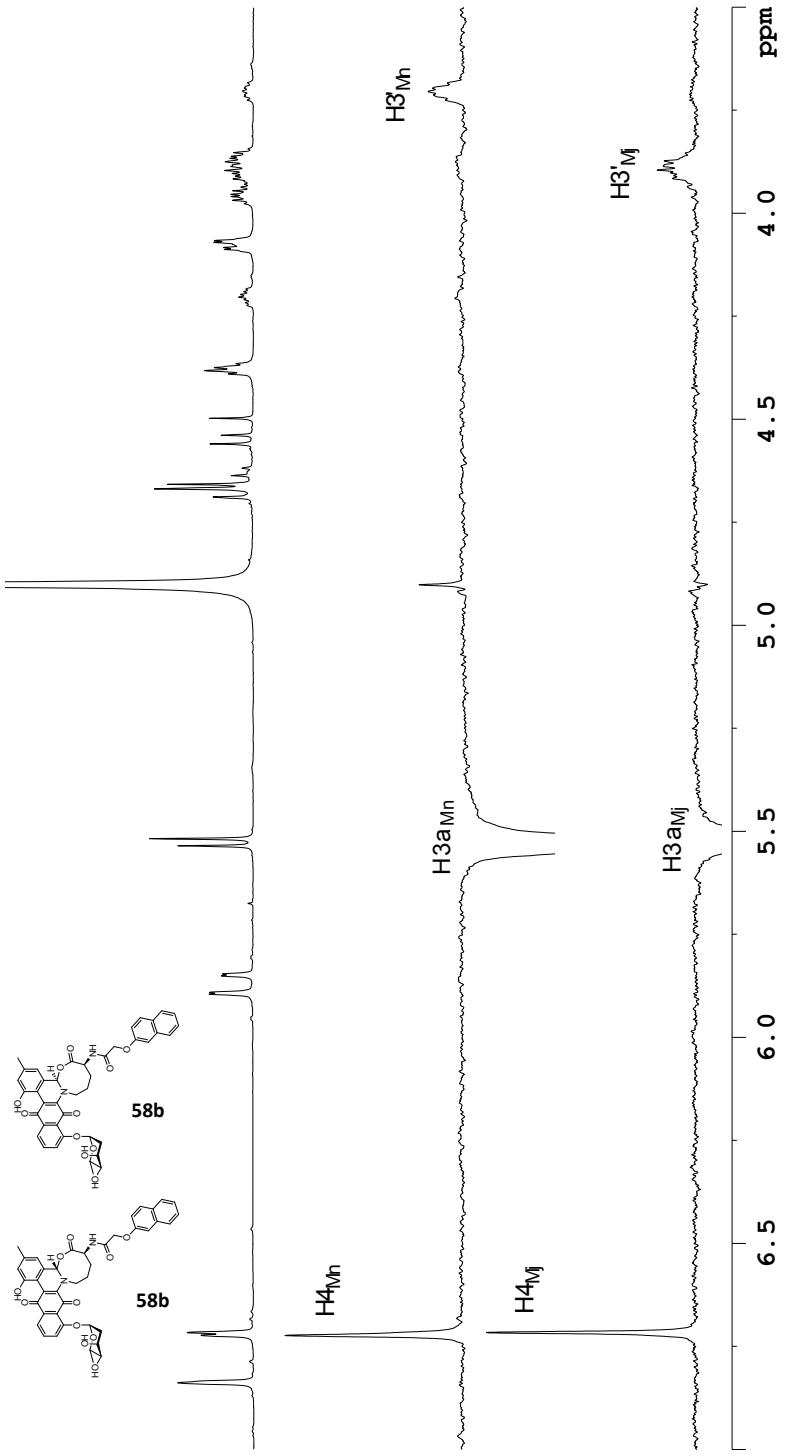

Overlay of ^{1}H-NMR spectrum of **58b** (top) with ROESY (700 MHz) showing irradiation of H3a$_{Mn}$ (middle), and H3a$_{Mj}$ (bottom) in MeOD-d$_4$.

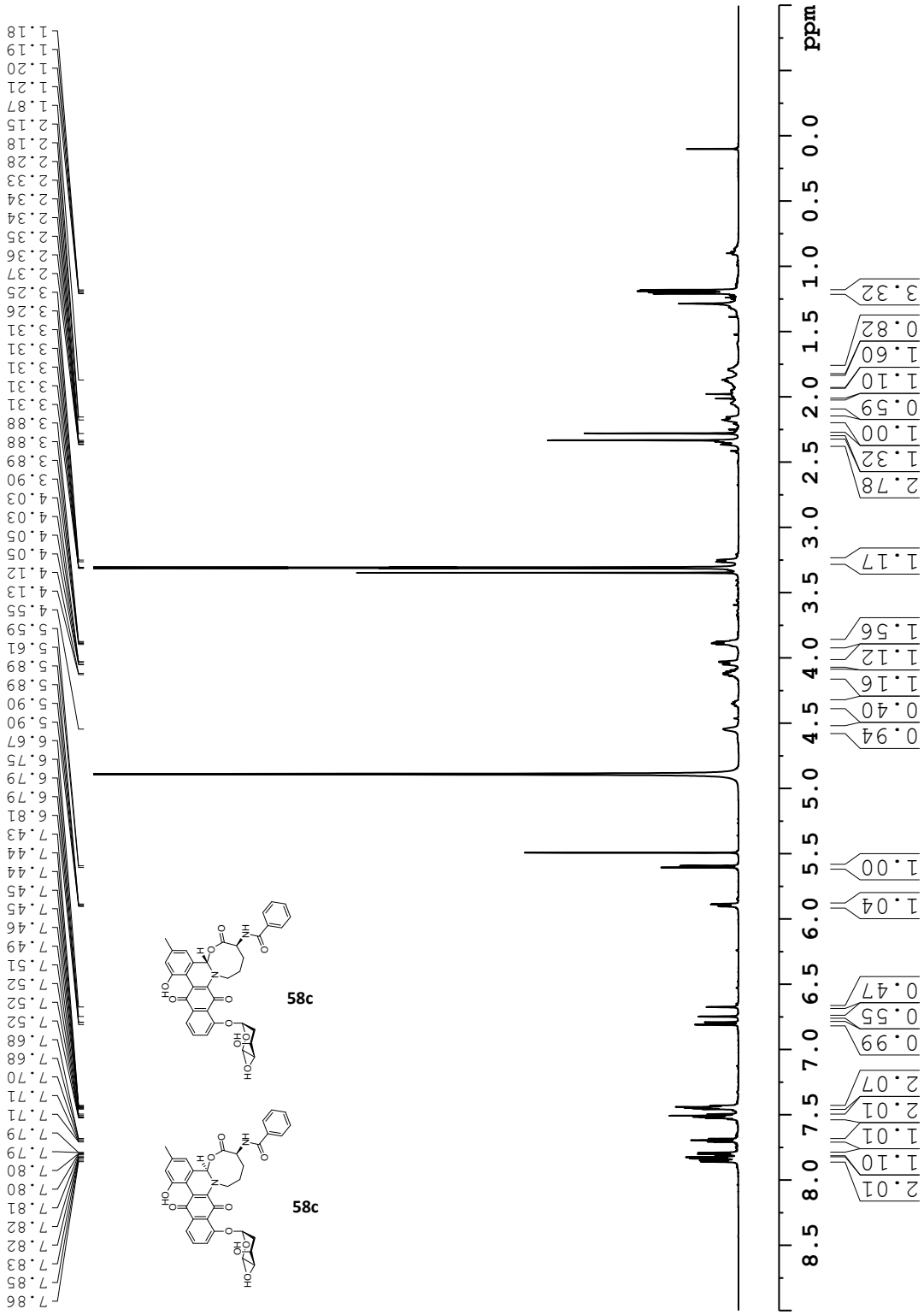

^{1}H-NMR spectrum of **58c** (diastereomeric mixture) in MeOD-d_4 (^{1}H: 700 MHz).

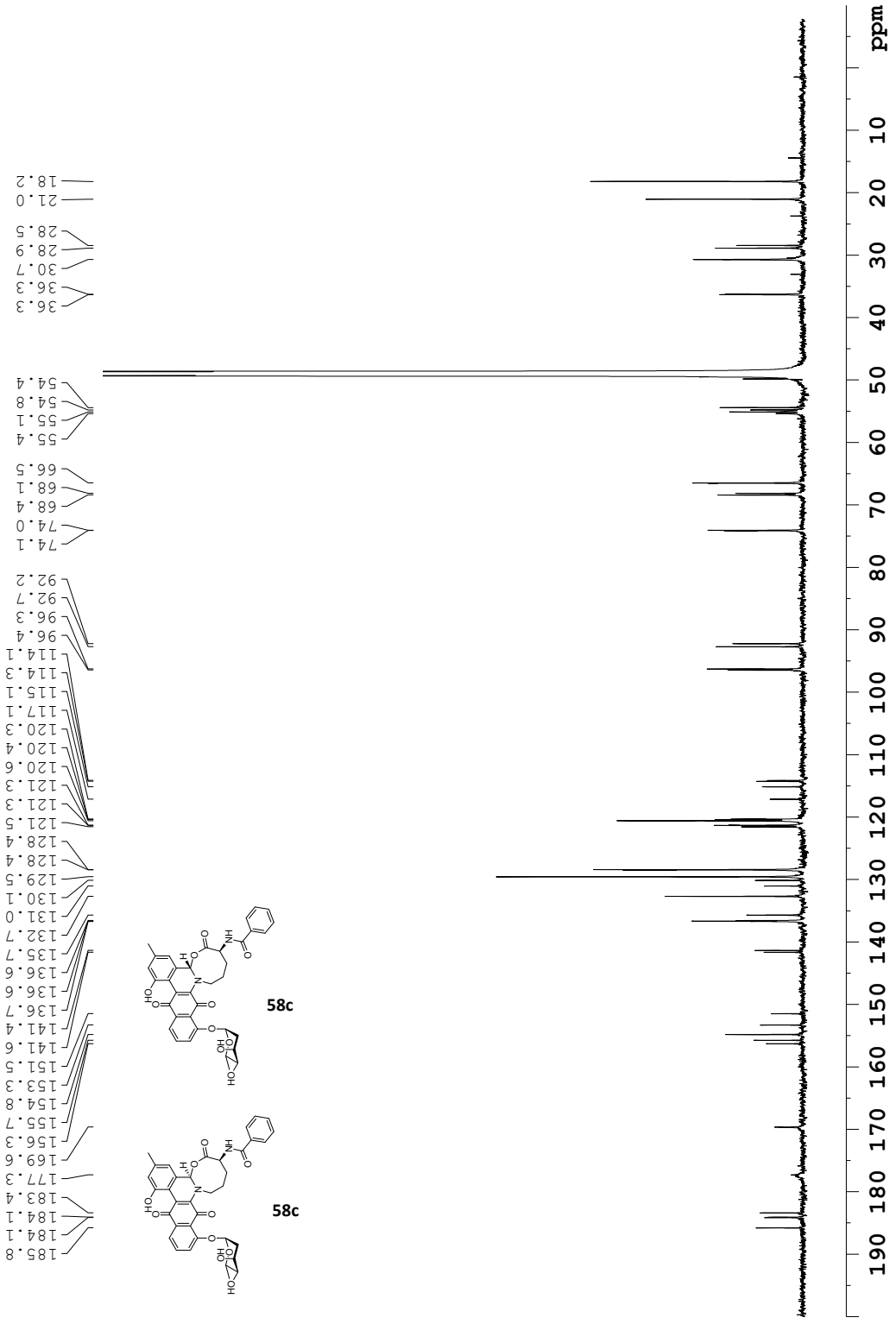

^{13}C-NMR spectrum of **58c** (diastereomeric mixture) in MeOD-d_4 (^{13}C: 176 MHz).

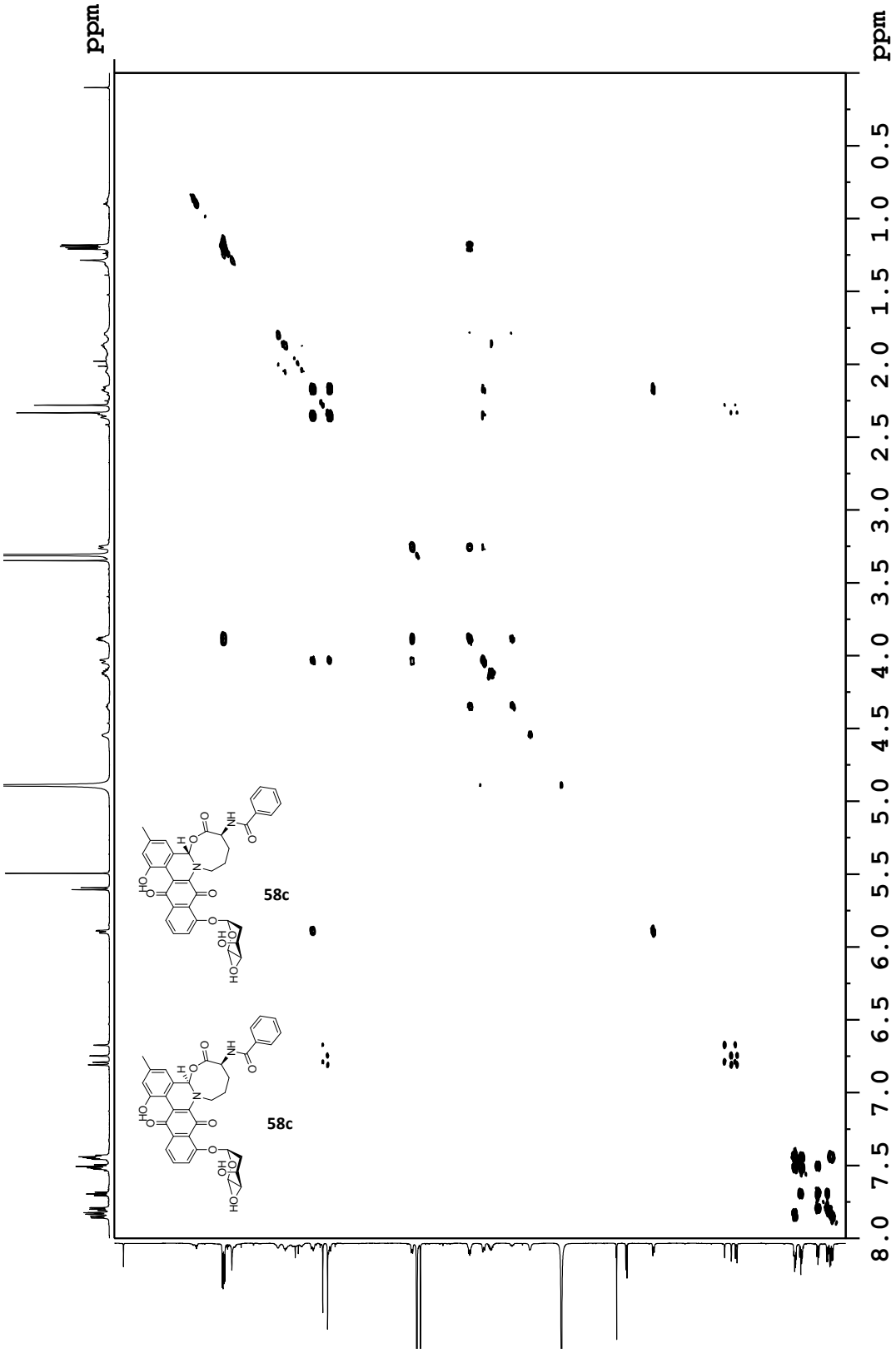

COSY (^{1}H-^{1}H) spectrum of **58c** (diastereomeric mixture) in MeOD-d_4 (700 MHz).

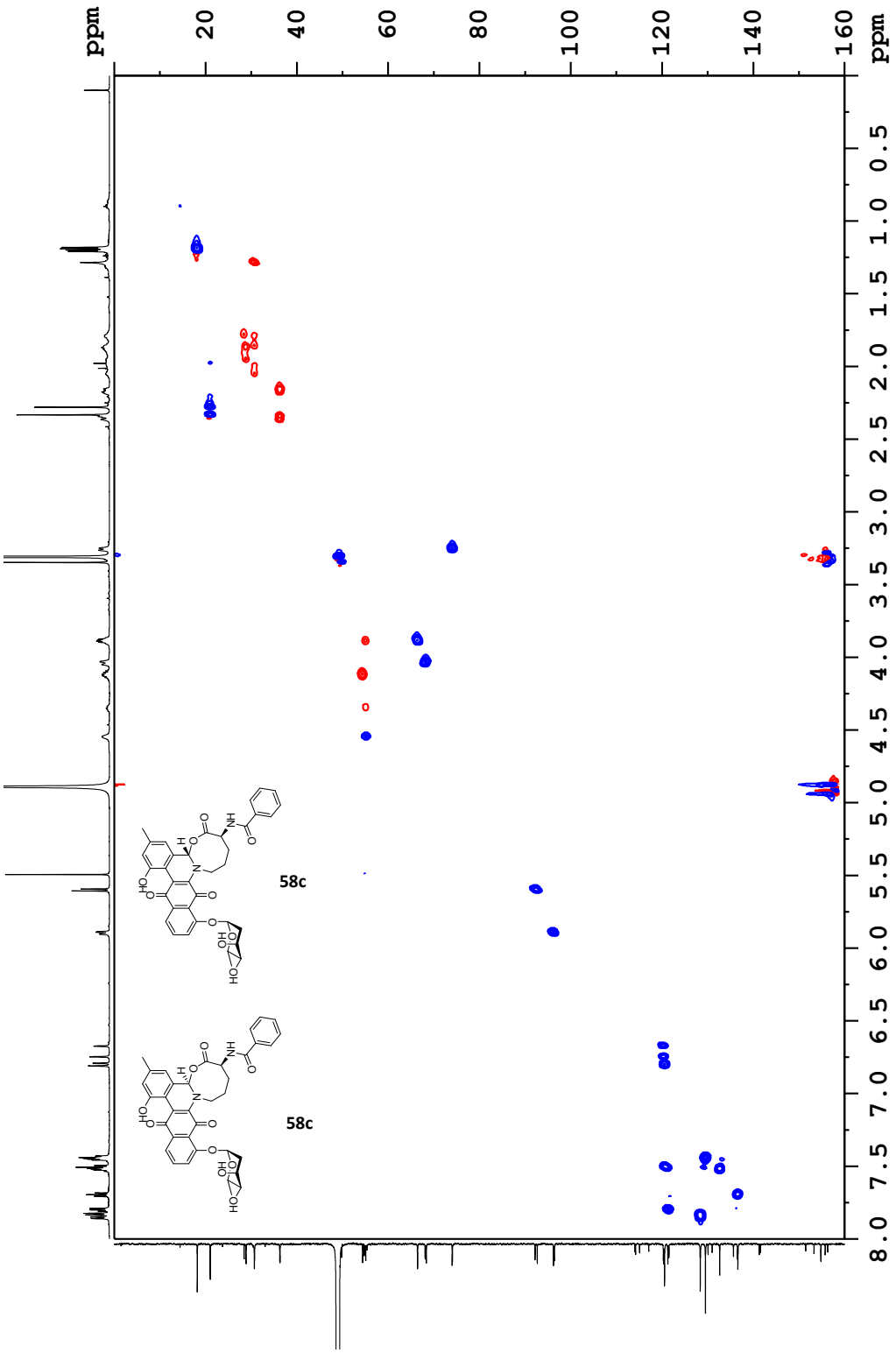

Edited-HSQC (^{1}H-^{13}C) spectrum of **58c** (diastereomeric mixture) in MeOD-d_4. Blue represents CH and CH_3 groups, red represents CH_2 groups.

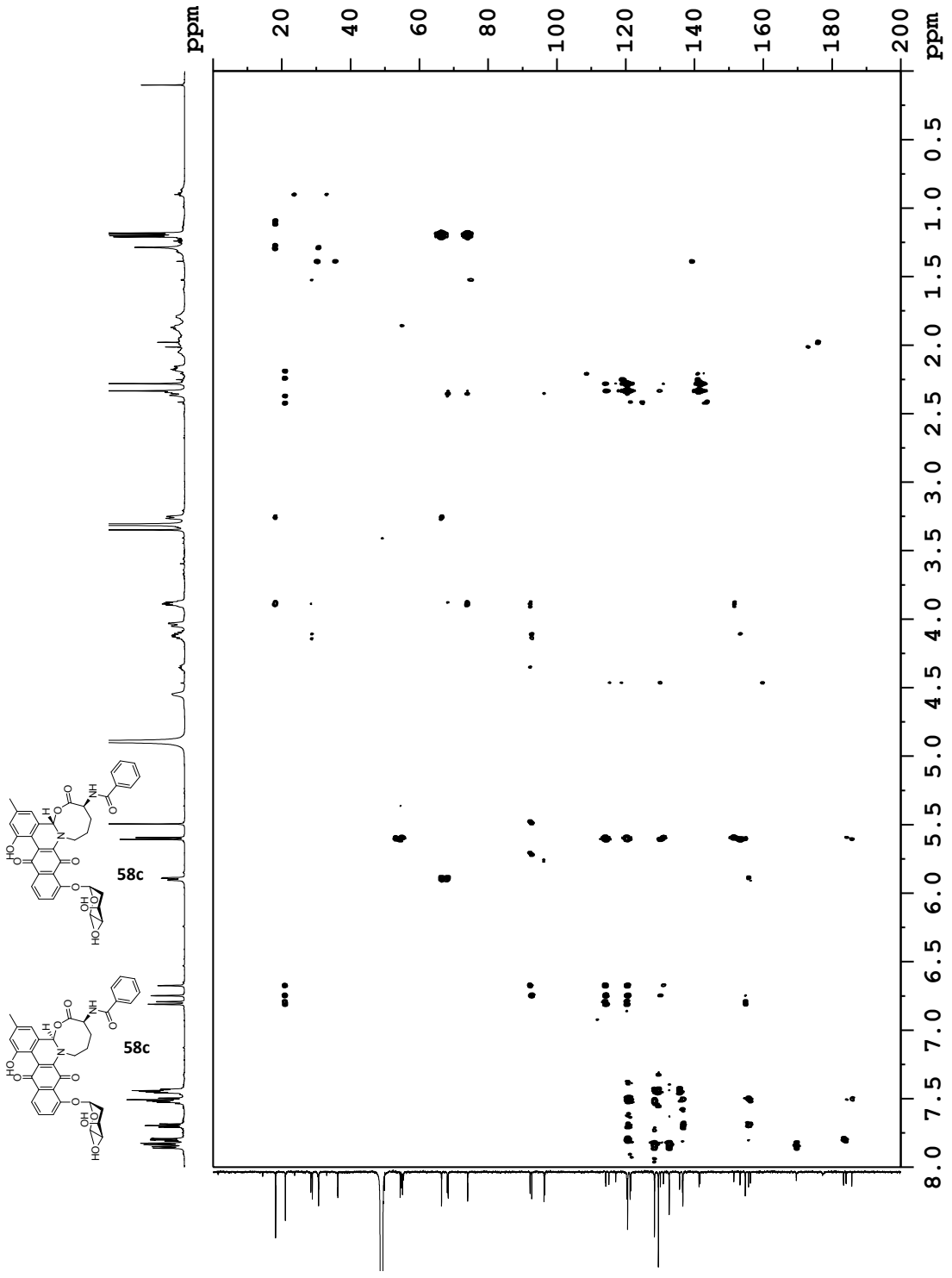

HMBC (^{1}H-^{13}C) spectrum of **58c** (diastereomeric mixture) in MeOD-d_4.

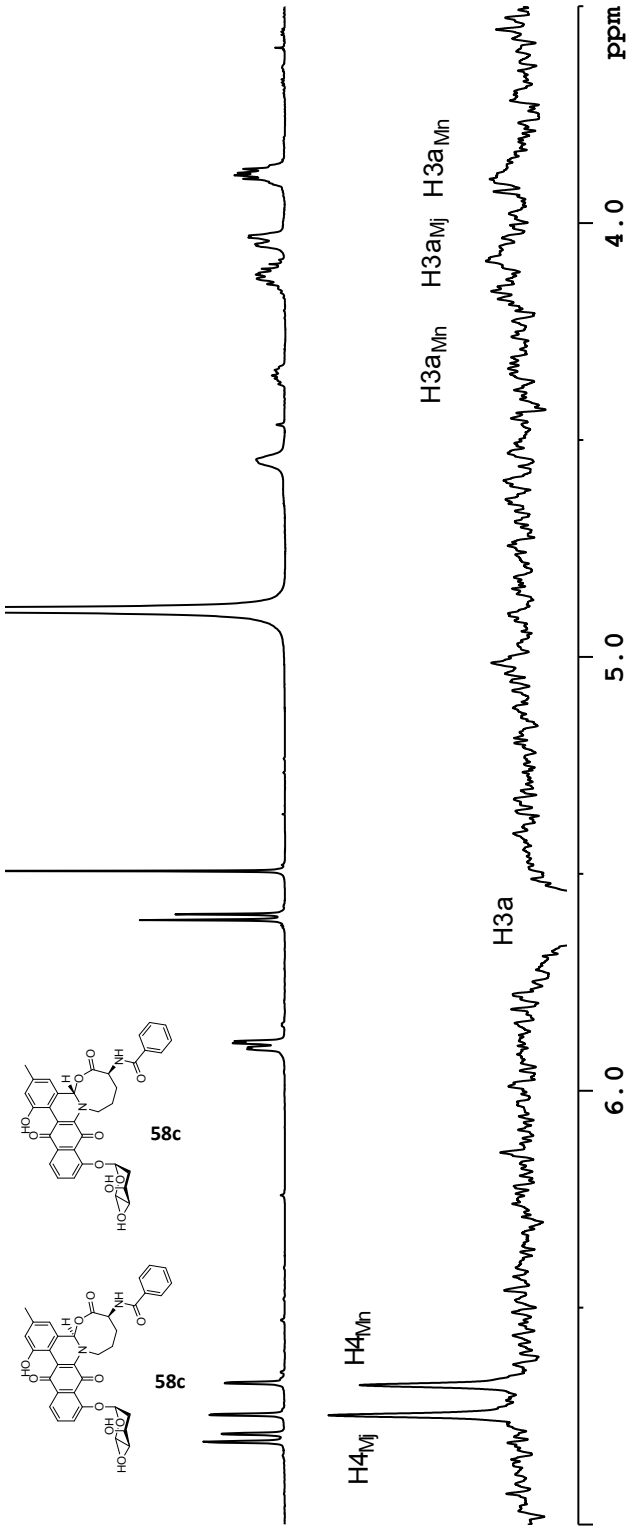

Overlay of ^{1}H-NMR spectrum of **58c** (top) with ROESY (500 MHz) showing irradiation of both $H3a_{Mn}$ and $H3a_{Mj}$ simultaneously (bottom), in MeOD-d_4.

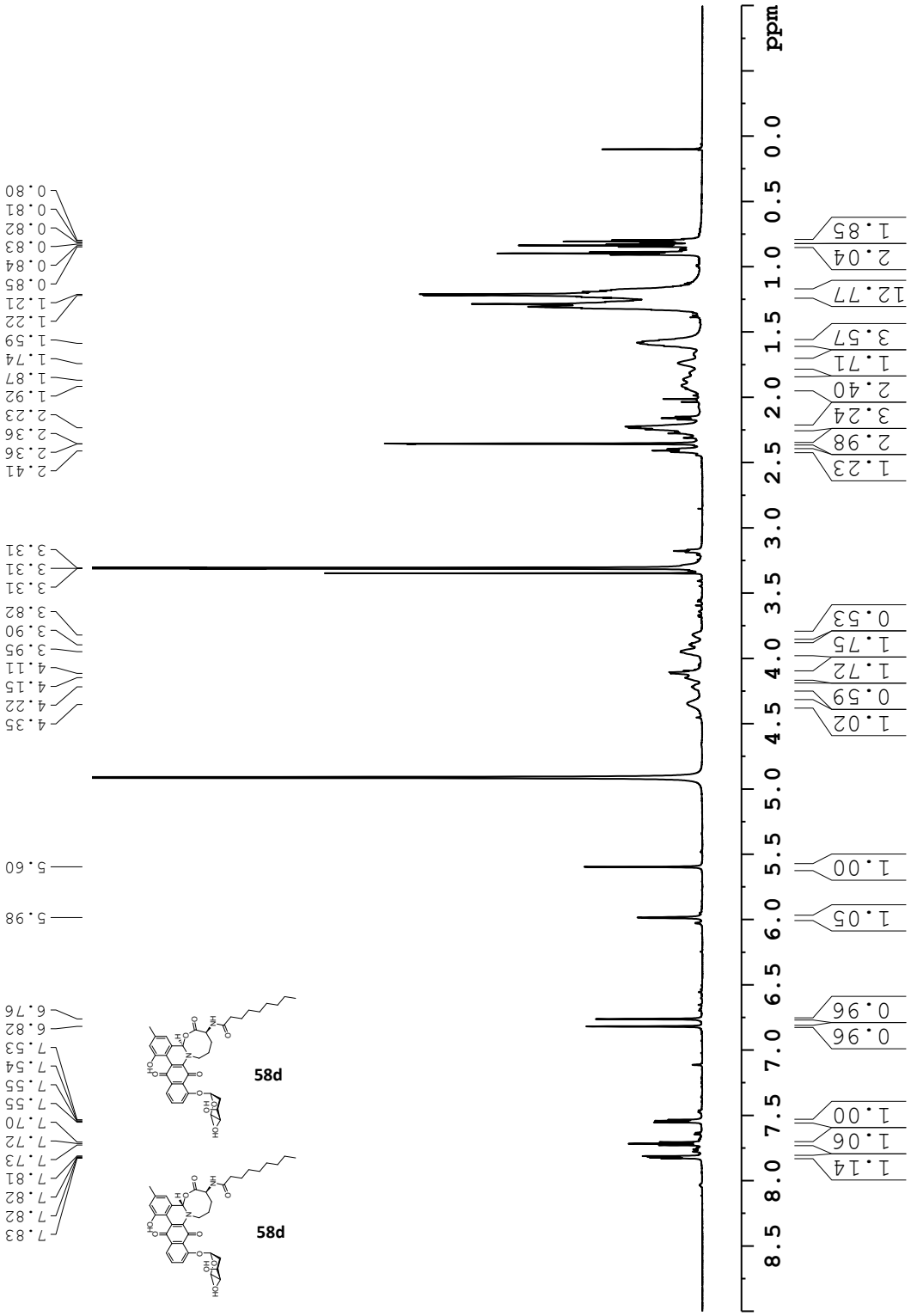

^{1}H-NMR spectrum of **58d** (diastereomeric mixture) in MeOD-d_4 (^{1}H: 700 MHz).

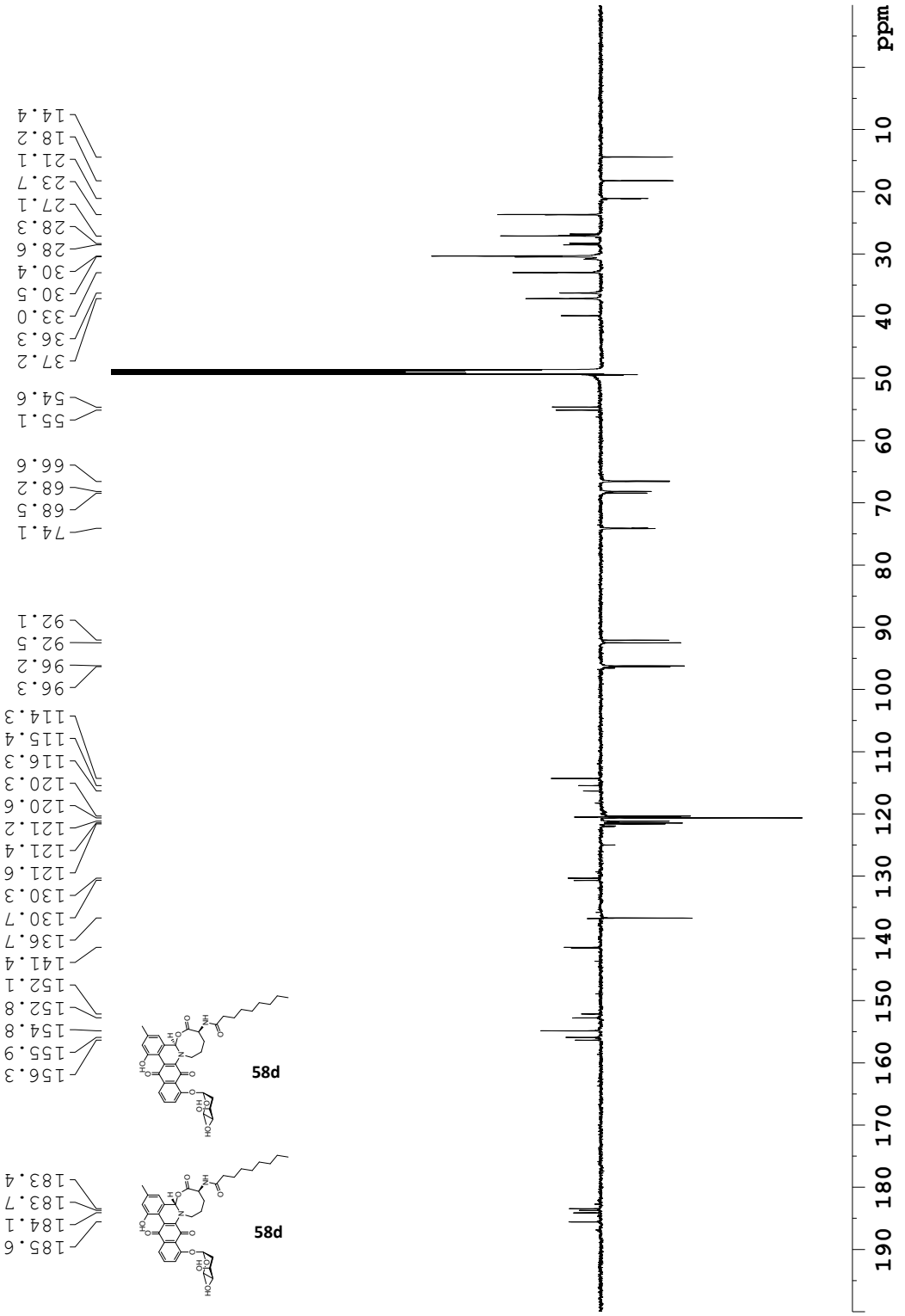

DEPTQ spectrum of **58d** (diastereomeric mixture) in MeOD-d_4 (^{13}C: 176 MHz).

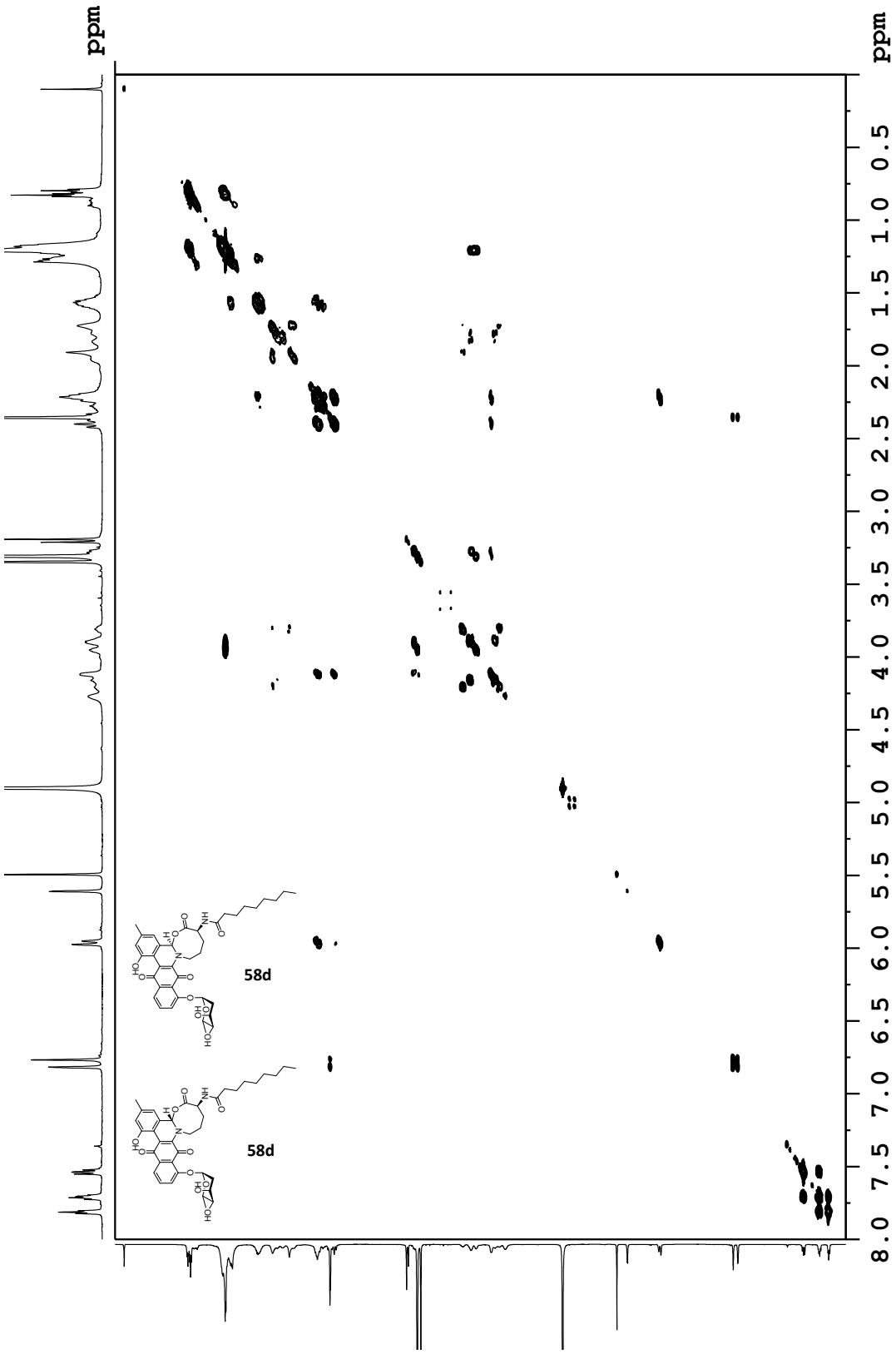

COSY (^{1}H-^{1}H) spectrum of **58d** (diastereomeric mixture) in MeOD-d_4 (700 MHz).

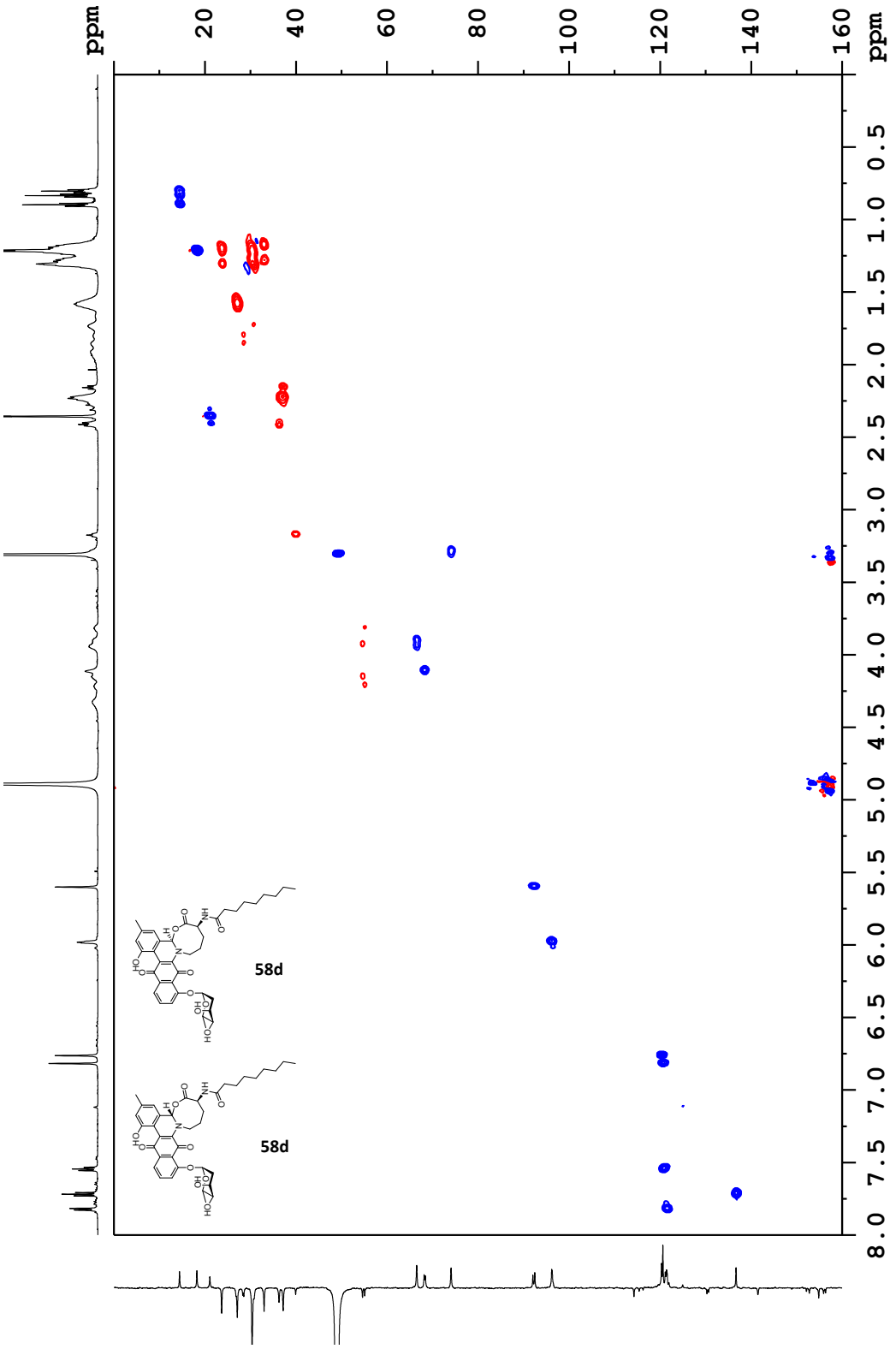

Edited-HSQC (^{1}H-^{13}C) spectrum of **58d** (diastereomeric mixture) in MeOD-d_4. Blue represents CH and CH_3 groups, red represents CH_2 groups.

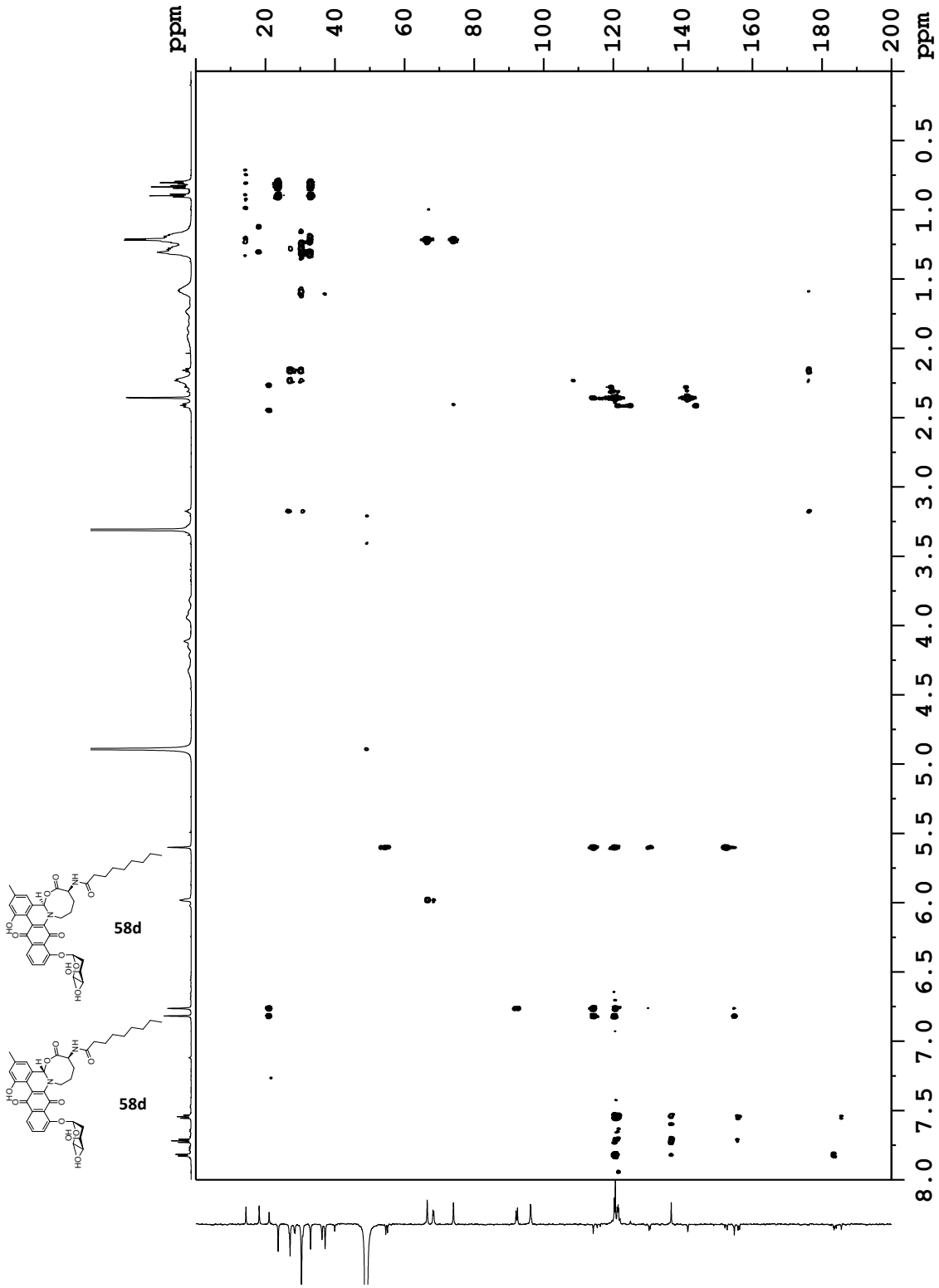

HMBC (^{1}H-^{13}C) spectrum of **58d** (diastereomeric mixture) in MeOD-d_4.

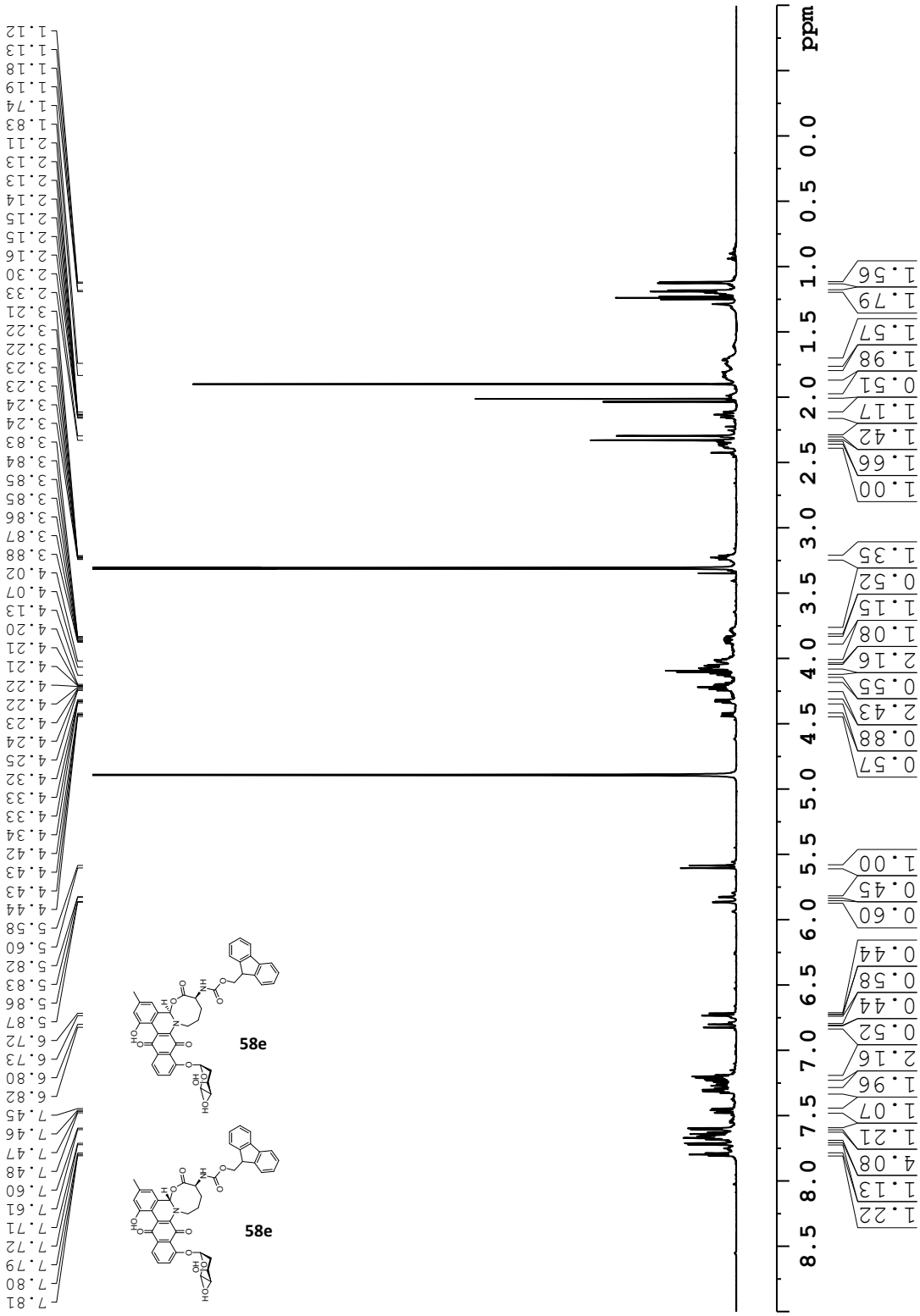

^{1}H-NMR spectrum of **58e** (diastereomeric mixture) in MeOD-d_4 (^{1}H: 700 MHz).
Note: Compound prone to breakdown over time in NMR tube/solvent.

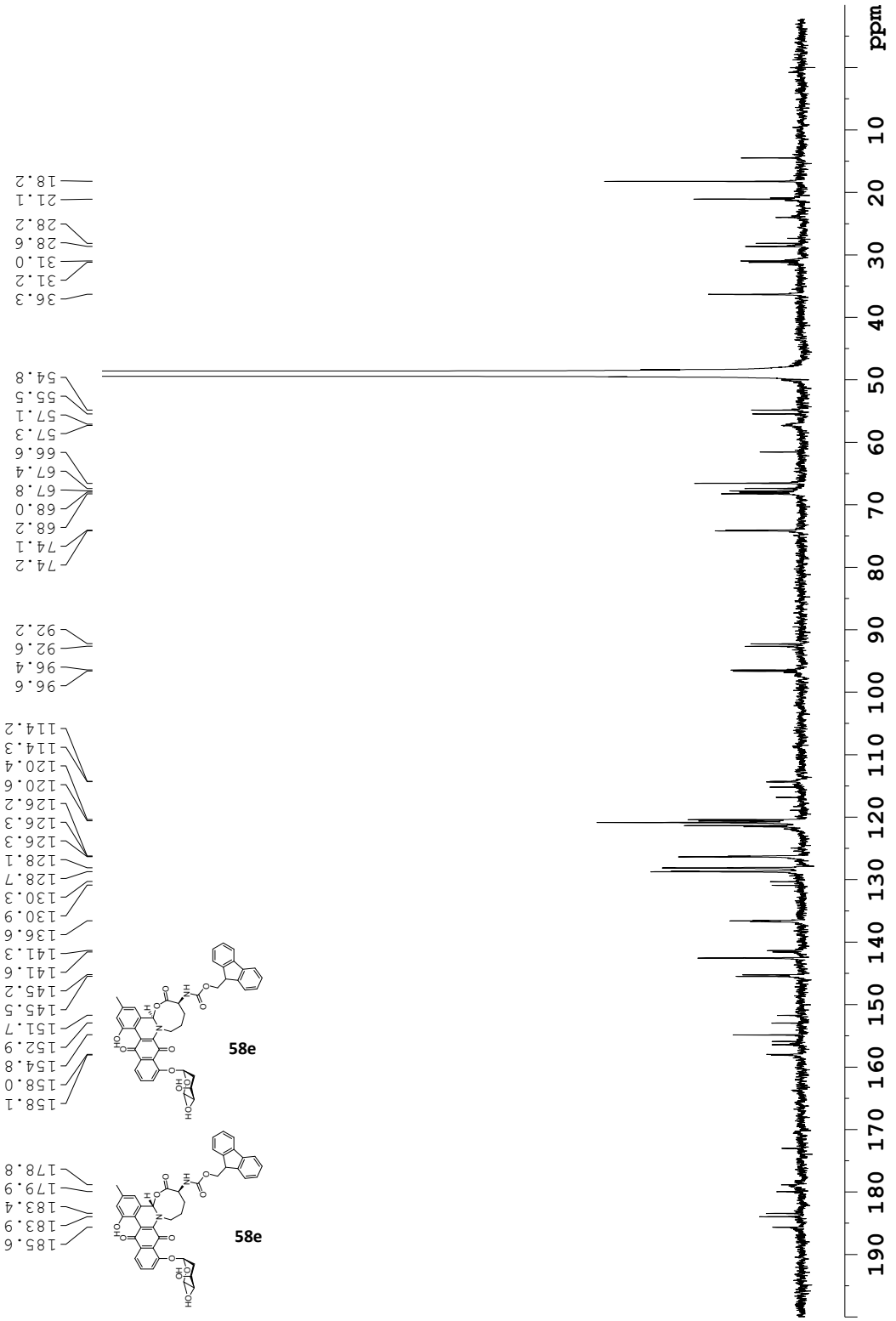

^{13}C-NMR spectrum of **58e** (diastereomeric mixture) in MeOD-d_4 (^{13}C: 176 MHz).

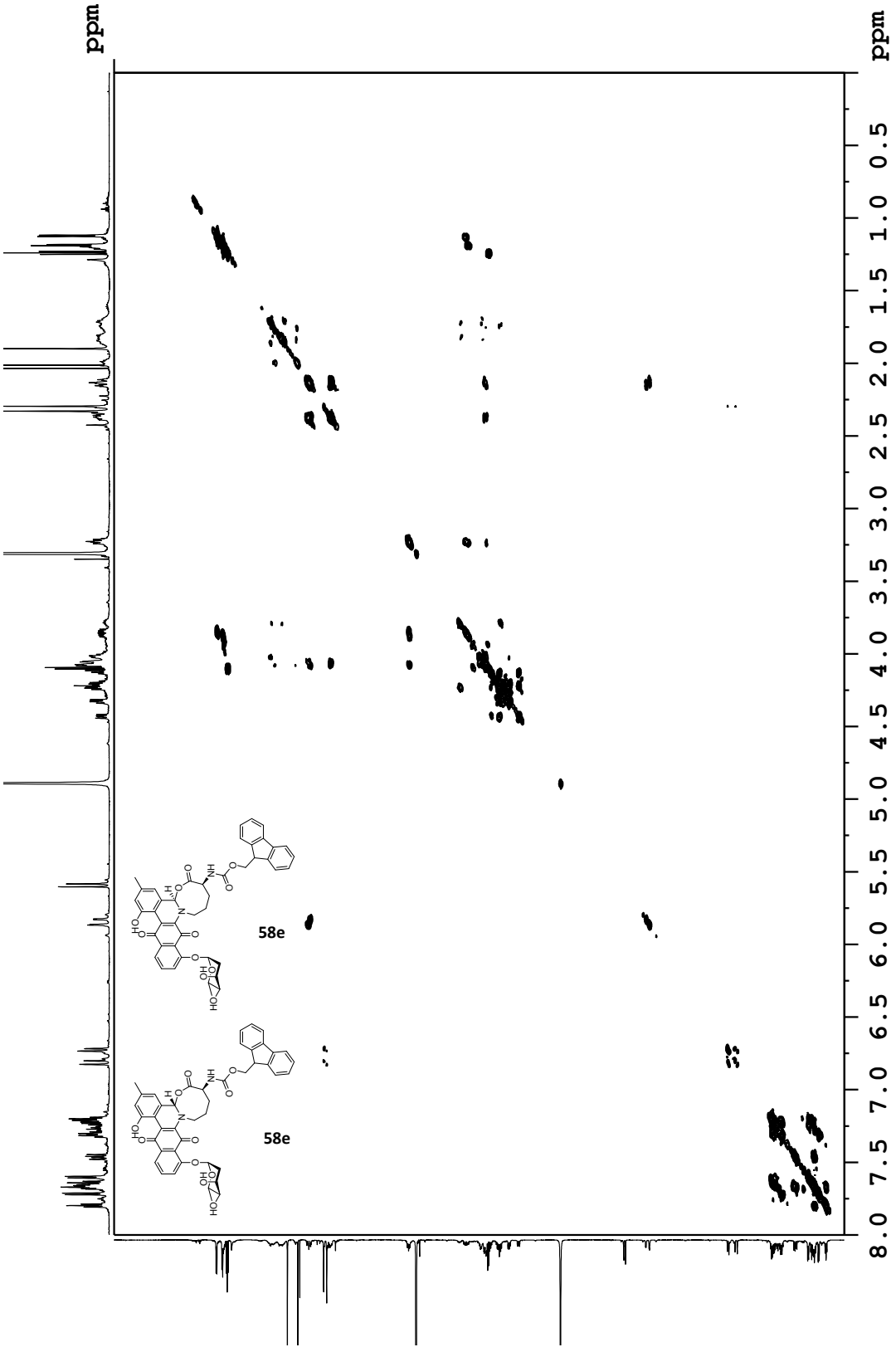

COSY (^{1}H-^{1}H) spectrum of **58e** (diastereomeric mixture) in MeOD-d_4 (700 MHz).

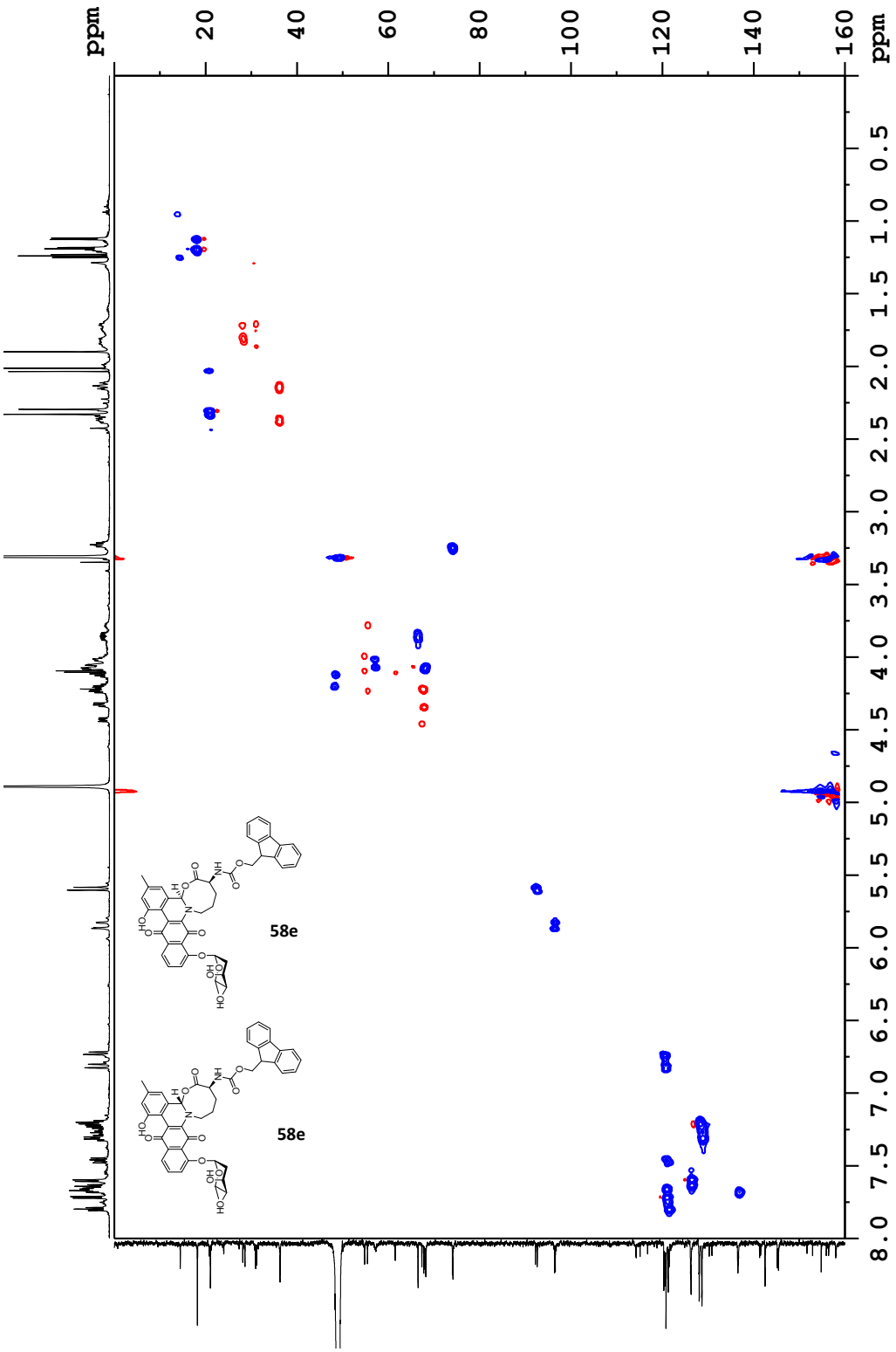

Edited-HSQC (^{1}H-^{13}C) spectrum of **58e** (diastereomeric mixture) in MeOD-d_4. Blue represents CH and CH_3 groups, red represents CH_2 groups.

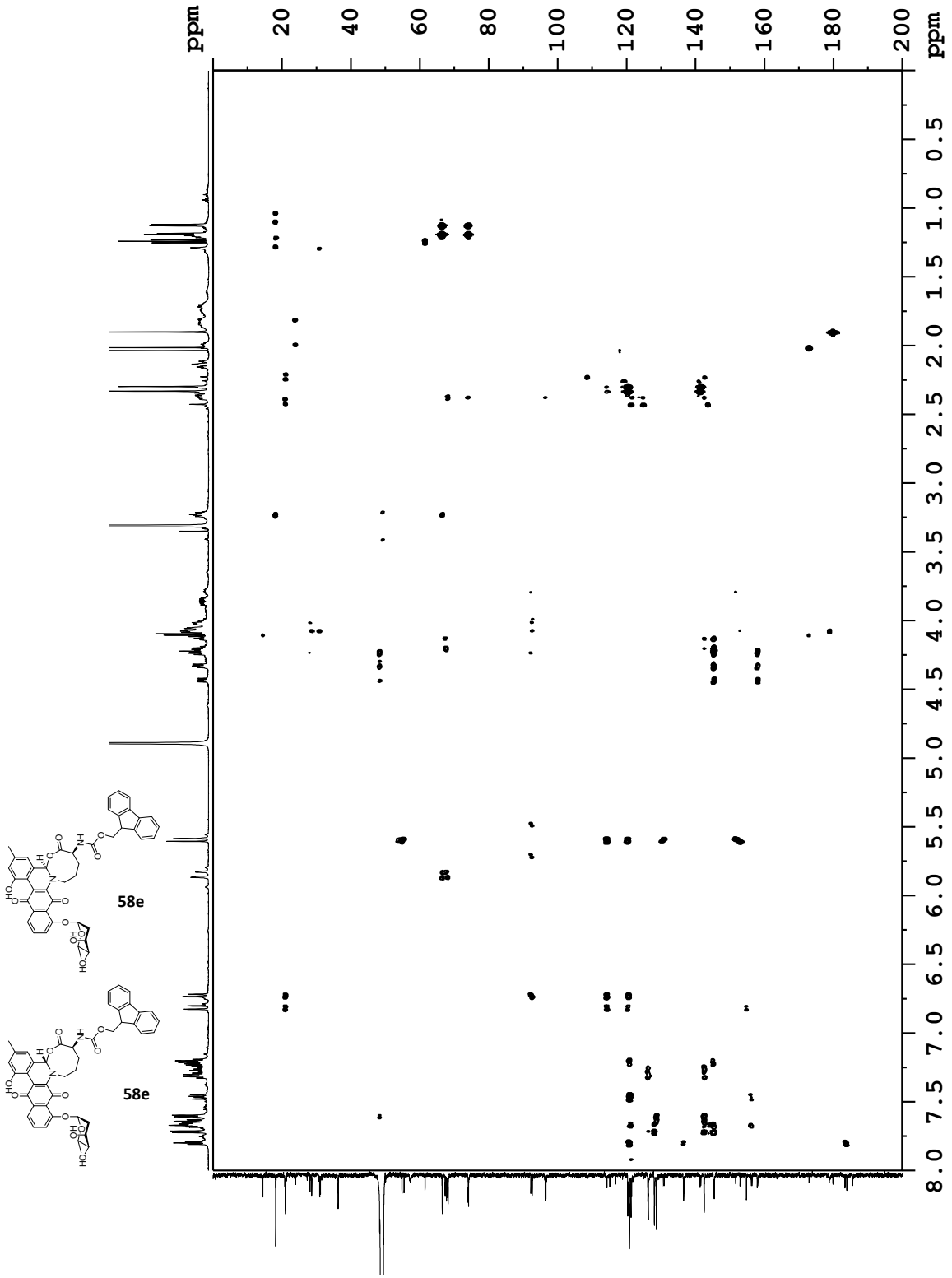

HMBC (^{1}H-^{13}C) spectrum of **58e** (diastereomeric mixture) in MeOD-d_4.

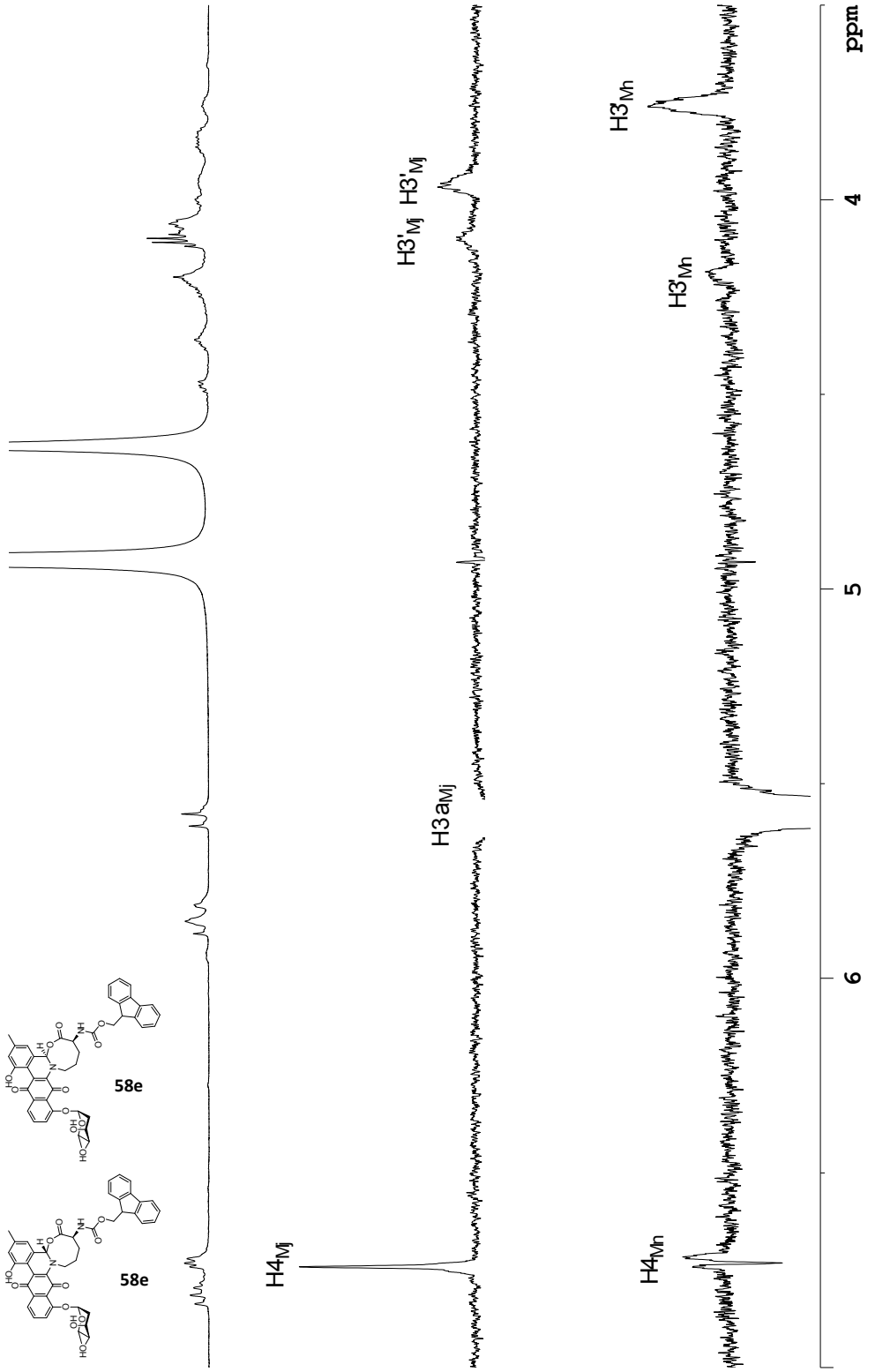

Overlay of ^{1}H-NMR spectrum of **58e** (top) with ROESY (500 MHz) showing irradiation of $H3a_{Mj}$ (middle), and $H3a_{Mn}$ (bottom) in MeOD-d_4.

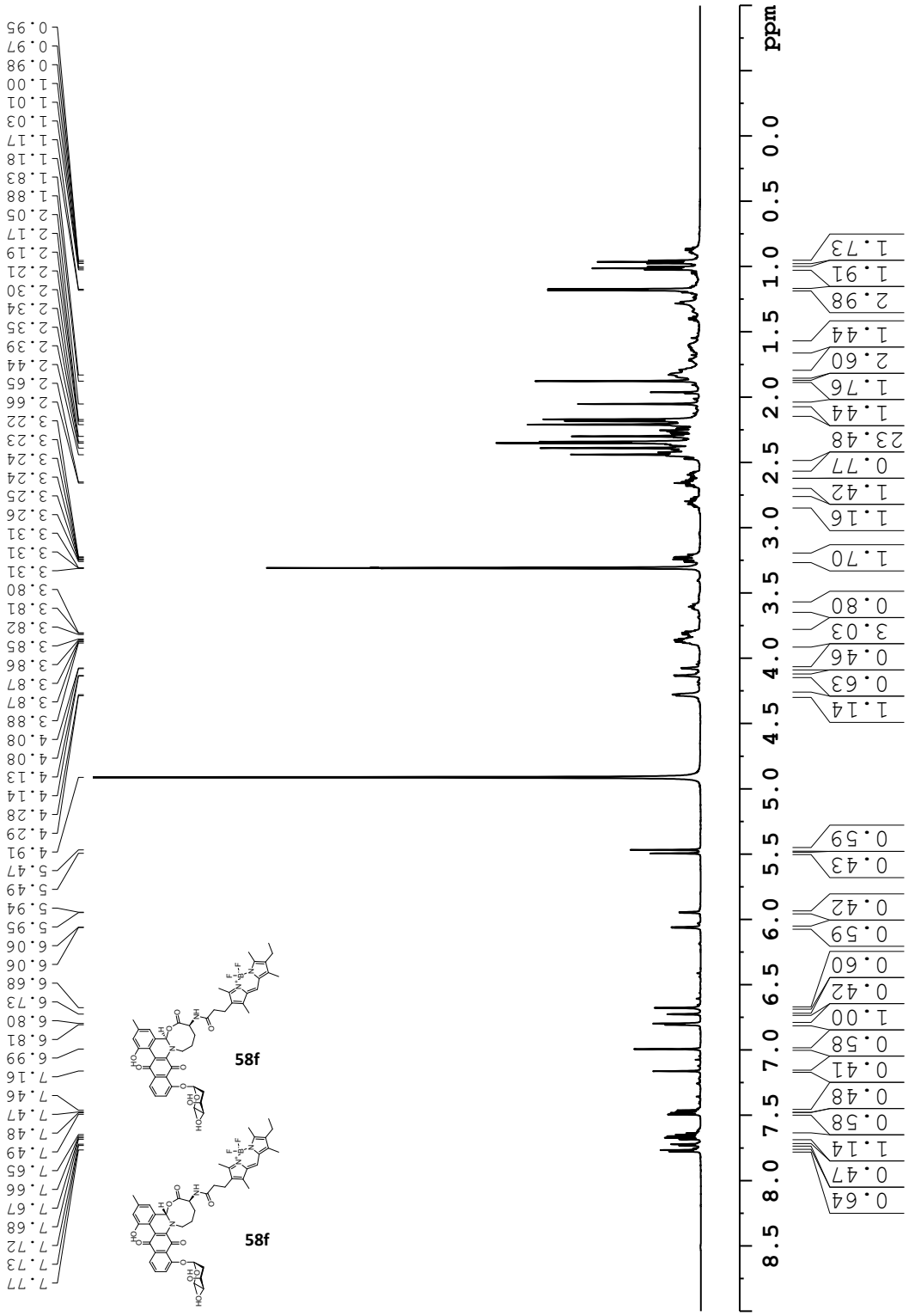

^{1}H-NMR spectrum of **58f** (diastereomeric mixture) in MeOD-d_4 (^{1}H: 700 MHz).

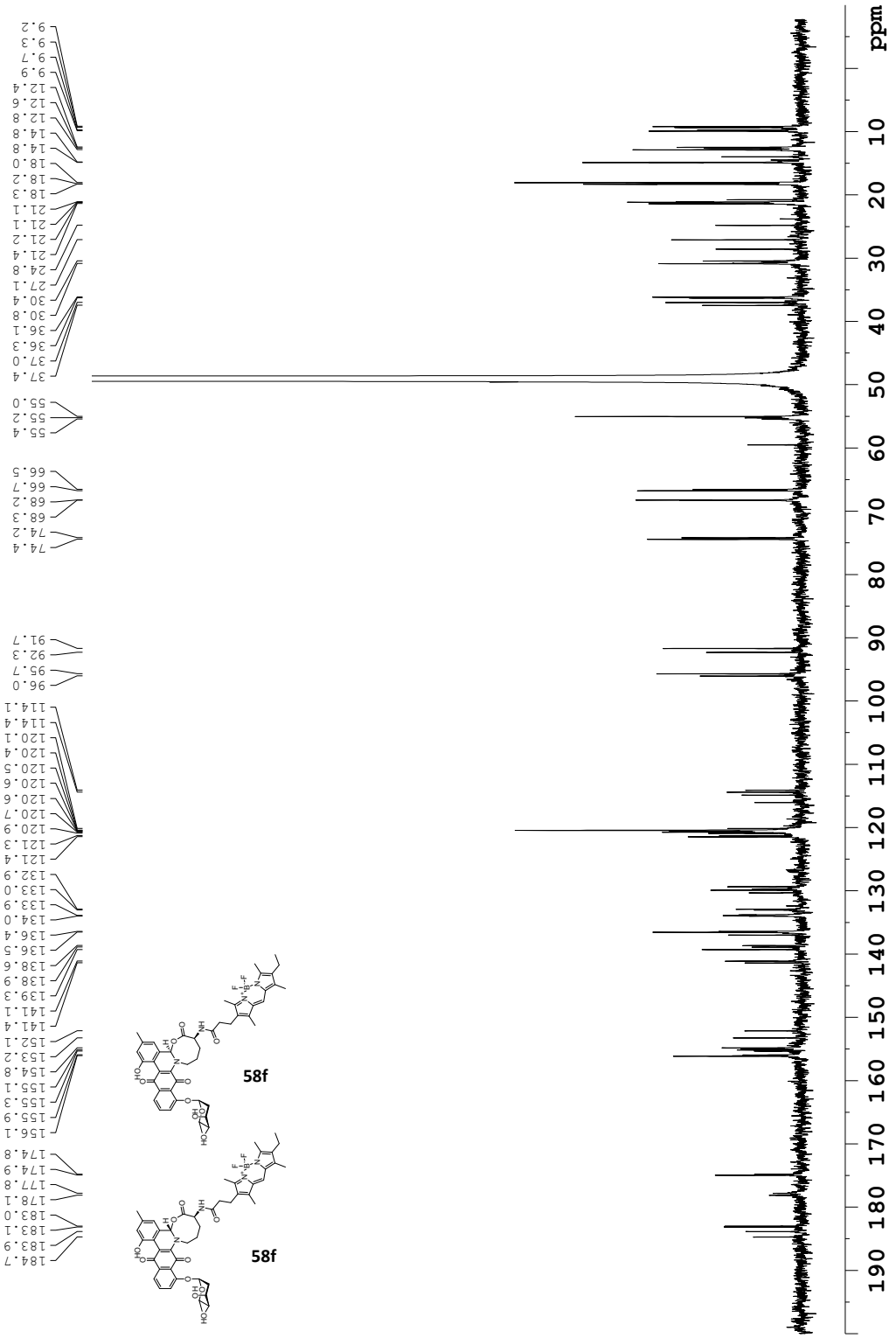

^{13}C-NMR spectrum of **58f** (diastereomeric mixture) in MeOD-d_4 (^{13}C: 176 MHz).

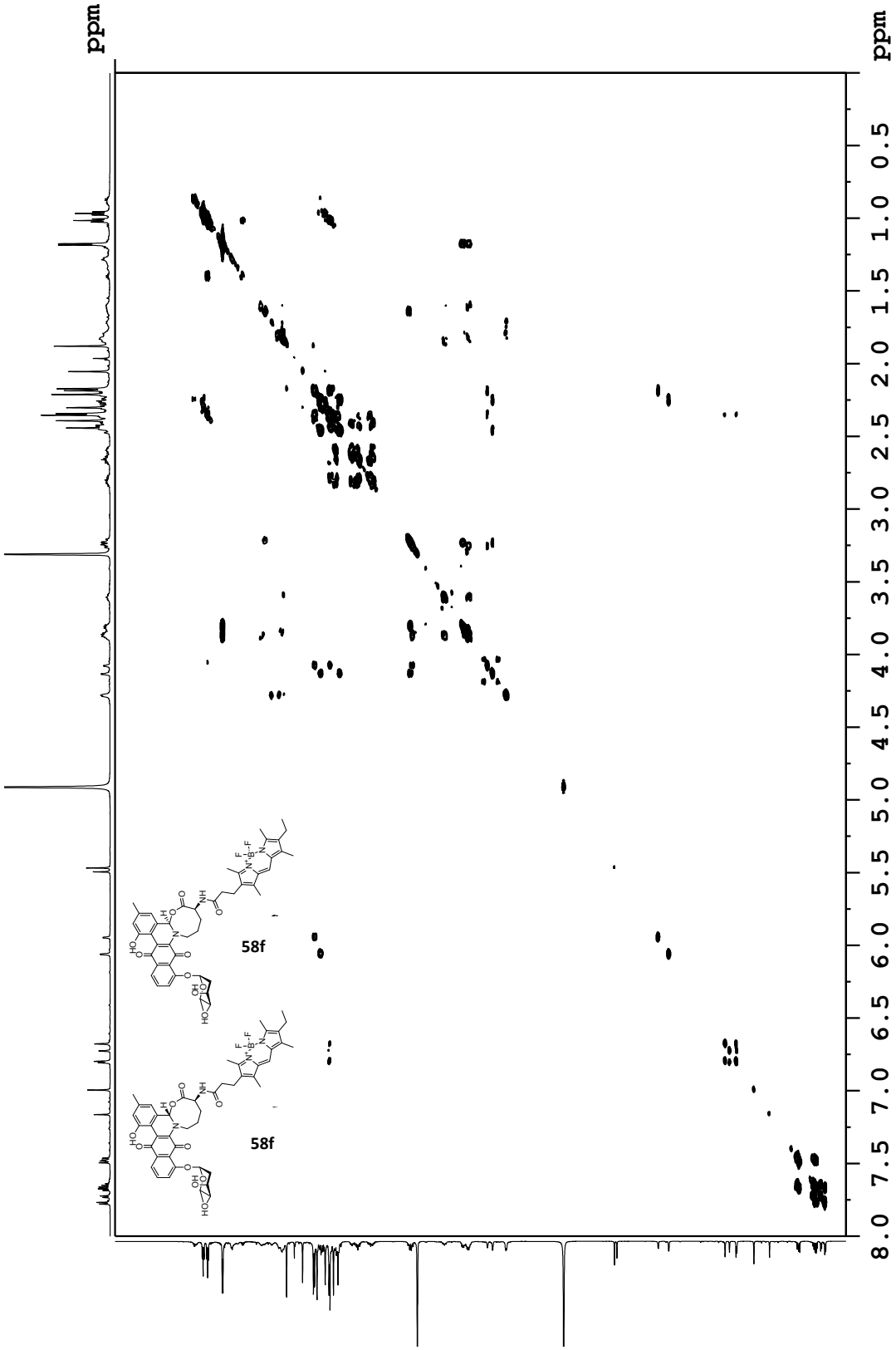

COSY (^{1}H-^{1}H) spectrum of **58f** (diastereomeric mixture) in MeOD-d_4 (700 MHz).

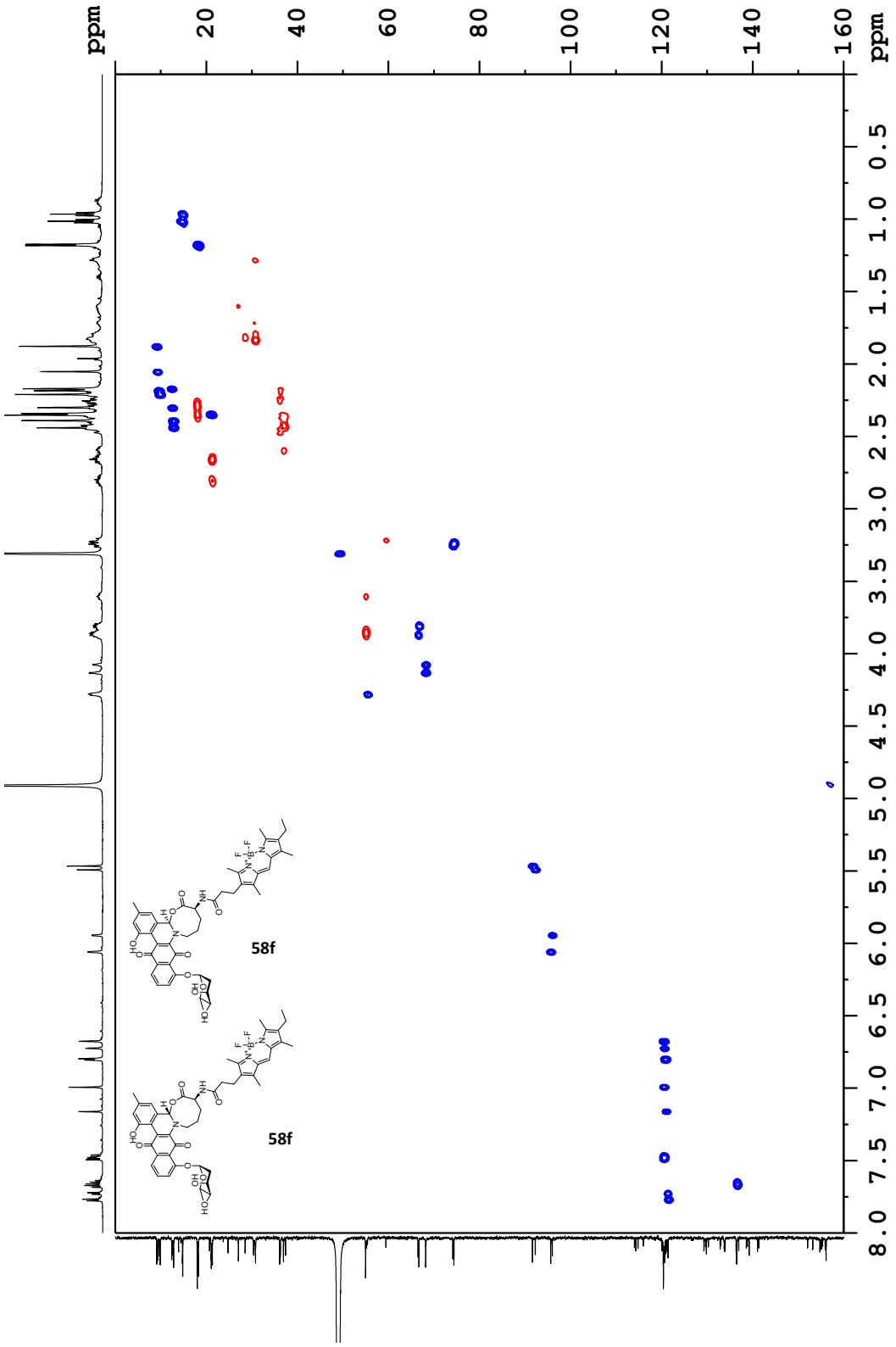

Edited-HSQC (^{1}H-^{13}C) spectrum of **58f** (diastereomeric mixture) in MeOD-d_4. Blue represents CH and CH_3 groups, red represents CH_2 groups.

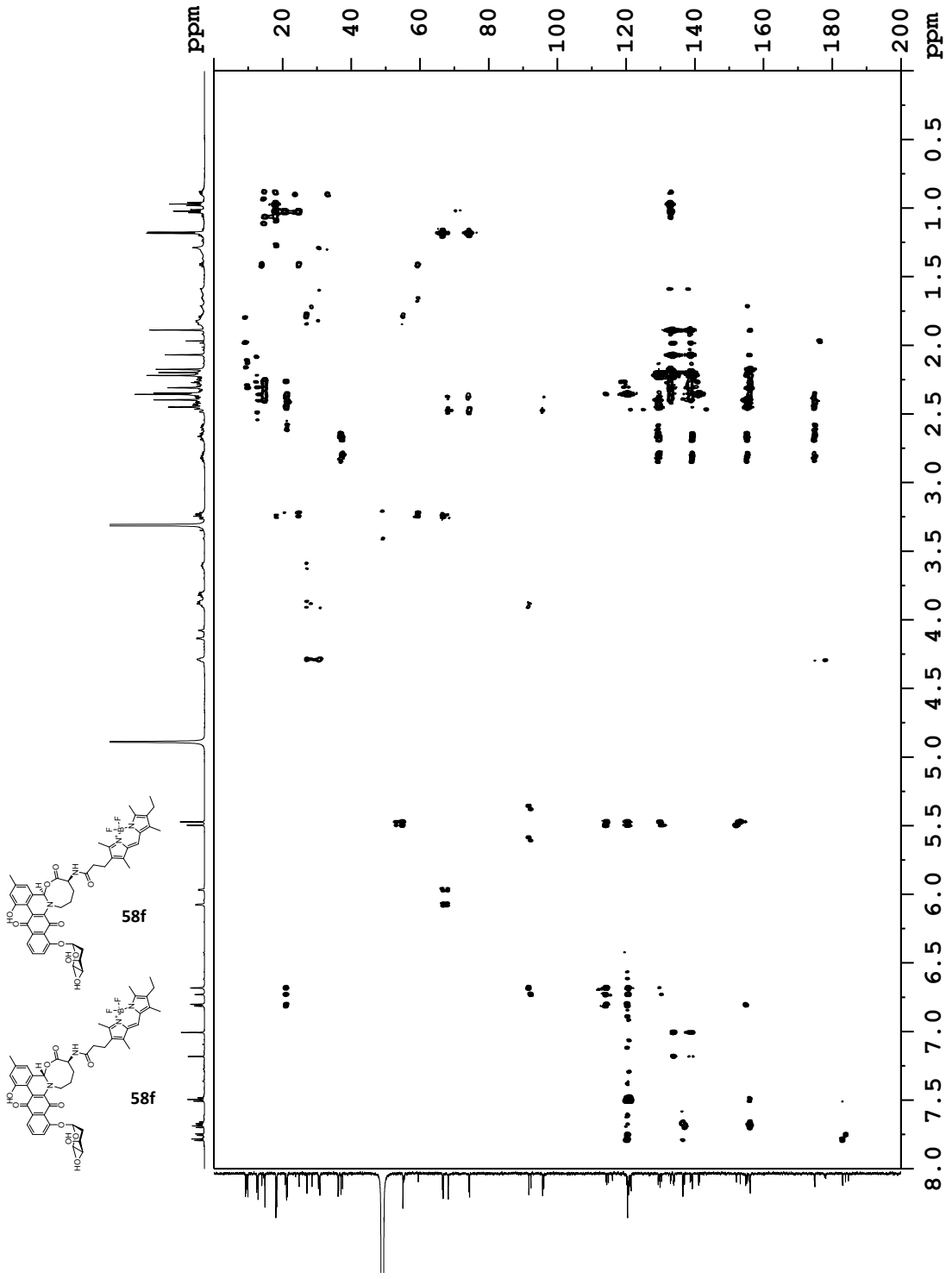

HMBC (^{1}H-^{13}C) spectrum of **58f** (diastereomeric mixture) in MeOD-d_4.

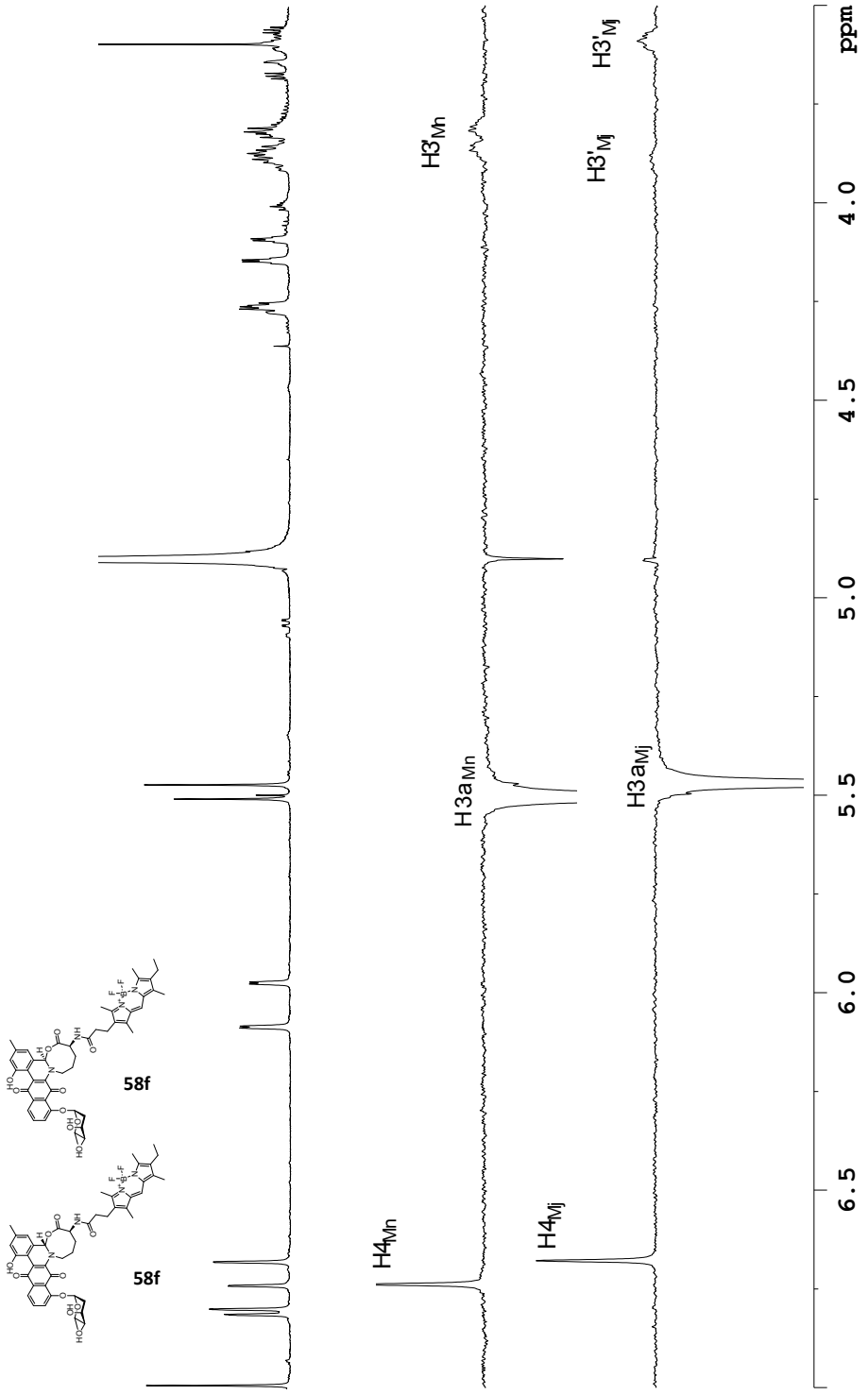

Overlay of ^{1}H-NMR spectrum of **58f** (top) with ROESY (700 MHz) showing irradiation of $H3a_{Mn}$ (middle), and $H3a_{Mj}$ (bottom) in MeOD-d_4.

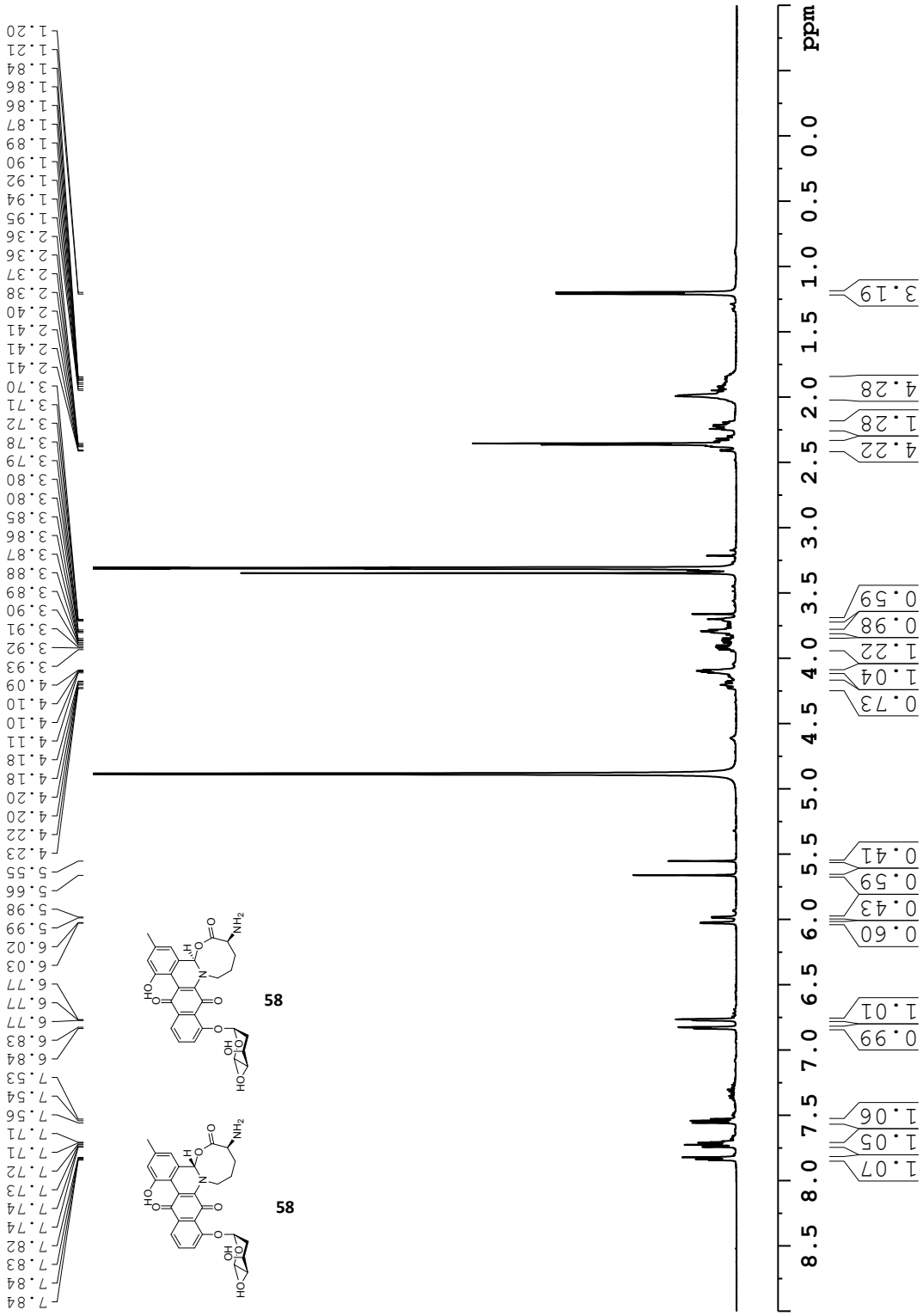

^{1}H-NMR spectrum of **58** (diastereomeric mixture) in MeOD-d_4 (^{1}H: 700 MHz). Note: Compound prone to breakdown over time in NMR tube/solvent.

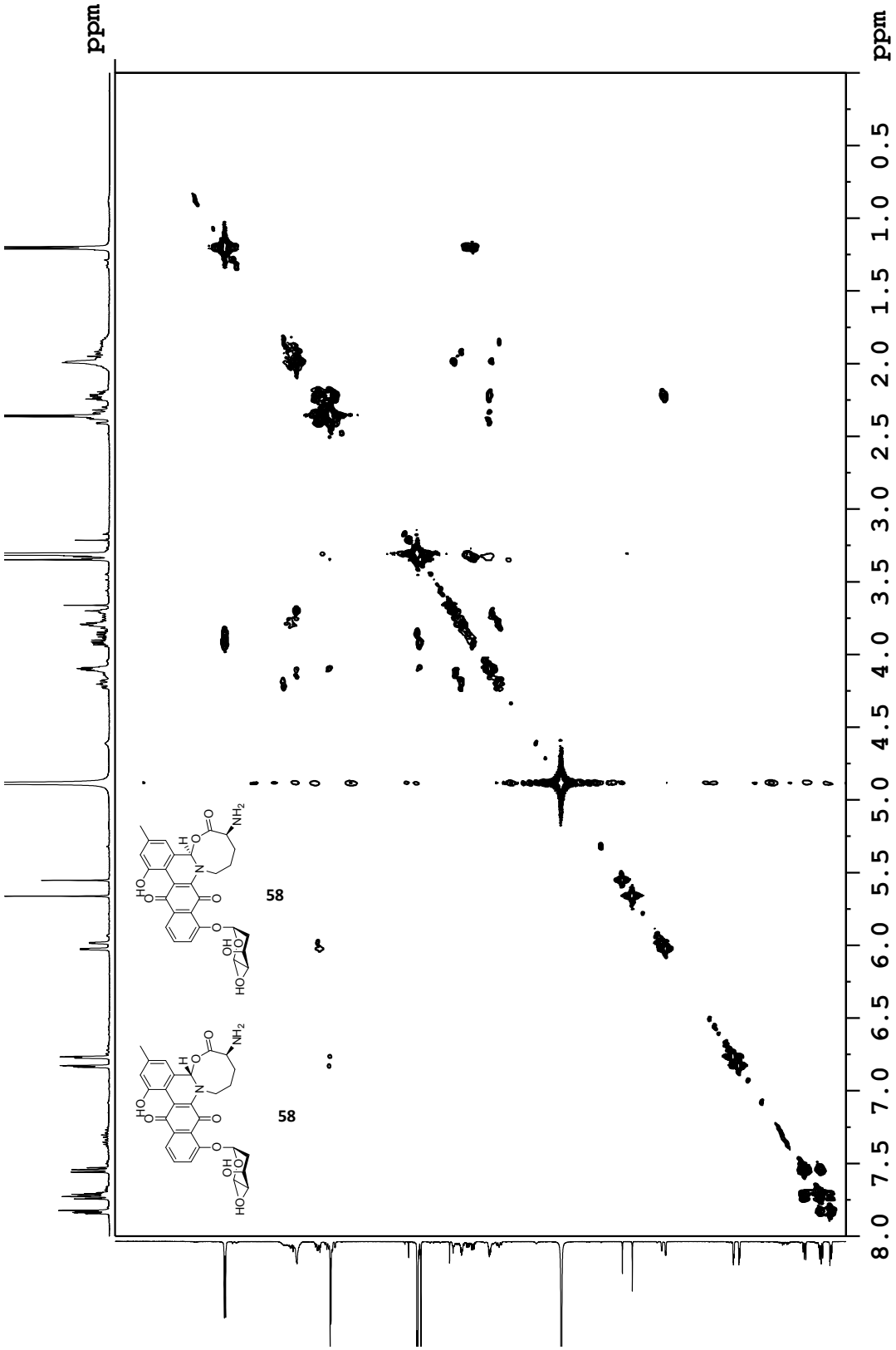

COSY (^{1}H-^{1}H) spectrum of **58** (diastereomeric mixture) in MeOD-d_4 (700 MHz).

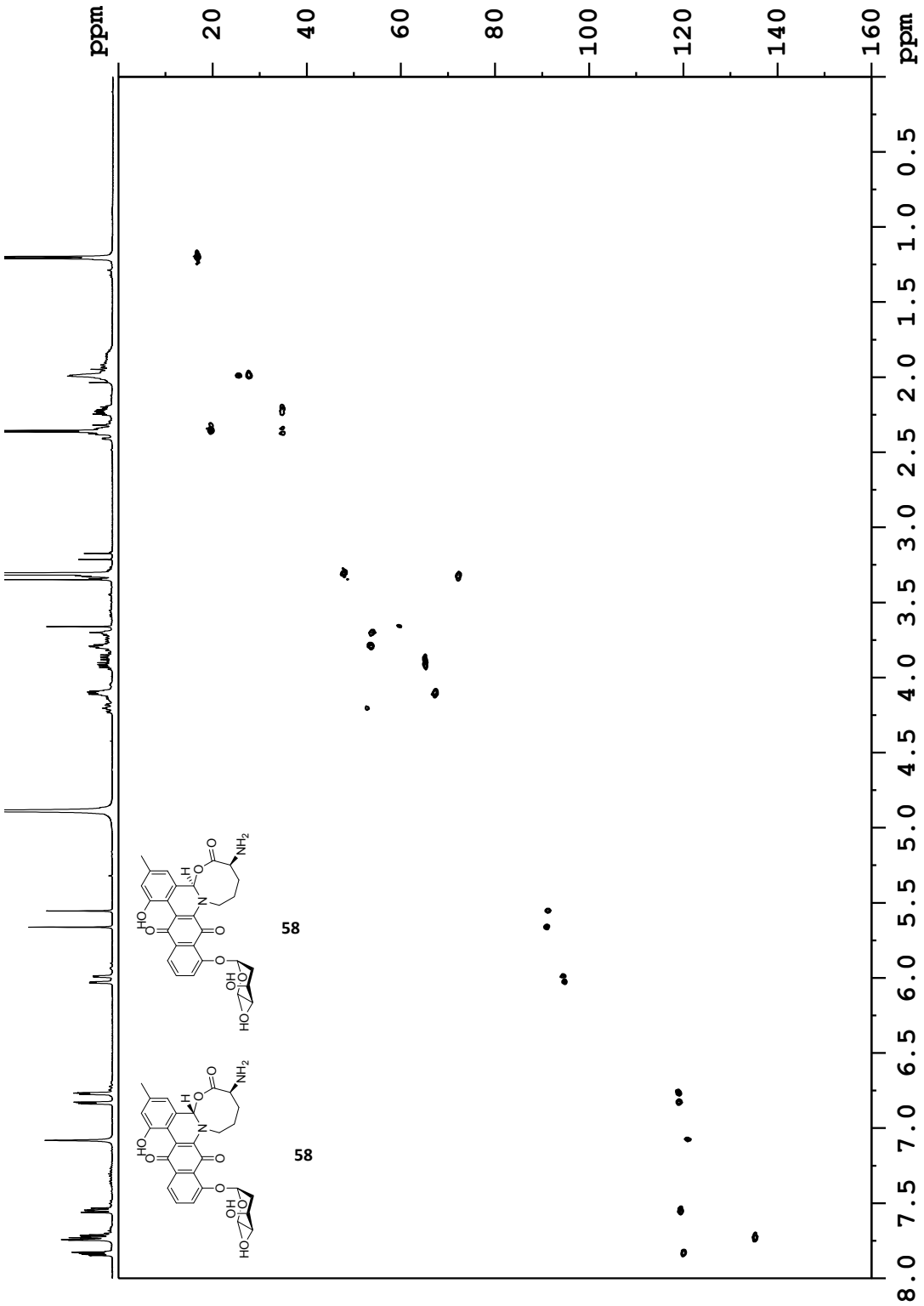

HSQC (^{1}H-^{13}C) spectrum of **58** (diastereomeric mixture) in MeOD-d_4.

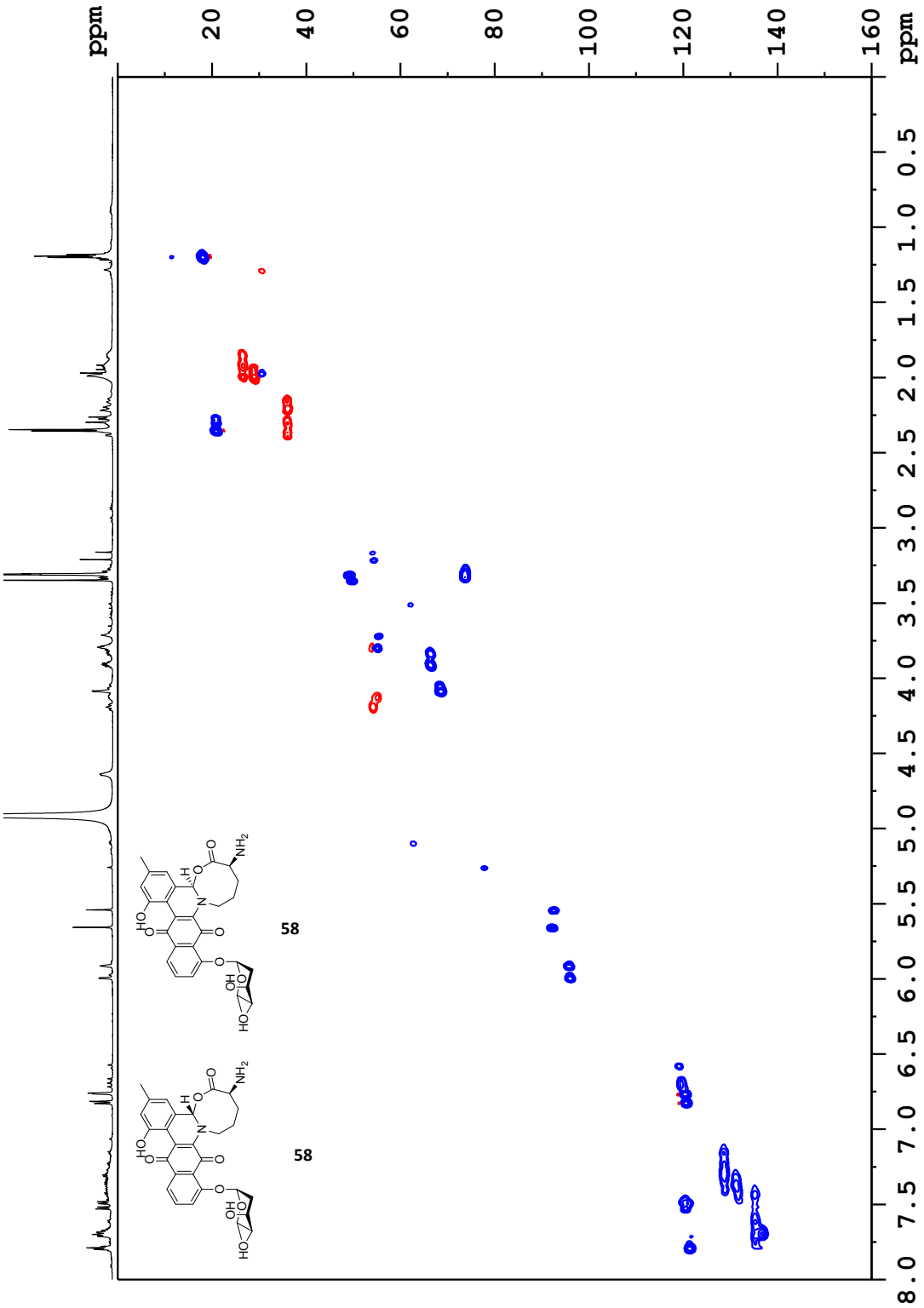

Edited-HSQC (^{1}H-^{13}C) spectrum of **58** (diastereomeric mixture) in MeOD-d_4. Blue represents CH and CH_3 groups, red represents CH_2 groups. Breakdown of **58** overtime in the NMR tube is observed in the aromatic region as a broad set of peaks between 7.1-7.5 ppm.

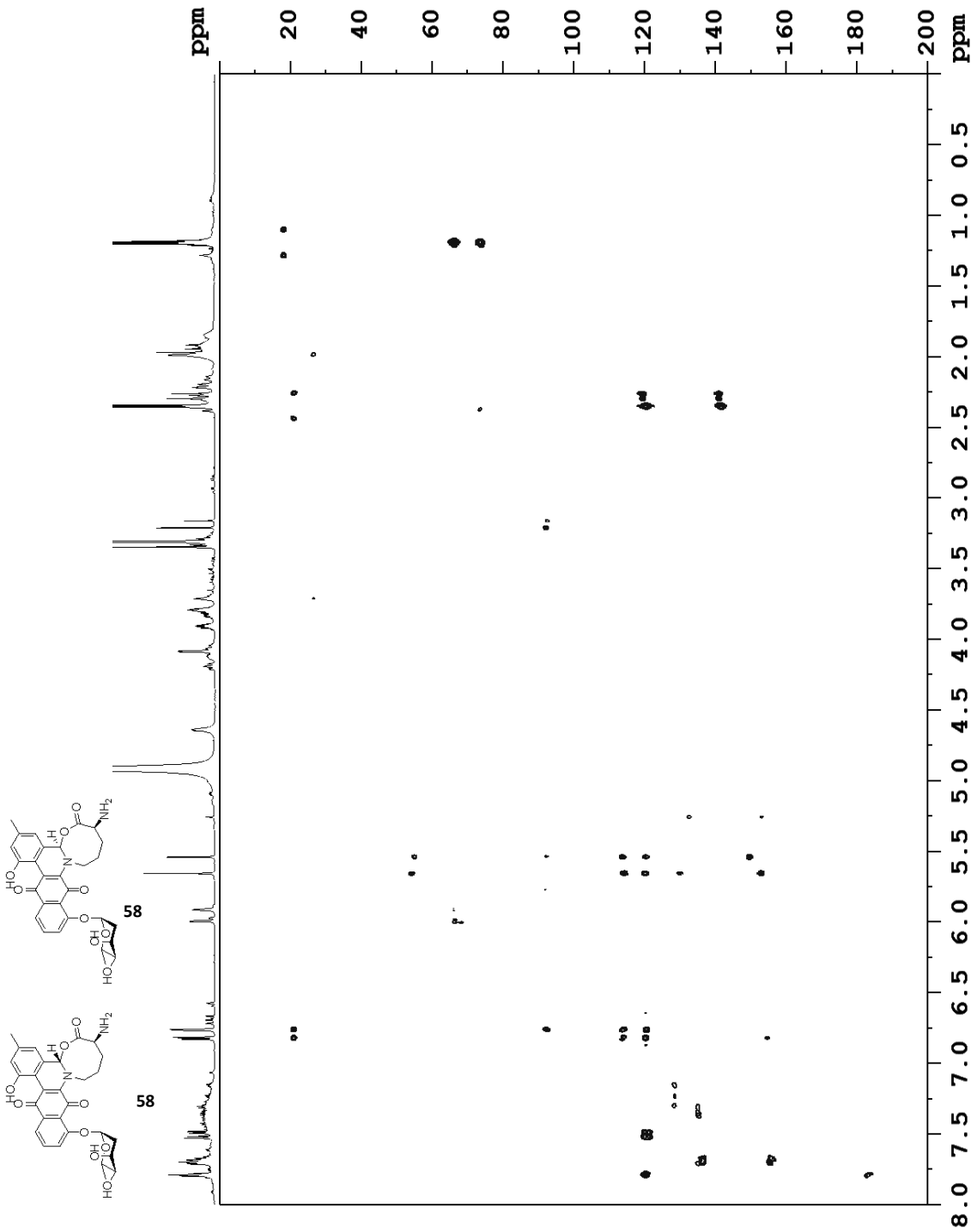

HMBC (^{1}H-^{13}C) spectrum of **58** (diastereomeric mixture) in MeOD-d_4. Breakdown of **58** overtime in the NMR tube is observed in the aromatic region as a broad set of peaks between 7.1-7.5 ppm.

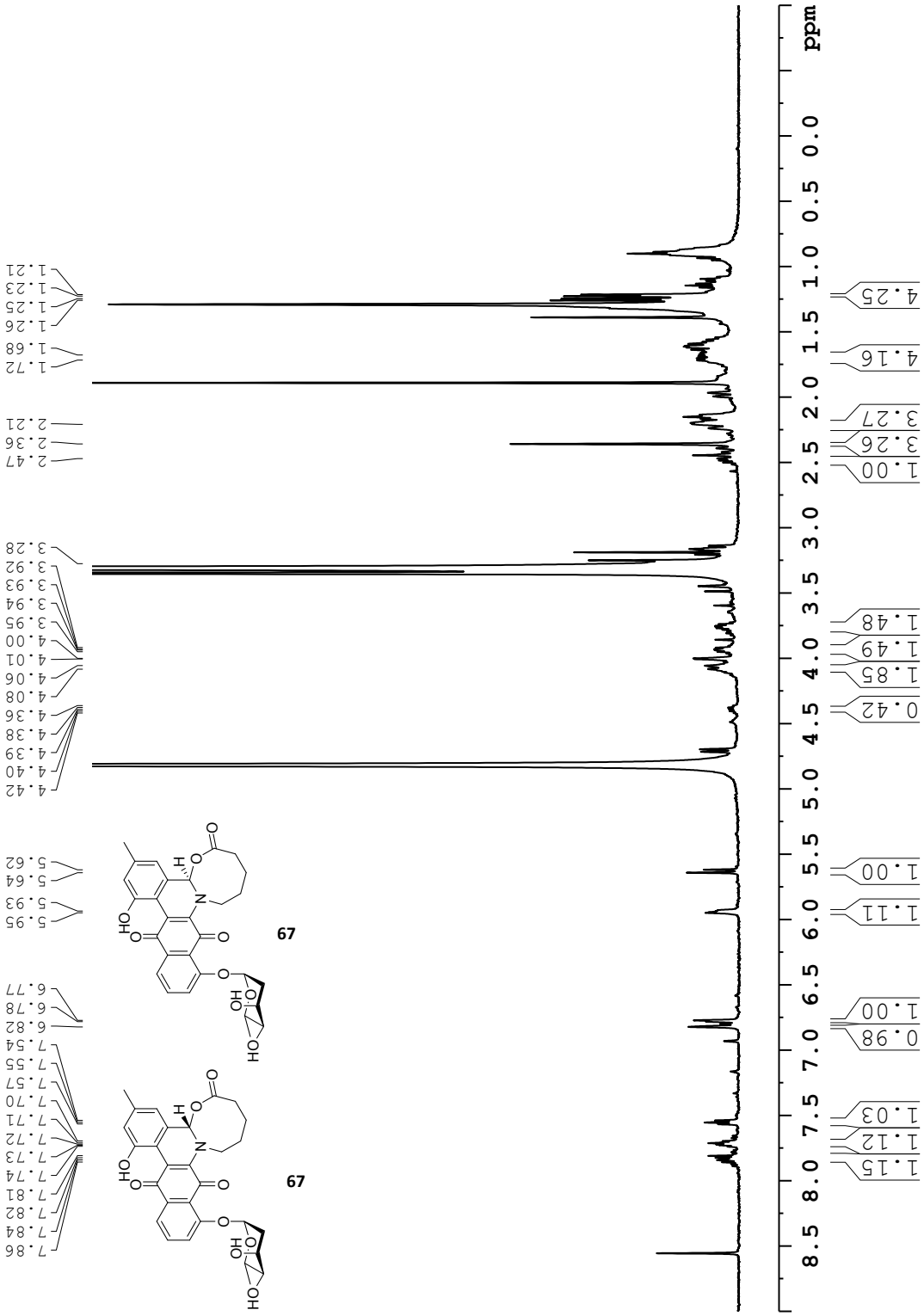

^{1}H-NMR spectrum of **67** (diastereomeric mixture) in MeOD-d_4 (^{1}H: 500 MHz).

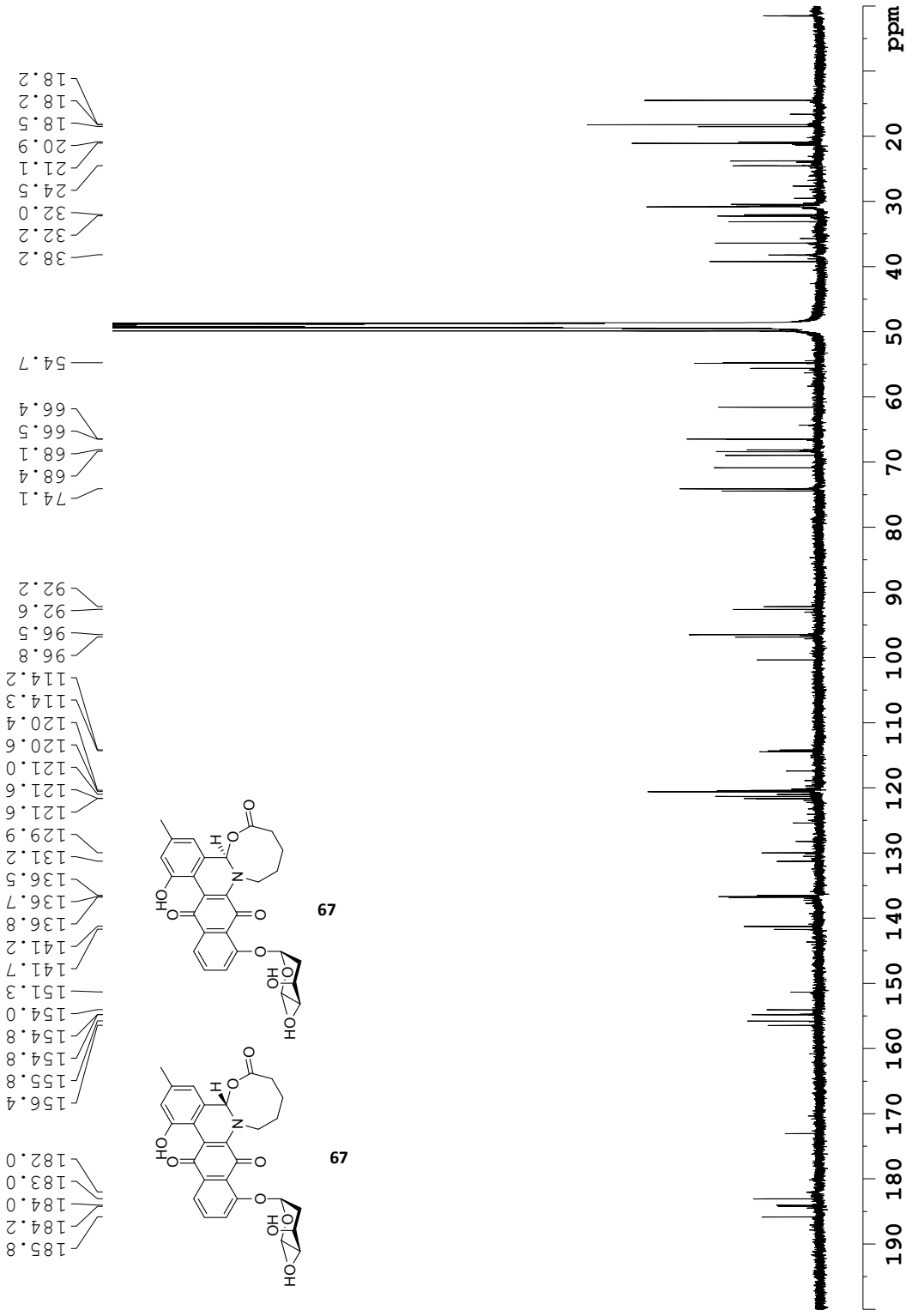

^{13}C-NMR spectrum of **67** (diastereomeric mixture) in MeOD-d_4 (^{13}C: 176 MHz).

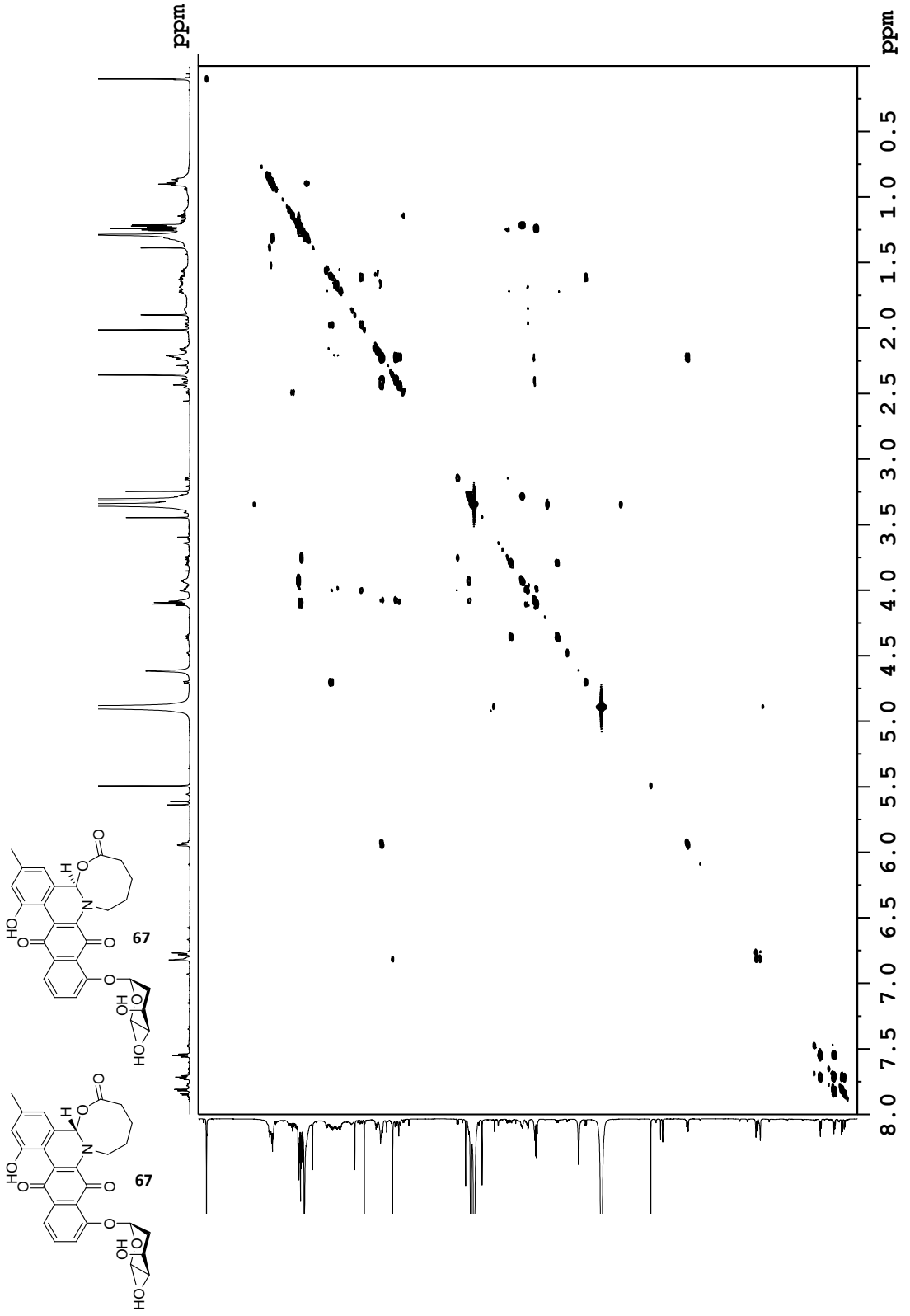

COSY (^{1}H-^{1}H) spectrum of **67** (diastereomeric mixture) in MeOD-d_4 (700 MHz).

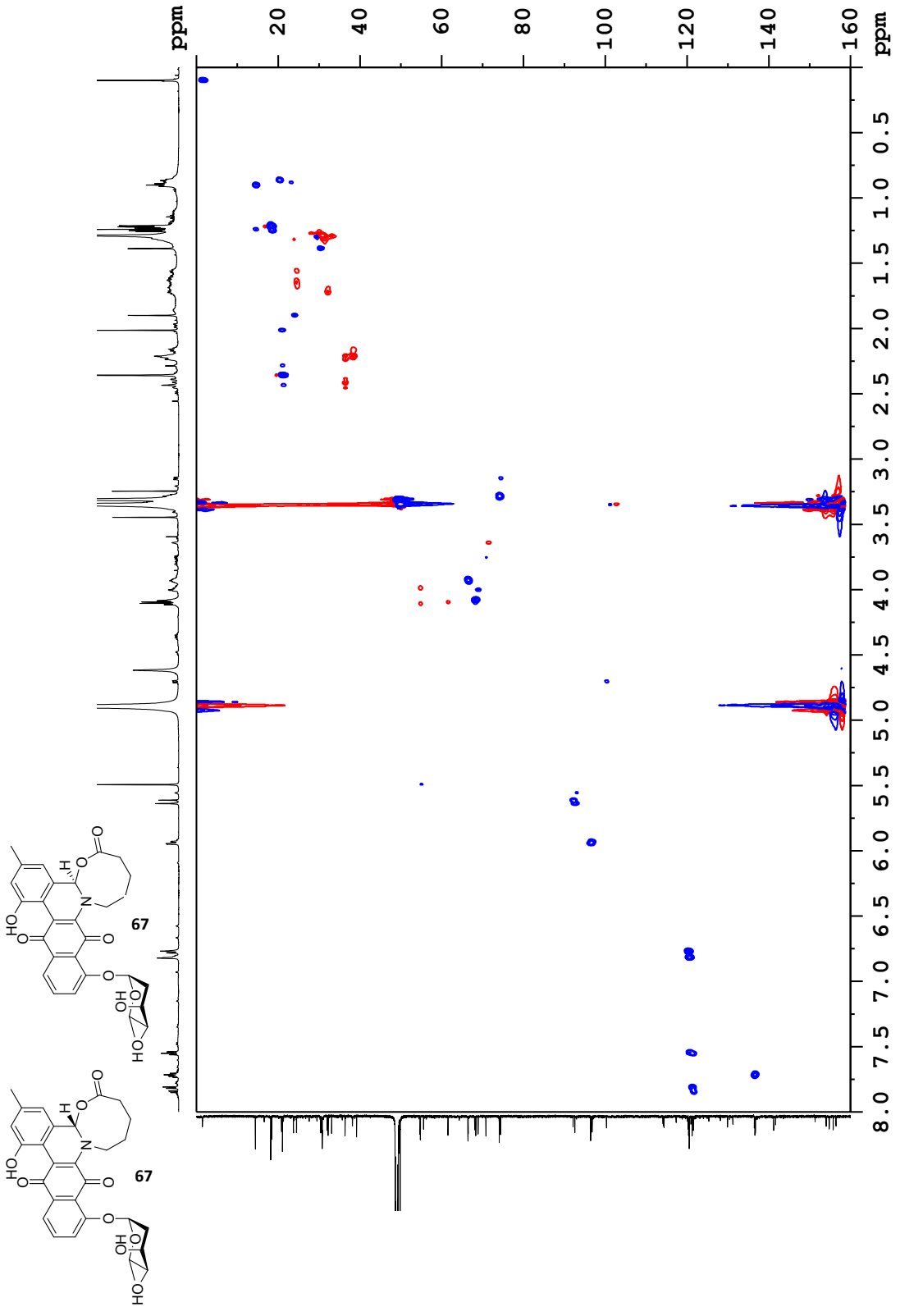

Edited-HSQC (^{1}H-^{13}C) spectrum of **67** (diastereomeric mixture) in MeOD-d_4. Blue represents CH and CH_3 groups, red represents CH_2 groups.

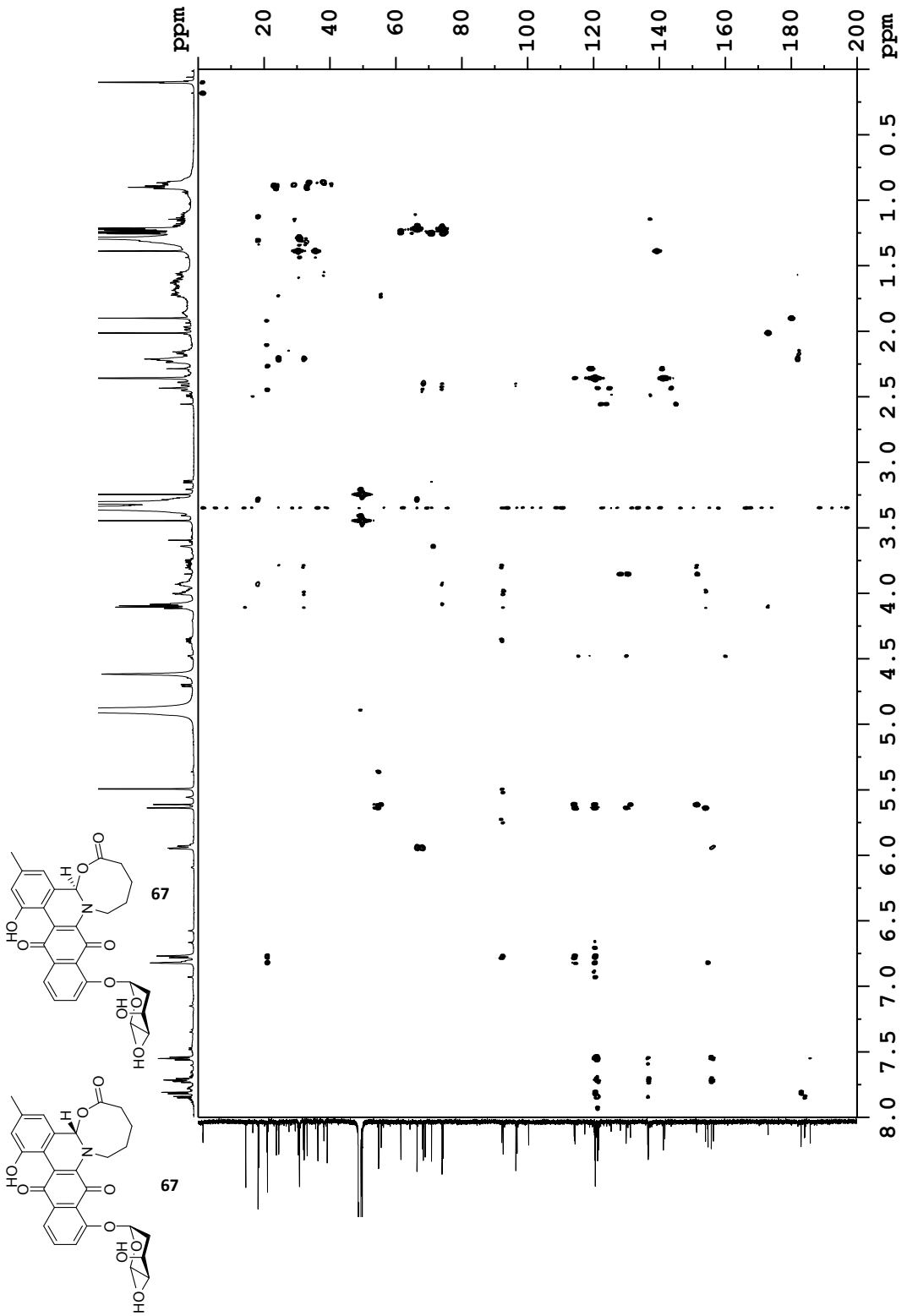

HMBC (^{1}H-^{13}C) spectrum of **67** (diastereomeric mixture) in MeOD-d_4.

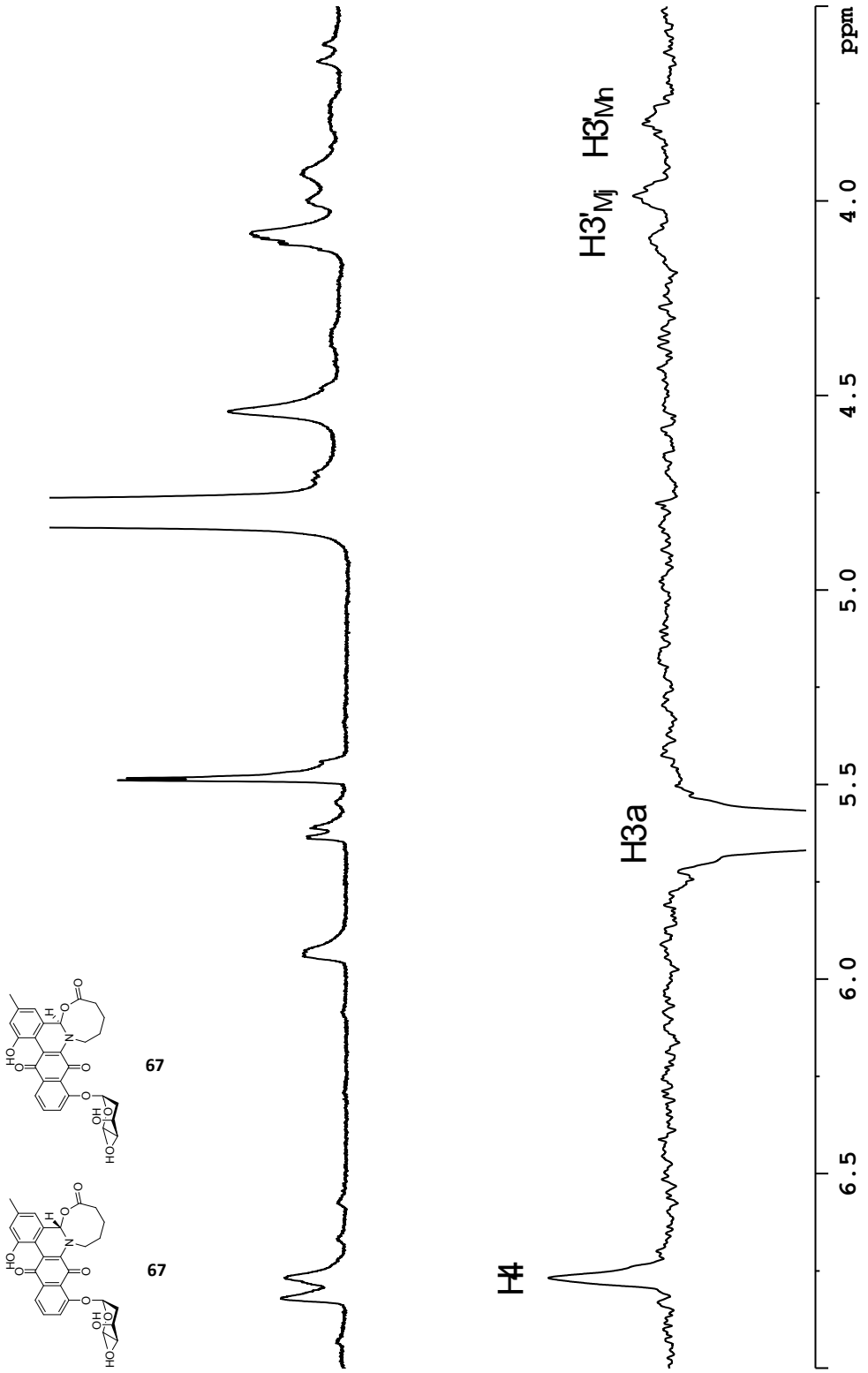

Overlay of ^{1}H-NMR spectrum of **67** (top) with NOESY (500 MHz) showing irradiation of both H3a$_{Mn}$ and H3a$_{Mj}$ simultaneously (bottom), in MeOD-d$_4$.

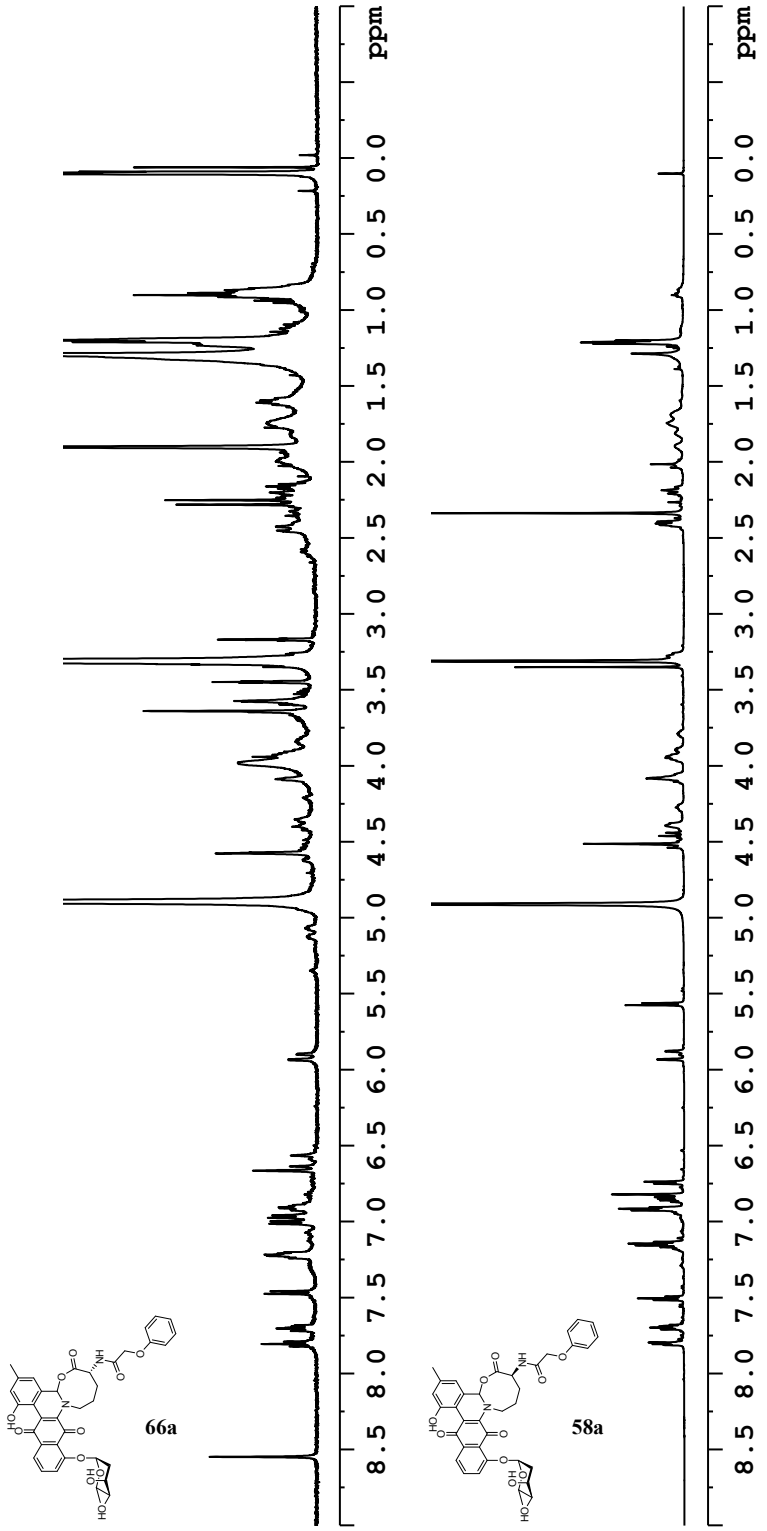

Overlaid ^{1}H-NMR of **66a**, (top) and **58a** (bottom). Compound **66a** was isolated in < 1 mg yield and was unable to be purified further.

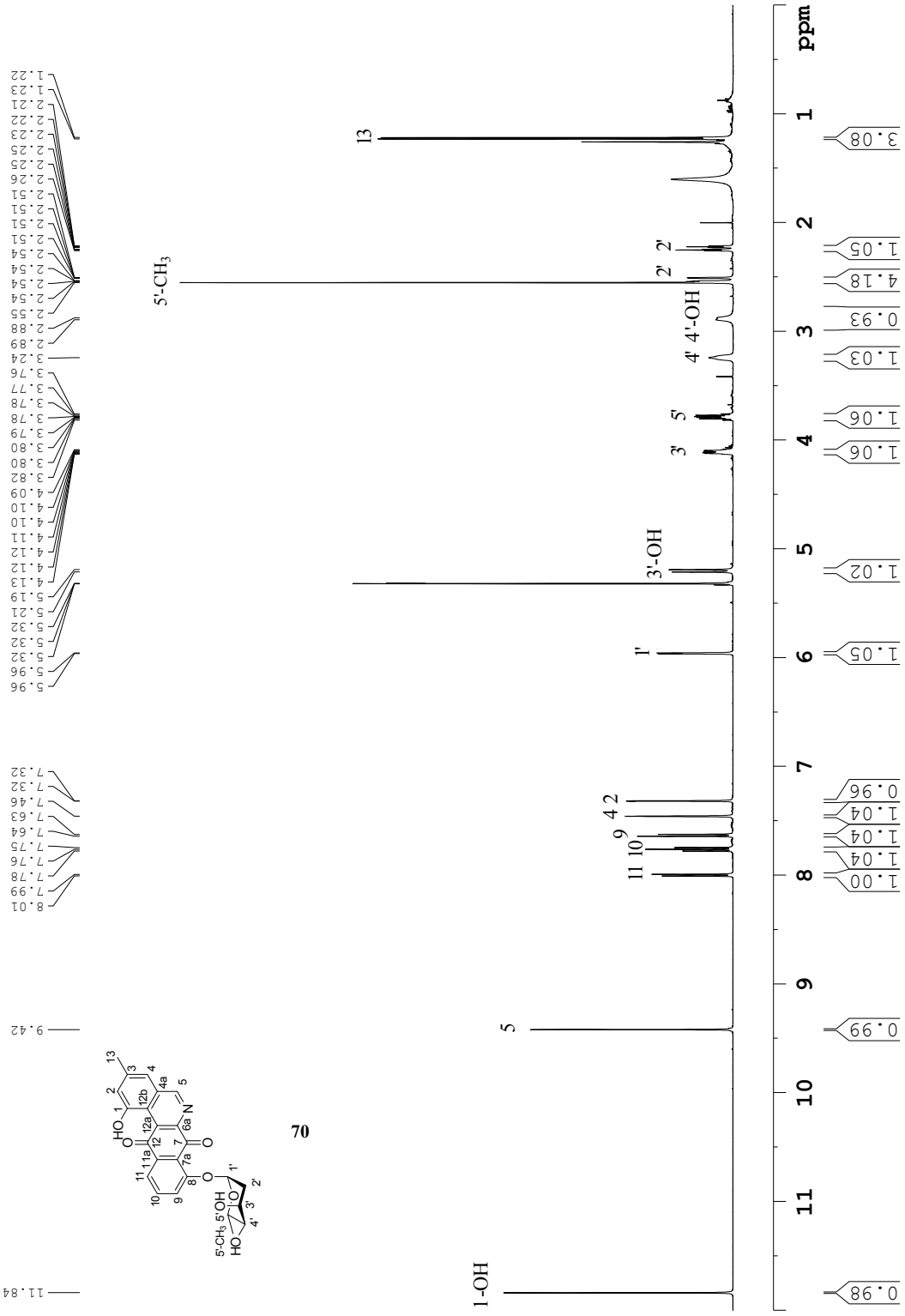

^{1}H-NMR spectrum of **70** in CD_2Cl_2 (^{1}H: 500 MHz).

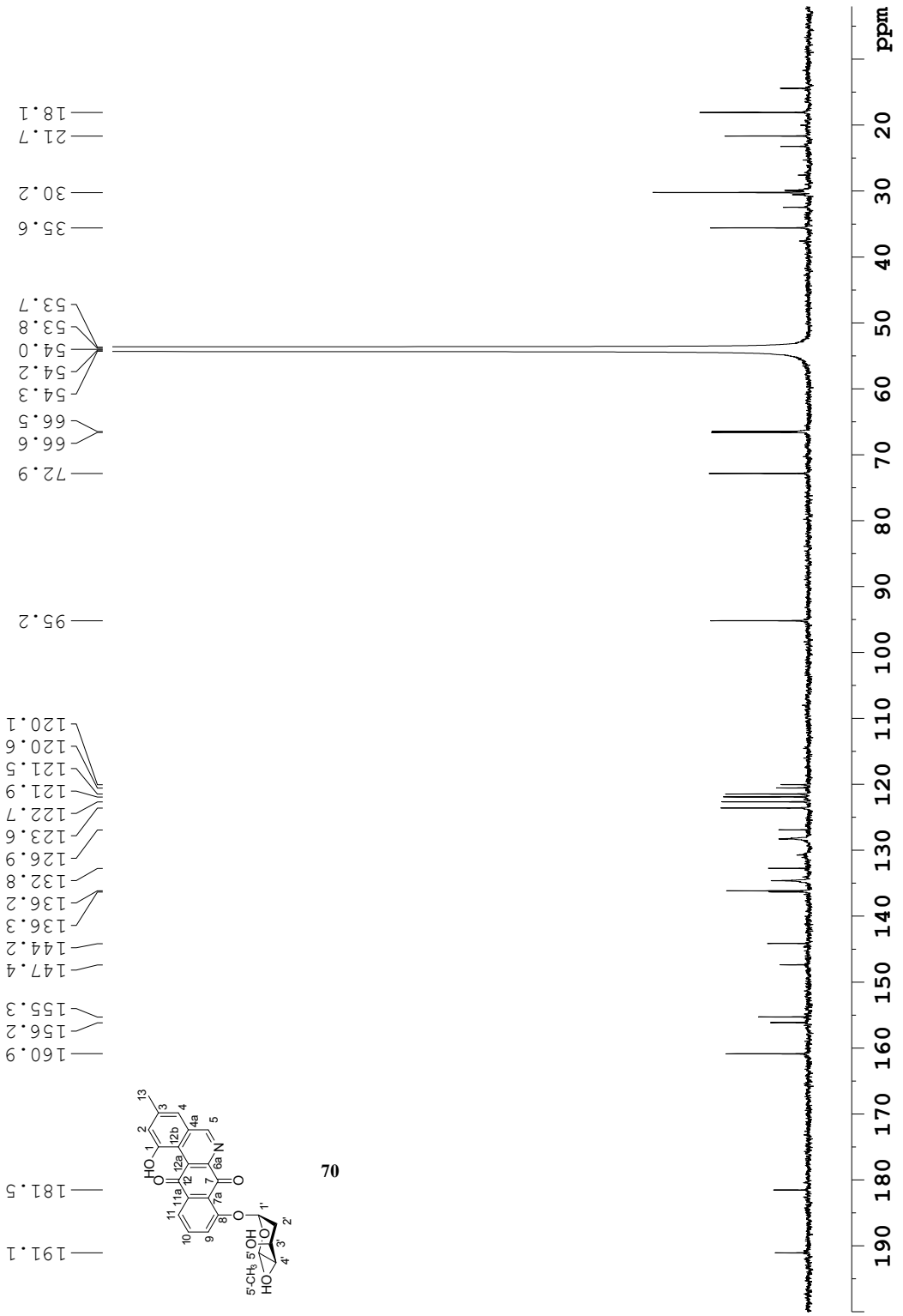

^{13}C-NMR spectrum of **70** in CD_2Cl_2 (^{13}C: 176 MHz).

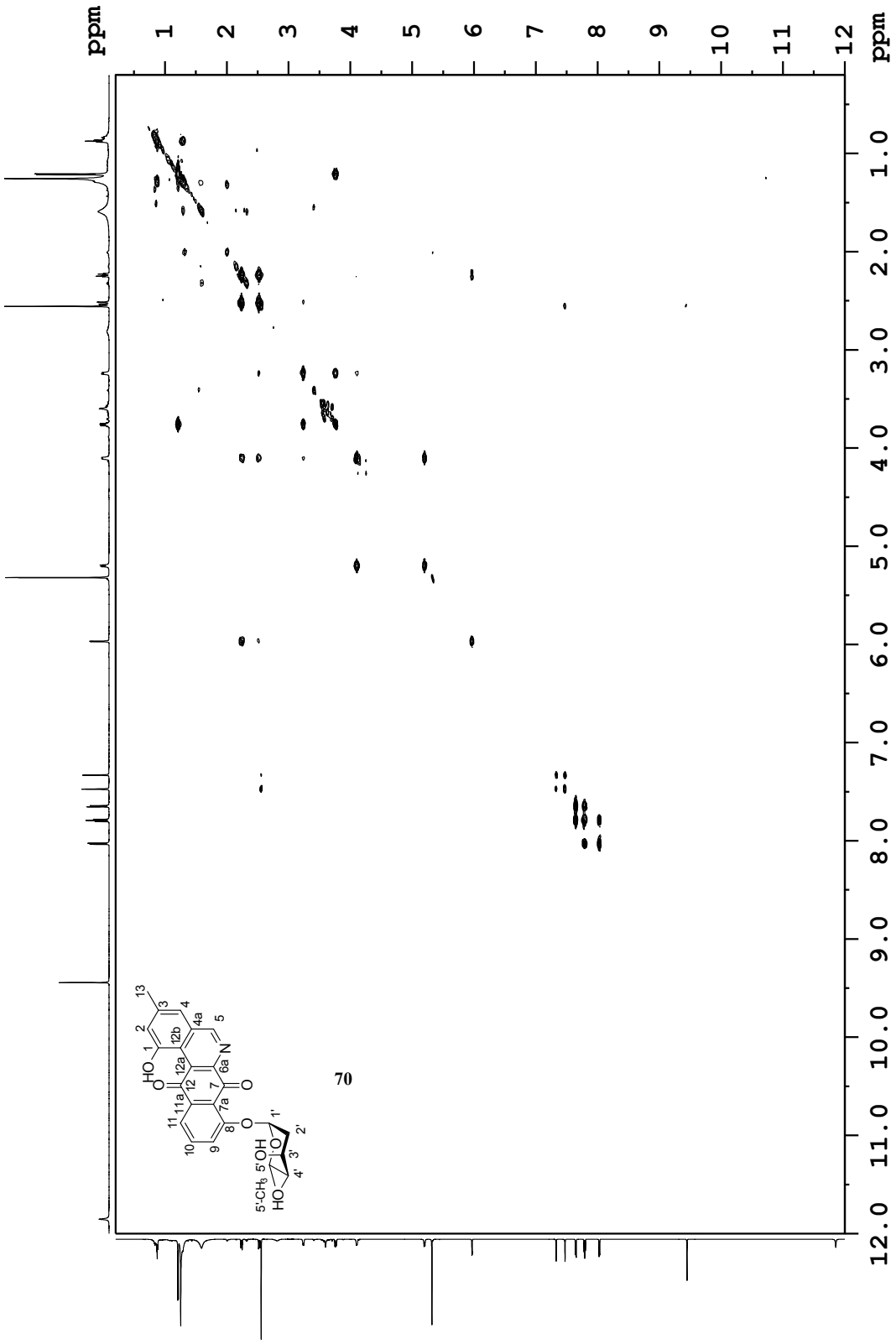

COSY (^{1}H-^{1}H) spectrum of **70** in CD_2Cl_2 (^{1}H: 700 MHz).

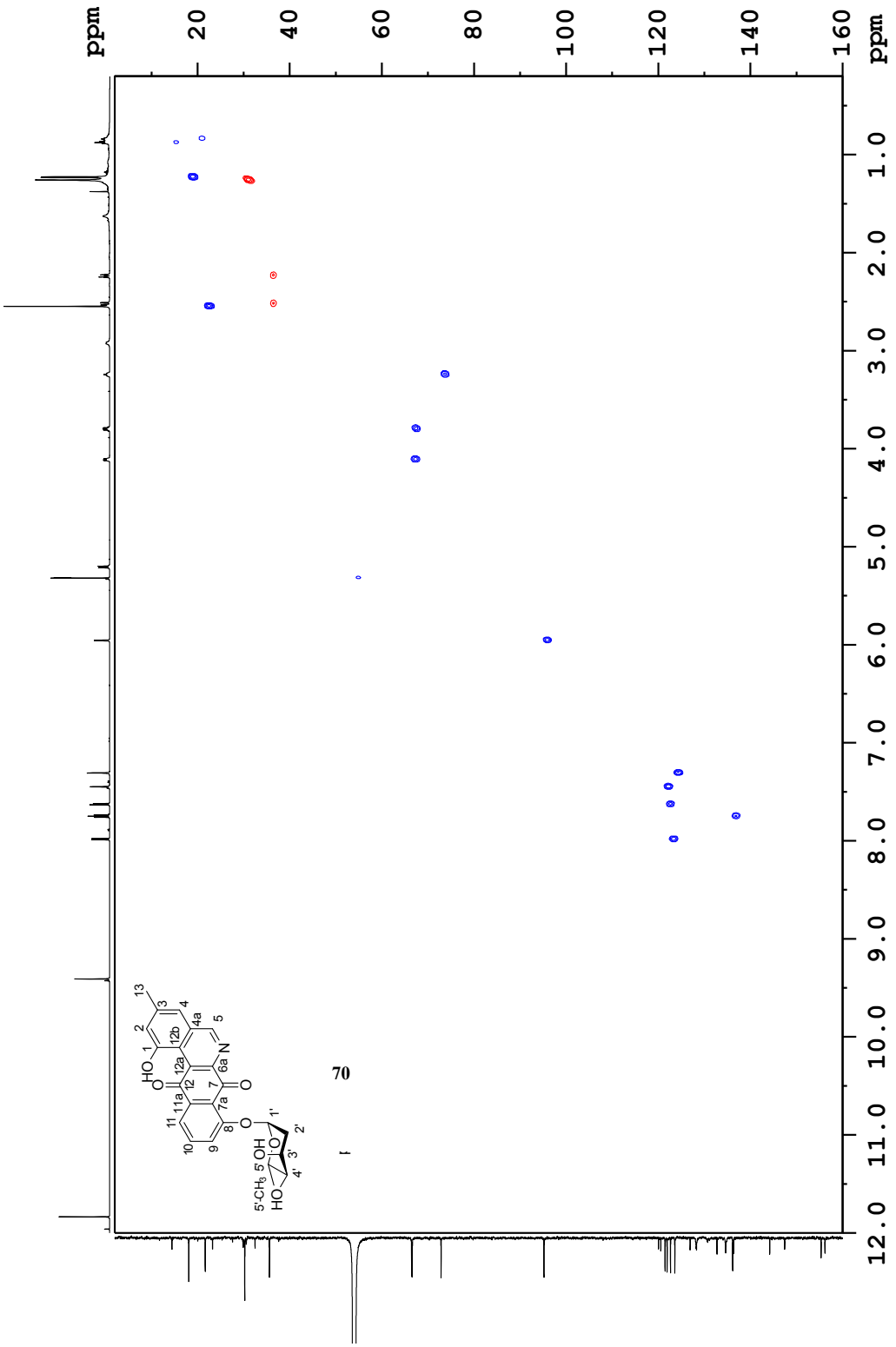

Edited-HSQC (^{1}H-^{13}C) spectrum of **70** in CD_2Cl_2 (^{1}H: 700 MHz; ^{13}C: 176 MHz). Blue represents CH and CH_3 groups, red represents CH_2 groups.

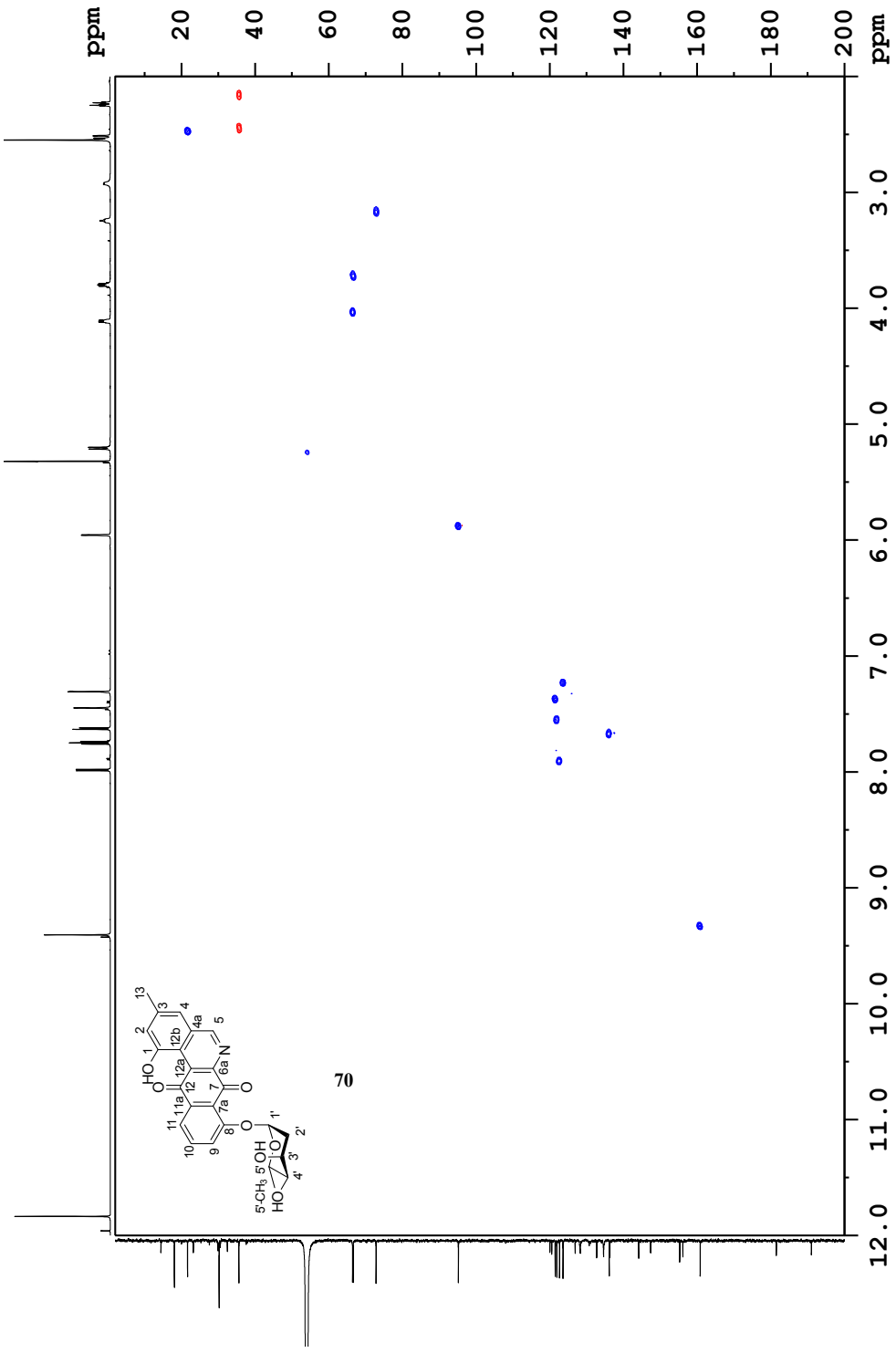

Edited-HSQC (^{1}H-^{13}C) spectrum of **70** in CD_2Cl_2 (^{1}H: 700 MHz; ^{13}C: 176 MHz) with expanded ^{13}C sweep-width to include C5. Blue represents CH and CH_3 groups, red represents CH_2 groups.

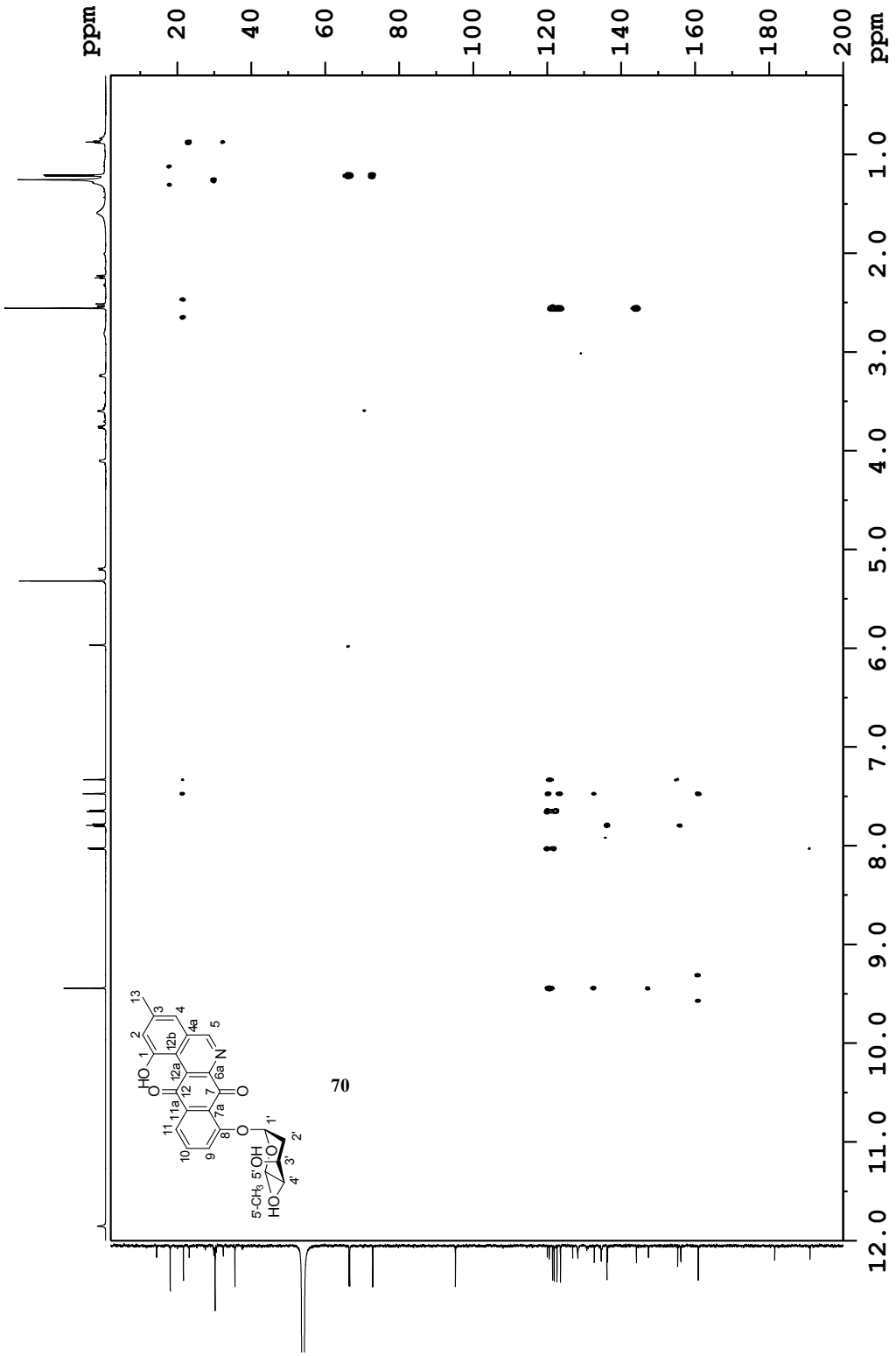

HMBC (^{1}H-^{13}C) spectrum of **70** in CD_2Cl_2 (^{1}H: 700 MHz; ^{13}C: 176 MHz).

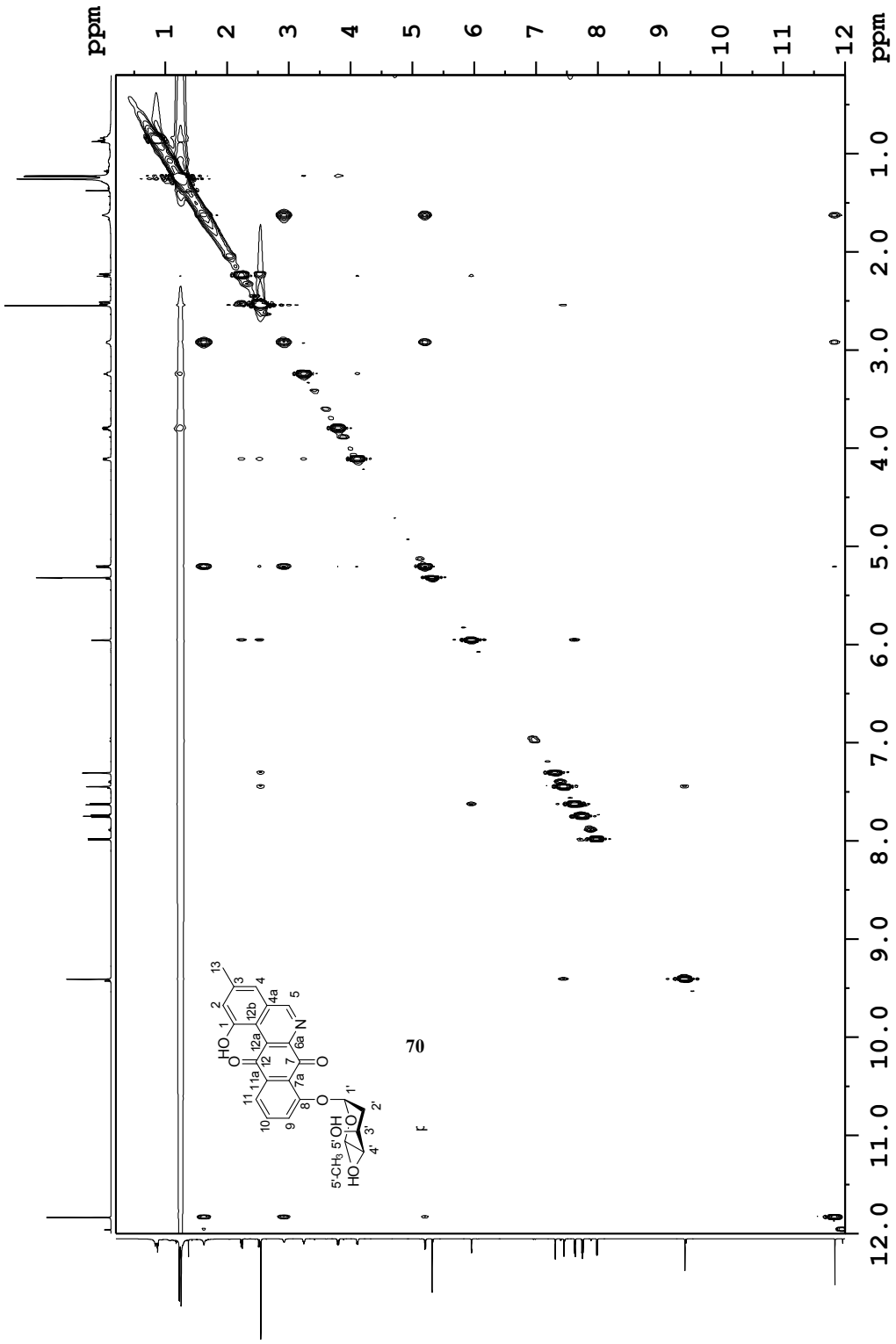

2D-NOESY (^{1}H-^{1}H) spectrum of **70** in CD_2Cl_2 (^{1}H: 700 MHz).

APPENDIX D: NATIONAL CANCER INSTITUTE (NCI) 60 DTP HUMAN TUMOR CELL LINE SCREENS CYTOTOXIC ACTIVITY AND COMPARE ANALYSIS

One dose NCI-60 tumor cell line screen of jadomycin Oct phenoxyacetylamide (**58a**) 211

One dose NCI-60 tumor cell line screen of jadomycin Oct benzoylamide (**58c**) 212

One dose NCI-60 tumor cell line screen of jadomycin Oct nonoylamide (**58d**) 213

One dose NCI-60 tumor cell line screen of jadomycin Oct BODIPY amide (**58f**) 214

One dose NCI-60 tumor cell line screen of L-digitoxosyl-phenanthroviridin (**70**) 215

Graphical representation of 5-dose NCI-60 tumor cell line screen assay, of **70**. 216

Tabulated 5-dose NCI-60 tumor cell line screen assay data in the presence and absence of **70**..... 217

5-dose NCI-60 tumor cell line screen assay $Log_{10}GI_{50}$, $Log_{10}TGI$ and $Log_{10}LC_{50}$ values for **70.**..... 218

Graphical overlay of all dose response curves for **70**. 219

GI_{50} (A), TGI (B), and LC_{50} (C) values (μM) for **70** grouped by cancer cell type..... 219

Standard COMPARE data comparing GI_{50} values of **70** versus GI_{50} values of the NCI Standard Agent Database 220

Standard COMPARE data comparing TGI values of **70** versus TGI values of the NCI Standard Agent Database 221

Standard COMPARE data comparing LC_{50} values of **70** versus LC_{50} values of the NCI Standard Agent Database. 222

Standard COMPARE data comparing GI_{50} values of **70** versus GI_{50} values of the NCI synthetic compounds database. 223

Standard COMPARE data comparing TGI values of **70** versus TGI values of the NCI synthetic compounds database. 224

Standard COMPARE data comparing LC_{50} values of **70** versus LC_{50} values of the NCI synthetic compounds database. 225

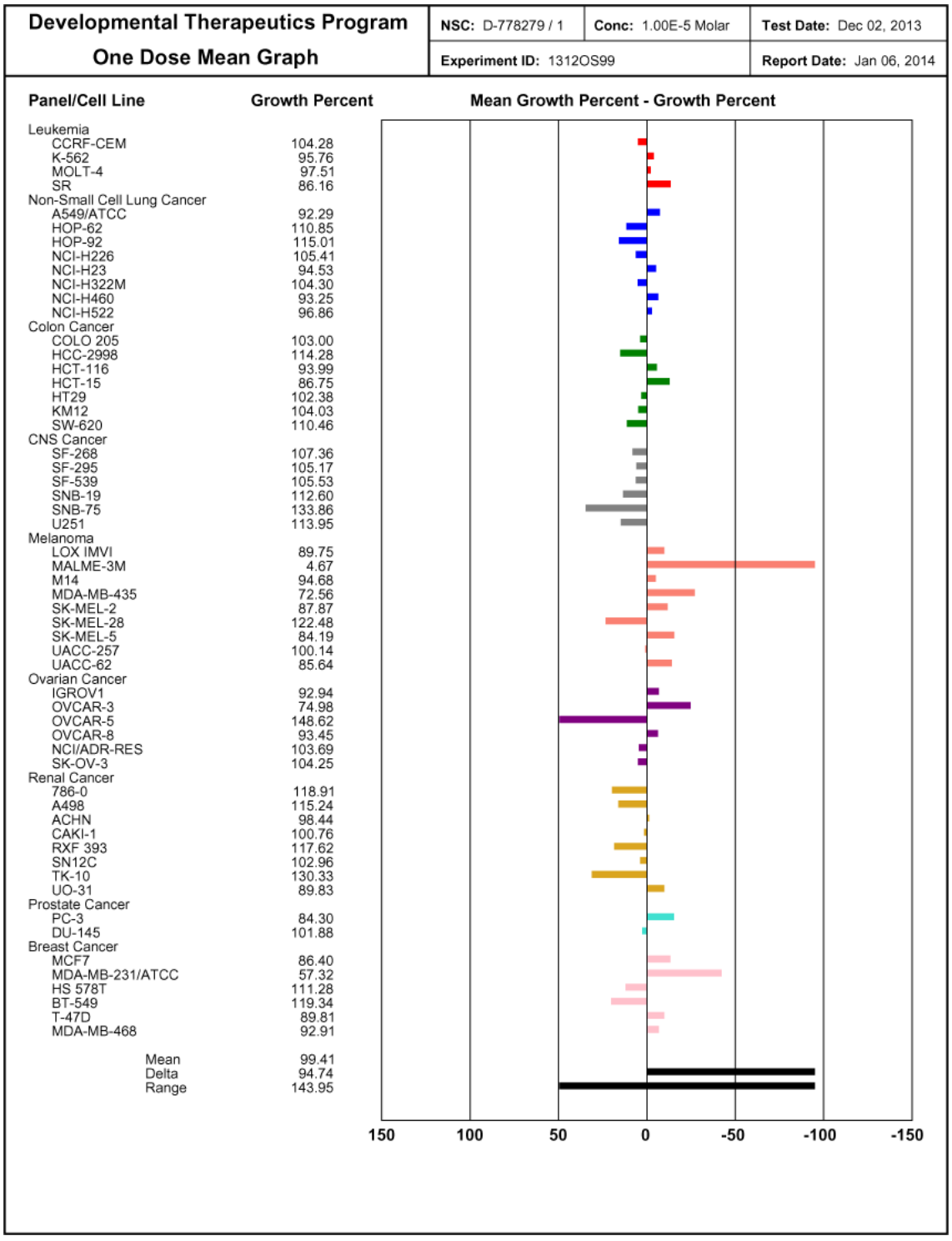

One dose NCI-60 tumor cell line screen of jadomycin Oct phenoxyacetylamide (**58a**) (1×10^{-5} M).

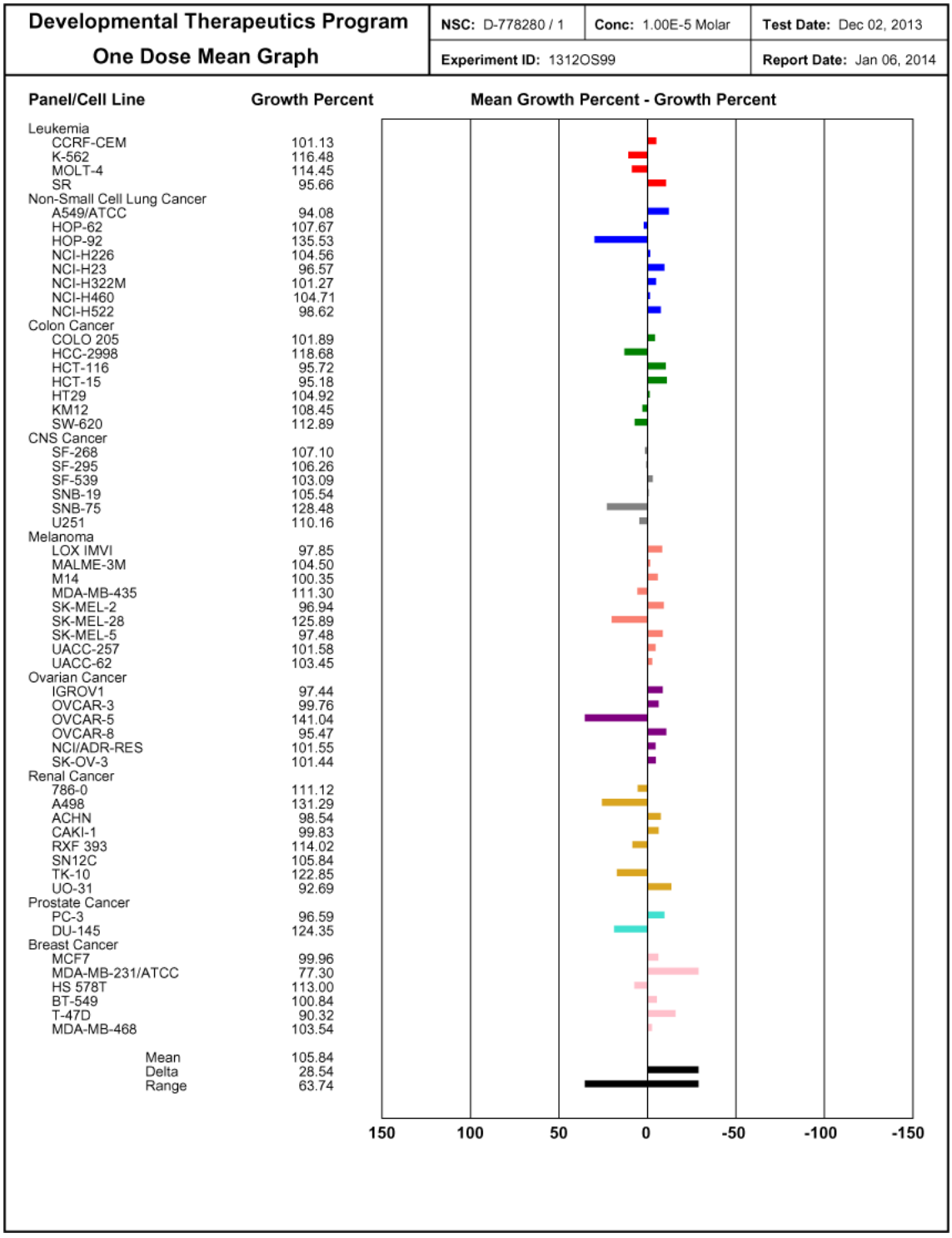

One dose NCI-60 tumor cell line screen of jadomycin Oct benzoylamide (**58c**) (1×10^{-5} M).

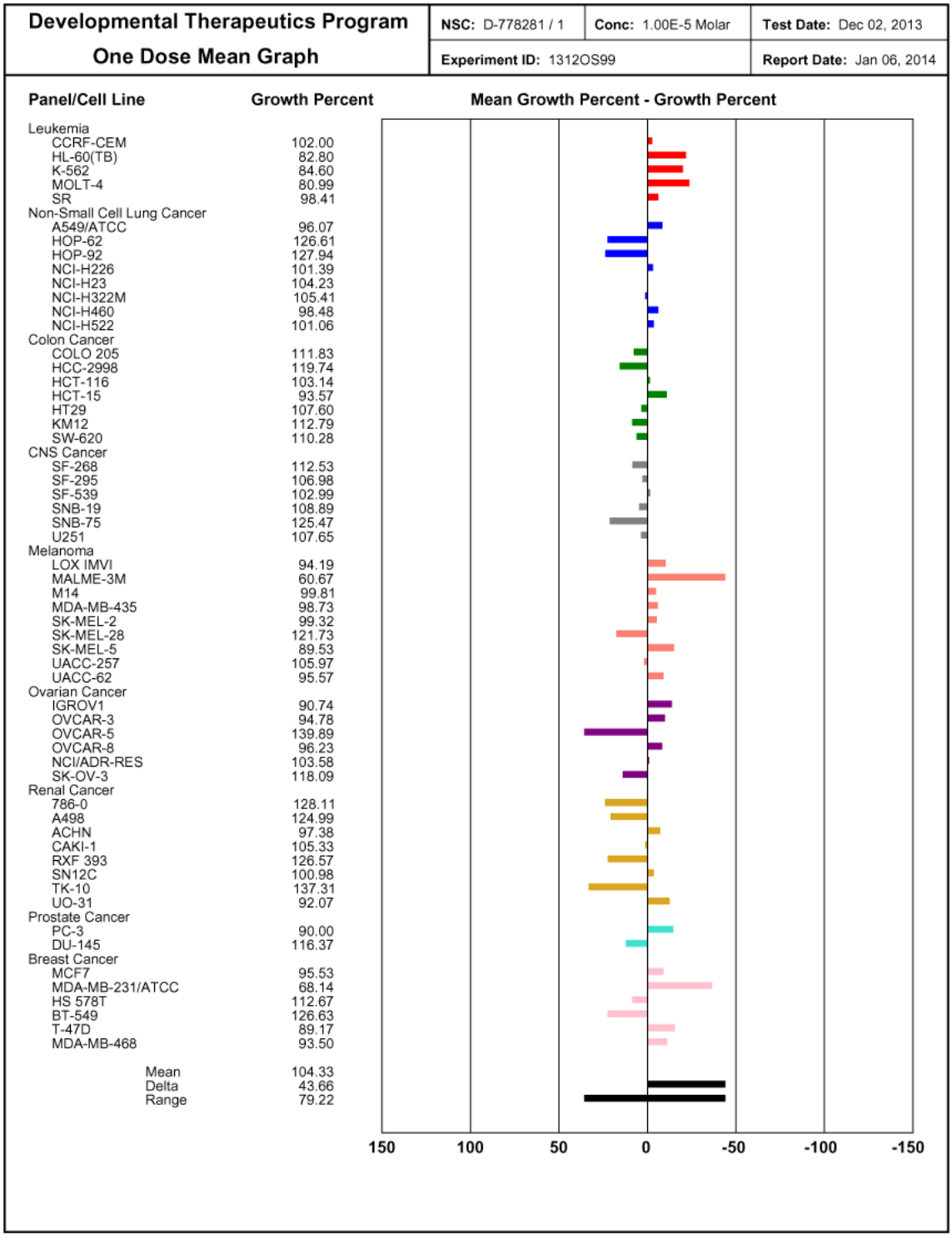

One dose NCI-60 tumor cell line screen of jadomycin Oct nonoylamide (**58d**) (1×10^{-5} M).

Developmental Therapeutics Program

One Dose Mean Graph

NSC: D-778282 / 1	Conc: 1.00E-5 Molar	Test Date: Dec 02, 2013
Experiment ID: 1312OS99		Report Date: Jan 06, 2014

Panel/Cell Line	Growth Percent
Leukemia	
CCRF-CEM	110.34
HL-60(TB)	136.54
K-562	92.79
MOLT-4	118.45
SR	95.65
Non-Small Cell Lung Cancer	
A549/ATCC	100.85
HOP-62	120.61
HOP-92	107.44
NCI-H226	99.73
NCI-H23	103.13
NCI-H322M	118.48
NCI-H460	97.49
NCI-H522	95.52
Colon Cancer	
COLO 205	107.80
HCC-2998	118.38
HCT-116	99.05
HCT-15	103.78
HT29	96.80
KM12	119.92
SW-620	110.30
CNS Cancer	
SF-268	117.70
SF-295	108.03
SF-539	105.75
SNB-19	107.32
SNB-75	132.76
U251	103.20
Melanoma	
LOX IMVI	96.48
MALME-3M	146.70
M14	104.88
MDA-MB-435	111.79
SK-MEL-2	104.41
SK-MEL-28	123.10
SK-MEL-5	98.19
UACC-257	108.10
UACC-62	103.97
Ovarian Cancer	
IGROV1	114.92
OVCAR-3	102.06
OVCAR-5	125.36
OVCAR-8	104.93
NCI/ADR-RES	103.18
SK-OV-3	116.59
Renal Cancer	
786-0	123.62
A498	118.11
ACHN	98.05
CAKI-1	105.25
RXF 393	120.93
SN12C	108.95
TK-10	123.30
UO-31	100.97
Prostate Cancer	
PC-3	97.81
DU-145	121.27
Breast Cancer	
MCF7	107.36
MDA-MB-231/ATCC	81.88
HS 578T	119.29
BT-549	123.55
T-47D	87.81
MDA-MB-468	105.78
Mean	109.41
Delta	27.53
Range	64.82

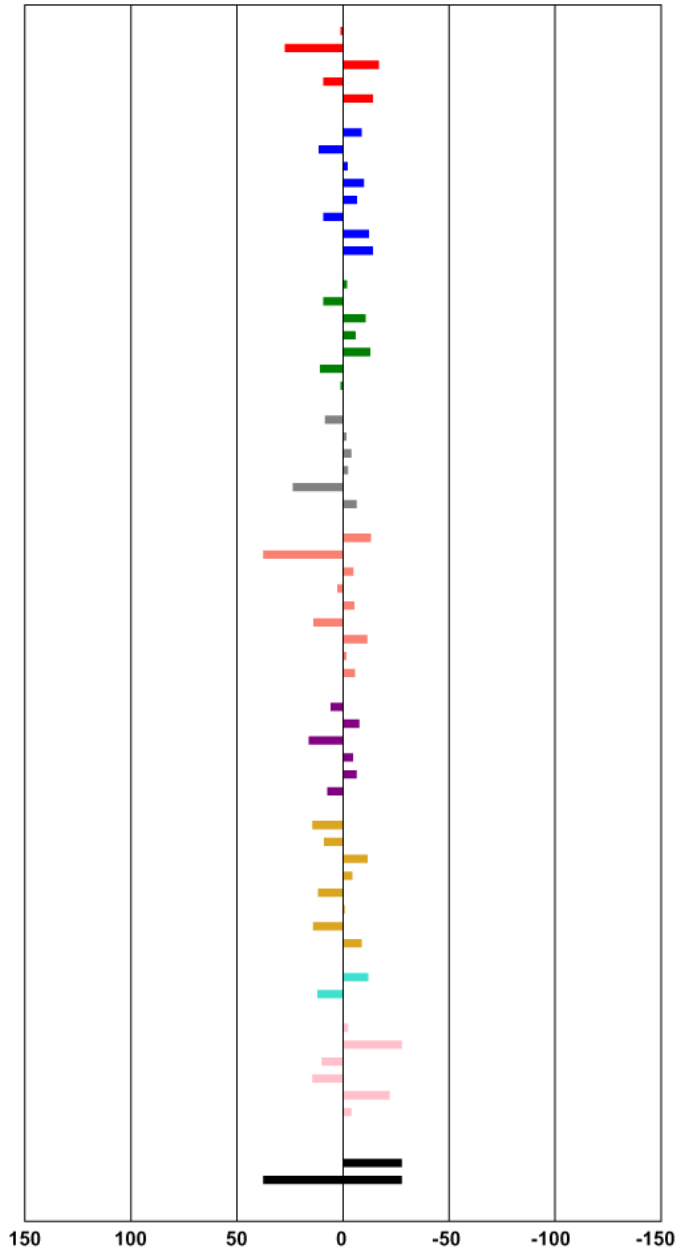

One dose NCI-60 tumor cell line screen of jadomycin Oct BODIPY amide (**58f**) (1×10^{-5} M).

Developmental Therapeutics Program

One Dose Mean Graph

NSC: D-778283 / 1	Conc: 1.00E-5 Molar	Test Date: Dec 02, 2013
Experiment ID: 1312OS99		Report Date: Jan 06, 2014

Panel/Cell Line	Growth Percent
Leukemia	
CCRF-CEM	1.46
HL-60(TB)	-19.48
K-562	-4.11
MOLT-4	-43.44
SR	-0.61
Non-Small Cell Lung Cancer	
A549/ATCC	-39.64
HOP-62	37.75
HOP-92	72.04
NCI-H226	69.76
NCI-H23	-35.78
NCI-H322M	-83.78
NCI-H460	-55.17
NCI-H522	-62.06
Colon Cancer	
COLO 205	-82.82
HCC-2998	-29.97
HCT-116	-26.02
HCT-15	-34.76
HT29	-26.30
KM12	13.31
SW-620	-52.16
CNS Cancer	
SF-268	9.29
SF-295	67.07
SF-539	-67.44
SNB-19	-8.63
SNB-75	-46.07
U251	-73.90
Melanoma	
LOX IMVI	-60.26
MALME-3M	-85.99
M14	-88.00
MDA-MB-435	-86.90
SK-MEL-2	8.75
SK-MEL-28	-41.46
SK-MEL-5	-93.30
UACC-257	-76.74
UACC-62	-66.45
Ovarian Cancer	
IGROV1	-34.68
OVCAR-3	-3.18
OVCAR-5	126.86
OVCAR-8	-2.09
NCI/ADR-RES	7.60
SK-OV-3	111.53
Renal Cancer	
786-0	66.39
A498	82.76
ACHN	21.07
CAKI-1	96.42
RXF 393	12.35
SN12C	-79.50
TK-10	112.27
UO-31	31.12
Prostate Cancer	
PC-3	0.64
DU-145	-91.35
Breast Cancer	
MCF7	-55.95
MDA-MB-231/ATCC	-27.55
HS 578T	-10.42
BT-549	25.66
T-47D	19.99
MDA-MB-468	-28.21
Mean	-12.81
Delta	80.49
Range	220.16

Mean Growth Percent - Growth Percent

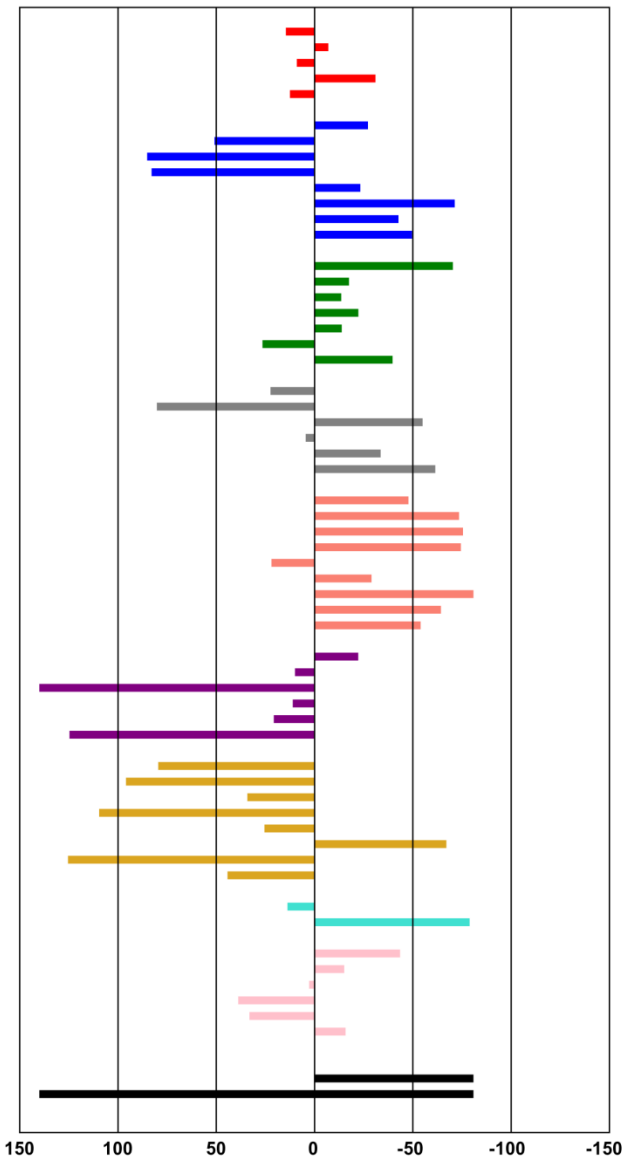

One dose NCI-60 tumor cell line screen of L-digitoxosyl-phenanthroviridin (**70**) (1 x 10^{-5} M).

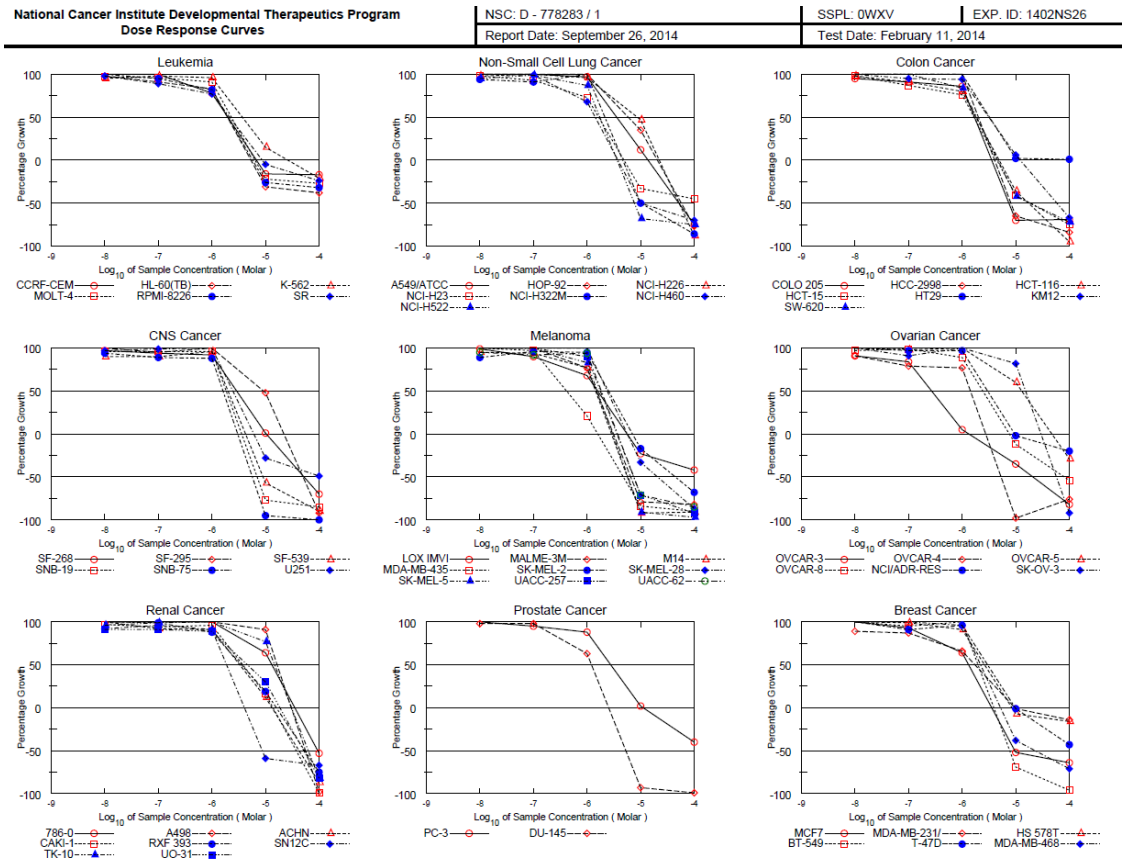

Graphical representation of 5-dose NCI-60 tumor cell line screen assay of **70**.

National Cancer Institute Developmental Therapeutics Program
In-Vitro Testing Results

NSC : D - 778283 / 1	Experiment ID : 1402NS26	Test Type : 08	Units : Molar
Report Date : September 26, 2014	Test Date : February 11, 2014	QNS :	MC :
COMI : L-digitoxosyl-phenanthroviridin (135199)	Stain Reagent : SRB Dual-Pass Related	SSPL : 0WXV	

			Log10 Concentration												
	Time		Mean Optical Densities					Percent Growth							
Panel/Cell Line	Zero	Ctrl	-8.0	-7.0	-6.0	-5.0	-4.0	-8.0	-7.0	-6.0	-5.0	-4.0	GI50	TGI	LC50
Leukemia															
CCRF-CEM	0.467	2.604	2.777	2.676	2.128	0.392	0.388	108	103	78	-16	-17	1.97E-6	6.74E-6	> 1.00E-4
HL-60(TB)	0.702	2.437	2.408	2.274	2.145	0.487	0.438	98	91	83	-31	-38	1.96E-6	5.37E-6	> 1.00E-4
K-562	0.202	1.834	1.756	1.800	1.770	0.441	0.161	95	98	96	15	-21	3.68E-6	2.61E-5	> 1.00E-4
MOLT-4	0.603	2.680	2.622	2.598	2.484	0.471	0.443	97	96	91	-22	-27	2.29E-6	6.39E-6	> 1.00E-4
RPMI-8226	0.696	2.465	2.487	2.372	2.142	0.518	0.475	101	95	82	-26	-32	1.97E-6	5.77E-6	> 1.00E-4
SR	0.509	2.225	2.186	2.043	1.832	0.485	0.388	98	89	77	-5	-24	2.14E-6	8.73E-6	> 1.00E-4
Non-Small Cell Lung Cancer															
A549/ATCC	0.518	2.621	2.681	2.689	2.560	0.762	0.131	103	103	97	12	-75	3.55E-6	1.36E-5	5.16E-5
HOP-92	1.360	1.854	1.885	1.883	1.887	1.532	0.312	106	106	107	35	-77	6.13E-6	2.05E-5	5.73E-5
NCI-H226	1.109	2.725	2.695	2.730	2.662	1.862	0.137	98	100	96	47	-88	8.52E-6	2.22E-5	5.24E-5
NCI-H23	0.480	1.394	1.373	1.327	1.150	0.321	0.263	98	93	73	-33	-45	1.65E-6	4.88E-6	> 1.00E-4
NCI-H322M	0.727	1.955	1.882	1.842	1.958	0.363	0.105	94	91	100	-50	-86	2.16E-6	4.64E-6	9.99E-6
NCI-H460	0.247	2.495	2.546	2.473	1.782	0.123	0.074	102	99	68	-50	-70	1.43E-6	3.76E-6	9.92E-6
NCI-H522	0.874	1.823	1.777	1.817	1.698	0.277	0.222	95	99	87	-68	-75	1.73E-6	3.63E-6	7.62E-6
Colon Cancer															
COLO 205	0.471	1.890	1.820	1.760	1.688	0.142	0.147	95	91	86	-70	-69	1.70E-6	3.56E-6	7.45E-6
HCC-2998	0.724	2.224	2.370	2.398	2.582	0.257	0.116	110	112	124	-65	-84	2.47E-6	4.55E-6	8.38E-6
HCT-116	0.282	2.067	2.035	1.911	1.713	0.181	0.016	98	91	80	-36	-95	1.82E-6	4.90E-6	1.74E-5
HCT-15	0.282	1.925	1.885	1.719	1.525	0.165	0.071	98	87	76	-41	-75	1.66E-6	4.42E-6	1.80E-5
HT29	0.194	1.001	1.072	1.065	1.045	0.214	0.203	109	108	105	2	1	3.45E-6	> 1.00E-4	> 1.00E-4
KM12	0.542	2.577	2.570	2.484	2.462	0.656	0.180	100	95	94	6	-67	3.16E-6	1.19E-5	5.86E-5
SW-620	0.272	1.895	1.888	1.915	1.642	0.157	0.075	100	101	84	-42	-72	1.87E-6	4.64E-6	1.80E-5
CNS Cancer															
SF-268	0.559	1.826	1.782	1.754	1.723	0.567	0.168	97	94	92	1	-70	2.88E-6	1.02E-5	5.22E-5
SF-295	0.685	2.617	2.624	2.522	2.676	1.613	0.058	100	95	103	48	-92	9.20E-6	2.21E-5	5.03E-5
SF-539	0.726	2.171	2.026	2.025	2.110	0.312	0.072	90	90	96	-57	-90	1.99E-6	4.23E-6	8.99E-6
SNB-19	0.467	1.892	1.834	1.830	1.839	0.107	0.072	96	96	96	-77	-85	1.85E-6	3.59E-6	6.97E-6
SNB-75	0.725	1.437	1.392	1.358	1.353	0.034	-0.005	94	89	88	-95	-100	1.61E-6	3.02E-6	5.66E-6
U251	0.544	2.605	2.553	2.580	2.620	0.389	0.275	97	99	101	-28	-49	2.47E-6	6.02E-6	> 1.00E-4
Melanoma															
LOX IMVI	0.192	1.647	1.628	1.501	1.179	0.147	0.111	99	90	68	-23	-42	1.57E-6	5.54E-6	> 1.00E-4
MALME-3M	0.677	1.344	1.343	1.456	1.193	0.142	0.124	100	117	77	-79	-82	1.49E-6	3.12E-6	6.51E-6
M14	0.494	1.708	1.643	1.633	1.425	0.040	0.045	95	94	77	-92	-91	1.44E-6	2.85E-6	5.64E-6
MDA-MB-435	0.452	2.199	2.248	2.150	0.819	0.071	0.047	103	97	21	-84	-90	4.16E-7	1.58E-6	4.72E-6
SK-MEL-2	1.110	2.176	2.054	2.132	2.124	0.916	0.358	89	96	95	-17	-68	2.52E-6	7.00E-6	4.43E-5
SK-MEL-28	0.692	2.126	2.154	2.186	2.197	0.467	0.088	102	104	105	-33	-87	2.51E-6	5.79E-6	2.08E-5
SK-MEL-5	0.665	3.073	3.102	3.087	2.661	0.058	0.020	101	101	83	-91	-97	1.54E-6	2.99E-6	5.79E-6
UACC-257	1.139	2.594	2.652	2.625	2.447	0.335	0.094	104	102	90	-71	-92	1.77E-6	3.63E-6	7.44E-6
UACC-62	0.675	2.467	2.377	2.327	2.362	0.193	0.101	95	92	94	-71	-85	1.85E-6	3.70E-6	7.42E-6
Ovarian Cancer															
OVCAR-3	0.484	1.486	1.399	1.325	0.539	0.313	0.087	91	84	5	-35	-82	2.71E-7	1.36E-6	2.06E-5
OVCAR-4	0.649	1.291	1.237	1.158	1.141	0.010	0.157	91	79	77	-98	-76	1.42E-6	2.74E-6	5.29E-6
OVCAR-5	0.561	1.674	1.673	1.650	1.692	1.229	0.400	100	98	102	60	-29	1.30E-5	4.75E-5	> 1.00E-4
OVCAR-8	0.546	2.630	2.567	2.604	2.408	0.481	0.251	97	99	89	-12	-54	2.45E-6	7.63E-6	8.02E-5
NCI/ADR-RES	0.509	1.690	1.706	1.653	1.654	0.497	0.410	101	97	97	-2	-20	2.97E-6	9.47E-6	> 1.00E-4
SK-OV-3	0.932	1.335	1.390	1.299	1.366	1.264	0.076	114	91	108	82	-92	1.53E-5	2.97E-5	5.75E-5
Renal Cancer															
786-0	0.732	2.531	2.614	2.575	2.716	1.878	0.346	105	102	110	64	-53	1.31E-5	3.52E-5	9.46E-5
A498	1.215	1.922	2.049	1.959	1.943	1.859	0.027	118	105	103	91	-98	1.65E-5	3.04E-5	5.59E-5
ACHN	0.576	2.082	2.076	1.967	1.947	0.756	0.076	100	92	91	12	-87	3.30E-6	1.32E-5	4.23E-5
CAKI-1	0.575	2.770	2.714	2.638	2.685	0.920	0.004	97	94	96	16	-99	3.75E-6	1.37E-5	3.72E-5
RXF 393	0.693	1.238	1.254	1.235	1.174	0.796	0.173	103	99	88	19	-75	3.56E-6	1.59E-5	5.41E-5
SN12C	0.727	2.573	2.432	2.492	2.411	0.296	0.239	92	96	91	-59	-67	1.88E-6	4.04E-6	8.68E-6
TK-10	0.969	1.938	1.896	1.930	2.328	1.720	0.179	96	99	140	77	-82	1.49E-5	3.07E-5	6.33E-5
UO-31	0.802	2.556	2.397	2.402	2.364	1.333	0.147	91	91	89	30	-82	4.61E-6	1.86E-5	5.21E-5
Prostate Cancer															
PC-3	0.614	2.618	2.612	2.509	2.370	0.661	0.371	100	95	88	2	-40	2.76E-6	1.14E-5	> 1.00E-4
DU-145	0.370	1.589	1.569	1.565	1.139	0.027	0.004	98	98	63	-93	-99	1.21E-6	2.54E-6	5.32E-6
Breast Cancer															
MCF7	0.348	2.100	2.104	1.972	1.477	0.166	0.126	100	93	64	-52	-64	1.33E-6	3.56E-6	9.53E-6
MDA-MB-231/ATCC	0.538	1.683	1.561	1.530	1.299	0.534	0.464	89	87	66	-1	-14	1.76E-6	9.75E-6	> 1.00E-4
HS 578T	1.120	2.191	2.226	2.182	2.096	1.046	0.942	103	99	91	-7	-16	2.63E-6	8.56E-6	> 1.00E-4
BT-549	1.331	1.969	2.024	1.936	1.990	0.413	0.060	109	95	103	-69	-96	2.04E-6	3.98E-6	7.76E-6
T-47D	0.637	1.371	1.388	1.306	1.339	0.634	0.366	102	91	96	-1	-43	2.98E-6	9.87E-6	> 1.00E-4
MDA-MB-468	0.761	1.553	1.627	1.618	1.519	0.475	0.223	109	108	96	-38	-71	2.20E-6	5.22E-6	2.36E-5

Tabulated 5-dose NCI-60 tumor cell line screen assay data in the presence and absence of **70**.

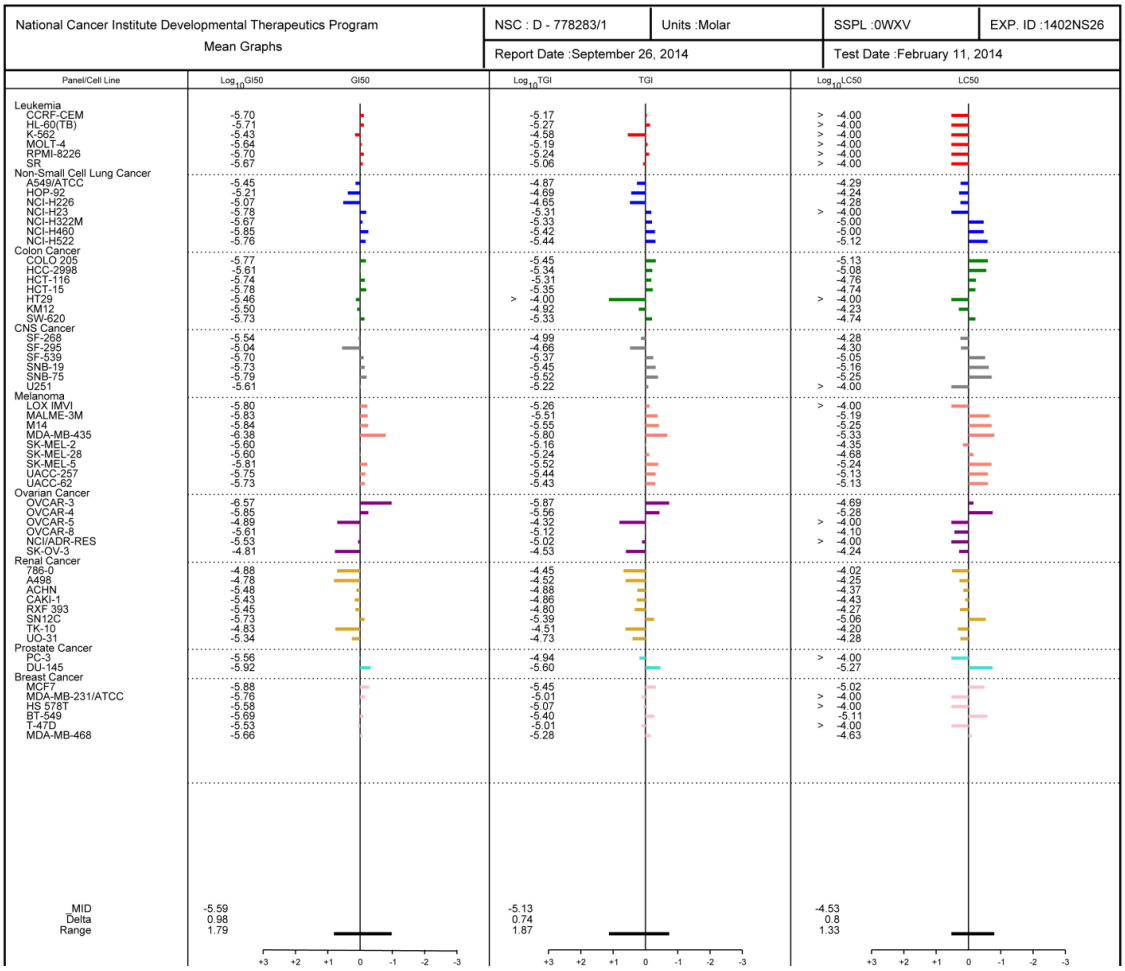

5-dose NCI-60 tumor cell line screen assay $Log_{10}GI_{50}$, $Log_{10}TGI$ and $Log_{10}LC_{50}$ values for **70.**

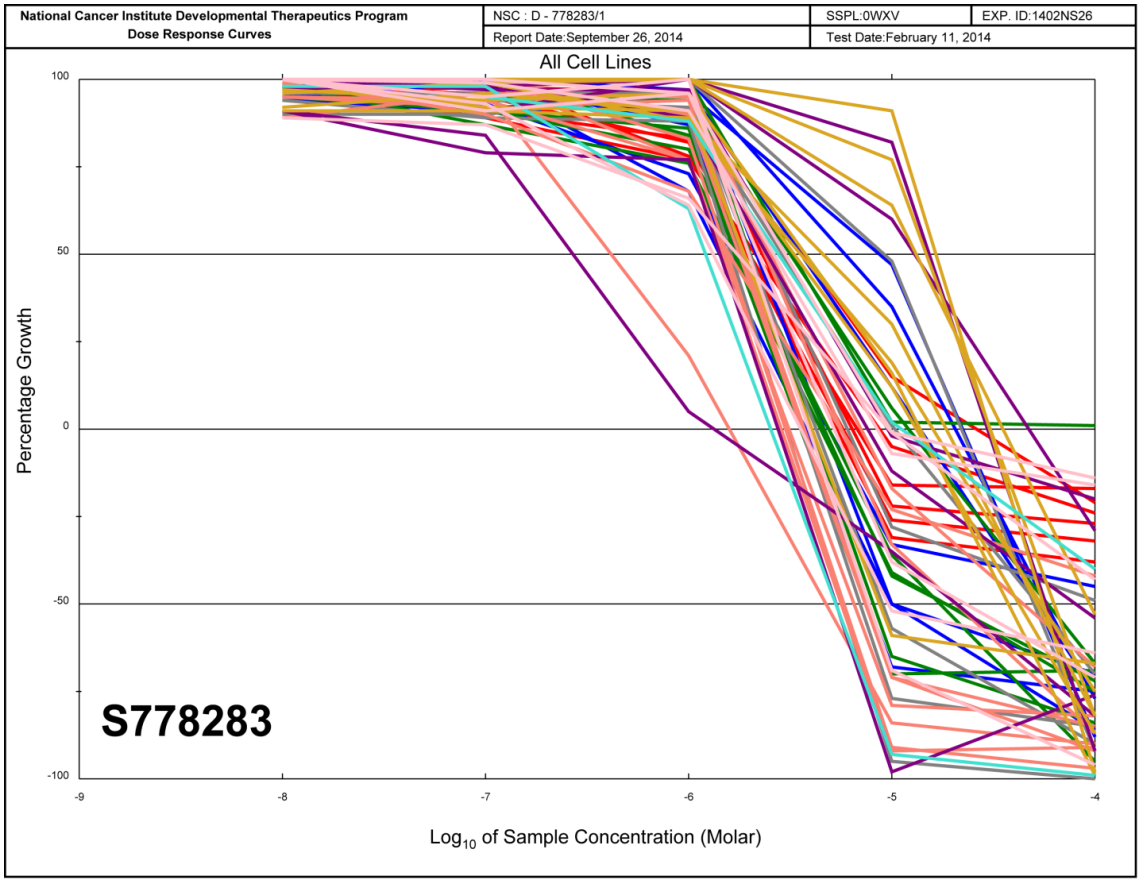

Graphical overlay of all dose response curves for **70**.

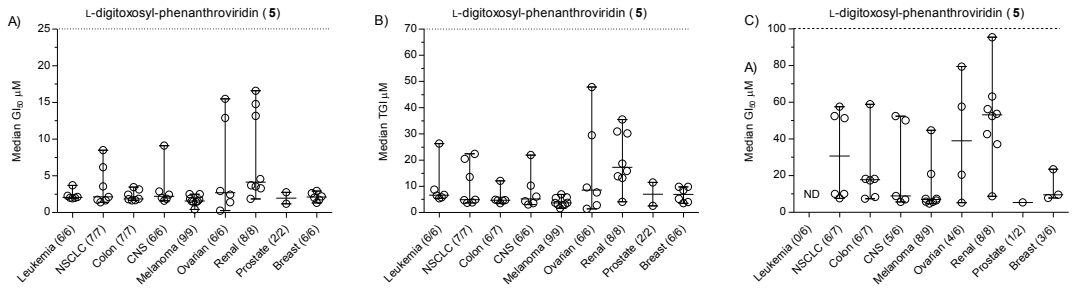

GI_{50} (A), TGI (B), and LC_{50} (C) values (µM) for **70** grouped by cancer cell type. Each open circle represents the GI_{50}, TGI or LC_{50} for an individual cancer cell line. The horizontal lines represent the median and range values for each group of cancer cells. The numbers in parentheses below the x-axis indicate the number of cell lines out of the total number of cell lines tested per group.

Standard COMPARE data comparing GI_{50} values of **70** versus GI_{50} values of the NCI Standard Agent Database.[a]

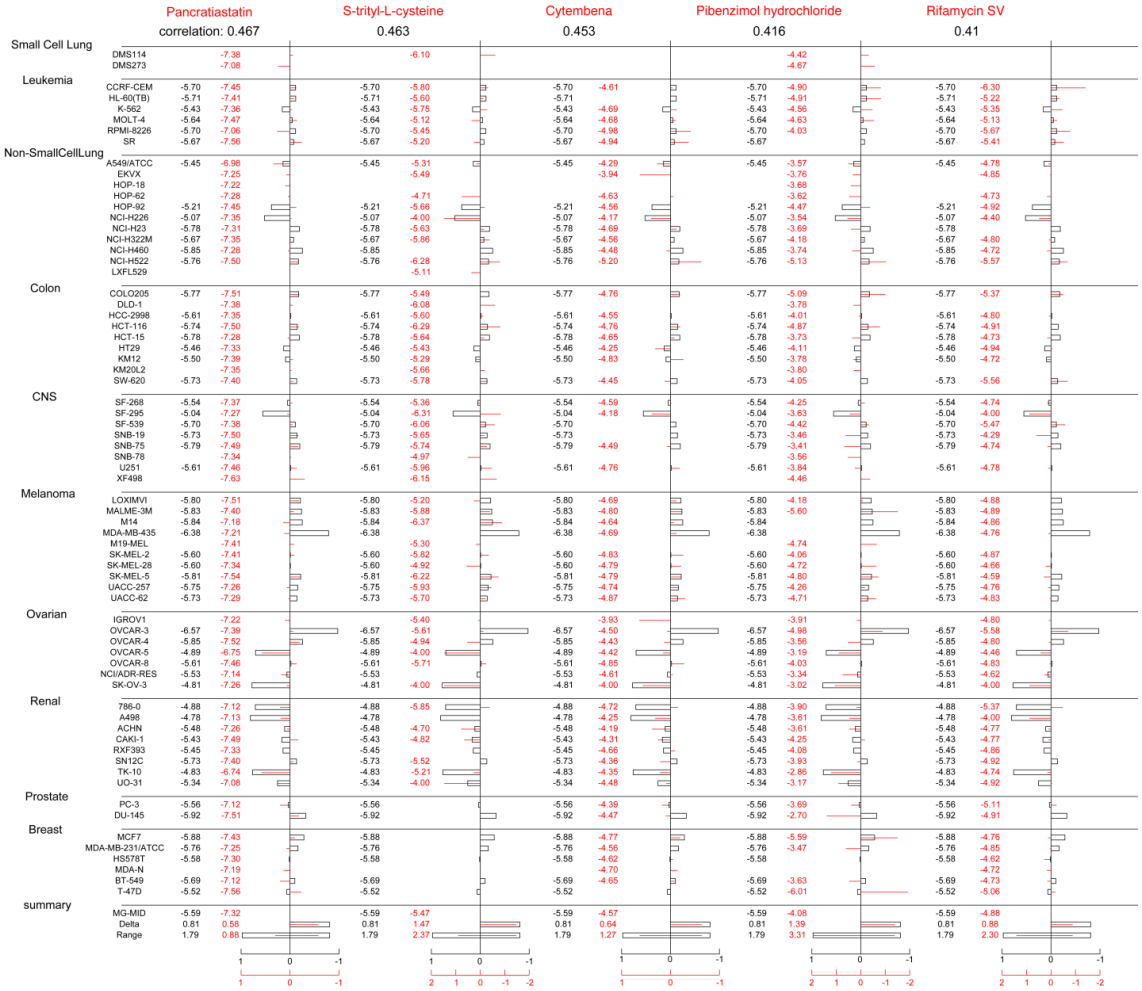

[a]The top five correlations are shown. GI_{50} values for compound **70** are represented in black as Log_{10} values. Compounds showing correlations to **70** are represented in red, the GI_{50} values associated with these compounds are represented as Log_{10} values. Correlation values are listed at the top of each column in black.

Standard COMPARE data comparing TGI values of **70** versus TGI values of the NCI Standard Agent Database.[a]

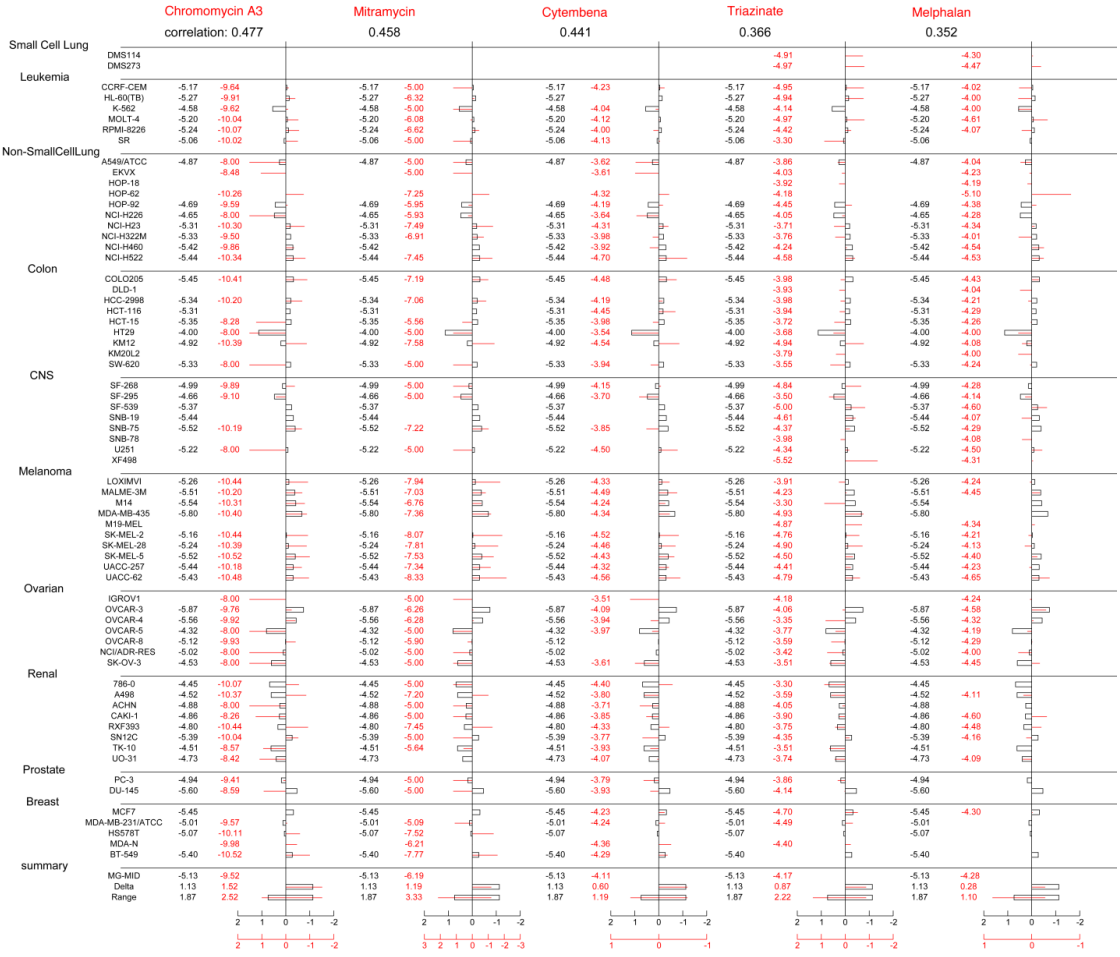

[a]The top five correlations are shown. TGI values for compound **70** are represented in black as Log_{10} values. Compounds showing correlations to **70** are represented in red, the TGI values associated with these compounds are represented as Log_{10} values. Correlation values are listed at the top of each column in black.

Standard COMPARE data comparing LC_{50} values of **70** versus LC_{50} values of the NCI Standard Agent Database.

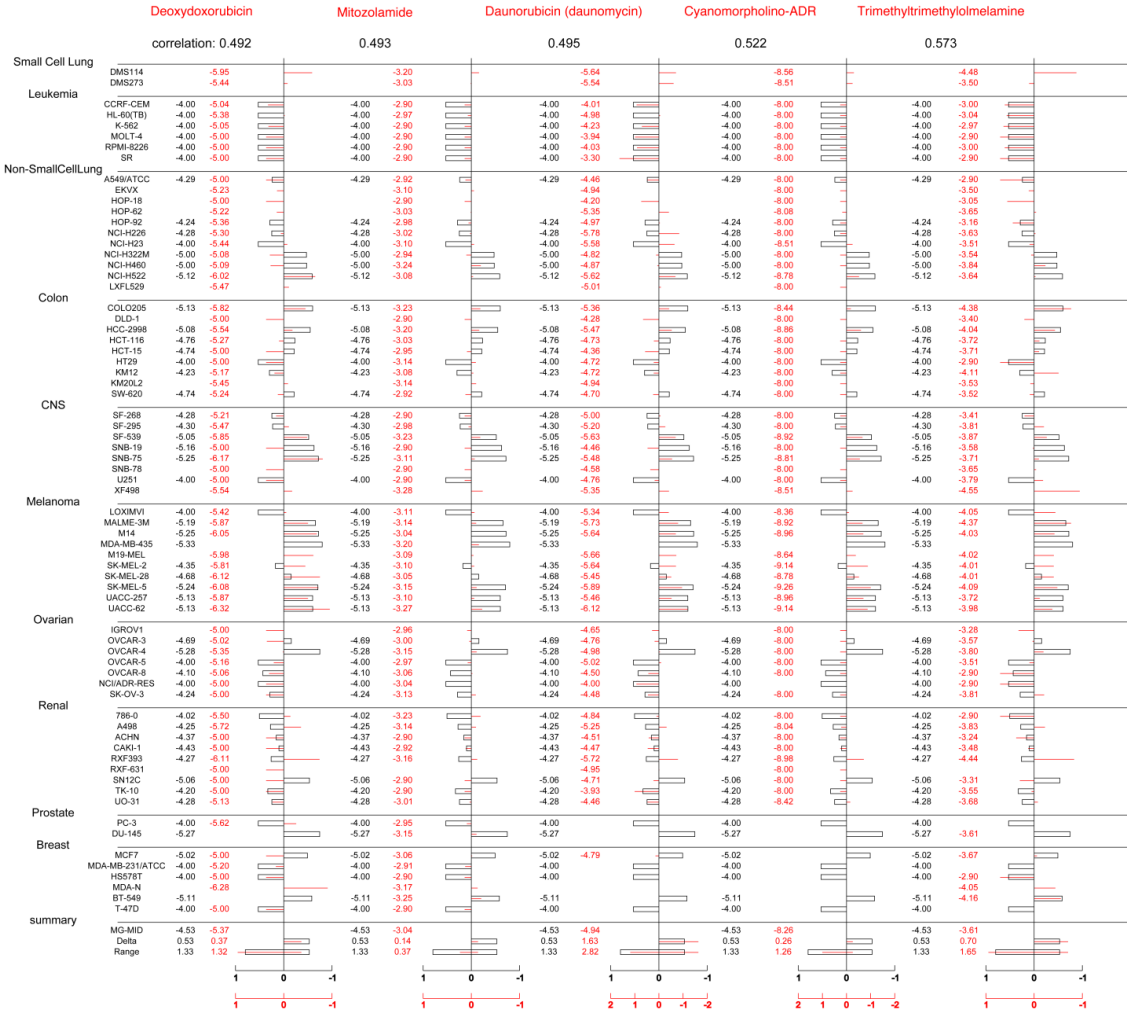

The top five correlations are shown. LC_{50} values for compound **70** are represented in black as Log_{10} values. Compounds showing correlations to **70** are represented in red, the LC_{50} values associated with these compounds are represented as Log_{10} values. Correlation values are listed at the top of each column in black.

Standard COMPARE data comparing GI_{50} values of **70** versus GI_{50} values of the NCI synthetic compounds database.

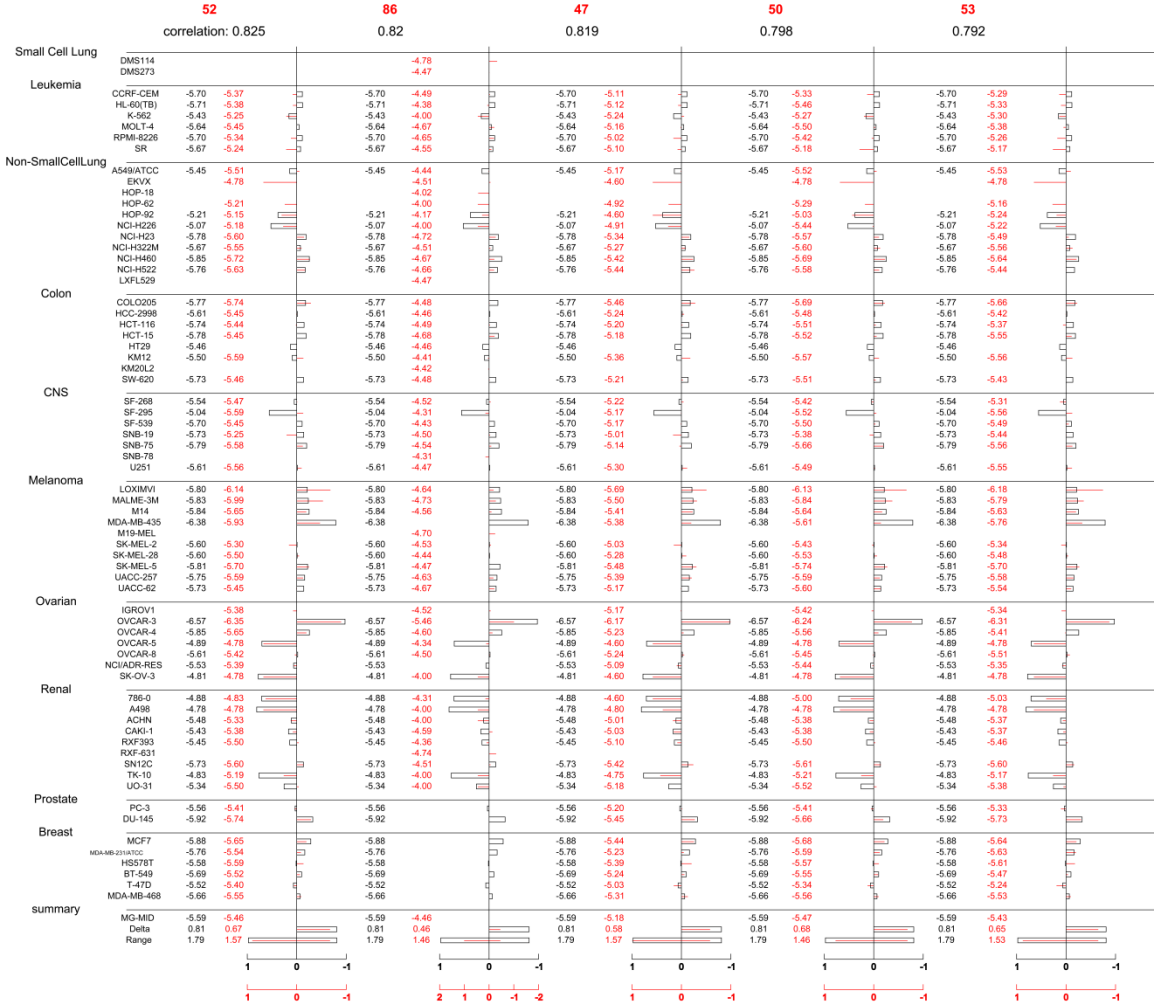

The top five correlations are shown. GI_{50} values for compound **70** are represented in black as Log_{10} values. Compounds showing correlations to **70** are represented in red, the GI_{50} values associated with these compounds are represented as Log_{10} values. Correlation values are listed at the top of each column in black.

Standard COMPARE data comparing TGI values of **70** versus TGI values of the NCI synthetic compounds database.

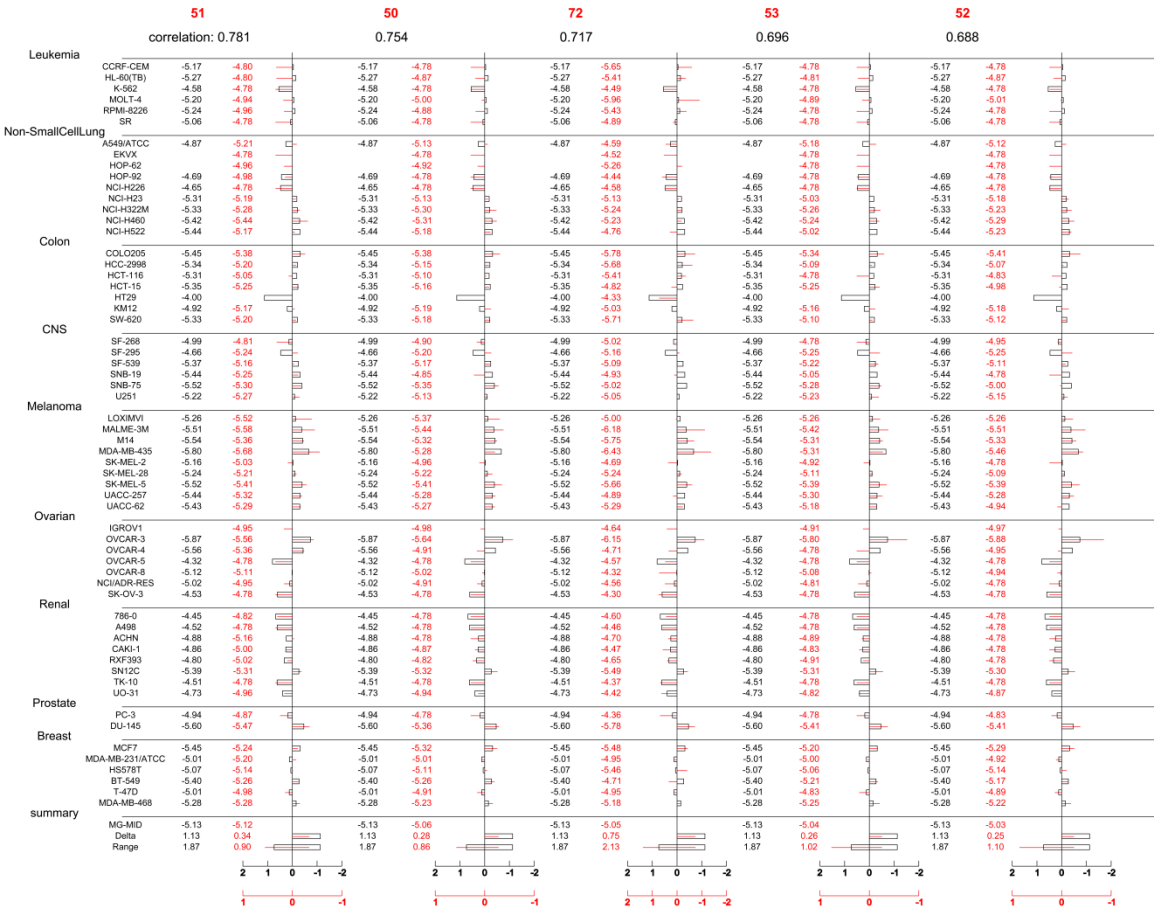

The top five correlations are shown. TGI values for compound **70** are represented in black as Log_{10} values. Compounds showing correlations to **70** are represented in red, the TGI values associated with these compounds are represented as Log_{10} values. Correlation values are listed at the top of each column in black.

Standard COMPARE data comparing LC_{50} values of **70** versus LC_{50} values of the NCI synthetic compounds database.

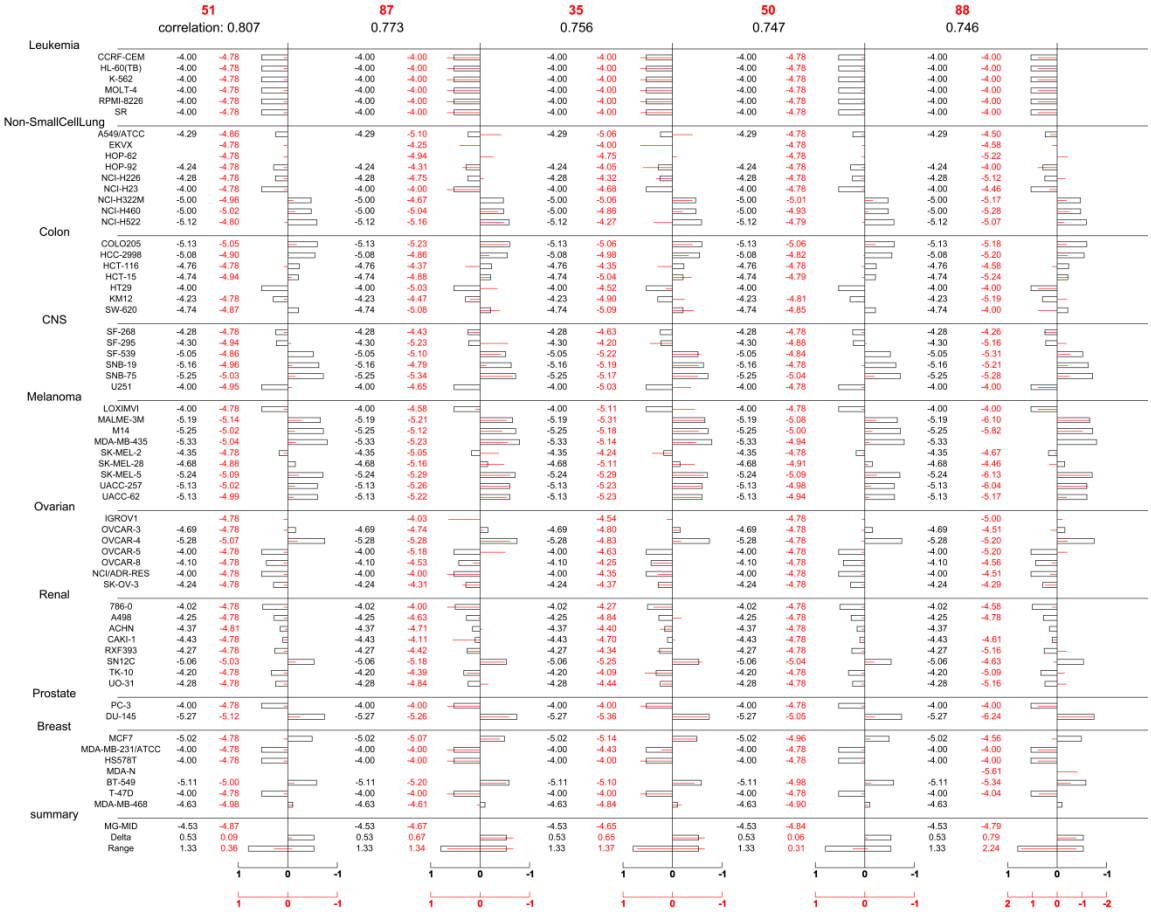

The top five correlations are shown. LC_{50} values for compound **70** are represented in black as Log_{10} values. Compounds showing correlations to **70** are represented in red, the LC_{50} values associated with these compounds are represented as Log_{10} values. Correlation values are listed at the top of each column in black.

APPENDIX E: JADX BINDING STUDIES INCLUDING BUFFERS, LC-MS/MS ANALYSIS, SPECTRAL DATA AND DOSE REPONSE BINDING CURVES

Multiple sequence alignment of JadX versus various homologous proteins 227

S. venezuelae ISP5230 WT and mutant growth curves in the presence of L-isoleucine (60 mM) 228

LC-MS/MS generates standard curve (linear region) of jadomycin B (**6**). 228

Final concentrations of **6** from comparative growths of *S. venezuelae* ISP5230 WT and mutants 228

LC-MS/MS generated standard curves (linear regions) of Jadomycin DS (**96**) (left) and chloramphenicol (**3**) (right). 229

Media and Buffers 229

Overlaid negative control WaterLOGSY NMR spectra of **96** 232

Overlaid WaterLOGSY NMR spectra of **96** in the presence of JadX 233

WaterLOGSY generated binding curves of **96** 234

Overlaid negative control WaterLOGSY NMR spectra of **3** 235

Overlaid WaterLOGSY NMR spectra of **3** in the presence of JadX 236

WaterLOGSY generated binding curves of **3** 237

Overlaid negative control WaterLOGSY NMR spectra of **96** in the presence of **3** 238

Overlaid WaterLOGSY NMR spectra of **96** in the presence of **3** 239

WaterLOGSY generated binding curves of **96** in the presence of **3** 240

Overlaid negative control WaterLOGSY NMR spectra of **3** in the presence of **96** 241

Overlaid WaterLOGSY NMR spectra of **3** in the presence of **96** 242

WaterLOGSY generated binding curves of **3** in the presence of **96** 243

```
HbmX     --------------MTATADYDSLARRLQALEDKEALRALMIRGWRALDR 36
GdmX     ---------------TATADYDSLARRLRALEDKEALRALMIRGWRALDR 35
GdmX     --------------MLPTPALDALTRRVRDLEDRDALHALMIRGWRALDR 36
JadX     MTTTDLTAVTTTDGPALAAELAELRATVRELSDRAAISAVCDRYAMHLDK 50
KinX     ----------------------------MTSSQSTADVAGLLDRYLINLDD 23
AzicU3   ---------------MTNTFTTEHDTLLRRLSDRAEISELLSLNWRALDA 35

HbmX     -KDWQTWIECWAEDAVLEFGPWEKIHGKEAVRAKVEEVESPYASMQHHIL 85
GdmX     -KDWQTWIECWAEDAVLEFGPWEKIHGKEAVRAKVEEVESPYASMQHHIL 84
GdmX     -KDWRAWSACWAEDAVLEFGPWQRIQGRAAIRAKVEEAESPYTSIQHHIL 85
JadX     DRGSDDWFGAVFTDDVHLVFPMGEYKGMDGLAAFQQMARTTFARTHHISG 100
KinX     DKLDDAWARGLFTEDAVVEFPMSRHEGIAGLAEYHSTALAAFARTQHIGS 73
AzicU3   -QDFDNADEMYTDDIELVVGGGEPITGLAEVVRITRELNVHYESTQHNGS 84

HbmX     NMHVDVAGDRATGIGYMWFVAVTEP------GSTSSPYSMGGPYDWEFRR 129
GdmX     NMHVDVEGDRATGIGYMWFVAVTAP------GSTSSPYSMGGPYDWEFRR 128
GdmX     NMQVDVAGDRATGIGYMWFVAVTAP------GRASAPYSMGGPYDWEFRR 129
JadX     AYAIDLRGDEATVRAHLTAFHVRDA------AAPSAHFAIGGHYDAHVVR 144
KinX     PAVVEIDGDRASLRCNIVSTHVHHPSDHPEDADRDPIFANGSLVTAEARR 123
AzicU3   SLGIELDGDRAVVTANVIGVLIGRAN-----EAPPVSVNVTG-ARVGVVR 128

HbmX     GPDGWLLVRQRLGVWWTDGEDTLRAFA---------------------- 156
GdmX     GPDGWLLVRQRLGVWWTDGEDTLRAFA---------------------- 155
GdmX     DGDGWLLARQRLGILWTDGEDTLRAFEAE-------------------- 158
JadX     TPEGWRIRSFTFDLVWNAGEAPGAKGHS--------------------- 172
KinX     TPEGWRLSLLSLRMIWVTGTAPRKADAGDRRDSTKRARWYGEDAPRTTAL 173
Azic     TERGWRMDRIELTPRYRYPVG---------------------------- 149
```

Multiple sequence alignment of JadX versus various homologous proteins using Clustal W. Highly conserved amino acids are bolded and underlined. The organisms involved are: HbmX (AAY28224), *S. hygroscopicus*; GdmX (AAO06915), *S. hygroscopicus*; GdmX (ZP_05004866), *S.clavuligerus*; JadX (AAK01935), *S. venezuelae*; KinX (AAO65342), *S. murayamaensi*; AzicU3 (ADB02840), *Kibdelosporangium* sp. MJ126-NF4.

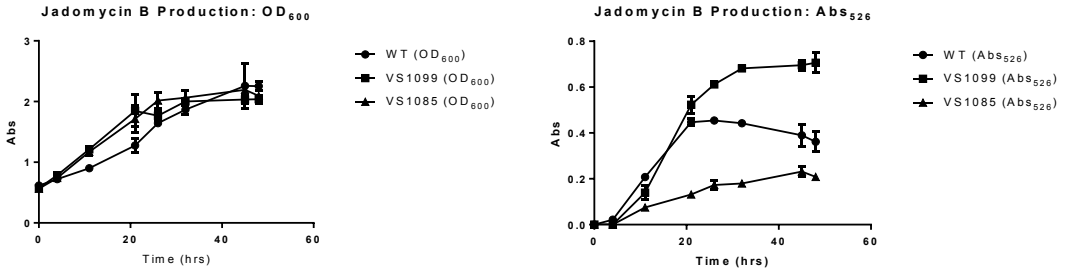

S. venezuelae ISP5230 WT and mutant growth curves in the presence of L-isoleucine (60 mM); (*Left*) Cellular growth curves (OD_{600}) of *S. venezuelae* ISP5230 WT (●), *S. venezuelae* ISP5230 VS1099 (■), and *S. venezuelae* ISP5230 VS1085 (▲) ethanol shocked and grown in MSM-Ile media. (*Right*) Absorbance of clarified growth media at λ = 526 nm (Abs_{526}), estimating coloured compound production of *S. venezuelae* ISP5230 WT (●), *S. venezuelae* ISP5230 VS1099 (■), and *S. venezuelae* ISP5230 VS1085 (▲) ethanol shocked and grown in MSM-Ile media.

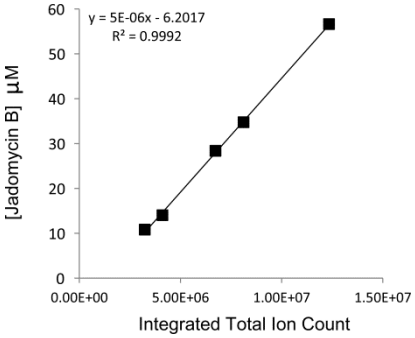

LC-MS/MS generated standard curve (linear region) of jadomycin B (**6**).

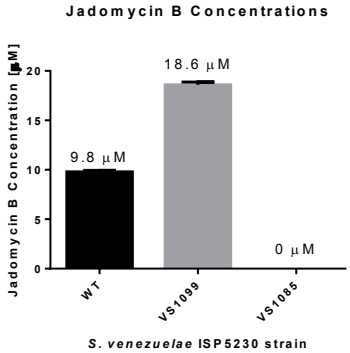

Final concentrations of **6** from comparative growths of *S. venezuelae* ISP5230 WT and mutants; *S. venezuelae* ISP5230 WT (black), *S. venezuelae* ISP5230 VS1099 (grey), and *S. venezuelae* ISP5230 VS1085 (white) after 48 h growth as determined by LC-MSMS analysis.

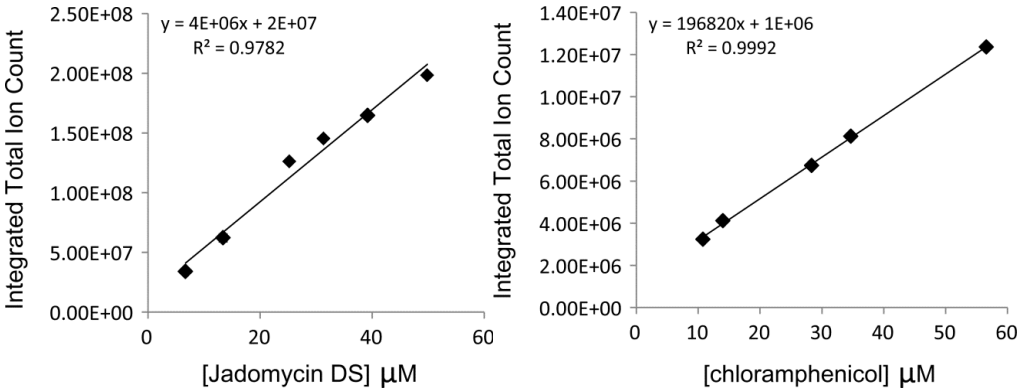

LC-MS/MS generated standard curves (linear regions) of jadomycin DS (**96**) (left) and chloramphenicol (**3**) (right).

Media and Buffers:

Maltose Yeast Malt Extract (MYM) Media

Maltose (0.4% w/v),
Yeast extract (0.4% w/v),
Malt extract (1% w/v); pH 7.0

MYM agar (E. *coli* growths)

MYM media supplemented with 1.5% agar

Minimal Salt Media (MSM)
$MgSO_4$ (0.4 g),
MOPS (1.9 g),
Salt solution (9 mL/L of 1% w/v NaCl and 1% w/v $CaCl_2$)
$FeSO_4 \cdot 7H_2O$ (4.5 mL/L of 0.2% w/v)
Trace mineral solution (4.5 mL/L)
pH 7.5
The trace mineral solution contained, per litre: $ZnSO_4 \cdot 7H_2O$ (880 mg), $CuSO_4 \cdot 5H_2O$ (39 mg), $MnSO_4 \cdot 4H_2O$ (6.1 mg), H_3BO_3 (5.7 mg), and $(NH_4)_6Mo_7O_{24} \cdot 4H_2O$ (3.7 mg).

Minimal Salt Media (MSM) With Amino Acid

MSM media supplemented with 60 mM of amino acid.

TE25 buffer (for lysis during genomic DNA extraction)

Tris-HCl pH 8	25 mM
EDTA pH 8	25 mM
Sucrose	0.3 M

2 × Kirby mix (for genomic DNA isolation)

SDS	2g
Sodium 4-aminosalicilate	12g
2 M Tris HCl pH 8	5mL
Equilibrated phenol pH 8	6mL
Distilled water	to 100mL

LB broth (*E. coli* growths)

Tryptone 10 g
Yeast Extract 5 g
NaCl 10 g
Dissolved in 1 L distilled water
pH 7.0

LB agar (*E. coli* growths)

LB broth supplemented with 1.5% agar

5 × M9 Salts (autoclaved)

KH_2PO_4 (15.0 g/L)
$NaHPO_4 \cdot 7H_2O$ (64.0 g/L)
NaCl (2.5 g/L)
NH_4Cl (5.0 g/L)
Dissolved in 1 L distilled water
pH adjusted to 7.2 with NaOH

^{15}N 5 × M9 Salts (autoclaved)

5× M9 salts solution with ^{15}N-ammonium chloride ($^{15}NH_4Cl$)

^{15}N-Minimal growth media (1 L)

^{15}N 5 × M9 Salts (200 mL) autoclaved separately
D-glucose (20% w/v) (20 mL) filter sterilized using 0.2 μm filter disks
100 × Basal Media Eagle Vitamin Solution (10.0 mL)
1 M $MgSO_4$ (2.0 mL) autoclaved separately
1 M $CaCl_2$ (0.1 mL) autoclaved separately
H_2O (770 mL) autoclaved separately
Mixed aseptically and divided into 4 × 250 mL fractions in sterile 1 L flasks.

Phosphate Buffered Saline (PBS) Buffer (Filter Sterilized)

$NaH_2PO_4 \bullet H_2O$ (6.9 g/L, 50 mM)
NaCl (8.482 g/L, 145 mM)
Dissolved in 1 L distilled H_2O
pH was adjusted to 7.6 or 6.6 (as needed) with NaOH solution (1 M).
Solutions were filter sterilized by passing through a 0.22 μm Millipore Durapore® Membrane filters.

dPBS Buffer

PBS buffer of a known pH (pH 7.6 or 6.6) was lyophilized for 48 h and dissolved in an equal volume of D_2O.

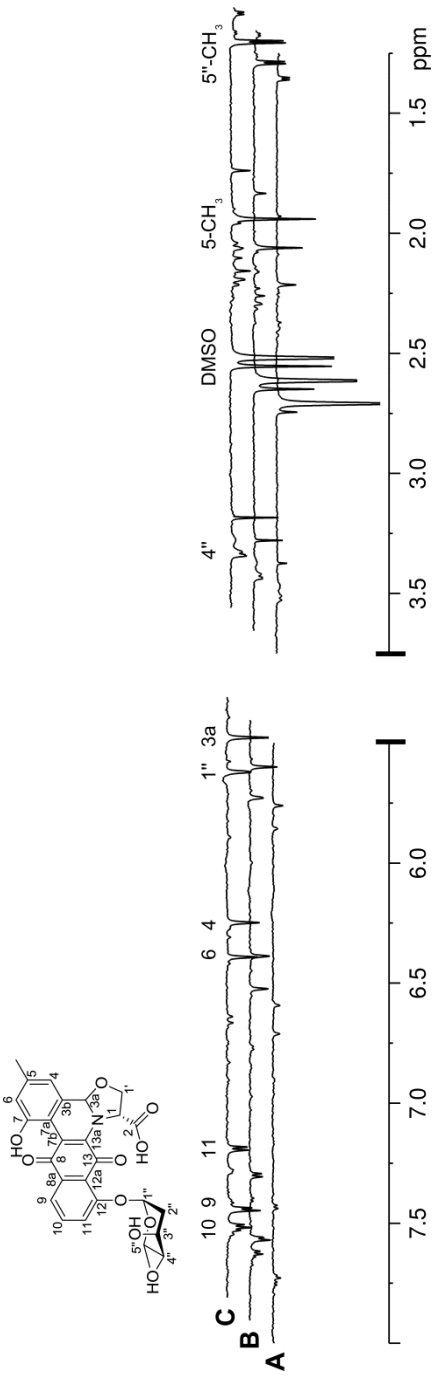

Overlaid negative control WaterLOGSY NMR spectra of **96**; (10% dPBS, 85% PBS, 5% DMSO-d_6) in the absence of JadX with varying concentrations of **96**: (*A*) 250 μM; (*B*) 750 μM; and (*C*) 1250 μM.

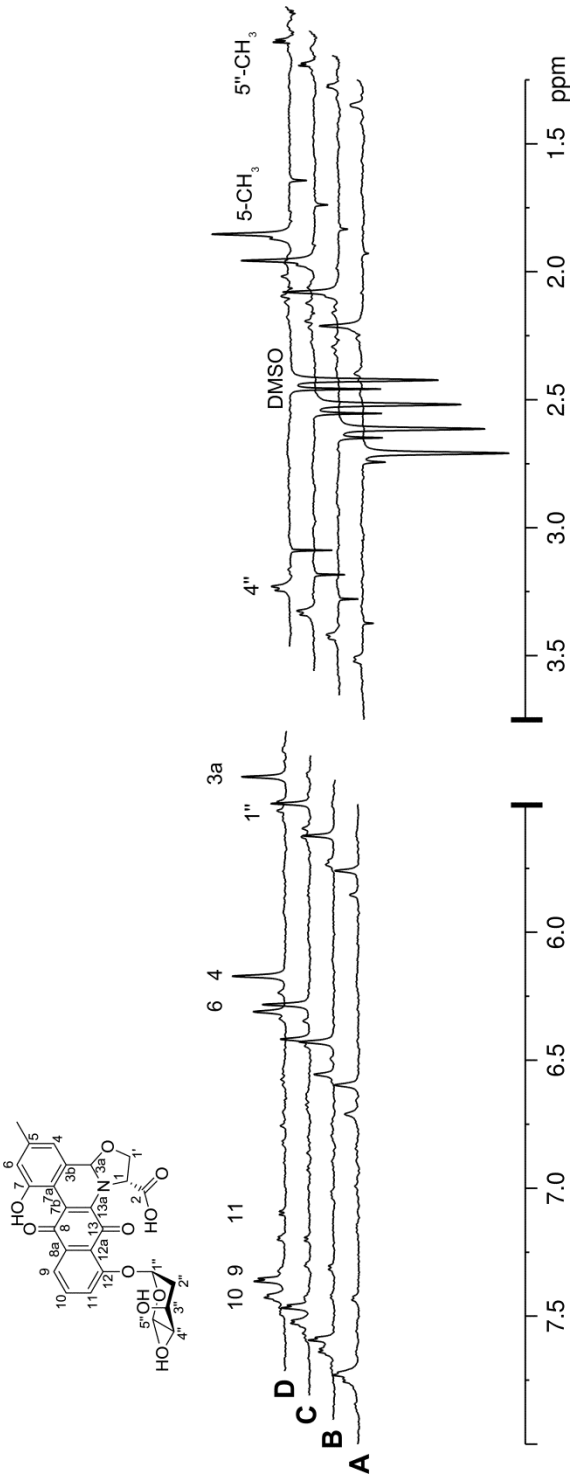

Overlaid WaterLOGSY NMR spectra of **96** in the presence of JadX; (10% dPBS, 85% PBS, 5% DMSO-d_6) in the presence of JadX (10 μM) with varying concentrations of **96**: (*A*) 250 μM; (*B*) 500 μM; (*C*) 750 μM; and (*D*) 1000 μM.

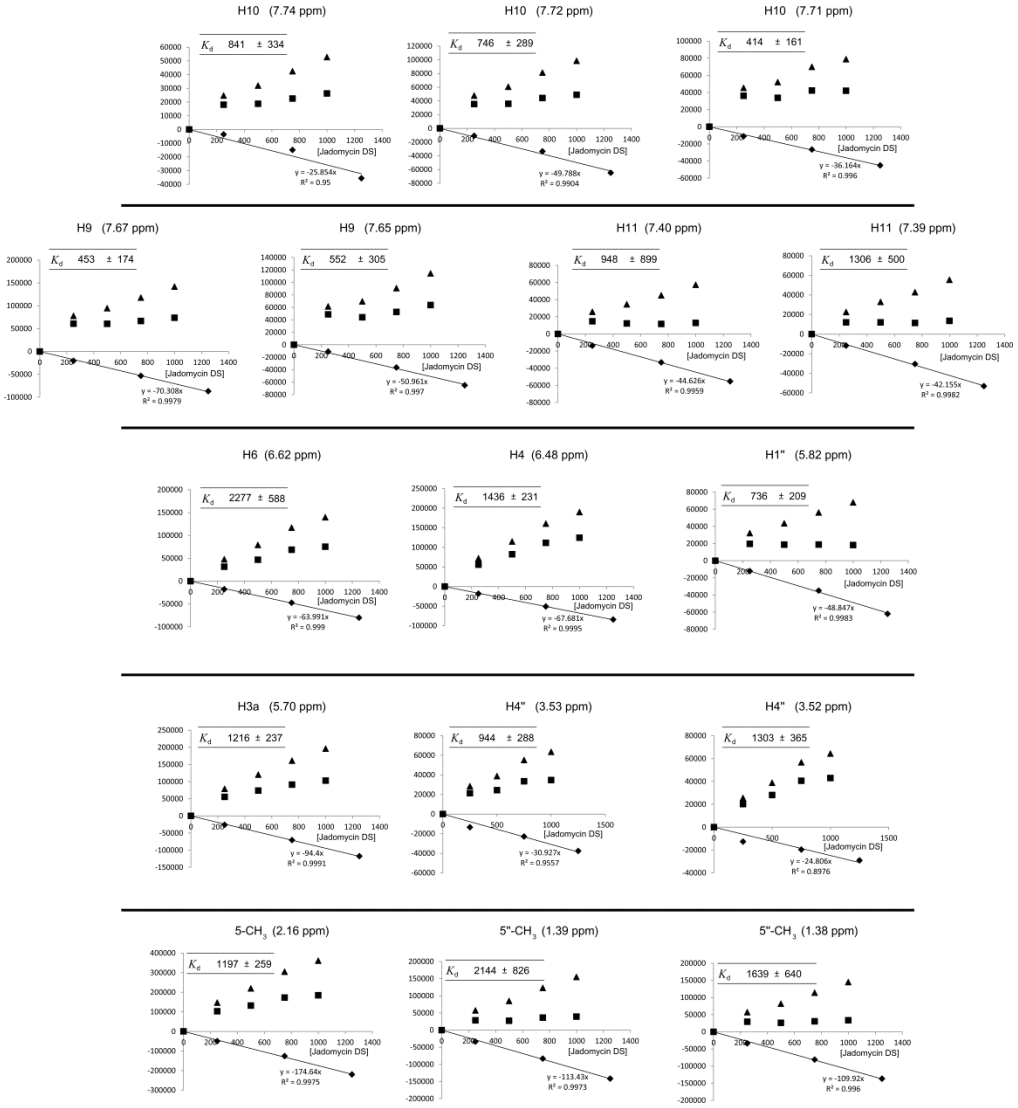

WaterLOGSY generated binding curves of **96** in the absence of JadX (♦), **96** in the presence of JadX (■), the difference of the binding and the non-binding standard (▲), and the linear fit (solid line). K_D value, in μM, is listed. The y-axis represents NMR signal intensity.

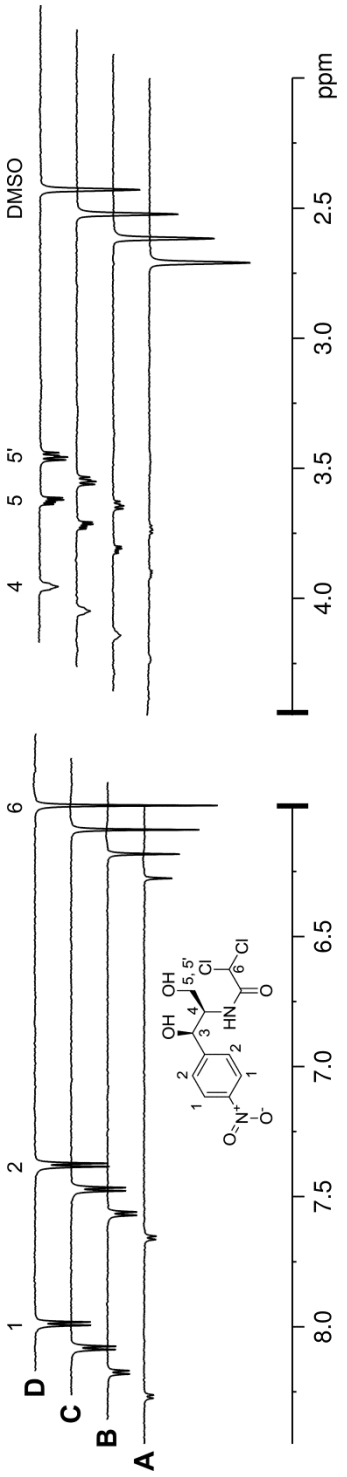

Overlaid negative control WaterLOGSY NMR spectra of **3**; (10% dPBS, 85% PBS, 5% DMSO-d_6) in the absence of JadX with varying concentrations of **3**: (*A*) 237 μM; (*B*) 710 μM; (*C*) 1183 μM; and (*D*) 1893 μM.

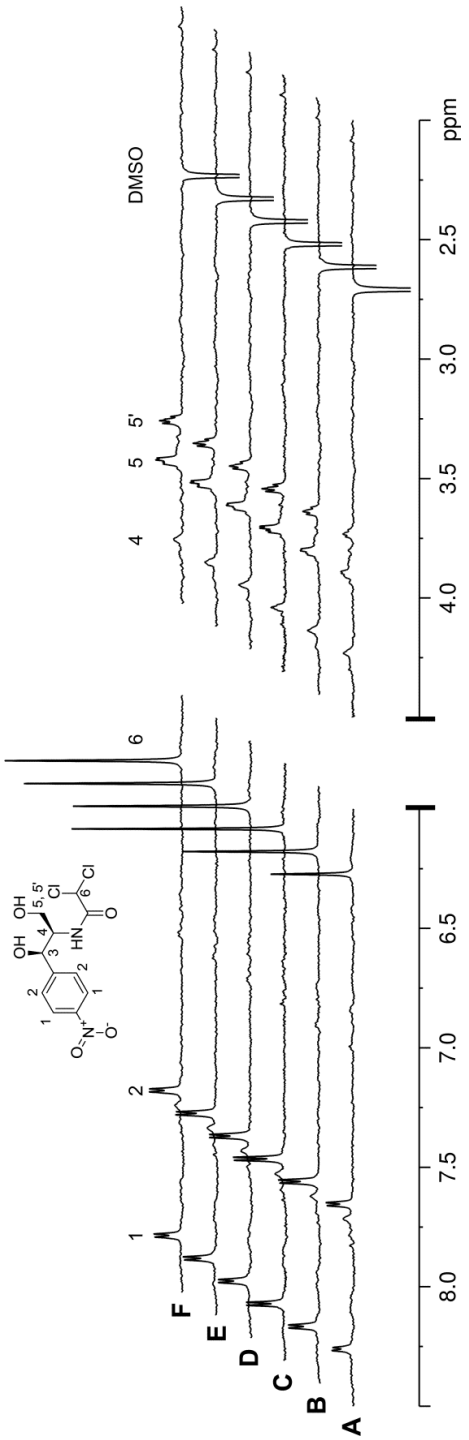

Overlaid WaterLOGSY NMR spectra of **3** in the presence of JadX; (10% dPBS, 85% PBS, 5% DMSO-d_6) in the presence of JadX (10 μM) with varying concentrations of **3**: (*A*) 237 μM; (*B*) 473 μM; (*C*) 710 μM; (*D*) 947 μM; (*E*) 1183 μM; and (*F*) 1420 μM.

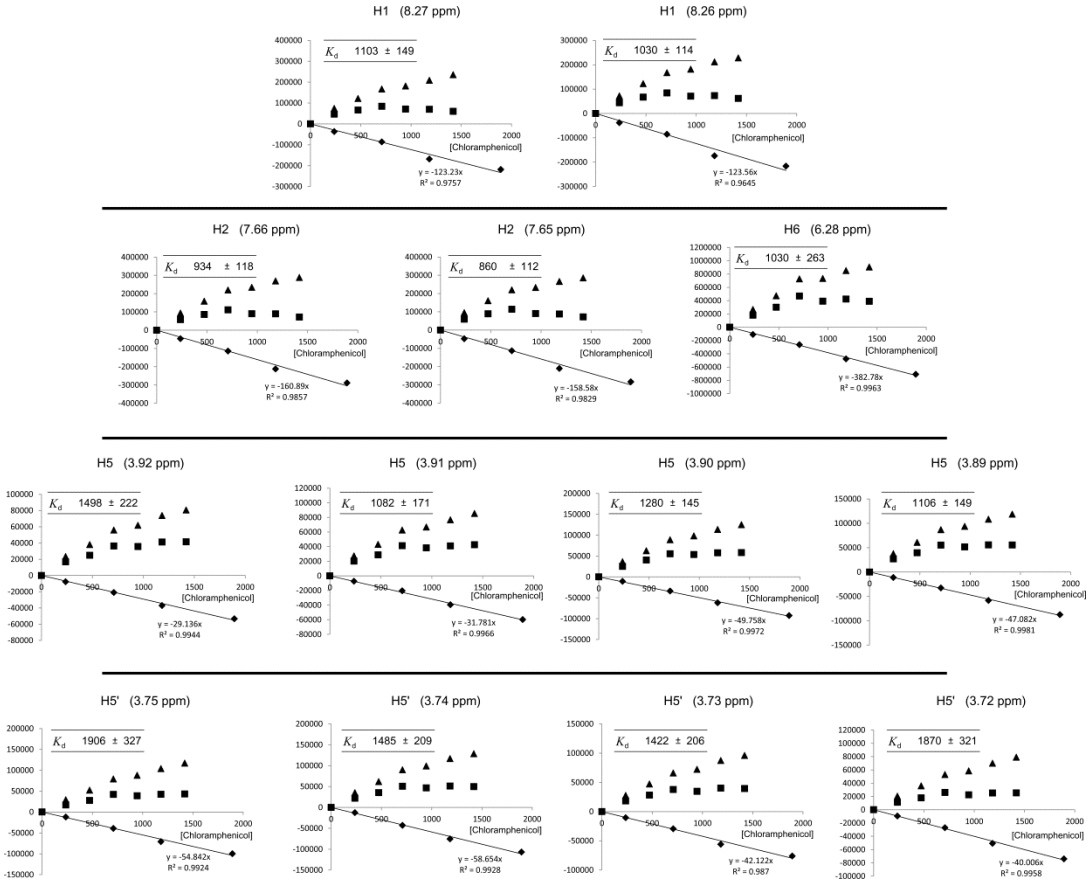

WaterLOGSY generated binding curves of **3**; in the absence of JadX (♦),in the presence of JadX (■), the difference of the binding and the non-binding standard (▲), and the linear fit (solid line). K_D value, in μM, is listed. The y-axis represents NMR signal intensity.

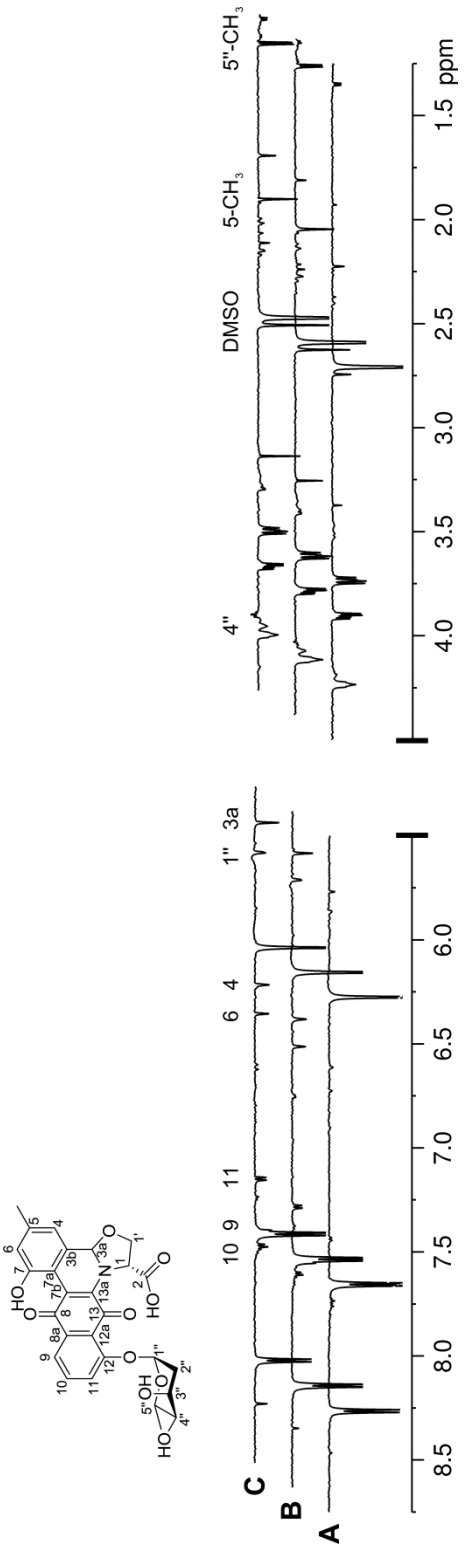

Overlaid negative control WaterLOGSY NMR spectra of **96** in the presence of **3**; (10% dPBS, 85% PBS, 5% DMSO-d_6) with **3** (2000 μM) in the absence of JadX with varying concentrations of **96**: (*A*) 250 μM; (*B*) 750 μM; and (*C*) 1250 μM.

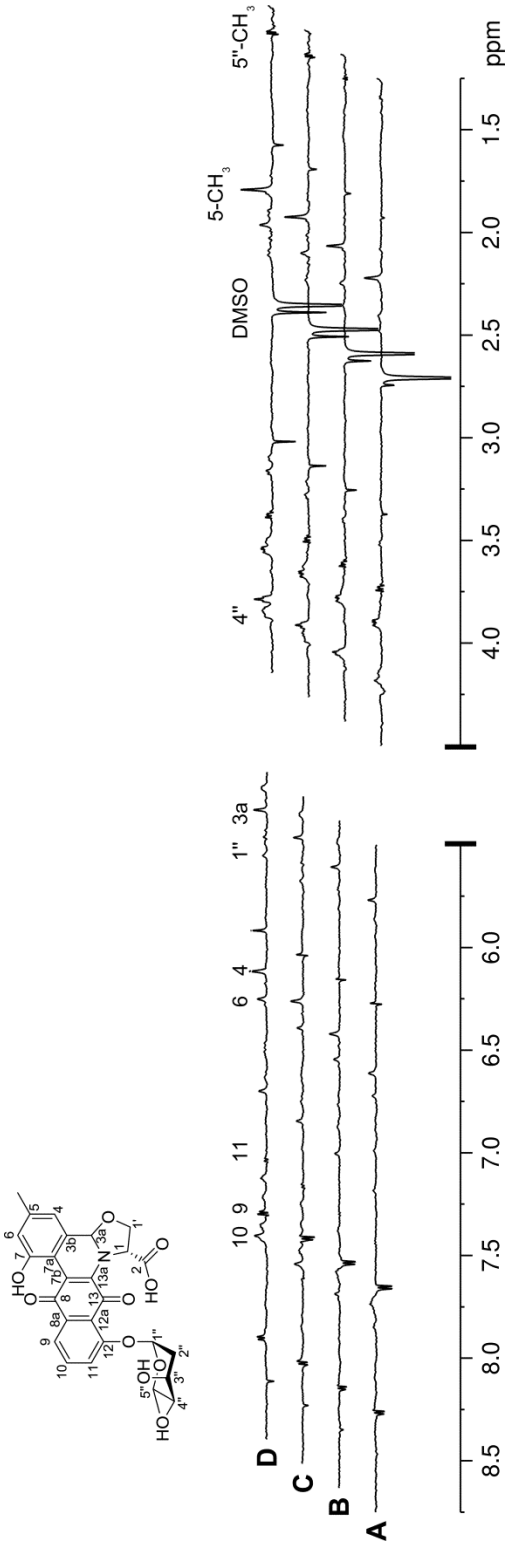

Overlaid WaterLOGSY NMR spectra of **96** in the presence of **3**; (10% dPBS, 85% PBS, 5% DMSO-d_6) in the presence of JadX (10 μM) and **3** (2000 μM) with varying jadomycin DS concentrations (*A*) 250 μM; (*B*) 500 μM; (*C*) 750 μM; and (*D*) 1000 μM.

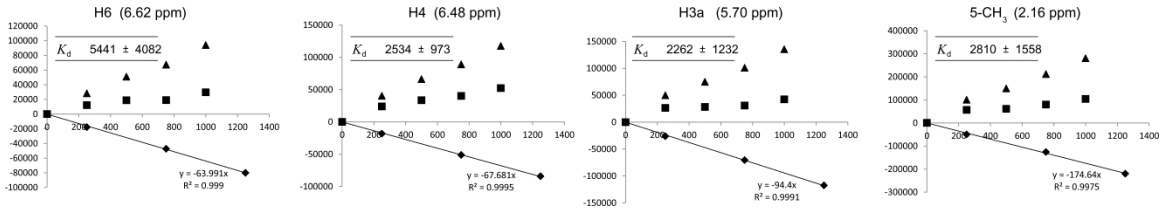

WaterLOGSY generated binding curves of **96** in the presence of **3** (2000 μM), in the absence of JadX (♦), in the presence of JadX (■), the difference of the binding and the non-binding standard (▲), and the linear fit (solid line). K_D value, in μM, is listed. The y-axis represents NMR signal intensity.

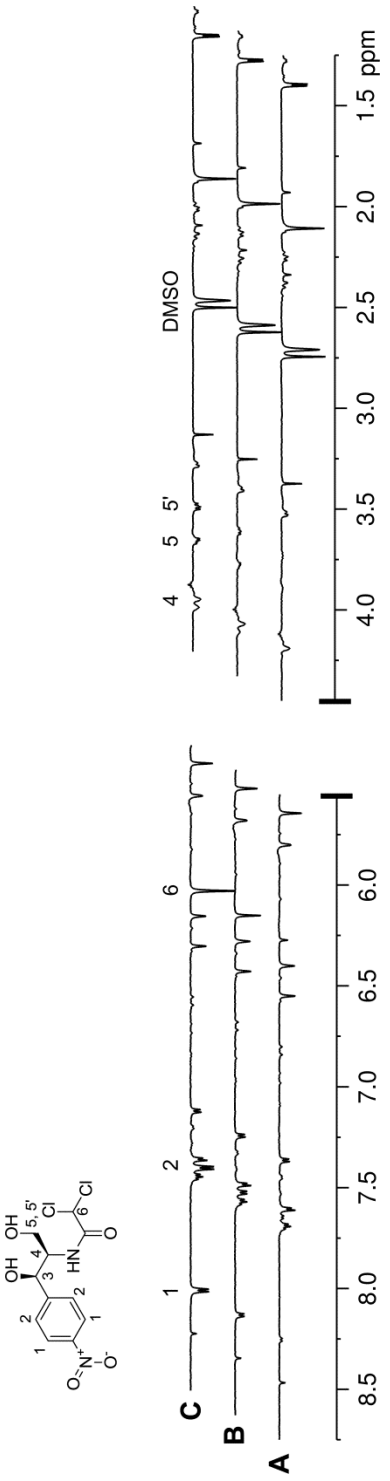

Overlaid negative control WaterLOGSY NMR spectra of **3** in the presence of **96**; (10% dPBS, 85% PBS, 5% DMSO-d_6) with **96** (2000 μM) in the absence of JadX with varying concentrations of **3**: (*A*) 250 μM; (*B*) 750 μM; and (*C*) 1500 μM.

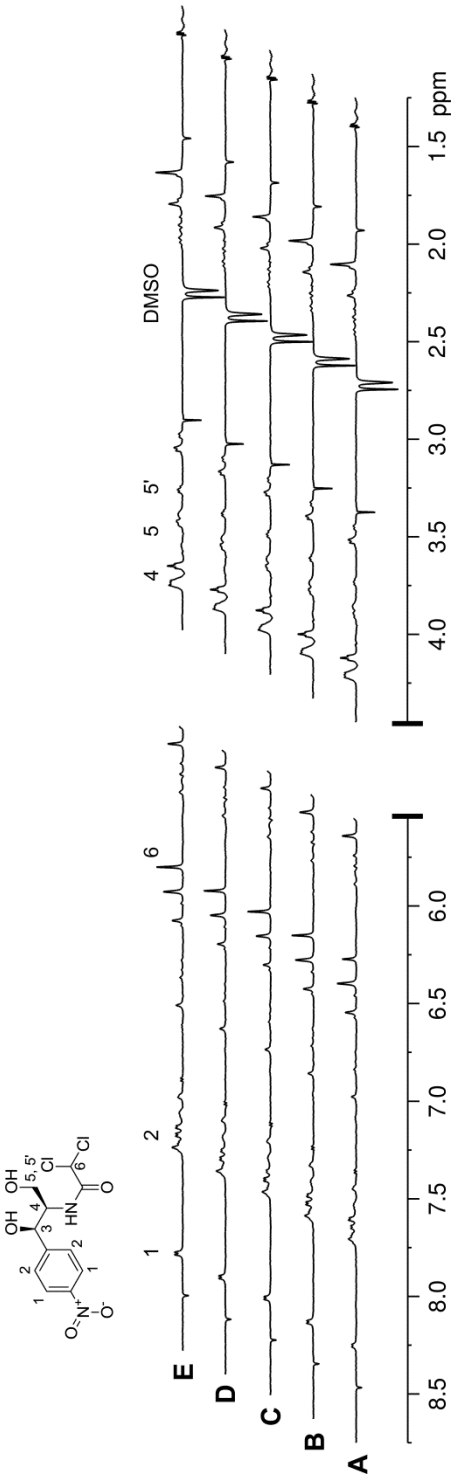

Overlaid WaterLOGSY NMR spectra of **3** in the presence of **96**; (10% dPBS, 85% PBS, 5% DMSO-d_6) in the presence of JadX (10 μM) and **96** (2000 μM) with varying concentrations of **3**: (*A*) 250 μM; (*B*) 500 μM; (*C*) 750 μM; (*D*) 1250 μM; and (*E*) 1450 μM.

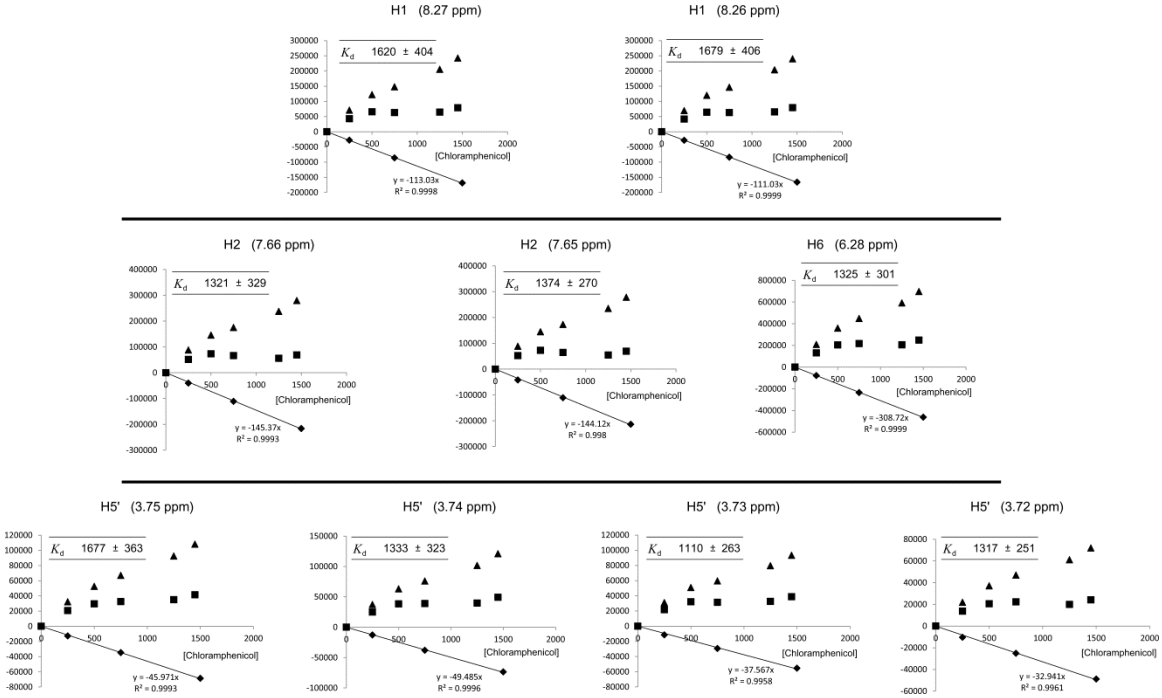

WaterLOGSY generated binding curves of **3** in the presence of **96** (2000 μM), in the absence of JadX (♦), in the presence of JadX (■), the difference of the binding and the non-binding standard (▲), and the linear fit (solid line). K_D value, in μM, is listed. The y-axis represents NMR signal intensity.